UNIVERSITAT RAMON LLULL

Development of cell-specific RNAi delivery vectors based on poly(β-amino ester)s with therapeutic applications

Nom i cognom/s de l'autor/a de la tesi

http://hdl.handle.net/10803/406136

C.I.F. G: 59069740 Universitat Ramon Llull Fundació Rgtre. Fund. Generalitat de Catalunya núm. 472 (28-02-90)

ADVERTIMENT. L'accés als continguts d'aquesta tesi doctoral i la seva utilització ha de respectar els drets de la persona autora. Pot ser utilitzada per a consulta o estudi personal, així com en activitats o materials d'investigació i docència en els termes establerts a l'art. 32 del Text Refós de la Llei de Propietat Intel·lectual (RDL 1/1996). Per altres utilitzacions es requereix l'autorització prèvia i expressa de la persona autora. En qualsevol cas, en la utilització dels seus continguts caldrà indicar de forma clara el nom i cognoms de la persona autora i el títol de la tesi doctoral. No s'autoritza la seva reproducció o altres formes d'explotació efectuades amb finalitats de lucre ni la seva comunicació pública des d'un lloc aliè al servei TDX. Tampoc s'autoritza la presentació del seu contingut en una finestra o marc aliè a TDX (framing). Aquesta reserva de drets afecta tant als continguts de la tesi com als seus resums i índexs.

ADVERTENCIA. El acceso a los contenidos de esta tesis doctoral y su utilización debe respetar los derechos de la persona autora. Puede ser utilizada para consulta o estudio personal, así como en actividades o materiales de investigación y docencia en los términos establecidos en el art. 32 del Texto Refundido de la Ley de Propiedad Intelectual (RDL 1/1996). Para otros usos se requiere la autorización previa y expresa de la persona autora. En cualquier caso, en la utilización de sus contenidos se deberá indicar de forma clara el nombre y apellidos de la persona autora y el título de la tesis doctoral. No se autoriza su reproducción u otras formas de explotación efectuadas con fines lucrativos ni su comunicación pública desde un sitio ajeno al servicio TDR. Tampoco se autoriza la presentación de su contenido en una ventana o marco ajeno a TDR (framing). Esta reserva de derechos afecta tanto al contenido de la tesis como a sus resúmenes e índices.

WARNING. The access to the contents of this doctoral thesis and its use must respect the rights of the author. It can be used for reference or private study, as well as research and learning activities or materials in the terms established by the 32nd article of the Spanish Consolidated Copyright Act (RDL 1/1996). Express and previous authorization of the author is required for any other uses. In any case, when using its content, full name of the author and title of the thesis must be clearly indicated. Reproduction or other forms of for profit use or public communication from outside TDX service is not allowed. Presentation of its content in a window or frame external to TDX (framing) is not authorized either. These rights affect both the content of the thesis and its abstracts and indexes.

C. Claravall, 1-3 | 08022 Barcelona | Tel. 93 602 22 00 | Fax 93 602 22 49 | info@url.edu | www.url.edu

C.I.F. G: 59069740 Universitat Ramon Llull Fundació Rgtre. Fund. Generalitat de Catalunya núm. 472 (28-02-90)

UNIVERSITAT RAMON LLULL

DOCTORAL THESIS

Title	Development of cell-specific RNAi delivery vectors based on poly(β-amino ester)s with therapeutic applications
Presented by	Pere Dosta Pons
Centre	IQS School of Engineering
Department	Bioengineering
Directed by	Dr. Salvador Borrós Gómez Dr. Victor Ramos Perez

This page left blank intentionally

A la meva família

This page left blank intentionally

A person who never made a mistake never tried anything new

Albert Einstein

This page left blank intentionally

Acknowledgments

En primer lloc, m'agradaria agrair als meus directors de tesis, en Dr. Salvador Borrós i en Dr. Victor Ramos per confiar en mi i donar-me l'oportunitat de realitzar aquesta tesis doctoral. Moltes gràcies Salvador per acollir-me al teu grup, ajudar-me en tot moment i per tot el que m'has ensenyat durant aquets anys. Gràcies per totes les oportunitats professionals que m'has donat, des de la col·laboració amb altres grups de recerca fins a l'estada a Emory. Admiro el teu entusiasme i optimisme permanent, el qual m'ha donat la confiança i llibertat per tirar endavant aquest projecte, i en aquesta tesis es reflecteix el seu resultat. Amb tu he crescut a nivell personal i professional. De tot cor, moltes gràcies per tot! També vull agrair profundament en Victor Ramos, ja que sense ell aquesta tesis no hagués sigut possible. Moltes gràcies per tots els teus consells, llargues reunions i per tot el que he aprés al teu costat. Cada dia em sorprèn més el teu pou de coneixement. Gràcies a tu he descobert la meva passió pel món de la investigació. Ha estat un plaer treballar al teu costat! No tinc suficients paraules per agrair-te tota la teva ajuda. Moltes gràcies Victor!

I am very grateful to Dr. Hanjoong Jo from Biomedical Department from Geogia Tech and Emory Univerity. Thank you for your confidence and everything that you have taught me. You transmitted me a lot of scientific values, teaching me to be strict and critic doing and analysing experiments. It was a pleasure to be in your Lab. Thank you Dr. Jo! I would like to thank you also all the members of Jo Lab. Especialment voldria donar les gràcies a en Joan Fernandez; amb tu, la meva etapa a Atlanta va ser molt més fàcil. Moltes gràcies per haver-me acollit des del minut zero i considerant-me un membre més de la teva família d'Atlanta. Rachel, Marwa and Leo, thank you for your help in the lab and for making my experience much more fun! You guys are great! I would also like to thank to Dr. Sandeep Kumar and Mr. Dong Wang for their help in the lab and their advice. Without you this thesis would not have been possible!

També voldria donar les gràcies al Dr. Maher Al-Atari de la Universitat Internacional de Barcelona per donar-me la oportunitat d'endinsar-me en un camp de recerca completament nou per mi. M'agradaria agrair a tots els membres del seu grup, per tractar-me tant bé en tot moment, fent-me sentir un membre més del seu grup. Tanmateix, m'agradaria fer una menció especial a la Raquel Nuñez i Sheyla Montori. Gràcies Raquel per tots els moments compartits, les llargues discussions de resultats i riures. Treballar amb gent com tu no te preu! Gràcies Sheyla per la teva ajuda en i els teus consells. Nomes puc dir que ha sigut un enorme plaer poder treballar amb vosaltres!

Aquests anys han sigut molt feliços gràcies a tots els amics que he conegut al laboratori i m'emporto per sempre. Sento una gran melancolia per estar acabant aquesta etapa i si fos per mi l'allargaria. En primer lloc m'agradaria donar les gràcies al grup de GEMAT, que es com la meva segona família. Realment no tinc paraules per descriure aqueta experiència viscuda, però estic segur

que serà difícil igualar-la. Gràcies al Lab Vell, sobretot a la Núria, Marina i Elena, per sempre estar disposades a donar-me un cop de mà en tot. Muchas gracias Nathaly por estar siempre a mi lado y por todo lo que me enseñaste justo llegar al laboratorio. Empezar una nueva etapa cómo esta con una persona como tú no tiene precio. ¡Muchas gracias por todo! També voldria agrair a tots aquells TFM i TFG que han fet possible aquesta tesis. Gràcies Gemma per totes les hores que vas passar ajudant-me amb tota la part de síntesis, crec que vas arribar just en el moment que més ho necessitava! Sense tu crec que encara estaria fent columnes! També vull agrair a la Marta, tota la seva feina feta. Va ser un autèntic plaer treballar amb tu. Estic segur que he aprés molt més jo de vosaltres que vosaltres de mi! Així que sense la vostra ajuda aquesta tesis tampoc hagués sigut possible.

Ara toca agrair als veterans del laboratori, i qui millor per començar que per en Robert Teixidó. Mai m'hauria pensat que poguéssim haver compartit tants moments, des de companys de pis, discussions de micropipetes i alguna sobre ciència, viatgets, visites a la Barraquer, sopars... Gràcies per tots els bons moments que hem passat i per estar sempre al meu costat. Gràcies Joan ajudar-me tantes vegades quan tenia problemes informàtics... Només us desitjo el millor en la vostra nova aventura com a emprenedors! Gràcies Anna Mas per extendre el meu propi llenguatge en el lab. Estic molt orgullós que una noia de Sant Cugat parli com un noi de Bor. Pensa que som molt poquets els que tenim l'habilitat de parlar aquest idioma!

I ara toca agrair els més jovenets del laboratori. Alba, Laura, Pol, Núria, Cris i Patri, m'ha encantat poder coincidir amb vosaltres durant aquesta última etapa de redacció. Muchísimas gracias Alba por estar siempre dispuesta a ayudarme, por tu carácter y por todos los momentos vividos juntos. ¡No cambies nunca Alba! Laura tu tranquil·la que quan jo vaig començar a fer síntesis estava com tu... i mira, alguna cosa em va sortir al final. Pol, ha sigut un plaer ser el teu assessor en la selecció i decoració del teu futur piset! Trobaré a faltar les nostres discussions de ciència interminables... Núria, me'n vaig tranquil sabent que tu seguiràs treballant amb els peri(beta-amino dosta)s. Cris, por estar siempre alegre, con este carácter da gusto trabajar contigo. I Patri, gràcies per compartir i fer que aquestes llargues tardes d'escriptura a la biblioteca siguessin més divertides.

I com em podia deixar d'agrair a tota aquella gent de Miercoles de Fiesta con Peri. Per vosaltres no tinc paraules, simplement que sou genials. Gràcies a vosaltres heu fet que aquesta ultima etapa d'escriptura sigues fins i tot divertida. Aquest grup no seria el mateix sense en German i en Tito, els quals sempre estan allà per donar-ho tot! Tito, sempre recordaré les nostres excursions en bici per Barcelona a altes hores de la nit. Teresaaa, ahora que nos has abandonado ya no es lo mismo. Te echamos mucho de menos. Gracias por todo, siempre tendrás un amigo en Barcelona. Mire, m'encanta el teu caràcter, ja que mai sap dir un no a unes cervesetes. Espero que això no canviï mai! I finalment, aquest grup no tindria sentit sense el Mario, que en els moments claus sempre esta allà! Moltes gràcies a tots!

Moltes gràcies al grup de Sagetis, amb vosaltres vaig aprendre moltes coses i crec que formeu un equip genial. Anna sempre recordaré la teva ajuda just quan vaig començar la tesis, moltes gràcies

per tot. Gracias Miguel Ángel por tus consejos buenísimos sobre síntesis, con tu ayuda todo ha sido mucho más fácil. Pau, que he de dir de tú... Admiro tant la teva vesant artística com científica! Trobaré molt a faltar aquells llargs cafés parlant de ciència! Sejin fue un placer todos los momentos pasados contigo, tanto dentro como fuera del laboratorio. I les noves incorporacions, Cris Castells i Cris Fornagera, crec que sou imprescindibles en aquest grup.

En segon lloc, m'agradaria agrair els grans moments passats en el grup d'Enginyeria de Teixits! Recordo un inici de tesis immillorable. Moltíssimes gràcies Mire, Lourdes i Alex pels grans moments viscuts! Per tots els viatgets visitant poblets, rutes i festetes... Gràcies Mire per ser com ets, sense tu aquest grup ja no es el que era! La única cosa que em consola es que potser ens tornem a trobar aviat en la meva següent aventura per Boston! Gràcies Lourdes per estar en tot moment disposada a ajudar-me. Y Alex, que tengo que decir... No puedo ni imaginar el montón de buenos momentos pasados juntos. Els quatre formàvem un gran equip! Trobo a faltar aquella època!

I evidentment no em puc deixar d'agrair els meus màsters preferits: Estela, Alex, Pau, Jorge, Jenny, Aitor, Anna, Su i Miquel. Ha sigut un enorme plaer passar tots aquets anys amb vosaltres. Des de que vàrem començar el màster no em parat de fer cosetes. Per lluny que estem sempre trobem una excusa per retrobar-nos. Crec que això ho diu tot de nosaltres. Gracies a aquest viatge que vaig començar amb vosaltres, he pogut arribar fins aquí.

I fora d'IQS, no puc deixar d'agrair a tota aquella gent que ha estat en tot moment al meu costat al llarg d'aquets anys. M'agradaria començar agraint a una de les persones que he compartit més moments, la Maria. Gràcies Maria per ser la millor companya de pis que he tingut. Han sigut uns 8 anys inoblidables. Crec que hem format un gran equip de pis! Sergi, tu també vas ser un dels millors companys de pis, però vàrem conviure menys temps. Però el que si que puc afirmar es que ets un gran amic. Gràcies per tot el que em viscut, des dels primers anys de residencia fins a la teva visita a Atlanta. Elena, sin duda fuiste uno de los mejores fichajes del piso. Gracias por tus historias realmente inmejorables. Robert, tu també has sigut molt bon companyeru de pisu. Gràcies Pablo per ser el que posa algú d'ordre al pis. Y como no... no me puedo dejar nuestro último fichaje, la Inmaculaaa! Immaculada, creo que nos llegamos a entender ya que hemos desarrollado nuestro propio idioma!

A la meva família, que ha estat al meu costat en tot moment. Els meus avis m'han donat els valors necessaris per tirar endavant, ajudant-me en tot moment i confiant amb tota la meva feina. Als meus pares, els quals que m'ho han donat tot. Mai us podré arribar a agrair l'esforç i sacrifici que heu arribat a fer perquè pogués arribar fins aquí. També es d'admirar la fe i confiança que heu dipositat amb mi, sense dubtar en cap moment de seguir apostant per mi. La meva germana Júlia, que la necessito sempre al meu costat. Admiro el seu caràcter emotiu i rialler, que m'ajuda a valorar les coses importants d'aquesta vida. Sento que som una gran família, per això us dedico aquesta tesis doctoral.

Pere Dosta Pons, 5 de Juliol de 2017

This page left blank intentionally

This thesis has been made thanks to the fellowship grant of personal novice investigator (FI) SUR funded by the DEC of the Government of Catalonia and the European Social Fund.

Credentials:

[2015 FI_B 00497]

[2016FI_B1 00211]

[2017FI_B2 00141]

This page left blank intentionally

Abstract

Development of cell-specific RNAi delivery vectors based on poly(ß-amino ester)s with therapeutic applications

RNAi technology has gained rapid promise for its potential therapeutic application for diseases caused by abnormal gene overexpression. Although RNAi delivery strategies have been widely studied and developed, concerns about their safety, cell-specificity and efficiency delivering prompts the development of alternative delivery methodologies capable of efficiently drive RNAi-based nucleic acids to the target cells in a safe manner. Recently, newly developed poly(β-amino ester)s (pBAEs) have emerged as an interesting choice for nucleic acid delivery due to their low toxicity, high biocompatibility, and simple chemical formulation. Here, we present an extended family of pBAEs that incorporate terminal oligopeptide moieties, containing both positive and negative amino acids, able to condense RNAi-based nucleic acids into discrete nanoparticles. Furthermore, we demonstrated that pBAE backbone hydrophobicity has a deep effect in the resulting polyplexes formulations. With this new approach, we have obtained delivery formulations with increased RNAi packaging capacity, stability, and transfection efficiency. In addition, *in vitro* and *in vivo* results have demonstrated that careful control of the pBAE oligopeptide composition is a powerful strategy to efficiently deliver nucleic acids in a cell-type dependent manner. These delivery vectors have specially shown great promise for difficult-to-transfect cells. For instance, pBAE formulations using a combination of arginine and aspartic acid oligopeptides were able to efficiently and simultaneously deliver anti-OCT3/4 siRNA, anti-NANOG siRNA, and RUNX2 plasmid to Dental Pulp Pluripotent Stem Cells in order to promote their osteogenic differentiation. At *in vivo* level, it has been found that a combination of lysine- and histidine- modified pBAEs was able to preferentially deliver siRNA to endothelial cells from the vasculature with low off-target effects.

Finally, polyplexes have been further optimized to selectively deliver RNAi-based nucleic acids via receptor-mediated endocytosis in order to selectively target diseased cells, while avoiding healthy cells populations from the same tissue. *In vivo* results demonstrated that the targeted delivery system proposed here was able to efficiently regulate gene expression in inflamed endothelial cells from atherosclerotic mice model, obtaining a promising therapeutic effect.

In conclusion, this thesis demonstrates that careful control of the composition of pBAE-nucleic acid formulations allows the fabrication of stable, specific and efficient delivery systems, resulting in promising delivery vectors that can be easily adapted for specific therapeutic applications.

This page left blank intentionally

Resumen

Development of cell-specific RNAi delivery vectors based on poly(ß-amino ester)s with therapeutic applications

Los ARNs de interferencia han demostrado tener un potencial terapéutico muy prometedor para el tratamiento de enfermedades debidas a la desregulación génica. Se han estudiado y desarrollado distintas técnicas de liberación de ARNs, sin embargo, las dudas sobre su seguridad, especificidad celular y eficiencia de transfección hacen necesario el desarrollo de metodologías de liberación alternativas, capaces de conducir de forma selectiva y segura los ARNs de interferencia hasta su diana. Recientemente, formulaciones poliméricas basadas en poly(β-amino ester)s (pBAEs) han surgido como una prometedora alternativa para la liberación de ácidos nucleicos, debido a su baja toxicidad, alta biocompatibilidad y simple formulación química. Concretamente, en este trabajo, se ha sintetizado una nueva familia de pBAEs que incorpora diferentes oligopéptidos catiónicos y aniónicos, capaces de condensar ARNs en partículas con tamaños nanométricos. Además, se ha demostrado que variando la hidrofobicidad de su estructura, se obtienen formulaciones poliméricas con distintas propiedades biofísicas. Considerando todos estos factores, se han diseñado sistemas de liberación de ARNs con una mayor capacidad de almacenamiento, estabilidad y eficacia de transfección. Además, se ha observado que controlado la composición oligopeptidica de los pBAEs es posible formular poliplejos con una elevada especificad celular, tanto a nivel *in vitro* como *in vivo.* Consecuentemente, estos nuevos sistemas de liberación muestran un elevado potencial para el tratamiento de líneas celulares difíciles o delicadas de transfectar. Por ejemplo, la combinación de pBAEs modificados con arginina y ácido aspártico forman poliplejos capaces de liberar eficientemente y simultáneamente anti-OCT3 / 4 siRNA, anti-NANOG siRNA y RUNX-2 plásmido sobre Dental Pulp Pluripotent Stem Cells, mejorando su diferenciación osteogénica. Por otra parte, a nivel *in vivo*, se ha observado que la combinación de pBAEs modificados con lisina e histidina forma poliplejos capaces de liberar preferencialmente ácidos nucleicos sobre células endoteliales de la vasculatura.

Finalmente, los poliplejos se han optimizado con el fin de liberar ARNs mediante endocitosis mediada por receptor sobre células enfermas, evitando efectos no deseados sobre las células sanas del mismo tejido. Mediante un ensayo *in vivo* utilizando un modelo de ateroesclerosis en ratón, se ha demostrado que el sistema de liberación diseñado es capaz de regular la expresión génica sobre células endoteliales inflamadas.

En conclusión, esta tesis demuestra que un cuidadoso diseño en la formulación de los poliplejos de ARN permite la fabricación de sistemas de liberación estables, específicos y eficientes, dando como resultado, vectores de liberación adaptables en función de la su aplicación terapéutica.

This page left blank intentionally

Resum

Development of cell-specific RNAi delivery vectors based on poly(ß-amino ester)s with therapeutic applications

Els ARNs de interferència han demostrat tenir un potencial terapèutic molt prometedor per tractar malalties causades per desregulació gènica. S'han estudiat i desenvolupat diferents tècniques d'alliberació d'ARNs, tot i així, els dubtes sobre la seva seguretat, especificitat cel·lular i eficiència de transfecció fan necessari el desenvolupament de metodologies d'alliberació alternatives, capaces de conduir de forma específica i segura els àcids nucleics fins a la seva diana terapèutica. Recentment, formulacions polimèriques basades en poly(β-amino ester)s (pBAEs) han sorgit com una opció per l'alliberació d'àcids nucleics degut a la seva baixa toxicitat, alta biocompatibilitat i formulació química simple. Concretament, en aquest treball, s'ha desenvolupat una nova família de pBAEs incorporant-los-hi en els seus extrems oligopèptids formats per aminoàcids catiònics i aniònics, capaços de condensar ARNs tot obtenint partícules amb mides manomètriques. A més, s'ha demostrat que variant la hidrofobicitat de la seva cadena central, s'obtenen formulacions polimèriques amb diferents propietats biofísiques. Tenint en compte les característiques prèviament descrites, s'han dissenyat sistemes d'alliberació d'ARNs amb una major capacitat d'emmagatzematge, estabilitat i eficàcia de transfecció. A més, s'ha observat que jugant amb la composició oligopeptidica dels pBAEs és possible controlar la seva especificitat cel·lular, tant a nivell *in vitro* com *in vivo.* Conseqüentment, aquets nous sistemes d'alliberació mostren un elevat potencial pel tractament de línies cel·lulars difícils o delicades de transfectar. Per exemple, la combinació de pBAEs modificats amb arginina i àcid aspàrtic formen poliplexes capaços d'alliberar eficientment anti-OCT3/4 siRNA, anti-NANOG siRNA i RUNX2 plasmid en Dental Pulp Pluripotent Stem Cells, millorant la seva diferenciació osteogènica. Per altra banda, a nivell *in vivo*, s'ha observat que la combinació de pBAEs modificats amb lisina i histidina forma poliplexes capaços d'alliberar preferencialment àcids nucleics sobre cèl·lules endotelials de la vasculatura.

Finalment, s'han optimitzat les nanopartícules amb la finalitat d'alliberar ARNs mitjançant endocitosis mediada per receptor sobre cèl·lules malaltes evitant efectes no desitjats sobre les cèl·lules sanes del mateix teixit. Mitjançant un assaig *in vivo* utilitzant un model d'ateroesclerosis en ratolí, s'ha demostrat que el sistema d'alliberament dissenyat és capaç de regular l'expressió gènica en cèl·lules endotelials inflamades.

En conclusió, aquesta tesi demostra que un disseny acurat en la formació dels poliplexes d' ARNs permet la fabricació de sistemes d'alliberació estables, específics i eficients, donant com a resultat, vectors d'alliberació fàcilment adaptables en funció de la seva aplicació terapèutica.

This page left blank intentionally

Table of Contents

This page left blank intentionally

Index of Figures

Figures from Chapter I

Figures from Chapter II

Figures from Chapter III

Figures from Chapter IV

Figures from Chapter V

Figures from Chapter VI

Index of Tables

Tables from Chapter I

Tables from Chapter II

Tables from Chapter III

Tables from Chapter IV

Tables from Chapter V

Tables from Chapter VI

List of Abbreviations

AcONa	Sodium acetate
cDNA	complementary Deoxyribonucleic Acid
COS-7	COS-7 cells (fibrolast-like cell line)
DAPI	4',6-diamidino-2-phenylindole
DCM	Dichloromethane
DLS	Dynamic Light Scattering
DMEM	Dulbecco's Modified Eagle Medium
DMSO	Dimethyl Sulfoxide
DNA	Deoxyribonucleic Acid
DPPSCs	Dental Pulp Pluripotent Stem Cells
DTT	Dithiothreitol
EDTA	Ethylenediaminetetraacetic Acid
FBS	Fetal Bovine Serum
FDA	Food and Drug Administration
FITC	Fluorescein IsoTioCyanate
FT-IR	Fourier Transform Infrared Spectroscopy
GAPDH	Glyceraldehyde 3-phosphate dehydrogenase
GFP	Green Fluorescent Protein
HCl	Chlorhydric Acid
HeLa-GFP	Human Cervical Carcinomal Cell Line Stably Expressing Green Fluorescent Protein
^{1}H-NMR	proton Nuclear Magnetic Resonance
HPLC	High-performance liquid chromatography
MDAMB231-GFP	Mammary Gland Cancer Cell Line Stably Expressing Green Fluorescent Protein
miRNA	micro Ribonucleic Acid
mRNA	messenger Ribonucleic Acid
MTS	3-(4,5-dimethylthiazol-2-yl)-5-(3-carboxymethoxyphenyl) -2-(4-sulfophenyl)-2H-tetrazolium
NANOG	Nanog homeobox
NaOH	Sodium Hydroxide
NHI	National Institutes of Health
NP	Nanoparticle
OCTA ¾	octamer-binding transcription factor 4
PAMAM	Poly(amidoamine)
pBAEs	Poly(β-aminoester)s
PBS	Phosphate Buffered Saline
PCL	Partial Carotid Ligation Technique
pDMAEMA	poly (dimethylaminoethyl methacrylate)
PEI	polyethylenimine
PEG	Polyethylene glycol
pHPMA	Poly[N-(2-hydroxypropyl)methacrylamide]
pGFP	Green Fluorescent Protein plasmid
PLL	poly(L-lysine)
PFA	Paraformaldehyde
RCA	Right Carotid
RISC	RNA-induced silencing complex

RNA	Ribonucleic Acid
RNAi	interference Ribonucleic Acid
RT-PCR	Real Time - Polymerase Chain Reaction
RUNX2	Runt-related transcription factor 2
LCA	Left Carotid
TIMP3	Metalloproteinase inhibitor 3
scrRNA	Scrambled Ribonucleic Acid
shRNA	Short-Hairpin RNA
siGFP	Silencer Green Fluorescent Protein
siICAM2	Silencer Intercellular adhesion molecule 2
siRNA	Small Interference Ribonucleic Acid
THF	Tetrahydrofuran
UV	Ultraviole

Chapter I

Introduction: RNAi delivery vectors

This page left blank intentionally

Introduction: RNAi delivery vectors

This chapter discusses the current status of RNAi therapy in clinical applications, highlighting therapeutic methodologies and their delivery approaches. Nowadays, RNAi is changing the way we treat diseases, however its efficacy in *in vivo* applications is limited due to the lack of delivery systems. In this thesis, special interest was focused on the development of delivery strategies based on polymeric vectors to overcome current delivery limitations.

1.1 Introduction

The term of “gene therapy” become a revolutionary way for the treatment of a wide range of genetic and acquired diseases. Mainly, gene therapy is a technique that uses nucleic acids to treat or prevent diseases instead of traditional approaches, including, drugs or different surgery procedures [1,2]. Therefore, instead of focusing on treating the symptoms of the disease, gene therapy is able to treat the genetic roots of the disease. In the future, this technique may allow doctors to treat a disorder by inserting genes into a patient’s, correcting the errors from the endogenic gene.

All of these concepts arose initially in early 1960’s when it was demonstrated that foreign nucleic acids could be introduced permanently, stably, functionally and heritably into mammalian cells [3]. With the arrival of recombinant DNA techniques, cloned genes were used to demonstrate that foreign genes could be used to correct genetic defects or mutations in mammalian cells [4]. After that, in late 1970’s, transfection techniques were combined with selection systems for cultured cells and recombinant DNA technology [4]. And in early 1980’s, retroviral vectors that are able to transfer genes into mammalian cells were developed. All these experiments proved the feasibility of transferring small genetic material into the genome, providing a potential therapeutic approached to treat genetic diseases. Therefore, during these years, gene therapy experienced an exponential growth. However, it is important to remember that in 1999 the worst case scenario for gene therapy became a reality, where the tragic death of Jesse Gelsinger occurred during a clinical assay [5]. After that, it was not until 2003 when China become the first country to approve the first gene therapy product for clinical use, Gendicine™ [6,7].

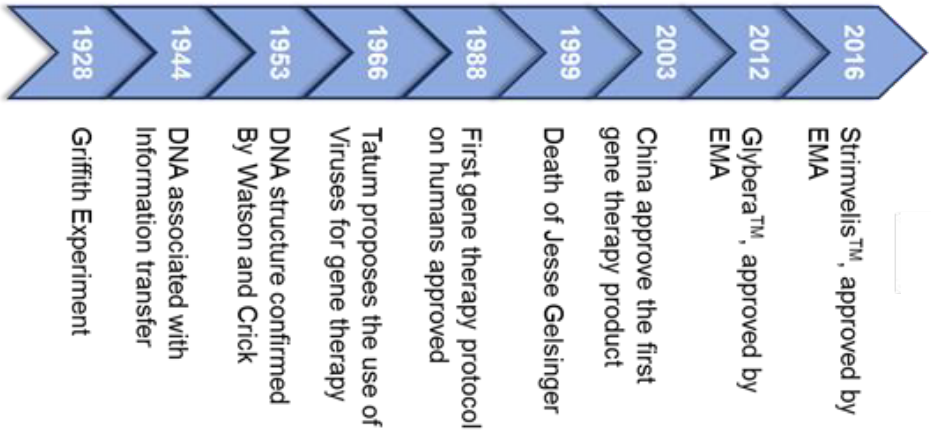

Figure I-1 Timeline highlighting important milestones of gene therapy from 1928 to the present (source: The Journal of Gene Medicine).

Nowadays, more than 2400 clinical trials are currently underway worldwide, with miles of patients enrolled, showing remarkable therapeutic benefits, where different genetic strategies have been used (source: www.wiley.co.uk/genmed/clinical). Generally, gene therapy has been classified depending on the methodology applied to treat the disease [8–10].

- Gene supplementation or correction: supplementation of damaged gen with functional copies of functional genes.
- Gene augmentation: to introduce a novel gene into the cell, in order to produce a novel function that is not exist in this cell or increase their expression.
- Gene silencing: this approach consists in the delivery of interfering RNA (RNAi) to induce post-transcriptional gene silencing by specific degradation of messenger RNA (mRNA).

Over the past decade, RNAi-based therapeutics have witnessed an explosion of interest due to their ability to efficiently control genome expression. For instance, RNAi is able to silence the post-transcriptional expression of specific target genes in order to prevent protein transcription [11], showing great potential in biomedical therapeutic applications for diseases caused by abnormal gene overexpression. In addition, usually RNAi-based nucleic acids act in the cell cytoplasm, avoiding intracellular barriers than other therapeutic genes have to reach, such as plasmidic DNA, making them more efficient [12].

Commonly, different types of endogenous/exogenous RNAs have been used to control gene expression, such as microRNA (miRNA), short interfering RNAs (siRNAs), short hairpin RNAs (shRNAs), and Dicer substrate RNAs (dsiRNAs). Each of these systems acts through different mechanisms, differing in their possible therapeutic potential and pharmacological complexity[13].

Although shRNA or dsiRNAi have been described, they are rarely used in current clinical trials due to their complexity[14,15].

Thus, currently, siRNA and miRNA are the most broadly used in therapeutic applications due to simplicity of manufacturing and well-described mechanism of action. They are characterized by the double-stranded of RNA formed by 20-25 pair bases of amino acid and they are generally distributed in both phylogenetic and physiological terms. The major difference between them is the way to downregulate the expression of specific target mRNAs. Where, siRNA binds completely to the target mRNA and the miRNA binds to the target mRNAs through partial complementary base pairing. Consequently, miRNA can have multiple mRNA targets, allowing the treatment of complex multigene diseases, such as cancers and neurodegenerative disorders, which require modulation of multiple pathways for effective treatment [16]. In contrast, siRNA only acts just in one target mRNA. Apart from this difference, they present similar silencing mechanism, as is explained in Figure I-2.

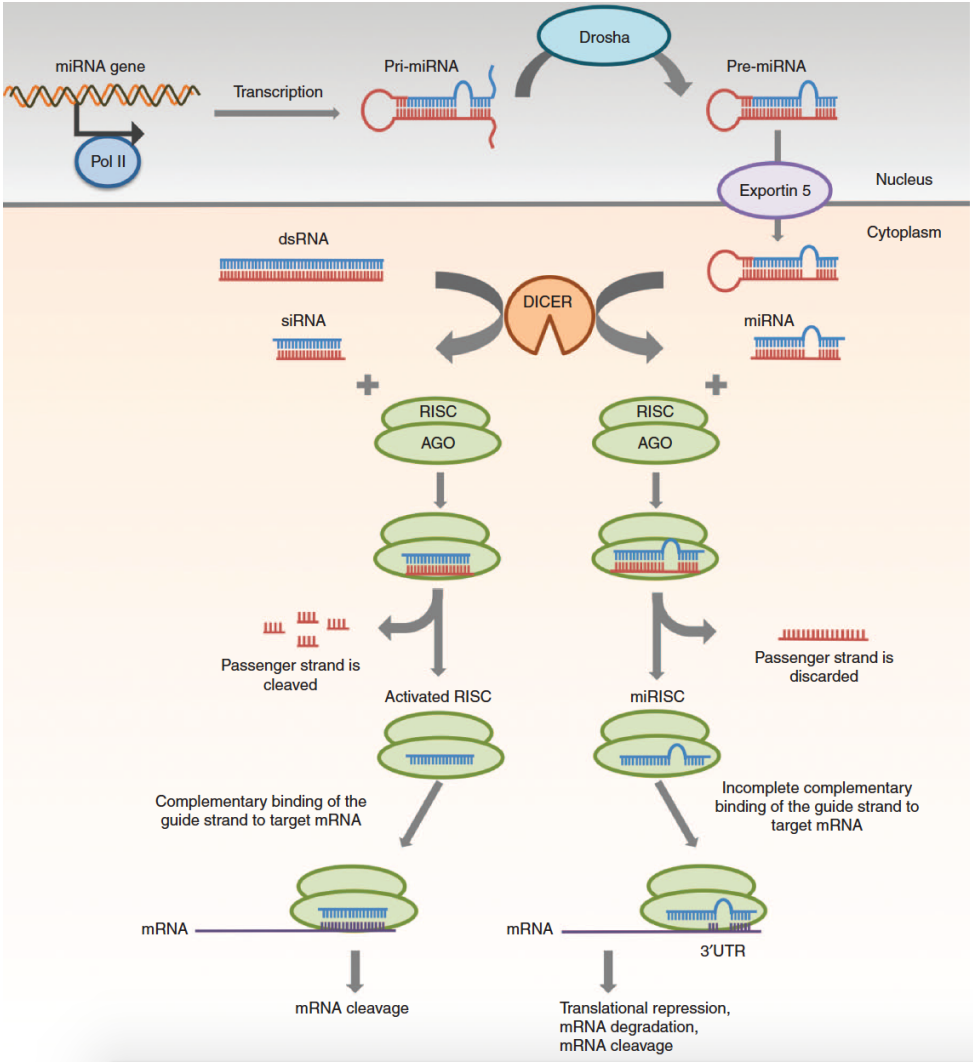

Figure I-2 Interference RNA pathways. **dsRNA** (either transcribed or artificially introduced) is processed by a specialized ribonuclease (RNase) III-like enzyme named Dicer in the cytoplasm into a smaller dsRNA molecule, known as the siRNA. The siRNA interacts with and is loaded with RNA-induced silencing complex (RISC). The endonuclease argonaute 2 (AGO2)

component of the RISC cleaves the passenger strand of the siRNA. In contrast the antisense strand remains associated with the RISC, which guide the RISC to its target mRNA. After that, siRNA completely binds to the target mRNA, which is cleaved by AGO2 protein (left side of the figure). **miRNA:** Transcription of miRNA gene is carried out by RNA polymerase II in the nucleus to give primary miRNA (pri-miRNA), which is double-stranded stem-loop structure. Then, pri-miRNA is cleaved by Drosha to form pre-miRNA. The pre-miRNA is transported by Exportin 5 to the cytoplasm where it is processed by Dicer into miRNA duplex of 18–25 nucleotides. The miRNA is loaded into the RISC where the passenger strand is discarded. In contrast the antisense strand remains associated with the RISC, which guide the RISC to its target mRNA through partially complementary binding. Finally, the target mRNA is inhibited via translational repression, degradation or cleavage (right side of the figure) [17].

Taking in account all these proprieties, the discovery of RNAi motivated new efforts for clinical therapeutic use. Since RNA was identified by Craig Mello and Andrew [18], many RNAi therapeutic approaches have revealed great potential. The first clinical trial of siRNA therapeutics was initiated in 2004 and microRNA therapeutics was initialed in 2013 [19]. To date, a wide range of RNAi-based dugs have been identified, reaching various stages of clinical trials [17,20]. Most of them are focus to cancer [21–23], infectious diseases [24,25], genetic disorders [26,27], cardiovascular diseases [28], ocular/retinal disorders [29–31], and antiviral disease [20,32], as shown Figure I-3.

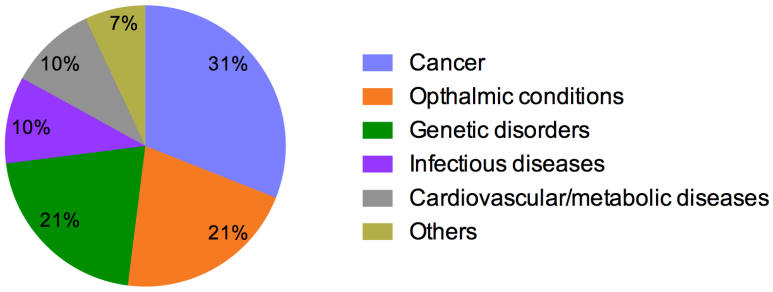

Figure I-3. Clinical trials distribution using siRNA and miRNA as a therapeutic RNAi. (source: clinicaltrials.gov).

However, the number of RNAi studies that reach advanced clinical trials is far from the values expected, where only 10 RNAi-based dugs are in phase II/III (Table I-1). The reason for that is the lack of efficient delivery systems for RNAi. It has been described that RNAi present low stability and it is rapidly identified by immune system and degraded by nucleases, limiting their therapeutic applicability [43].

Table I-1 Current advanced clinical trials. RNAi-based drugs in Phase II and Phase III [17]

Drug	Chemistry / formulation	Route	Disease	Phase	Refs
PF-04523655 (PF-655)	Naked siRNA, O-methylated	IVT	AMD, DME	II	[30,31]
QPI-1002* (I5NP)	Naked siRNA, O-methylated	IV	AKI DGF	II	*Source: Quark Pharmaceuticals, Inc. USA.*
QPI-1007	Naked siRNA, O-methylated	*IVT*	*NAION* Glaucoma	*III*	*Source: Quark Pharmaceuticals, Inc. USA.*
TKM-080301 (TKM-PLKI)	*siRNA/SNALP*	*IV*	*Solid tumors, HCC, NET, ACC lymphoma*	*II/III*	[33]
Atu027	*siRNA/LIPOPLEX*	*IV*	*Pancreatic cancer*	*I/II*	[34]
SYL040012	*Naked siRNA*	*Eye drops*	*Ocular hyertension, glaucome*	*II*	[35,36]
SYL1001	*Naked siRNA*	*Eye drops*	*Ocular pain Dry Eye Syndrome*	*II*	[37]
Patisiran (ALN-TTR02)	*siRNA/lipid particle, ApoE*	*IV*	*TTR-mediated Amyloidosis*	*III*	[26,38]
siGI2D-LODER	*siRNA/miniature PLGA device*	*Intratumoral*	*Pancreatic cáncer*	*II*	[39]
Miravisen	*AntimiR, antisense oligodeoxynucleotide LNA, PS*	*SC*	*Hepatitis C infection*	*II*	[40–42]

Recently, improvements in RNAi synthesis have been used to stabilize siRNA or miRNA, making them more resistant to external degradation and less prone to immune recognition. For instance, it has been reported that a simple chemical modification in the 2´-position of the ribose and substitution of phosphorothioate linkages protect siRNAs from nuclease digestion and prolongs their half-life [44]. Moreover, 2´-modifications can also be used to prevent recognition by innate immune receptors and overcome off-target effects. Regardless of the improvements in RNAi stability, RNAi efficiency has been increased by playing with RNAi structure modifications, such as LNA and unlocked nucleic acid [45]. These modifications introduce chemical asymmetry into duplex siRNA by blocking the passenger strand entry and promote RISC loading of the guide strand [46]. Taking into account these modifications, among others that have not been described, current modified RNAi molecules are more stable in physiological medium, however usually not enough to be therapeutically useful.

Despite RNAi stability, RNAi delivery presents other drawbacks that need to be addressed. For instance, RNAi molecules are too large and negatively charged to cross the lipid bilayer and enter to the cells. Only some chemically modified small single strand RNAi, such as anti-miRNA, has been reported to be able to cross cellular membranes[47]. However, once small single-strand RNAi are in the cell cytosol, they remain trapped inside of the endosome[48], limiting their therapeutic efficiency. Besides, modified RNAi is not able to be delivered in a tissue-specific-manner, giving high number of off-target effects over other cells lines o tissues [49].

To overcome these limitations, a delivery strategy to promote efficient and safe RNAi delivery to the right target cells is required. Therefore, an accurate evaluation of a series of parameters, such as the type of therapeutic nucleic acids (large DNA or small RNAi), target cells, and administration route, is needed for each therapeutic application (Figure I-4).

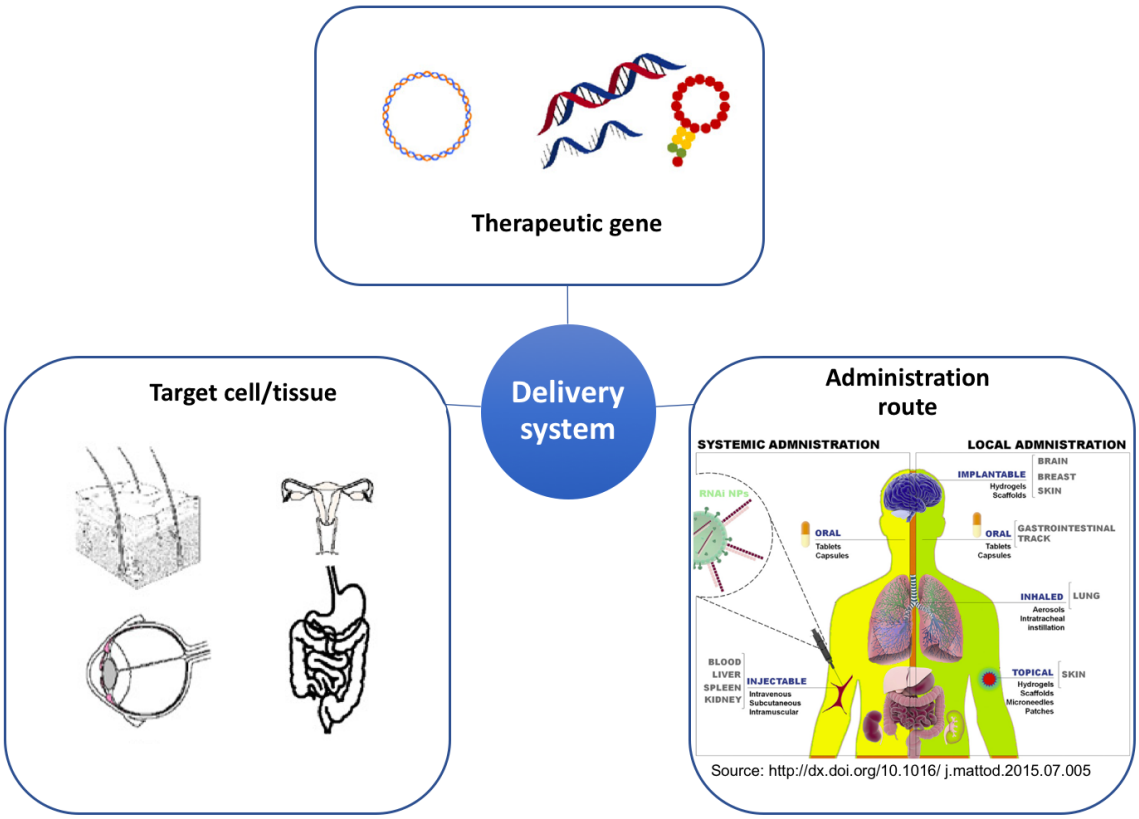

Figure I-4. Mainly requirements to design a RNAi delivery system. **Therapeutic gene:** A large type of nucleic acids with potential therapeutic function are now available. This includes plasmidic DNA, oligonucleotids, and a broad series of small non-coding nucleic acids. **Target cell/tissue:** Delivery vector have to be designed to exclusively target specific cells or tissues, avoiding other cells lines. **Administration route**: Describes the way to reach the final tissue, which is going to play a key role for delivery vector design.

The administration route is one of the most important parameter, because it limits the final approach. Currently, two different delivery strategies have been described, local and systemic delivery. Local delivery may overcome some of the limitations associated with systemic administration, and may allow the use of simple formulations and lower doses, resulting in higher bioavailability due to the simple accessibility to the target tissue. Usually, local delivery has been explored for the treatment of solid tumors, skin disease, and eye disease [50,51]. For instance, a combination of polyplexes with hydrogel matrixes or scaffolds have demonstrated a positive effect against cancer [52–54]. Then, scaffolds have been used to protect and control RNAi-based nucleic acids release, obtaining a therapeutic effect at the specific target.

However, for a wide range of diseases such as, cardiovascular, infectious or some cancers, RNAi molecules have to be delivered systemically in a tissue-specific manner. For this purpose, a long circulating delivery system is generally the most effective mechanism. Usually RNAi-based nucleic acids are delivered via intravenous, intraperitoneal, or oral administration. Nevertheless, as previously discussed, systemic delivery presents several limitations. Once delivery vectors are injected into the bloodstream, they have to avoid protein interactions and protect their therapeutic cargo from enzymatic degradation and immune system. In addition, delivery vectors should overcome different biophysical barriers, avoid non-target tissue clearance and phagocyte recognition [55].

Nevertheless, systemic delivery is taking advantage over local deliver during the last years. For example, before 2008, only 1 out of 8 new RNAi clinical candidates was systemically administered, while in 2012 at least half of newly developed RNAi-drugs were systemically administered [49,56], and currently 70% of advanced clinical trials were systemically administrated. These data suggest that important improvements in delivery strategies for systemic delivery have been developed, approaching them to ideal delivery strategy.

Typically, there are two different types of vectors: viral and non-viral. Initially, viruses were widely used to develop efficient vectors for the delivery of therapeutic genes [57–69]. Viruses present high rate of transfection due to thousands of years of evolution. However, they present several issues, such as limited packaging capacity, high large-scale production costs, poor target-selectivity, and safety risks [70,71]. Despite its commonly described limitations, viral vectors are rarely used in RNAi therapy, because periodic RNAi administrations are needed in in order to efficiently treat a disease. It has been descried that several administrations of viral vectors can cause immunological response, limiting their applicability.

Alternatively, non-viral vectors have attracted increasing attention in the past two decades because they offer many advantages over viral systems. Some of these advantages are their simple large-scale production, stability and low immunogenicity after periodic administrations [72,73]. Therefore, non-viral vectors have been increasingly explored as safe and effective alternatives that are easier to prepare and can deliver large payloads of nucleic acids, which it is the key to design an effective RNAi delivery strategy. Nowadays, non-viral vectors for RNAi delivery can be classified in three groups: lipid-based delivery systems, polymeric-based delivery systems, and conjugated-based delivery systems, as shown Figure I-5 [73,74].

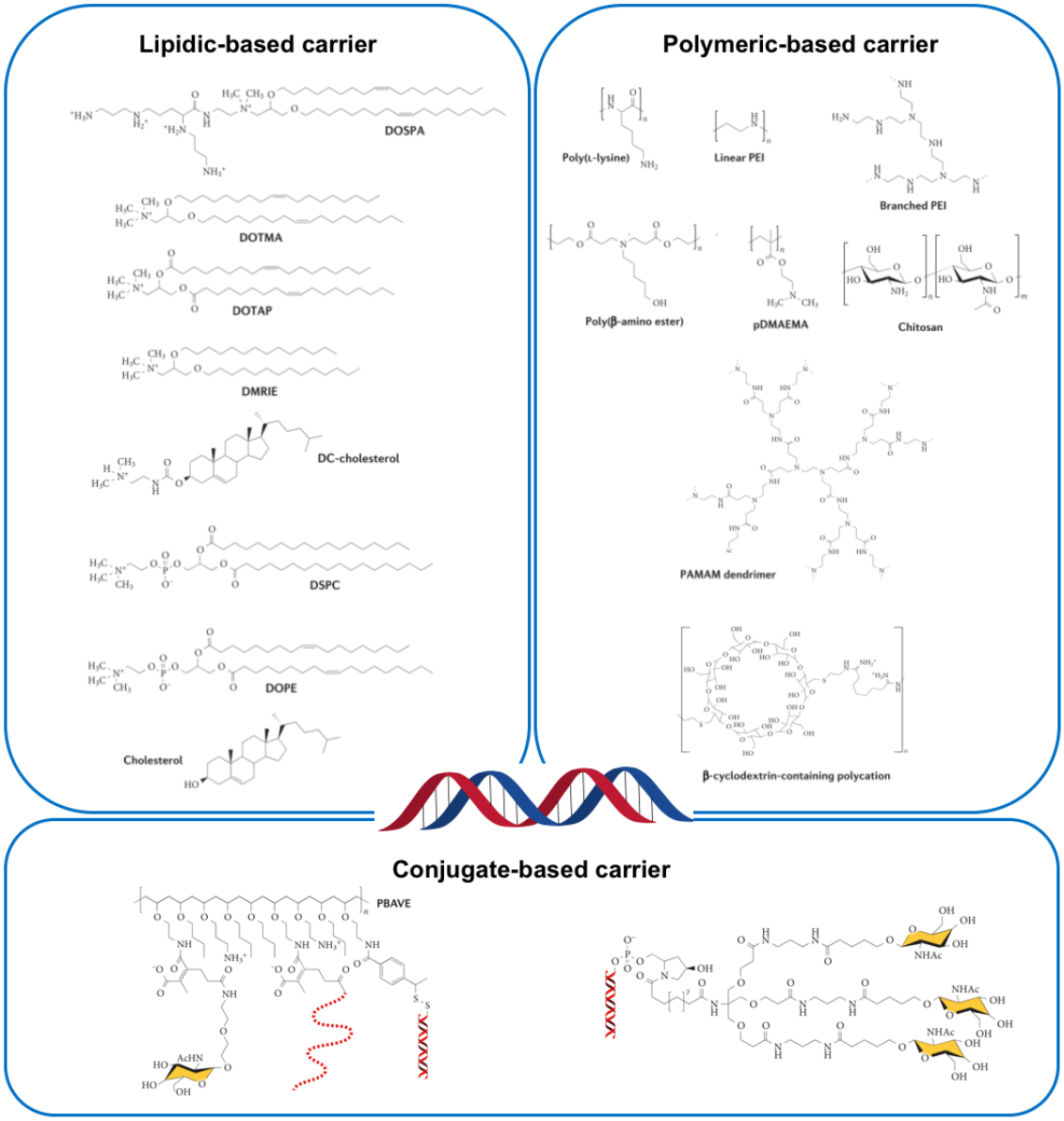

Figure I-5 Chemical structure of non-viral vectors currently used. **Lipids-based carriers** (Liposomal formulation typically used a mixture of cationic lipid and neutral lipid in their formulation)**:** 1,2-dioleoyl-3-trimethylammonium propane (DOTAP), N-[1-(2,3-dioleyloxy)propyl]-N,N,N- trimethylammonium chloride (DOTMA), 2,3-dioleoyloxy- N-[2-(sperminecarboxamido)ethyl]-N,N-dimethyl-1- propanaminium (DOSPA), dioctadecyl amido glycil spermine (DOGS), 3,[N-(N1,N-dimethylethylenediamine)-carbamoyl]cholesterol (DC-chol), 1,2-Distearoyl-sn-glycero-3-phosphocholine (DSPC), 1,2-Dioleoyl-sn-glycero-3-phosphoethanolamine (DOPE), and Cholesterol. **Polymeric-based carriers**: Poly(l‑lysine), polyethylenimine (PEI), poly[(2-dimethylamino) ethyl methacrylate] (pDMAEMA), carbohydrate-based polymers such as chitosan and β-cyclodextrin-containing polycations, polyamidoamine (PAMAM) dendrimers, and degradable poly(β-amino ester)s polymers. **Conjugate-based carriers:** Dynamic PolyConjugate (DPC) and triantennary N-acetylgalactosamine (GalNAc) [74].

Lipid-based vectors are among the most widely used non-viral nucleic acid carriers for *in vivo* applications [75–80]. Lipid nanoparticles are formed spontaneously by electrostatic and hydrophobic interactions between hydrophobized polycations and nucleic acids. Typically, cationic lipids, such as DOTMA, are characterized structurally by three components: the polar head-group, a hydrophobic chain, and a linker between these two regions [81]. Tailoring polar and hydrophobic domains of

cationic lipids large libraries of lipids can obtain, such as DOSPA, DOTAP, DMRIE, and DC-Cholesterol. In addition, neutral lipids, such as DOPE or Cholesterol, have been included in liposomal formulations as 'helper lipids' in order to enhance transfection efficiency and stability [82]. Currently, lipid-based vectors are being used in different clinical trials, such as stable nucleic-acid particle (SNAP). For instance, Silence Therapeutics has developed a SNAP-based formulation, which consist of a cationic lipid, a helper lipid, and PEG-lipid targeting the protein kinase N3 in patients with advanced solid cancer [83]. However, some concerns about their safety have arisen after toxicity of certain lipid formulation has been reported [84–86].

Cationic polymers are an attractive alternative to lipid-base formulations. Polyplexes are formed by electrostatic interactions between the positive charge groups of polycations and nucleic acids. Poly(l‑lysine) (PLL) [87] and polyethylenimine (PEI) [88] are the first polymers and the most commonly used as gene delivery vectors. Chemical structure of PEI polymer provides high transfection efficiency, high nucleic acid condensation, and high endosomal escape. However, it is reported that PEI induces high cytotoxicity. Further studies demonstrated that PEI cytotoxicity strongly depends on its structural proprieties, specially of their molecular weight [89] and their linear versus the branched forms [90]. Nevertheless, in order to improve safety and efficacy, other polymers have been studied, such as poly(amidoamine) dendrimer (PAMAM) [91], chitosan [92,93], poly(β-amino ester) (PAE) [94–96], among others. For example, cyclodextrin polymer-based nanoparticle was the first used targeted nanoparticle for siRNA delivery in clinical assays for cancer treatment [21].

Taking advantage of lipidic and polymeric vectors, combinations of both have been reported in order to create systems that combine the best of each delivery vectors. For instance, the combination of hydrophobic hexadecylated PEI with different lipids is able to maintain gene silencing for longer periods of times in *in vitro* assays [97]. Furthermore, mixtures of lipidic and polymeric formulations, also known as lipidoids, exhibit promising results of RNAi delivery *in vitro* and *in vivo* assays [98,99].

On the other hand, conjugate-based RNAi delivery system is the newest approach in RNAi delivery field. Several promising formulations have been designed though covalent attachment of delivery ligands to RNAi-based drugs, such as carbohydrates, peptides, and polyamines [100]. Currently, the most clinically advanced formulations are Dynamic PolyConjugates (DPCs) and triantennary N-acetylgalactosamine (GalNAc), which commonly are used to target hepatocytes [101]. However, in order to target others organs than liver using conjugate-based delivery systems is still challenging.

Among of promising RNAi delivery systems have been developed during the last years, showing promising *in vitro* and *in vivo* efficiencies. Currently, lipid-base formulations are the most used in clinical trials, however cytotoxic effects have been reported after several administrations. Furthermore, a recent study has demonstrated that around 70 % of RNAi taken up by cells is not able to escape from the endosome, limiting their therapeutic utility [102]. In order to overcome these drawbacks, polymer-based nanoparticles are being developed, showing less cytotoxic effects and better endosomal scape.

Within the polymer-based vectors, poly (β-amino ester)s (pBAEs) are an interesting choice due to their low toxicity and high biocompatibility [94–96,103]. pBAEs were discovered by David M. Lynn at 2000 as a safe alternative to previously existing polymeric vectors [94]. These polymers possess highly sought characteristics, such as simple synthesis and easily chemically modifications, as shown Figure I-6.

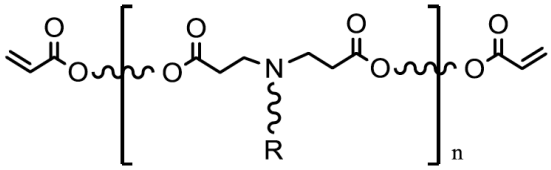

Figure I-6. Poly (β-amino ester)s (pBAEs) chemical structure.

PBAEs backbone is characterized by repeating ester groups that are biodegradable through hydrolysis and esterases in the cell cytoplasm. Therefore, pBAEs cytotoxicity is low due to the accumulation in cell cytoplasm is reduced and the resulting products derived from hydrolysis are not toxic. Moreover, the presence of protonable amines in their structure allows improved endosomal escape of complexes due to the proton sponge effect [104].

Taking these proprieties into account, different types of poly(β-amino ester)s have been formulated and used successfully in a number of therapeutic applications including vaccination [105], gene therapy for cancer and ophthalmology [106–108], gene silencing [109,110] and stem cell modification [111,112]. However, current pBAEs present some drawbacks that have to be further improved when they are used for systemic delivery, such as stability or tissue targeting.

Previously in our group, a new family of pBAE has been synthetized in order to overcome such limitations. Particularly, end-capping groups were modified using different positive amino acid moieties, such as arginine, lysine, and histidine. Results demonstrated that oligopeptide-modified pBAE achieve better cellular viability and higher transfection efficacy than previously chemically end-modified pBAE, however their stability under physiological is still challenging [96].

Then, the main objective of this thesis **is the development of efficient strategy to specifically drive therapeutic nucleic acids to desired tissue or target cells, avoiding current off-target effects.** Polymers based on pBAEs have been used due their high biodegradability and low toxicity compared to current non-viral vectors. Taking into account their easy synthesis and manipulation, the effect of structural modifications has been explored to design a specific formulation depending on the needs of their final target.

In order to achieved the main objective, the following goals were proposed:

- To develop and characterize a library of poly(β-amino ester)s with different oligopeptide terminations in order design safe, efficient, and cell-specific polyplexes. **(Chapter II).**
- To evaluate the ability of new cell-specific polymers to efficiently deliver RNAi into difficult-to-transfect cell types, such as Dental Pulp Pluripotent Stem Cells (DPPSCs) **(Chapter III).**
- Increase the RNAi polyplexes stability and nucleic acids packaging capacity considering their *in vivo* applications **(Chapter IV).**
- To evaluate the ability of new stable and cell-specific polymers to preferentially deliver siRNA to endothelial cells **(Chapter V).**
- To develop a targeted nanoparticle formulation to deliver therapeutic RNAi (anti-miR712) to diseased cells, avoiding healthy cells from the same tissue **(Chapter VI).**

1.2 Content of this Dissertation

Poly(β-amino ester) polymers are promising candidates for RNAi delivery since they possess a high degree of biocompatibility, low toxicity, and high transfection efficiency. In addition, pBAE structure allows simple modifications, paving the way to the design-tailored polymer formulations in function of their final therapeutic application, making them effective delivery vectors for future clinical development. Thus, different pBAE chemical modifications are presented in this work to overcome common delivery vectors limitations, such as cell-targeting and stability in physiological media.

First, modification of pBAE termini groups are explored using different cationic and anionic oligopeptide moieties to efficiently condense RNAi into discrete nanoparticle with tuneable surface charge, in order to design a cell-specific polymer formulation **(Chapter II).** This study investigates the relationship between oligopeptide moiety formulation and cell-specificity.

Chapter III goes a step further exploring the use of our previously developed and characterized delivery system in osteogenesis. Through a collaboration with Dr. Maher Atari Laboratory from Universitat Internacional de Catalunya (UIC) in Barcelona, our end target was to improve the differentiation of Dental Pulp Pluripotent Stem Cells (DPPSC)s towards an osteoblast cell line to develop bone regenerative therapies, by silencing OCTA ¾ and NANOG pluripotency genes and overexpressing key osteogenic genes.

Although the design of cell/tissue specific polyplexes is a key factor to avoid off-targets effects, the stability of the pBAEs in physiological media also have a direct influence on its therapeutic efficiency. **Chapter IV** seeks to explore how to develop a stable, efficient, and tissue specific family of poly(β-amino ester)s playing with their hydrophobicity. As a result, we developed a wide range polymers combining different oligopeptides formulations with different pBAE backbone structures, which their composition differs from traditional cationic polymers for their enough stability and functionality, making them closer for in vivo applications.

Chapter V is focused in the optimization and evaluation of these newly developed stable and cell-specific pBAEs to preferentially deliver siRNA to endothelial cells from mice vasculature. This work was mainly performed at Coulter Department of Biomedical Engineering at Georgia Institute of Technology and Emory University in Atlanta (USA) in collaboration with Dr. Hanjoong Jo laboratory.

The last part of this thesis is centered to specifically deliver RNAi-based nucleic acids to diseased cells from tissue. Some disease only occurred in certain cell populations, such as atherosclerosis, limiting the use of our previously designed cell-specifics polyplexes. Currently, targeting delivery represents a promising approach to overcome this limitation. Then, in **Chapter VI** targeted polyplexes based on previous designed pBAEs were formulated. In collaboration with Dr. Hanjoong Jo laboratory, our designed targeted polyplexes were used to deliver a therapeutic RNAi (anti-miR712) to inflamed endothelial cells from the vasculature in order to treat atherosclerosis disease.

1.3 References

[1] I.M. Verma, N. Somia, Gene therapy - promises, problems and prospects, Nature. 389 (1997) 239–242. doi:10.1038/38410.

[2] N. Somia, I.M. Verma, Gene therapy: trials and tribulations., Nat. Rev. Genet. 1 (2000) 91–99. doi:10.1038/35038533.

[3] W.S. Hunter, Elizabeth, Szybalski, GENETICS OF HUMAN CELL LINES, IV. DNA-MEDIATED HERITABLE TRANSFORMATION OF A BIOCHEMICAL TRAIT, 1962.

[4] T. Friedmann, A brief history of gene therapy, Nature. 2 (1992) 93–98. doi:10.1038/ng1092-93.

[5] T. Wirth, N. Parker, S. Ylä-Herttuala, S. Yl-Herttuala, History of gene therapy, Gene. 525 (2013) 162–169. doi:10.1016/j.gene.2013.03.137.

[6] Z. Peng, Current Status of Gendicine in China: Recombinant Human Ad-p53 Agent for Treatment of Cancers, Hum. Gene Ther. 16 (2005) 1016–1027. doi:10.1089/hum.2005.16.1016.

[7] J.M. Wilson, Gendicine: the first commercial gene therapy product., Hum. Gene Ther. 16 (2005) 1014–5. doi:10.1089/hum.2005.16.1014.

[8] J.A. Broderick, P.D. Zamore, MicroRNA therapeutics, Gene Ther. 18 (2011) 1104–1110. doi:10.1038/gt.2011.50.

[9] N.J. Caplen, Gene therapy progress and prospects. Downregulating gene expression: the impact of RNA interference., Gene Ther. 11 (2004) 1241–1248. doi:10.1038/sj.gt.3302324.

[10] P. Shankar, N. Manjunath, J. Lieberman, The Prospect of Silencing Disease Using RNA Interference, 293 (2005) 1367–1373.

[11] G.J. Hannon, RNA interference, Nature. 418 (2002) 24–26.

[12] S.F. Dowdy, Overcoming cellular barriers for RNA therapeutics, Nat. Biotechnol. 35 (2017) 222–229. doi:10.1038/nbt.3802.

[13] G.R. Rettig, M.A. Behlke, Progress Toward In Vivo Use of siRNAs-II, Mol. Ther. 20 (2012) 483–512. doi:10.1038/mt.2011.263.

[14] D.D. Rao, J.S. Vorhies, N. Senzer, J. Nemunaitis, siRNA vs. shRNA: Similarities and differences, Adv. Drug Deliv. Rev. 61 (2009) 746–759. doi:10.1016/j.addr.2009.04.004.

[15] J. Chery, RNA therapeutics: RNAi and antisense mechanisms and clinical applications, HHS Public Access. 4 (2016) 35–50.

[16] Y. Tomari, P.D. Zamore, Perspective: machines for RNAi., Genes Dev. 19 (2005) 517–29. doi:10.1101/gad.1284105.

[17] J.K.W. Lam, M.Y.T. Chow, Y. Zhang, S.W.S. Leung, siRNA Versus miRNA as Therapeutics for Gene Silencing, Mol. Ther. - Nucleic Acids. 4 (2015) e252. doi:10.1038/mtna.2015.23.

[18] a Fire, S. Xu, M.K. Montgomery, S. a Kostas, S.E. Driver, C.C. Mello, Potent and specific genetic interference by double-stranded RNA in Caenorhabditis elegans., Nature. 391 (1998) 806–11. doi:10.1038/35888.

[19] G. Ozcan, B. Ozpolat, R.L. Coleman, A.K. Sood, G. Lopez-Berestein, Preclinical and clinical development of siRNA-based therapeutics, Adv. Drug Deliv. Rev. 87 (2015) 108–119. doi:10.1016/j.addr.2015.01.007.

[20] R. Titze-de-Almeida, C. David, S.S. Titze-de-Almeida, The Race of 10 Synthetic RNAi-Based Drugs to the Pharmaceutical Market, Pharm. Res. 34 (2017) 1339–1363. doi:10.1007/s11095-017-2134-2.

[21] M.E. Davis, The First Targeted Delivery of siRNA in Humans via a Self-Assembling, Cyclodextrin Polymer-Based Nanoparticle: From Concept to Clinic, Mol. Pharm. 6 (2009) 659–668. doi:10.1021/mp900015y.

[22] M.E. Davis, J.E. Zuckerman, C.H.J. Choi, D. Seligson, NIH Public Access, 464 (2010) 1067–1070. doi:10.1038/nature08956.Evidence.

[23] J.E. Zuckerman, T. Hsueh, R.C. Koya, M.E. Davis, A. Ribas, siRNA knockdown of ribonucleotide reductase inhibits melanoma cell line proliferation alone or synergistically with temozolomide., J. Invest. Dermatol. 131 (2011) 453–60. doi:10.1038/jid.2010.310.

[24] M.R. Zamora, M. Budev, M. Rolfe, J. Gottlieb, A. Humar, J. DeVincenzo, A. Vaishnaw, J. Cehelsky, G. Albert, S. Nochur, J.A. Gollob, A.R. Glanville, RNA Interference Therapy in Lung Transplant Patients Infected with Respiratory Syncytial Virus, Am. J. Respir. Crit. Care Med. 183 (2011) 531–538. doi:10.1164/rccm.201003-0422OC.

[25] J. DEVINCENZO, J. CEHELSKY, R. ALVAREZ, S. ELBASHIR, J. HARBORTH, I. TOUDJARSKA, L. NECHEV, V. MURUGAIAH, A. VLIET, A. VAISHNAW, Evaluation of the safety, tolerability and pharmacokinetics of ALN-RSV01, a novel RNAi antiviral therapeutic directed against respiratory syncytial virus (RSV), Antiviral Res. 77 (2008) 225–231. doi:10.1016/j.antiviral.2007.11.009.

[26] T. Coelho, D. Adams, A. Silva, P. Lozeron, P.N. Hawkins, T. Mant, J. Perez, J. Chiesa, S. Warrington, E. Tranter, M. Munisamy, R. Falzone, J. Harrop, J. Cehelsky, B.R. Bettencourt, M. Geissler, J.S. Butler, A. Sehgal, R.E. Meyers, Q. Chen, T. Borland, R.M. Hutabarat, V.A. Clausen, R. Alvarez, K. Fitzgerald, C. Gamba-Vitalo, S. V. Nochur, A.K. Vaishnaw, D.W.Y.Y. Sah, J.A. Gollob, O.B. Suhr, Safety and Efficacy of RNAi Therapy for Transthyretin Amyloidosis, N. Engl. J. Med. 369 (2013) 819–829. doi:10.1056/NEJMoa1208760.

[27] A. Sehgal, S. Barros, L. Ivanciu, B. Cooley, J. Qin, T. Racie, J. Hettinger, M. Carioto, Y. Jiang, J. Brodsky, H. Prabhala, X. Zhang, H. Attarwala, R. Hutabarat, D. Foster, S. Milstein, K. Charisse, S. Kuchimanchi, M.A. Maier, L. Nechev, P. Kandasamy, A. V Kel'in, J.K. Nair, K.G.

Rajeev, M. Manoharan, R. Meyers, B. Sorensen, A.R. Simon, Y. Dargaud, C. Negrier, R.M. Camire, A. Akinc, An RNAi therapeutic targeting antithrombin to rebalance the coagulation system and promote hemostasis in hemophilia, Nat. Med. 21 (2015) 492–497. doi:10.1038/nm.3847.

[28] K. Fitzgerald, M. Frank-Kamenetsky, S. Shulga-Morskaya, A. Liebow, B.R. Bettencourt, J.E. Sutherland, R.M. Hutabarat, V.A. Clausen, V. Karsten, J. Cehelsky, S. V. Nochur, V. Kotelianski, J. Horton, T. Mant, J. Chiesa, J. Ritter, M. Munisamy, A.K. Vaishnaw, J.A. Gollob, A. Simon, Effect of an RNA interference drug on the synthesis of proprotein convertase subtilisin/kexin type 9 (PCSK9) and the concentration of serum LDL cholesterol in healthy volunteers: a randomised, single-blind, placebo-controlled, phase 1 trial, Lancet. 383 (2014) 60–68. doi:10.1016/S0140-6736(13)61914-5.

[29] P.K. Kaiser, R.C.A. Symons, S.M. Shah, E.J. Quinlan, H. Tabandeh, D. V Do, G. Reisen, J. a Lockridge, B. Short, R. Guerciolini, Q.D. Nguyen, RNAi-based treatment for neovascular age-related macular degeneration by Sirna-027., Am. J. Ophthalmol. 150 (2010) 33–39.e2. doi:10.1016/j.ajo.2010.02.006.

[30] Q.D. Nguyen, R.A. Schachar, C.I. Nduaka, M. Sperling, A.S. Basile, K.J. Klamerus, K. Chi-Burris, E. Yan, D.A. Paggiarino, I. Rosenblatt, A. Khan, R. Aitchison, S.S. Erlich, Phase 1 dose-escalation study of a siRNA targeting the RTP801 gene in age-related macular degeneration patients, Eye. 26 (2012) 1099–1105. doi:10.1038/eye.2012.106.

[31] Q.D. Nguyen, R.A. Schachar, C.I. Nduaka, M. Sperling, K.J. Klamerus, K. Chi-Burris, E. Yan, D.A. Paggiarino, I. Rosenblatt, R. Aitchison, S.S. Erlich, Evaluation of the siRNA PF-04523655 versus Ranibizumab for the Treatment of Neovascular Age-related Macular Degeneration (MONET Study), Ophthalmology. 119 (2012) 1867–1873. doi:10.1016/j.ophtha.2012.03.043.

[32] B.L. Davidson, P.B. McCray, Current prospects for RNA interference-based therapies, Nat. Rev. Genet. 12 (2011) 329–340. doi:10.1038/nrg2968.

[33] et al. . Ramanathan RK, Hamburg, S.I., Borad, M.J., Seetharam, M., Kundranda, M.N., Lee, P., A phase I dose-escalation study of TKM-080301, a RNAi therapeutic directed against polo-like kinase 1 (PLK1), in patients with advanced solid tumors: Expansion cohort evaluation of biopsy samples for evidence of pharmacodynamic effects of PLK1 inhibition., Cancer Res. 73 (2013) [Abstract].

[34] B. Schultheis, D. Strumberg, A. Santel, C. Vank, F. Gebhardt, O. Keil, C. Lange, K. Giese, J. Kaufmann, M. Khan, J. Drevs, First-in-Human Phase I Study of the Liposomal RNA Interference Therapeutic Atu027 in Patients With Advanced Solid Tumors, J. Clin. Oncol. 32 (2014) 4141–4148. doi:10.1200/JCO.2013.55.0376.

[35] G. V, P. K, T. K, M. FJ, J. J, G. J, U. F, A. A, G. E, Moreno-Montanes, Phase 2 of bamosiran (SYL040012), a novel RNAi based compound for the treatment of increased intraocular pressure associated to glaucoma, Invest Ophthalmol Vis Sci. [abstract] (2014).

[36] J. Moreno-Montañés, B. Sádaba, V. Ruz, A. Gómez-Guiu, J. Zarranz, M.V. González, C. Pañeda, A.I. Jimenez, Phase I Clinical Trial of SYL040012, a Small Interfering RNA Targeting β-Adrenergic Receptor 2, for Lowering Intraocular Pressure, Mol. Ther. 22 (2014) 226–232. doi:10.1038/mt.2013.217.

[37] J. AI, C. JMB, M.-M. J, J.-A. I, M.-N. F, P. K, T. K, P. C, M. T, RuzV, GonzalezV, Results of clinical trials with a novel RNA based therapy (SYL1001) to treat patients with ocular pain associated to dry eye disease., Invest Ophthalmol Vis Sci. 12 (2016) 2878.

[38] O.B. Suhr, T. Coelho, J. Buades, J. Pouget, I. Conceicao, J. Berk, H. Schmidt, M. Waddington-Cruz, J.M. Campistol, B.R. Bettencourt, A. Vaishnaw, J. Gollob, D. Adams, Efficacy and safety of patisiran for familial amyloidotic polyneuropathy: a phase II multi-dose study, Orphanet J. Rare Dis. 10 (2015) 109. doi:10.1186/s13023-015-0326-6.

[39] T. Golan, E.Z. Khvalevsky, A. Hubert, R.M. Gabai, N. Hen, A. Segal, A. Domb, G. Harari, E. Ben David, S. Raskin, Y. Goldes, E. Goldin, R. Eliakim, M. Lahav, Y. Kopleman, A. Dancour, A. Shemi, E. Galun, RNAi therapy targeting KRAS in combination with chemotherapy for locally advanced pancreatic cancer patients, Oncotarget. 6 (2015) 24560–24570. doi:10.18632/oncotarget.4183.

[40] H.L.A. Janssen, H.W. Reesink, E.J. Lawitz, S. Zeuzem, M. Rodriguez-Torres, K. Patel, A.J. van der Meer, A.K. Patick, A. Chen, Y. Zhou, R. Persson, B.D. King, S. Kauppinen, A.A. Levin, M.R. Hodges, Treatment of HCV Infection by Targeting MicroRNA, N. Engl. J. Med. 368 (2013) 1685–1694. doi:10.1056/NEJMoa1209026.

[41] M.H. van der Ree, A.J. van der Meer, J. de Bruijne, R. Maan, A. van Vliet, T.M. Welzel, S. Zeuzem, E.J. Lawitz, M. Rodriguez-Torres, V. Kupcova, A. Wiercinska-Drapalo, M.R. Hodges, H.L.A. Janssen, H.W. Reesink, Long-term safety and efficacy of microRNA-targeted therapy in chronic hepatitis C patients, Antiviral Res. 111 (2014) 53–59. doi:10.1016/j.antiviral.2014.08.015.

[42] S. Ottosen, T.B. Parsley, L. Yang, K. Zeh, L.-J. van Doorn, E. van der Veer, A.K. Raney, M.R. Hodges, A.K. Patick, In Vitro Antiviral Activity and Preclinical and Clinical Resistance Profile of Miravirsen, a Novel Anti-Hepatitis C Virus Therapeutic Targeting the Human Factor miR-122, Antimicrob. Agents Chemother. 59 (2015) 599–608. doi:10.1128/AAC.04220-14.

[43] D. Bumcrot, M. Manoharan, V. Koteliansky, D.W.Y. Sah, RNAi therapeutics: a potential new class of pharmaceutical drugs, Nat. Chem. Biol. 2 (2006) 711–719. doi:10.1038/nchembio839.

[44] Y. Chiu, T.M. Rana, siRNA function in RNAi : A chemical modification analysis, RNA Soc. 9 (2003) 1034–1048. doi:10.1261/rna.5103703.2000.

[45] N.M. Snead, J.R. Escamilla-Powers, J.J. Rossi, A.P. McCaffrey, 5′ Unlocked Nucleic Acid Modification Improves siRNA Targeting, Mol. Ther. - Nucleic Acids. 2 (2013) e103. doi:10.1038/mtna.2013.36.

[46] A.L. Jackson, Position-specific chemical modification of siRNAs reduces “off-target” transcript silencing, RNA. 12 (2006) 1197–1205. doi:10.1261/rna.30706.

[47] D.J. Son, S. Kumar, W. Takabe, C. Woo Kim, C.-W. Ni, N. Alberts-Grill, I.-H. Jang, S. Kim, W. Kim, S. Won Kang, A.H. Baker, J. Woong Seo, K.W. Ferrara, H. Jo, The atypical mechanosensitive microRNA-712 derived from pre-ribosomal RNA induces endothelial inflammation and atherosclerosis, Nat. Commun. 4 (2013) 3000. doi:10.1038/ncomms4000.

[48] R.L. Juliano, X. Ming, K. Carver, B. Laing, Cellular Uptake and Intracellular Trafficking of Oligonucleotides: Implications for Oligonucleotide Pharmacology, Nucleic Acid Ther. 24 (2014) 101–113. doi:10.1089/nat.2013.0463.

[49] D. Haussecker, Current issues of RNAi therapeutics delivery and development, J. Control. Release. (n.d.). doi:http://dx.doi.org/10.1016/j.jconrel.2014.07.056.

[50] L.L. Wang, J.A. Burdick, Engineered Hydrogels for Local and Sustained Delivery of RNA-Interference Therapies, Adv. Healthc. Mater. 6 (2017) 1601041. doi:10.1002/adhm.201601041.

[51] K. Schwabe, A. Ewe, C. Kohn, T. Loth, A. Aigner, M.C. Hacker, M. Schulz-Siegmund, Sustained delivery of siRNA poly- and lipopolyplexes from porous macromer-crosslinked gelatin gels, Int. J. Pharm. 526 (2017) 178–187. doi:10.1016/j.ijpharm.2017.04.065.

[52] N. Segovia, M. Pont, N. Oliva, V. Ramos, S. Borrós, N. Artzi, Hydrogel Doped with Nanoparticles for Local Sustained Release of siRNA in Breast Cancer, Adv. Healthc. Mater. 4 (2015) 271–280. doi:10.1002/adhm.201400235.

[53] C.E. Nelson, M.K. Gupta, E.J. Adolph, J.M. Shannon, S. a Guelcher, C.L. Duvall, Sustained local delivery of siRNA from an injectable scaffold., Biomaterials. 33 (2012) 1154–61. doi:10.1016/j.biomaterials.2011.10.033.

[54] M.K. Nguyen, O. Jeon, M.D. Krebs, D. Schapira, E. Alsberg, Sustained localized presentation of RNA interfering molecules from in situ forming hydrogels to guide stem cell osteogenic differentiation, Biomaterials. 35 (2014) 6278–6286. doi:10.1016/j.biomaterials.2014.04.048.

[55] M.L. Bobbin, J.J. Rossi, RNA Interference (RNAi)-Based Therapeutics: Delivering on the Promise?, Annu. Rev. Pharmacol. Toxicol. 56 (2016) 103–122. doi:10.1146/annurev-pharmtox-010715-103633.

[56] D. Haussecker, The Business of RNAi Therapeutics in 2012, Mol. Ther. - Nucleic Acids. 1 (2012) e8. doi:10.1038/mtna.2011.9.

[57] S.A. Stewart, D.M. Dykxhoorn, D. Palliser, H. Mizuno, E.Y. Yu, D.S. An, D.M. Sabatini, I.S.Y. Chen, W.C. Hahn, P.A. Sharp, R.A. Weinberg, C.D. Novina, Lentivirus-delivered stable gene silencing by RNAi in primary cells, (2003) 493–501. doi:10.1261/rna.2192803.rapid.

[58] S. Alimperti, P. Lei, J. Tian, S.T. Andreadis, A novel lentivirus for quantitative assessment of gene knockdown in stem cell differentiation, Gene Ther. 19 (2012) 1123–1132.

doi:10.1038/gt.2011.208.

[59] Y.P.O.I. Liu, M.A. Vink, J. Westerink, E.V.A.R.D.E. Arellano, P. Konstantinova, O.T.E.R. Brake, B.E.N. Berkhout, Titers of lentiviral vectors encoding shRNAs and miRNAs are reduced by different mechanisms that require distinct repair strategies, Rna. 16 (2010) 1328–1339. doi:10.1261/rna.1887910.3.

[60] P.A. Campochiaro, E.H. Sohn, T.A. Mir, A.K. Lauer, S. Naylor, M.C. Anderton, M. Kelleher, R. Harrop, S. Ellis, K.A. Mitrophanous, Lentiviral Vector Gene Transfer of Endostatin / Angiostatin for Macular Degeneration (GEM) Study, 28 (2017) 99–111. doi:10.1089/hum.2016.117.

[61] Y. Motegi, K. Katayama, F. Sakurai, T. Kato, T. Yamaguchi, H. Matsui, M. Takahashi, K. Kawabata, H. Mizuguchi, An effective gene-knockdown using multiple shRNA-expressing adenovirus vectors, J. Control. Release. 153 (2011) 149–153. doi:10.1016/j.jconrel.2011.04.009.

[62] R.G. Crystal, Adenovirus: The First Effective In Vivo Gene Delivery Vector, Hum. Gene Ther. 25 (2014) 3–11. doi:10.1089/hum.2013.2527.

[63] M.L. Hirsch, L. Green, M.H. Porteus, R.J. Samulski, Self-complementary AAV mediates gene targeting and enhances endonuclease delivery for double-strand break repair, Gene Ther. 17 (2010) 1175–1180. doi:10.1038/gt.2010.65.

[64] L.H. Vandenberghe, J.M. Wilson, G. Gao, Tailoring the AAV vector capsid for gene therapy, 16 (2009) 311–319. doi:10.1038/gt.2008.170.

[65] C. Qiao, Z. Yuan, J. Li, B. He, H. Zheng, C. Mayer, J. Li, X. Xiao, C. Hill, Liver-specific microRNA-122 target sequences incorporated in AAV vectors efficiently inhibits transgene expression in the liver, 18 (2013) 403–410. doi:10.1038/gt.2010.157.Liver-specific.

[66] N. Clément, J.C. Grieger, Manufacturing of recombinant adeno-associated viral vectors for clinical trials, Mol. Ther. - Methods Clin. Dev. 3 (2016) 16002. doi:10.1038/mtm.2016.2.

[67] Y. Shen, J. Nemunaitis, Herpes simplex virus 1 (HSV-1) for cancer treatment, Cancer Gene Ther. 2 (2006) 975–992. doi:10.1038/sj.cgt.7700946.

[68] Y. Wang, H. Su, Y. Yang, Y. Hu, L. Zhang, P. Blancafort, L. Huang, Systemic Delivery of Modified mRNA Encoding Herpes Simplex Virus 1 Thymidine Kinase for Targeted Cancer Gene Therapy, Mol. Ther. (2013) 1–10. doi:10.1038/mt.2012.250.

[69] R.S. Tomar, H. Matta, P.M. Chaudhary, Use of adeno-associated viral vector for delivery of small interfering RNA, Oncogene. 22 (2003) 5712–5715. doi:10.1038/sj.onc.1206733.

[70] C.E. Thomas, A. Ehrhardt, M.A. Kay, Progress and problems with the use of viral vectors for gene therapy, Nat. Rev. Genet. 4 (2003) 346–358. doi:10.1038/nrg1066.

[71] I. a Pringle, S.C. Hyde, D.R. Gill, Non-viral vectors in cystic fibrosis gene therapy: recent developments and future prospects., Expert Opin. Biol. Ther. 9 (2009) 991–1003. doi:10.1517/14712590903055029.

[72] A. Kamen, O. Henry, Development and optimization of an adenovirus production process, J. Gene Med. 6 (2004) 184–192.

[73] M. Foldvari, D.W. Chen, N. Nafissi, D. Calderon, L. Narsineni, A. Rafiee, Non-viral gene therapy: Gains and challenges of non-invasive administration methods, J. Control. Release. 240 (2016) 165–190. doi:10.1016/j.jconrel.2015.12.012.

[74] H. Yin, R.L. Kanasty, A.A. Eltoukhy, A.J. Vegas, J.R. Dorkin, D.G. Anderson, Non-viral vectors for gene-based therapy, Nat. Rev. Genet. 15 (2014) 541–555. doi:10.1038/nrg3763.

[75] C. Zylberberg, K. Gaskill, S. Pasley, S. Matosevic, Engineering liposomal nanoparticles for targeted gene therapy, Gene Ther. (2017). doi:10.1038/gt.2017.41.

[76] P.P. Karmali, A. Chaudhuri, Cationic liposomes as non-viral carriers of gene medicines: Resolved issues, open questions, and future promises, Med. Res. Rev. 27 (2007) 696–722. doi:10.1002/med.20090.

[77] C. Zylberberg, S. Matosevic, Bioengineered liposome–scaffold composites as therapeutic delivery systems, Ther. Deliv. 8 (2017) 425–445. doi:10.4155/tde-2017-0014.

[78] V. Perri, M. Pellegrino, F. Ceccacci, A. Scipioni, S. Petrini, E. Gianchecchi, A. Lo Russo, S. De Santis, G. Mancini, A. Fierabracci, Use of short interfering RNA delivered by cationic liposomes to enable efficient down-regulation of PTPN22 gene in human T lymphocytes, PLoS One. 12 (2017) e0175784. doi:10.1371/journal.pone.0175784.

[79] K.B. Knudsen, H. Northeved, P. Kumar EK, A. Permin, T. Gjetting, T.L. Andresen, S. Larsen, K.M. Wegener, J. Lykkesfeldt, K. Jantzen, S. Loft, P. Møller, M. Roursgaard, In vivo toxicity of cationic micelles and liposomes, Nanomedicine Nanotechnology, Biol. Med. 11 (2015) 467–477. doi:10.1016/j.nano.2014.08.004.

[80] A. Kheirolomoom, C.W. Kim, J.W. Seo, S. Kumar, D.J. Son, M.K.J. Gagnon, E.S. Ingham, K.W. Ferrara, H. Jo, Multifunctional Nanoparticles Facilitate Molecular Targeting and miRNA Delivery to Inhibit Atherosclerosis in ApoE –/– Mice, ACS Nano. 9 (2015) 8885–8897. doi:10.1021/acsnano.5b02611.

[81] M.A. Mintzer, E.E. Simanek, Nonviral vectors for gene delivery., Chem. Rev. 109 (2009) 259–302. doi:10.1021/cr800409e.

[82] W. Li, F.C. Szoka, Lipid-based Nanoparticles for Nucleic Acid Delivery, Pharm. Res. 24 (2007) 438–449. doi:10.1007/s11095-006-9180-5.

[83] M. Aleku, P. Schulz, O. Keil, A. Santel, U. Schaeper, B. Dieckhoff, O. Janke, J. Endruschat, B. Durieux, N. Roder, K. Loffler, C. Lange, M. Fechtner, K. Mopert, G. Fisch, S. Dames, W. Arnold, K. Jochims, K. Giese, B. Wiedenmann, A. Scholz, J. Kaufmann, Atu027, a Liposomal Small Interfering RNA Formulation Targeting Protein Kinase N3, Inhibits Cancer Progression, Cancer Res. 68 (2008) 9788–9798. doi:10.1158/0008-5472.CAN-08-2428.

[84] Z. Ma, J. Li, F. He, A. Wilson, B. Pitt, S. Li, Cationic lipids enhance siRNA-mediated interferon response in mice, Biochem. Biophys. Res. Commun. 330 (2005) 755–759. doi:http://dx.doi.org/10.1016/j.bbrc.2005.03.041.

[85] M.C. Filion, N.C. Phillips, Toxicity and immunomodulatory activity of liposomal vectors formulated with cationic lipids toward immune effector cells., Biochim. Biophys. Acta. 1329 (1997) 345–56. doi:10.1016/S0005-2736(97)00126-0.

[86] K.A. Whitehead, R. Langer, D.G. Anderson, Knocking down barriers: advances in siRNA delivery, 8 (2009). doi:10.1038/nrd2742.

[87] M. Yamagata, T. Kawano, K. Shiba, T. Mori, Y. Katayama, T. Niidome, Structural advantage of dendritic poly(l-lysine) for gene delivery into cells, Bioorg. Med. Chem. 15 (2007) 526–532. doi:10.1016/j.bmc.2006.09.033.

[88] A. von Harpe, H. Petersen, Y. Li, T. Kissel, Characterization of commercially available and synthesized polyethylenimines for gene delivery, J. Control. Release. 69 (2000) 309–322. doi:10.1016/S0168-3659(00)00317-5.

[89] W.T. Godbey, K.K. Wu, A.G. Mikos, Size matters : Molecular weight affects the efficiency of poly (ethylenimine) as a gene delivery vehicle, J. Biomed. Mater. Res. 45 (1998) 268–275.

[90] L. Wightman, R. Kircheis, V. Rssler, S. Carotta, R. Ruzicka, M. Kursa, E. Wagner, Different behavior of branched and linear polyethylenimine for gene deliveryin vitro andin vivo, J. Gene Med. 3 (2001) 362–372. doi:10.1002/jgm.187.

[91] V. Leiro, S.D. Santos, A.P. Pego, Delivering siRNA with Dendrimers: In Vivo Applications., Curr. Gene Ther. (2017). doi:10.2174/1566523217666170510160527.

[92] D. Lee, W. Zhang, S. a. Shirley, X. Kong, G.R. Hellermann, R.F. Lockey, S.S. Mohapatra, Thiolated Chitosan/DNA Nanocomplexes Exhibit Enhanced and Sustained Gene Delivery, Pharm. Res. 24 (2006) 157–167. doi:10.1007/s11095-006-9136-9.

[93] H.Q. Mao, K. Roy, V.L. Troung-Le, K. a Janes, K.Y. Lin, Y. Wang, J.T. August, K.W. Leong, Chitosan-DNA nanoparticles as gene carriers: synthesis, characterization and transfection efficiency., J. Control. Release. 70 (2001) 399–421. http://www.ncbi.nlm.nih.gov/pubmed/11182210.

[94] D.M. Lynn, R. Langer, Degradable Poly(β-amino esters): Synthesis, Characterization, and Self-Assembly with Plasmid DNA, J. Am. Chem. Soc. 122 (2000) 10761–10768. doi:10.1021/ja0015388.

[95] P. Dosta, N. Segovia, A. Cascante, V. Ramos, S. Borrós, Surface charge tunability as a powerful strategy to control electrostatic interaction for high efficiency silencing, using tailored oligopeptide-modified poly(β-amino ester)s (PBAEs), Acta Biomater. 20 (2015) 82–93. doi:http://dx.doi.org/10.1016/j.actbio.2015.03.029.

[96] N. Segovia, P. Dosta, A. Cascante, V. Ramos, S. Borrós, Oligopeptide-terminated poly(β-amino ester)s for highly efficient gene delivery and intracellular localization., Acta Biomater. 10 (2014) 2147–58. doi:10.1016/j.actbio.2013.12.054.

[97] H.-Y. Xue, H.-L. Wong, Solid Lipid–PEI Hybrid Nanocarrier: An Integrated Approach To Provide Extended, Targeted, and Safer siRNA Therapy of Prostate Cancer in an All-in-One Manner, ACS Nano. 5 (2011) 7034–7047. doi:10.1021/nn201659z.

[98] X. Wang, A. Bodman, C. Shi, D. Guo, L. Wang, J. Luo, W.A. Hall, Tunable Lipidoid-Telodendrimer Hybrid Nanoparticles for Intracellular Protein Delivery in Brain Tumor Treatment, Small. 12 (2016) 4185–4192. doi:10.1002/smll.201601234.

[99] I.C. Turnbull, A.A. Eltoukhy, D.G. Anderson, K.D. Costa, Lipidoid mRNA Nanoparticles for Myocardial Delivery in Rodents, in: 2017: pp. 153–166. doi:10.1007/978-1-4939-6588-5_10.

[100] H. Lönnberg, Solid-Phase Synthesis of Oligonucleotide Conjugates Useful for Delivery and Targeting of Potential Nucleic Acid Therapeutics, Bioconjug. Chem. 20 (2009) 1065–1094. doi:10.1021/bc800406a.

[101] D.B. Rozema, D.L. Lewis, D.H. Wakefield, S.C. Wong, J.J. Klein, P.L. Roesch, S.L. Bertin, T.W. Reppen, Q. Chu, A. V. Blokhin, J.E. Hagstrom, J.A. Wolff, Dynamic PolyConjugates for targeted in vivo delivery of siRNA to hepatocytes, Proc. Natl. Acad. Sci. 104 (2007) 12982–12987. doi:10.1073/pnas.0703778104.

[102] G. Sahay, W. Querbes, C. Alabi, A. Eltoukhy, S. Sarkar, C. Zurenko, E. Karagiannis, K. Love, D. Chen, R. Zoncu, Y. Buganim, A. Schroeder, R. Langer, D.G. Anderson, Efficiency of siRNA delivery by lipid nanoparticles is limited by endocytic recycling, Nat. Biotechnol. 31 (2013) 653–658. doi:10.1038/nbt.2614.

[103] G.T. Zugates, N.C. Tedford, A. Zumbuehl, S. Jhunjhunwala, C.S. Kang, L.G. Griffith, D. a Lauffenburger, R. Langer, D.G. Anderson, Gene delivery properties of end-modified poly(beta-amino ester)s., Bioconjug. Chem. 18 (2007) 1887–96. doi:10.1021/bc7002082.

[104] M.S. Kim, D.S. Lee, H. Park, J. Kim, Modulation of Poly (β -amino ester) pH-Sensitive Polymers by Molecular Weight Control, 13 (2005) 147–151.

[105] S.R. Little, D.M. Lynn, Q. Ge, D.G. Anderson, S. V Puram, J. Chen, H.N. Eisen, R. Langer, Poly-beta amino ester-containing microparticles enhance the activity of nonviral genetic vaccines, Proc. Natl. Acad. Sci. U. S. A. 101 (2004) 9534–9539.

[106] Y. Huang, G.T. Zugates, W. Peng, D. Holtz, C. Dunton, J.J. Green, N. Hossain, M.R. Chernick, R.F.P. Jr, D.G. Anderson, J.A. Sawicki, Nanoparticle-Delivered Suicide Gene Therapy Effectively Reduces Ovarian Tumor Burden in Mice, Cancer Res. 69 (2010) 6184–6191. doi:10.1158/0008-5472.CAN-09-0061.

[107] C.D. Kamat, R.B. Shmueli, N. Connis, C.M. Rudin, J.J. Green, C.L. Hann, Poly(beta-aminoester) nanoparticle-delivery of p53 has activity against small cell lung cancer in vitro and in vivo, Mol. Cancer Ther. . (2013). doi:10.1158/1535-7163.MCT-12-0956.

[108] unsJoel C. Shine, S.B. Sunshine, I. Bhutto, J.T. Handa, J.J. Green, Poly(β-amino ester)-nanoparticle mediated transfection of retinal pigment epithelial cells in vitro and in vivo., PLoS One. 7 (2012) e37543. doi:10.1371/journal.pone.0037543.

[109] S.Y. Tzeng, B.P. Hung, W.L. Grayson, J.J. Green, Cystamine-terminated poly(beta-amino ester)s for siRNA delivery to human mesenchymal stem cells and enhancement of osteogenic differentiation, Biomaterials. 33 (2012) 8142–8151. doi:10.1016/j.biomaterials.2012.07.036.

[110] D. Jere, C.-X. Xu, R. Arote, C.-H. Yun, M.-H. Cho, C.-S. Cho, Poly(β-amino ester) as a carrier for si/shRNA delivery in lung cancer cells, Biomaterials. 29 (2008) 2535–2547. doi:10.1016/j.biomaterials.2008.02.018.

[111] J.J. Green, B.Y. Zhou, M.M. Mitalipova, C. Beard, R. Langer, R. Jaenisch, D.G. Anderson, Nanoparticles for gene transfer to human embryonic stem cell colonies., Nano Lett. 8 (2008) 3126–30. doi:10.1021/nl8012665.

[112] F. Yang, S. Cho, S. Mi, S.R. Bogatyrev, D. Singh, J.J. Green, Y. Mei, S.M. Son, S.R. Bogatyrev, D. Singh, J.J. Green, Y. Mei, S. Park, S.H. Bhang, B.-S. Kim, R. Langer, D.G. Anderson, Genetic engineering of human stem cells for enhanced angiogenesis using biodegradable polymeric nanoparticles, Proc. Natl. Acad. Sci. U. S. A. 107 (2010) 3317–22. doi:10.1073/pnas.0905432106.

Chapter II

Design of efficient and cell-specific delivery vectors using poly(β-amino ester)s

Originally published as:

N. Segovia, P. Dosta, A. Cascante, V. Ramos, S. Borrós, “Oligopeptide-terminated poly(β-amino ester)s for highly efficient gene delivery and intracellular localization”., **Acta Biomater**. Vol. 10, pp. 2147–58, May 2014.

P. Dosta, N. Segovia, A. Cascante, V. Ramos, and S. Borrós, “Surface charge tunability as a powerful strategy to control electrostatic interaction for high efficiency silencing, using tailored oligopeptide-modified poly(β-amino ester)s (PBAEs),” ***Acta Biomater.***, vol. 20, pp. 82–93, Jul. 2015.

This page left blank intentionally

Design of efficient and cell-specific delivery vectors using poly(β-amino ester)s

This chapter describes the synthesis of extended family of pBAEs that incorporate terminal oligopeptide moieties synthesized from both positive and negative amino acids. Polymer formulations of mixtures of oligopeptide-modified pBAEs are capable of condensing RNAi into discrete nanoparticles. In addition, we have demonstrated that efficient delivery of nucleic acids in a cell-type dependent manner can be achieved by careful control of the pBAE formulation, making them a powerful strategy for developing delivery systems for future RNAi therapy applications.

2.1 Introduction

As previously discussed in chapter I, RNAi therapy emerged a valuable tool for the therapeutic treatment for many diseases, becoming a new paradigm in medicine with enormous therapeutic potential [1]. However, the lack of safe, specific, and efficient delivery vectors is the principal handicap of this field, which limit their applicability.

One of the biggest obstacle are the different barriers that RNAi-nanoparticles have to overcome until it reach their target mRNA [2]. Beside stability barriers, efficient RNAi delivery to the target cell is also a challenging proses. Cellular entrance of RNAi nanoparticles most often occurs thought endocytosis. After that, endocytosed RNAi nanoparticles are entrapped in membrane-bound endocytic vesicles, which fuse with early endosome and become increasingly acidic, where RNAi nanoparticles have to scape in order to be therapeutic. Then, the development of strategies to overcome the intracellular barriers that delivery vectors have to overcome, also has attracted much of the work investigating the mechanism of synthetic delivery methods [3].

First, delivery vectors have to efficiently bind to the negatively-charged cell membranes and get internalized. Because polyplexes are held together electrostatically and typically present highly positively charged surfaces, the nature and the extent of their surface charge condition not only their interaction with the cell surface but also with other charged surfaces. Indeed, vector interactions with proteins and glycosaminoglycans (GAGs) found in the extracellular matrix or the cell surface may interfere with the interactions between polyplexes and the cell surface, resulting in decreased delivery efficiency [4–6]. Tailoring of the surface properties of the delivery vehicles, especially the surface charge, may significantly influence the way they interact with the cell surface and ultimately influence their performance [7][8][9]. Coating of the surface of polyplexes with hydrophilic polymers, such as polyethylene glycol (PEG) [10,11] or poly[N-(2-hydroxypropyl)methacrylamide] (pHPMA) [12–14], may

significantly alter the surface charge of the vector. The addition of such polymer coatings forms a physical barrier around the polyplexes that provides steric stabilization and protection from unwanted interactions, but may also hamper the required interactions for cellular uptake. In addition to polymer conjugation, another promising approach is the formation of ternary complexes by shielding the peripheral cationic charges with layers of anionic polymers, such as polyacrylic acid [9] or hyaluronic acid [15]. Controlled addition of anionic polymers on pre-formed polyplexes results in the formation of a negatively charged shell that may improve the disadvantages of their strong cationic charge, such as cytotoxicity and non-specific binding to physiological molecules. Recently, it was demonstrated that electrostatic coating of nucleic acid nanoparticles prepared from poly(β-amino ester) is a simple and effective method to modify the function and the toxicity of nanoparticles and may have the potential to promote tissue-specific RNAi and gene delivery [16,17].

Poly(β-amino ester) polymers are synthesized through classical Michael addition reaction involving the conjugation of either a primary amine or a bis(secondary amine) monomer with a diacrylate ester, in a one-step reaction without the production of any byproducts [18].

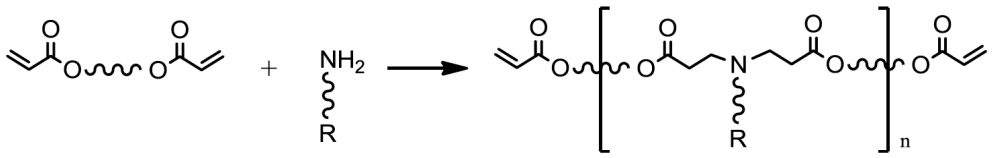

Figure II-1 Synthesis of pBAEs by Michael-type addition reaction.

Since different backbone structures can be ease designed, Anderson et. al. synthetized a large family of 2350 structurally unique pBAEs using high-throughput combinatorial chemistry [19,20]. Results showed that polymer structure have a direct influence to RNAi or DNA binding ability and delivery efficiency, finding that C32 polymer structure was one of the best formulations [21]. In addition, targeting ligands or endosomolytic moieties can be easily incorporated in the polymer backbone using different conjugation or polymerization techniques. Their use allows a high degree of flexibility in the final polymer formulation, which can be tuned for particular purposes [22–24].

Previously in our group, we developed a family of poly(β-amino ester) polymers with oligopeptide-modified termini that has proven high gene delivery and excellent biocompatibility. Previous results have demonstrated that tailored formulations of different cationic oligopeptide-terminated poly(β-amino ester) polymers are capable of rendering nanoparticles with specific features, obtaining a different intracellular localization. For instance, when pBAE was end-caped with arginine peptide previous results demonstrated arginine-modified poly(β-amino ester)s showed preferential localization around the perinuclear region, while complexes formed with poly(β-amino ester)s end-modified with lysine or histidine oligopeptides were preferentially observed in the cytoplasm or around the cellular membrane, respectively [25].

Taking into account previously observed oligopeptide-modified pBAE features, in this chapter, we have expanded the use of oligopeptide end-modification by exploring the use of mixtures of cationic and/or anionic oligopeptide-modified pBAE as delivery systems for RNAi therapy. As a result, we have developed formulations of anionic and/or cationic pBAE polymer mixtures as a simple method to tailor the surface charge of the resulting nanoparticles in order to avoid non-desired proteins interactions, while maintaining their ability to mediate efficient gene silencing. Consequently, wide family of polyplexes with different oligopeptide formulation have been designed, which may be used to delivery vector customization in function of their therapeutic application. Therefore, their easy adaptability makes them a promising alternative to transfect challenging cells lines, such as stem cells. In the next chapter, newly formulated positive/negative oligopeptide mixture have been tested to deliver siRNA into Dental Pluripotent Stem Cells.

Then, the main objective of this chapter is the development of a family of polymers (pBAEs) with different formulation strategies, which are able to efficiently condense RNAi into discrete nanoparticle with tuneable surface charge proprieties, in order to design a cell-specific and cell-efficient polymer formulation.

In order to achieve this objective, the following tasks were proposed:

- Synthesis and biophysical characterization positive and negative oligopeptide end-modified pBAEs.
- Study of GFP knockdown efficiency and viability using newly designed positive and negative oligopeptide pBAE in different cells lines.
- Determination of beneficial effects in terms of cell-specificity and transfection efficiency of newly developed oligopeptide end-modified pBAEs.

2.2 Materials and Methods

2.2.1 Materials

Reagents and solvents used for synthesis were purchased from Sigma Aldrich and Panreac. CR3 (H-Cys-Arg-Arg-Arg-NH2), CK3 (H-Cys- Lys-Lys-Lys-NH2), CH3 (H-Cys-His-His-His-NH2), CD3 (H-Cys-Asp-Asp-Asp-NH2) and CE3 (H-Cys-Glu-Glu-Glu-NH2) peptides were obtained from GL Biochem (Shanghai) Ltd with a purity of at least 98%. Derivatization kit (AccQ-TagTM Ultra) was obtained from Waters and Amino acid standard H was purchased from Sigma Aldrich. Silencer RNA against Green Fluorescent Protein (GFP) was obtained from Thermo Scientific Dharmacon. HeLa-GFP and MDA MB321 cell lines were obtained from Cell Biolabs and all of them were maintained at 37°C in 5% CO2 atmosphere in complete DMEM, containing 10% fetal bovine serum, 100 units/mL penicillin, 100 µg/mL streptomycin, 2 mM L-glutamine and 0.1 mM MEM Non-Essential Amino Acids (NEAA).

2.2.2 Synthesis of pBAEs polymers

Poly(β-amino ester)s were synthesized following a two-step procedure, described in the literature. First, an acrylate-terminated polymer was synthesized by addition reaction of primary amines with diacrylates (at 1:1.2 molar ratio of amine:diacrylate). Then, pBAEs were obtained by end-capping modification of the resulting acrylate-terminated polymer with different kind of amine- and thiol-bearing moieties. Synthesized structures were confirmed by ^{1}H-NMR and FT-IR analysis. NMR spectra were recorded in a 400 MHz Varian (Varian NMR Instruments, Claredon Hills, IL) and methanol-d4 was used as solvent. IR spectra were obtained using a Nicolet Magna 560 (Thermo Fisher Scientific, Waltham, MA) with a KBr beamsplitter, using methanol as solvent in evaporated film. Molecular weight determination was conducted on an HPLC Elite LaChrom system (VWR-Hitachi) equipped with a GPC Shodex KF-603 column, 6,0 mmID x 150mm, and THF as mobile phase. The molecular weight was calculated by comparison with the retention times of polystyrene standards.

2.2.2.1 Synthesis of oligopeptide end-modified pBAEs

In general, oligopeptide-modified pBAEs were obtained by end-modification of acrylate-terminated polymer C32 with thiol-terminated oligopeptide at 1:2,5 molar ratio in dimethyl sulfoxide (DMSO). The mixture was stirred overnight at room temperature and the resulting polymer was obtained by precipitation in a mixture of diethyl ether and acetone at 7:3 (v/v) ratio.

The following synthetic procedure to obtain tri-arginine end-modified pBAE polymer, C32-CR3, is shown as an example: A solution of C32 (0.15 g, 0.06 mmol) dissolved in DMSO (2 mL) and a solution of H-Cys-Arg-Arg-Arg-NH2 (CR3) (0.11 g, 0.15 mmol) in DMSO (1 mL) were mixed and stirred overnight at room temperature. End-modified polymer R3C-C32-CR3 was obtained by precipitation and dried under vacuum.

Table II-1 summarizes the quantity of different oligopeptides needed to synthetize the new family of cationic- and anionic- end-modified pBAEs from 0.15 g of C32 polymer.

Table II-1. Summary of the quantity of different oligopeptides to synthetize the PBAEs studied.

	MW (g/mol)	Quantity (mg)	Quantity (mmol)
CR3·4HCl	734.56	110.18	0.15
CK3·4HCl	650.52	97.58	0.15
CH3·4HCl	677.42	101.61	0.15
CD3·HCl	501.92	75.29	0.15
CE3·HCl	544.00	81.6	0.15

- C32-CR3

IR (evaporated film): ν = 721, 801, 834, 951, 1029, 1133 (C-O), 1201, 1421, 1466, 1542, 1672 (C=O, from peptide amide), 1731 (C=O, from ester), 2858, 2941, 3182, 3343 (N-H, O-H) cm^{-1}

^{1}H-NMR (400 MHz, CD_3OD, TMS) (ppm): δ = 4.41-4.33 (br, NH_2-C(=O)-CH-NH-C(=O)-CH-NH-C(=O)-CH-NH-C(=O)-CH-CH_2-, 4.11 (t, CH_2-CH_2-O), 3.55 (t, CH_2-CH_2-OH), 3.22 (br, NH_2-C(=NH)-NH-CH_2-, OH-$(CH_2)_4$-CH_2-N-), 3.04 (t, CH_2-CH_2-N-), 2.82 (dd, -CH_2-S-CH_2), 2.48 (br, -N-CH_2-CH_2-C(=O)-O), 1.90 (m, NH_2-C(=NH)-NH-$(CH_2)_2$-CH_2-CH-), 1.73 (br, -O-CH_2-CH2-CH2-CH_2-O), 1.69 (m, NH_2-C(=NH)-NH-CH_2-CH_2-CH_2-), 1.56 (br, -CH_2-CH_2-CH_2-CH_2-OH), 1.39 (br, -N-$(CH_2)_2$-CH_2-$(CH_2)_2$-OH).

- C32-CK3

IR (evaporated film): ν = 721, 799, 834, 1040, 1132, 1179 (C-O), 1201, 1397, 1459, 1541, 1675 (C=O, from peptide amide), 1732 (C=O, from ester), 2861, 2940, 3348 (N-H, O-H) cm^{-1}

^{1}H-NMR (400 MHz, CD_3OD, TMS) (ppm): δ = 4.38-4.29 (br, NH_2-$(CH_2)_4$-CH-), 4.13 (t, CH_2-CH_2-O-),3.73 (br,NH_2-CH-CH_2-S-), 3.55 (t, CH_2-CH_2-OH), 2.94 (br, CH_2-CH_2-N-, NH_2-CH_2-$(CH_2)_3$-CH-), 2.81 (dd, -CH_2-S-CH_2), 2.57 (br, -N-CH_2-CH_2-C(=O)-O), 1.85 (m, NH_2-$(CH_2)_3$-CH_2-CH-), 1.74 (br, -O-CH_2-CH2-CH2-CH_2-O), 1.68 (m, NH_2-CH_2-CH_2-$(CH_2)_2$-CH-), 1.54 (br, -CH_2-CH_2-CH_2-CH_2-OH), 1.37 (br, -N-$(CH_2)_2$-CH_2-$(CH_2)_2$-OH).

- C32-CH3

IR (evaporated film): ν = 720, 799, 832, 1040, 1132, 1201, 1335, 1403, 1467, 1539, 1674 (C=O, from peptide amide), 1731 (C=O, from ester), 2865, 2941, 3336 (N-H, O-H) cm^{-1}

^{1}H-NMR (400 MHz, CD_3OD, TMS) (ppm): δ = 8.0-7.0 (br -N(=CH)-NH-C(=CH)-) 4.61-4.36 (br, -CH2-CH-), 4.16 (t, CH_2-CH_2-O-), 3.55 (t, CH_2-CH_2-OH), 3.18 (t, CH_2-CH_2-N-, 3.06 (dd, -CH_2-CH-), 2.88 (br, OH-$(CH_2)_4$-CH_2-N-), 2.82 (dd, -CH_2-S-CH_2-), 2.72 (br, -N-CH_2-CH_2-C(=O)-O), 1.75 (br, -O-CH_2-CH2-CH2-CH_2-O), 1.65 (m, NH_2-CH_2-CH_2-$(CH_2)_2$ -CH-), 1.58 (br, -CH_2-CH_2-CH_2-CH_2-OH), 1.40 (br, -N-$(CH_2)_2$-CH_2-$(CH_2)_2$-OH).

- C32-CD3

IR (evaporated film): ν = 720, 799, 830, 954, 1028, 1131, 1199, 1403, 1468, 1588, 1677 (C=O, from peptide amide), 1731 (C=O, from ester), 2940, 3368 (N-H, O-H) cm^{-1}

^{1}H-NMR (400 MHz, MeOD, TMS) (ppm): δ = 4.56-4.44 (br, NH_2-C(=O)-C<u>H</u>-NH-C(=O)-C<u>H</u>-NH-C(=O)-C<u>H</u>-NH-C(=O)-C<u>H</u>-CH_2-), 4.19 (br,NH_2-C<u>H</u>-CH_2-S), 4.00 (t, CH_2-C<u>H_2</u>-O), 3.34 (t, CH_2-C<u>H_2</u>-OH), 2.98 (dd, -C<u>H_2</u>-S-C<u>H_2</u>), 2.57-2.48 (t, -CH-C<u>H_2</u>-COO-), 2.40 (br, -N-CH_2-C<u>H_2</u>-C(=O)-O), 1.60 (br, -O-CH_2-C<u>H</u>2-C<u>H</u>2-CH_2-O), 1.38 (br, -C<u>H_2</u>-CH_2-C<u>H_2</u>-CH_2-OH), 1.20 (br, -N-$(CH_2)_2$-C<u>H_2</u>-$(CH_2)_2$-OH).

- C32-CE3

IR (evaporated film): ν = 720, 799, 830, 955, 1030, 1131, 1199, 1403, 1542, 1675 (C=O, from peptide amide), 1731 (C=O, from ester), 2865, 2940, 3340 (N-H, O-H) cm^{-1}

^{1}H-NMR (400 MHz, MeOD, TMS) (ppm): δ = 4.25-4.21 (br, NH_2-C(=O)-C<u>H</u>-NH-C(=O)-C<u>H</u>-NH-C(=O)-C<u>H</u>-NH-C(=O)-C<u>H</u>-CH_2-), 4.15 (br,NH_2-C<u>H</u>-CH_2-S), 4.00 (t, CH_2-C<u>H_2</u>-O), 3.34 (t, CH_2-C<u>H_2</u>-OH), 2.95 (dd, -C<u>H_2</u>-S-C<u>H_2</u>), 2.57-2.44 (t, -C<u>H</u>-CH_2-CH_2-COO-, -CH-C<u>H_2</u>-CH_2-COO-, -CH-CH_2-C<u>H_2</u>-COO-), 2.21 (br, -N-CH_2-C<u>H_2</u>-C(=O)-O), 1.60 (br, -O-CH_2-C<u>H</u>2-C<u>H</u>2-CH_2-O), 1.38 (br, -C<u>H_2</u>-CH_2-C<u>H_2</u>-CH_2-OH), 1.23 (br, -N-$(CH_2)_2$-C<u>H_2</u>-$(CH_2)_2$-OH).

2.2.3 Nanoparticle formation and biophysical characterization

Polymer:siRNA complexes at different weight ratios were prepared by mixing equal volumes of siRNA at 0.01 µg/µL with polymers at different concentrations in AcONa buffer solution (25 mM, pH 5.5). C32-CR3 at 200:1 weight ratio is shown as an example: 4 µL of siRNA (0.25 µg/µL) was diluted in 96 µL of acetate buffer to obtain a final concentration of 0.01µg/µL. 2 µL of C32-CR3 (100 µg/µL) was diluted in 98 µL of acetate buffer to obtain a final concentration of 2 µg/µL. Then, siRNA was added over polymer solution and was mixed by pipetting, followed by vortexing for 5 seconds and was incubated at room temperature for 30 minutes.

2.2.3.1 Gel retardation assay

To perform siRNA retardation assay, different polymer:siRNA (w/w) ratios was added over agarose gel (2.5% of agarose w/v) in Tris-Acetate-EDTA (TAE) buffer containing ethidium bromide (1 µg/mL). Finally, samples were run for 1 hour at 80V (Apelex PS 305, France) and siRNA bands were visualized by UV irradiation.

2.2.3.2 Dynamic Light Scattering (DLS)

Particle size and surface charge measurements of the complexes were determined by Dynamic Light Scattering (DLS) at room temperature with a Zetasizer Nano ZS (Malvern Instruments Ltd, United Kingdom, 4-mW laser) using a wavelength of 633 nm. Measurements were carried out mixing 200 µL of complexes in AcONa buffer solution (25 mM, pH 5.0) with 3 mL of PBS 1x buffer solution (pH 7.4). Results were plotted as mean and standard deviation of triplicates analysed by intensity.

2.2.3.3 Buffering Capacity

The buffering capacity of end modified pBAEs was determined by acid-base titration. Briefly, 50µL of polymer at 100 mg/mL was dissolved in 5 mL with 150 mM NaCl at final concentration of 1mg/mL. Then, solution pH was adjusted to pH 10 with 0.1 M NaOH. The titration curve was performed by addition of 10 µL aliquots of 0.1 M HCl and pH was measured after each addition with pH meter (Crison Basic 20+, Crison Instruments). This step was repeated until pH solution was stabilized at pH 2.

2.2.4 Transfection of cells with siRNA silencing of green fluorescent protein with siRNA-siGFP

Cellular transfection was carried out using siGFP in MDA MB231 and HeLa GFP cells. Cells were seeded in 96-well plates at 8,000 cells/well and incubated overnight to roughly 80% confluence prior to performing the transfection experiments. Polymer:siRNA complexes were prepared as described previously at 200:1 ratio with AcONa buffer (25mM, pH 5.0). Cells were washed with PBS 1x and siRNA complexes, containing 5 pmol of siGFP, were added at a final concentration of 50nM in serum free medium. Then, cells were incubated for 3 h at 37°C in 5% CO_2 atmosphere. After 3h, the remaining complexes were removed and replaced with 100 µL of DMEM supplemented with 10% FBS, 1% Glutamine and 1% Streptomycin/Penicillin. Polyplus Interferin was used as positive control of transfection, and untreated cells were used as negative control.

Silencing of GFP using polymer:siRNA complexes was measured using flow cytometry (BD LSRFortessa cell analyser). Before, cells were trypsinized with 60 µL of trypsin and fixed with 100 µL of paraformaldehyde (PFA) at 1% and 100 µL of completed medium. A total of 2000 cells were analysed per sample, and fluorescence gating was determined using samples receiving no treatment and treated with commercial polymer (PolyPlus Interferin). Finally, the data was analysed by BD LSRFortessa cell analyser software.

2.2.5 Cellular uptake of fluorescently labelled siRNA with different oligopeptide formulations

Cellular transfection was realized using labelled siRNA (AF546) in MDA MB231 and HeLa GFP cells. Transfection assay was performed in the same manner than previous explain. After 3h, the remaining complexes were removed and cells were trypsinized with 60 µL of trypsin and fixed with 100 µL of paraformaldehyde (PFA) at 1% and 100 µL of completed medium.

2.2.6 Cell viability assay

The influence of siRNA complexes on cell viability was determined using the MTS assay (CellTiter 96® AQueous One Solution Cell Proliferation Assay, Promega Corporation, USA) at 48 h post-transfection as instructed by the manufacturer. Briefly, transfection assay was performed as earlier described. Forty-eight hours later, the medium was removed, cells were washed with PBS 1x and complete medium supplemented with 20% MTS reagent (v/v) was added. Then, cells were incubated

at 37ºC and absorbance was measured every 30 minutes using plate reader (Elx808 Biotek Instruments Ltd, USA) until appropriate absorbance values were obtained.

2.2.7 Amino acid analysis

Amino acid analysis was carried out using nanoparticles loaded with siRNA, as previously explained. 500 µL of nanoparticles using different polymer mixtures at 200:1 weigh ratio were prepared in order to analyse the polymer composition in the resulting nanoparticles. Nanoparticles were filtrated using Amicon Ultra-0.5 centrifugal filters with a membrane of 30 kDa to remove free polymer, this is polymer that did not form nanoparticles. Nanoparticles were washed twice using PBS. Afterwards, purified nanoparticles were mixed with milli-Q water and 12 M HCl solution containing 1% phenol a volume ratio nanoparticle/HCl/milli-Q water 33/50/17 for hydrolysis. Next, mixtures were added into 20 mL vial and inserted in the oven for hydrolysis during 22 hours at 120ºC. After hydrolysis, samples were placed in UPLC vials and evaporated under a stream of nitrogen. Then, each sample was resuspended in 200 µL of 0.1M HCl solution containing 0.147 mg/mL Norvaline as internal standard. Prior to analysis, samples were derivatized by mixing 20 µL of each sample with 60 µL of borate buffer and 20 µL of amino acid derivatizing reagent (AccQ•Tag Ultra Derivatization Kit). The resulting mixture was vortexed, incubated for 1 minute at room temperature and finally incubated for 10 minutes at 55ºC. Finally, the samples were analysed by UPLC following the manufacturer instructions.

2.2.8 Statistical analysis

Statistical analyses were carried out with Graph-Pad Prism (GraphPad Software). All error bars reported are SD unless otherwise indicated. Pairwise comparisons were performed using one-way Student t-tests. Differences between groups were considered significant at P values below 0.05 (* $p < 0.05$, ** $p < 0.01$, *** $p < 0.001$)

2.3 Results and discussion

2.3.1 Synthesis of oligopeptide-modified pBAEs

A new family of bioinspired polymers based on oligopeptide-modification of poly(β-amino ester)s have been designed for efficient RNAi delivery. In order to study the influence of oligopeptide composition on transfection efficiency, viability and cell-specificity, oligopeptide-modified poly(β-amino ester)s were synthesized and biophysically characterized.

Firstly, synthesis of end-modified poly(β-amino ester) polymers was performed via a two-step procedure, as similarly described in materials and methods (Figure II-2).

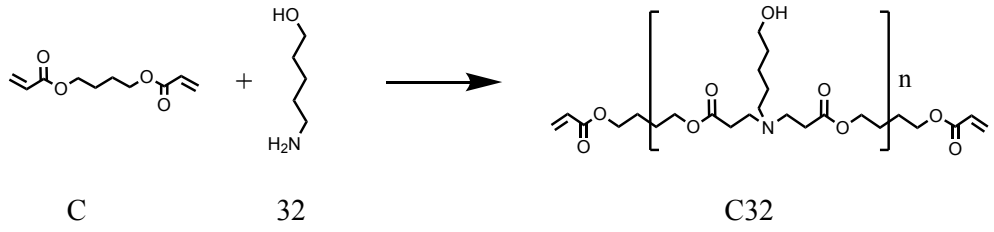

Figure II-2. Synthesis scheme of Poly β-Amino esters. C32 polymer was obtained by addition of the amine to the diacrylate.

Acrylate-terminated C32 intermediate polymer was obtained by conjugate addition of 5-amino-1-pentanol (32) to 1,4-butanediol diacrylate (C) using a slight excess of 1,4-butanediol diacrylate [26][25]. Polymerization was confirmed by ^{1}H-NMR. In addition, polymer molecular weight was corroborate using HPLC-SEC and the resulting C32 polymer had an apparent average molecular weight of approximately 2,500 g/mol (relative to polystyrene standards) and a polydispersity (M_w/M_n) of 1.81, showing a rather broad statistical distribution of polymer chain lengths. Moreover, the average molecular weight was further confirmed by ^{1}H-NMR, and an average molecular weight of approximately 2000 g/mol was obtained. The obtained average molecular weight and polydispersity distributions are in good agreement with the polymer molecular weight achieved in previous studies at the working ratio 1:1.2 (amine-to-diacrylate) [27].

Based on previous data, it was found that chemical-modifications of C32 polymer improved gene transfection. However, previously described end-capping structures based on primary amines or synthetic structures presented some cytotoxicity effects [28]. Then, in order to overcome this limitation, we proposed to modify C32 polymer using natural end-capping, as is shown in Table II-2.

Table II-2 Oligopeptide-moieties used for poly(β-amino ester)s end-capping.

Poly (β-amino ester)s	R	Oligopeptide
Arginine modified pBAEs, R3C-C32-CR3	SH-Cys-Arg-Arg-Arg-$CONH_2$	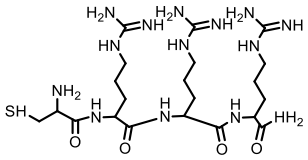
Lysine modified pBAEs, K3C-C32-CK3	SH-Cys-Lys-Lys-Lys-$CONH_2$	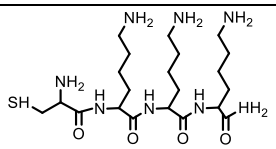
Histidine modified pBAEs, H3C-C32-CH3	SH-Cys-His-His-His-$CONH_2$	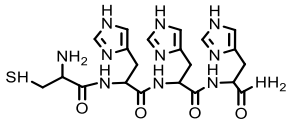
Aspartate acid modified pBAEs, D3C-C32-CD3	SH-Cys-Asp-Asp-Asp-$CONH_2$	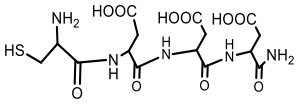
Glutamate acid modified pBAEs, E3C-C32-CE3	SH-Cys-Glu-Glu-Glu-$CONH_2$	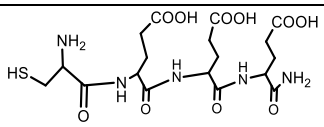

C32 polymer was further modified using oligopeptide moieties via addition of the thiol group of cysteine-terminated cationic and anionic oligopeptides to the acrylate-terminated end-groups of C32 polymer, as is shown in Figure II-3.

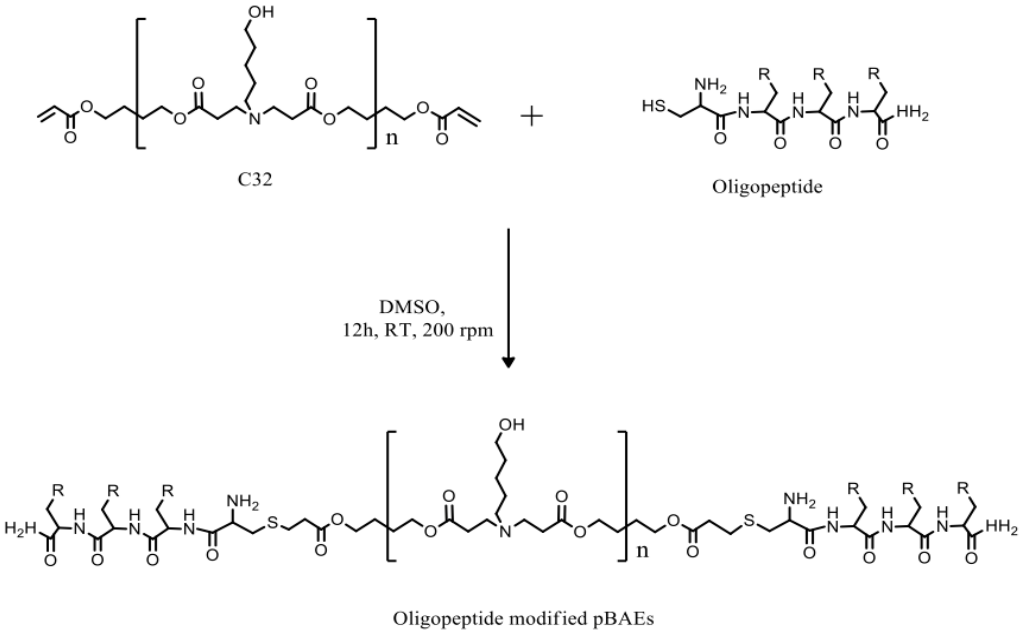

Figure II-3. Structure and synthetic scheme of oligopeptide-modified pBAEs. The synthesis was carried out in DMSO solvent, at room temperature with stirring and overnight. R terminal can be arginine-, lysine-, histidine-, glutamic acid- and aspartic acid-oligopeptide.

Oligopeptide-terminated pBAEs were characterized in terms of molecular structure by ^{1}H-NMR and FT-IR. The chemical structure of new oligopeptide-modified pBAEs was confirmed by the disappearance of acrylate signals and the presence of signals typically associated with amino acid moieties. Both ^{1}H-NMR and FT-IR spectra were in good agreement with the expected synthesized structures and signals from both C32 and the modifying moieties could be observed (materials and methods).

Resulting polymers can show different behavior according to their chemical structures. It can be observed that lysine contains primary amine, arginine contains a guanidinium group and histidine contains tertiary amines. Primary amine and guanidinium group can be easily protonated at acid pH, but tertiary groups needed more acid environment to be protonated. However, all of these polymers have the same structure and only change the side chain of the oligopeptide. In addition, the main difference between anionic oligopeptides is the extra methylene in the side chain of the glutamic acid residues in E3C-C32-CE3, which may confer a slightly higher hydrophobic character than in D3C-C32-CD3. Glutamate and aspartate end-modified pBAEs side chains have a pKa of 4.07 and 3.86, respectively. Therefore, these polymers are negatively charged at psychological pH (7.4). In this case, these polymers cannot be used to condense RNAi because these have the same charge than RNAi. However, these polymers can provide several advantages when are combined with cationic end-modified pBAEs, as previously it has been explained in the introduction. For instance, anionic modified pBAEs may be able to interact with cationic end-modified pBAEs to balance pBAEs charge and improve encapsulation efficiency of nucleic acids. Furthermore, anionic modified pBAEs (also combined with cationic modified-pBAEs) can play an important role in complex destabilization inside of cell, improving nucleic acids release.

2.3.2 Nanoparticle formation and biophysical characterization

Once oligopeptide-terminaed pBAE have been synthetized using positive and negative peptides, they usability was tested. In order to characterized the ability of newly developed polymers to perform polyplexes, different biophysical assays were performed. Polymers formulations were characterized by agarose gel retardation and Dynamic Light Scattering (DLS).

First of all, nanoparticles were formed by mixing polymer dissolved in DMSO with siRNA in acetate buffer. When polymers are dissolved in acetate buffer at pH 5.0, these are protonated and are able to interact with negatively charged siRNA by electrostatic forces. Then, these complexes were mixed with PBS at pH 7.4, which contributes to nanoparticle formation due to the hydrophobicity of the central polyester chain.

2.3.2.1 Agarose gel electrophoresis retardation assay

The siRNA-binding capability of the newly synthesized poly(β-amino ester)s polymers was evaluated by agarose gel electrophoresis at different polymer-to-siRNA ratios (w/w), ranging from 10:1 to 400:1 (Figure II-4).

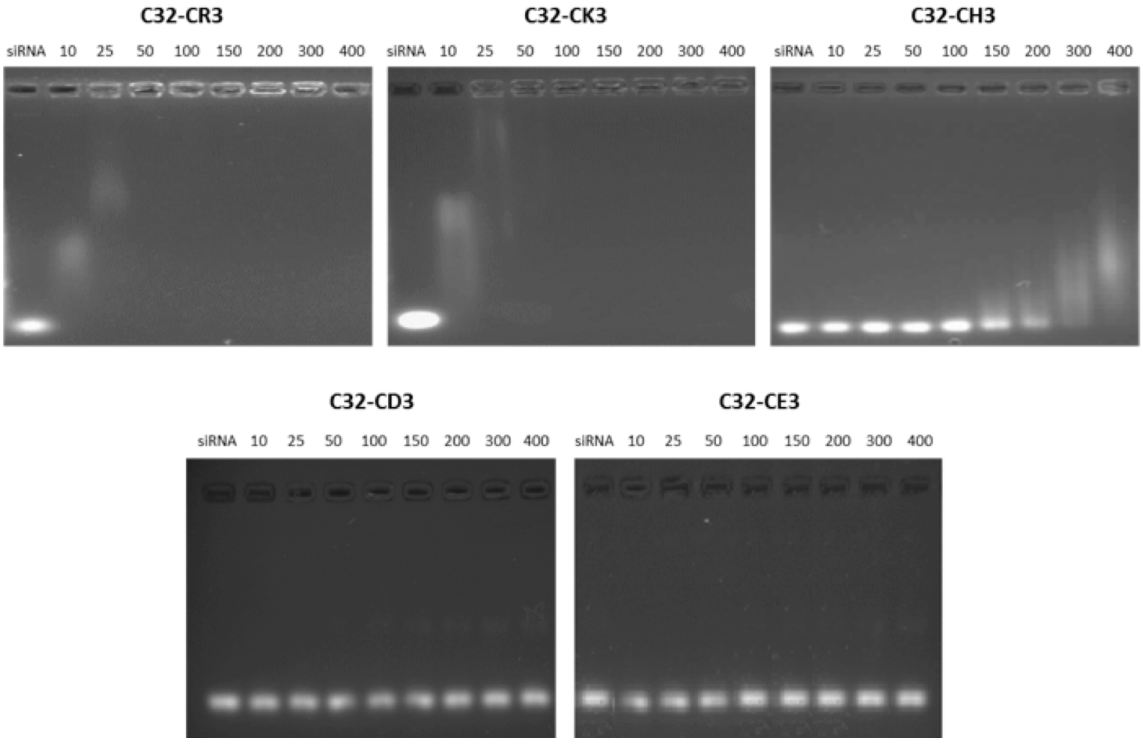

Figure II-4. Gel retardation assay of oligopeptide-terminated PBAES using siGFP siRNA at various weigh ratios. Polymer:siRNA complexes were prepared at different ratios (w/w) ranging from 1:10 to 1:400. Polyplexes were freshly prepared prior the assay and loaded into 2,5% agarose gel containing ethidium bromide and was run 1h hour at 80V.

Arginine- and lysine-terminated poly(β-amino ester)s, C32-CK3 and C32-CR3, showed complete siRNA retardation at 50:1 pBAE-siGFP ratios. In contrast, when siRNA was complexed with histidine-terminated polymers, C32-CH3, polymer-siGFP ratios of 300:1 or higher were required to impede siRNA mobility. Then, histidine-terminated pBAE does not fully complex siRNA between studied ratios. Histidine chemical structure is composed of tertiary amines. In contrast, lysine and arginine are formed by primary and secondary amides, which are readily protonated compared to tertiary amides. Therefore, lysine- and arginine- terminated pBAEs are able to condense more siRNA than histidine complexes.

In addition, complexes prepared with both aspartic and glutamic acid-modified poly(β-amino ester)s, C32-CD3 and C32-CE3, revealed no gel retardation. As previously commented, these results suggest that although the pBAE polymeric chains possess tertiary amines, the negative charges originated from aspartic or glutamic acid residues make complexation unfavourable.

2.3.2.2 Buffering capacity of oligopeptide modified pBAE

Poly(β-amino ester)s possesses high endosomal buffering capacity, which facilitates the endosomal escape of the complexes via the hypothetical proton sponge effect [29], as commented in Chapter I. Oligopeptide modified poly(β-amino ester)s synthetized differ in composition of amino groups, providing us an opportunity to compare the influence of buffering capacity and proton sponge behaviour in physiological environment. In order to evaluate the buffering effect, titration curves of positive and negative oligopeptide-modified pBAE, were performed as described in materials and methods.

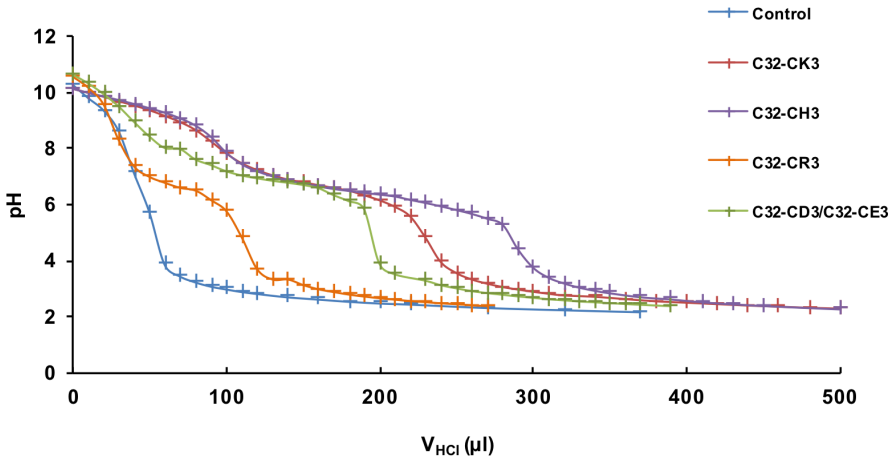

Figure II-5. Proton sponge effect. Titration curve of end modified PBAEs at 1 mg/mL. A solution of polymer (1mg/mL of polymer) in 5 mL of 150mM NaCl was titrated to pH 10 until pH 2 with 0.1M HCl. Control refers to titration of a solution that does not contain polymer.

The highest buffering capacity was observed with histidine-terminated poly(β-amino ester), which demonstrated high buffering in the pH range between 7.5 and 5.3. Lysine, aspartic acid and glutamic acid modified poly(β-amino ester)s presented suitable buffering capacity until pH 5.9. In contrast, poly(β-amino ester)s end-capped with arginine oligopeptides only showed limited buffering capacity in the range between 7.4 and 6.4. Since all polymers come from the same acrylate-terminated pre-polymer C32, the additional buffering capacity observed res from tertiary amine from pBAE backbone. In the negative control, no buffering capacity was observed, therefore DMSO without polymer does not have buffering capacity.

In general, polymers having tertiary amines in their structure show higher buffering effect at the endosomal pH range between 5.0 and 7.5, like histidine-terminated pBAEs, which causes an increase in osmotic pressure that results in disruption of the endosome [29]. Therefore, histidine-terminated poly(β-amino ester)s can play an important role in polymer formulations for acids nucleic delivery.

2.3.2.3 Determination of the nanoparticle size and zeta potential of complexes via Dynamic Light Scattering

In gel retardation assay, we have determined the minimum polymer:siRNA ratio able to fully condense siRNA. The next step towards characterizing RNA complexation with oligopeptide-modified pBAEs is to determine the size of the resulting complexes. Ideally, complexes should be obtained as discrete nanoparticles with average diameters comprised between 100 and 400 nm, which are suitable for cellular uptake. Particle size analysis using DLS is used to obtain the average hydrodynamic radius of the polymer:siRNA complexes. In addition, complexes are further characterized by measuring their zeta potential in order to determine the charge on the surface of the nanoparticles.

The first step was to determine the optimal conditions for nanoparticle formation, then a gradient of polymer-siRNA complexes was performed. Therefore, 100:1, 200:1 and 300:1 ratios were analyzed by DLS using freshly prepared complexes of arginine-, lysine- and histidine- modified poly(β-amino ester)s (Figure II-6), which are able to condense nucleic acids as previously observed in Figure II-4.

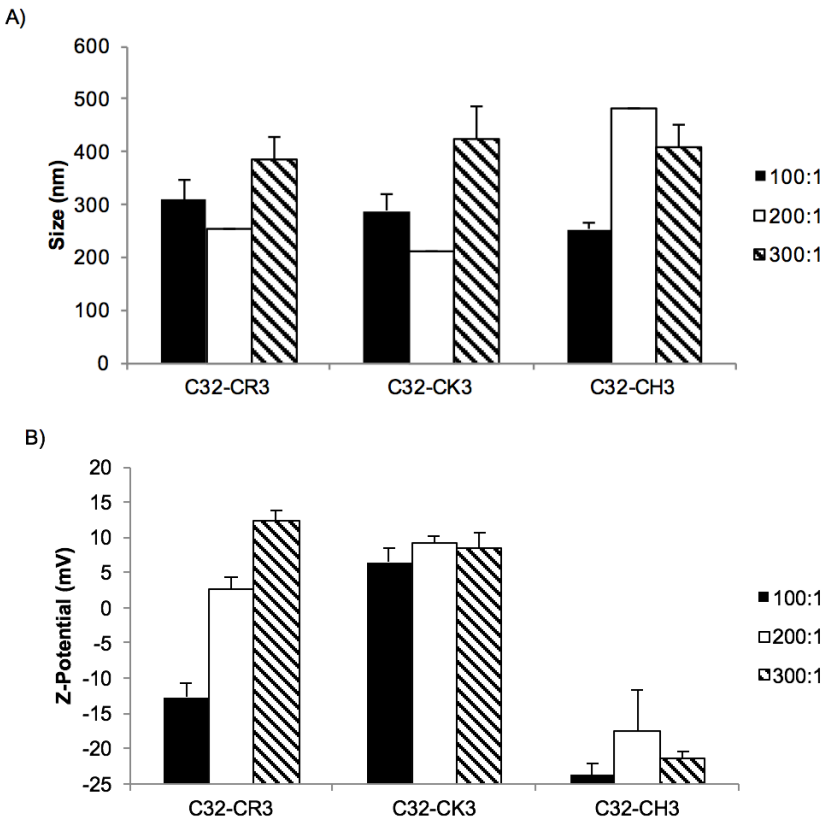

Figure II-6. Biophysical characterization of oligopeptide-modified pBAEs. Average hydrodynamic diameter (a) and zeta potential determination (b) of pBAE:siRNA nanoparticles prepared at 100:1, 200:1 and 300:1 polymer:siGFP ratio (w/w) with different oligopeptide-modified pBAE polymers determined by DLS. Results are shown as mean and standard deviation of triplicates analysed by intensity.

The average hydrodynamic diameter of particles obtained upon complexation of siRNA with oligopeptide-modified pBAEs ranged from 200 nm to 500 nm depending on the nature of the modifying amino acid and the ratio. In general, nanoparticles showed the smallest hydrodynamic diameters at 200:1 ratios. Interestingly, nanoparticles prepared from polymers modified with arginine-containing oligopeptides, C32-CR3, showed little size variation, ranging from 310 to 386 nm, when the polymer/siRNA ratio was increased. In contrast, complexes made of lysine-bearing polymers, C32-CK3, showed a greater size heterogeneity depending on the pBAE/siRNA ratio. On the other hand, end-modified poly(β-amino ester)s with histidine-oligopeptide presented a higher particle size at 200:1 polymer:siRNA ratio or higher.

Zeta Potential results showed that the w/w ratio of pBAE:siRNA had a deep influence on the resulting surface charge of the complexes. In general, it was observed that zeta potential increased at higher pBAEs:siRNA ratios. The highest zeta potential at the lower polymer:siRNA ratio was obtained for Lysine end-modified pBAE achieving a positive zeta potential of 10mV at 100:1 ratio. For ratios greater than 200:1 (polymer/siRNA), all tested polymers resulted in complexes having a positive surface charge, except for histidine-modified poly(β-amino ester)s. The presence of tertiary amines in its chemical structure makes that side chain pka lower than lysine and arginine amino acids, therefore this polymer requires a more acidic environment for obtaining a protonated structure that is able to condense siRNA.

With the purpose of obtaining nanoparticles with positive or even slightly negative charged surfaces, as previously discussed, 200:1 polymer:siRNA ratio is needed as Figure II-6 is shown. Moreover, at this ratio complexes present a size average between 200 nm and 300nm, except H3C-C32-CH3. However, histidine residues provide high buffering capacity to further enhance endosome escape. Therefore, a combination of different cationic pBAEs would be a good strategy to improve siRNA transfection.

2.3.3 Tailoring of the size and the zeta potential of nanoparticles using positively-charged oligopeptide-modified pBAEs

According to the previous results, the average hydrodynamic diameter and the zeta potential of pBAE/siRNA nanoparticles showed a high dependence on the chemical nature of the modifying amino acid. In order to determine whether the properties of the pBAE/siRNA particles could be further tailored by incorporating different oligopeptide/amino acid chemistries in the polyplexes, mixtures of different oligopeptide-modified pBAE polymers were used to complex siRNA and the physicochemical properties of the resulting particles were determined by DLS (Figure II-7).

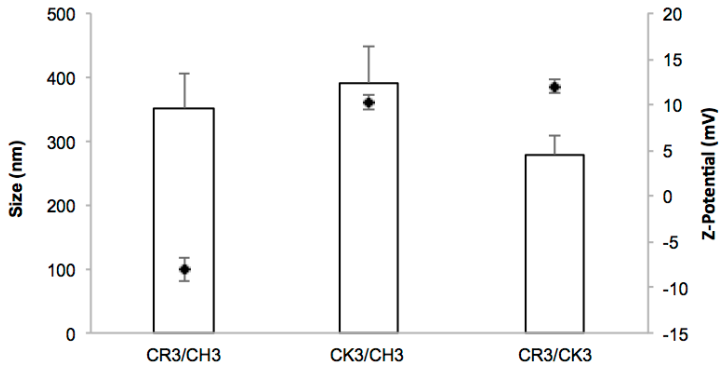

Figure II-7. Average hydrodynamic diameter and zeta-potential distributions of pBAEs mixtures modified with cationic oligopeptides. All particles were prepared at a pBAE/siRNA ratio of 200:1 (w/w).

The use of binary formulations of different oligopeptide-modified pBAEs had a significant influence on the size and zeta potential of the resulting nanoparticles, while the polydispersity index was maintained low. Mixtures of arginine- and histidine-modified pBAEs resulted in negatively charged nanoparticles with an intermediate average hydrodynamic diameter, when compared to nanoparticles obtained from arginine or histidine-modified polymers alone, 351 nm *vs.* 255 and 481 nm, respectively. In contrast, nanoparticles obtained from a mixture of lysine- and histidine-modified pBAEs resulted in positively charged complexes with an average hydrodynamic diameter of nearly 400 nm. Interestingly, when arginine- and lysine-modified pBAEs were combined with siRNA, positively charged (12 mV) nanoparticles below 300 nm in diameter were obtained.

2.3.3.1.1 Tailoring of the size and the zeta potential of nanoparticles using positively- and negatively-charged oligopeptide-modified pBAEs

Although poly(β-amino ester) polymers end-modified with oligopeptides bearing either aspartic or glutamic acid residues were not able to complex siRNA *per se* at w/w ratios up to 400:1 pBAE/siRNA, these negatively-charged pBAE polymers were mixed with other positively-charged pBAE polymers in order to obtain nanoparticles with varying size and zeta potential, similarly as shown in Figure II-7. Different weight-to-weight ratios of cationic and anionic oligopeptide-modified pBAEs were formulated with siRNA and the physicochemical properties of the resulting nanoparticles were determined using dynamic light scattering measurements. First, different formulations of lysine-modified pBAE, as the cationic polymer, and glutamic acid-modified pBAE, as the anionic polymer, at ratios ranging from 95:5 to 50:50 (w/w) were complexed with siRNA and the average hydrodynamic diameter and zeta potential were determined (Figure II-8).

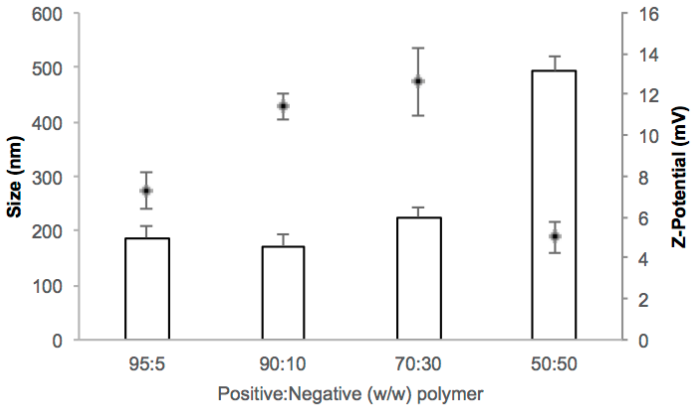

Figure II-8. Average hydrodynamic diameter and zeta-potential distributions of nanoparticles prepared from siGFP and CK3/CE3 polymer at different C32-CK3 and C32-CE3 proportions. All complexes were prepared at a pBAE/siRNA ratio of 200:1 (w/w).

Experimental determination of the nanoparticle size revealed that the average hydrodynamic diameter remained approximately constant at 200 nm for ratios up to 70:30 (w/w) cationic/anionic mixtures. However, the zeta potential of complexes obtained at ratios up to 70:30 cationic/anionic showed a significant increase with increasing presence of anionic oligopeptide-modified pBAEs in the formulation, i.e. from 7.3 mV for 95:5 ratio to 12.6 mV for 70:30 ratio. In contrast, when the ratio of cationic/anionic pBAE formulations was increased to 50:50 (w/w) resulted in nanoparticles having a significantly greater average hydrodynamic diameter, exceeding 500 nm and a positive zeta potential of 5.1 mV, suggesting that complexation was destabilized.

To further assess the binding ability of mixtures of cationic- / anionic- oligopeptide modified pBAEs at 70:30 ratio, agarose gel retardation assay was carried out, as shown Figure II-9.

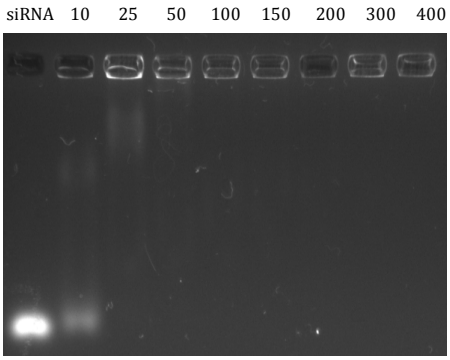

Figure II-9. Gel retardation assay of positive/negative oligopeptide-terminated PBAES 7:3 (w/w) using siRNA. Polymer:siRNA complexes were formed at different ratio from 1:10 (w/w) to 1:400 (w/w). Nanoparticles was realized using lysine as positive oligopeptide end-modified pBAEs and acid aspartic as negative oligopeptide end-modified pBAEs. Polyplexes were incubated at room temperature for 30 minutes, each sample was loaded into 2,5% agarose gel containing ethidium bromide and was run 1h hour at 80 V.

Gel retardation assay showed a fully siRNA complexation at ratios higher than 50:1, obtaining a similar behaviour than lysine oligopeptide-modified pBAEs. Then, these results suggest a favourable complexation when anionic modified pBAE was mixed with cationic modified pBAE.

Then, in order to evaluate the effect of the amino acid nature on the physicochemical properties of other cationic/anionic formulations, the size and zeta potential was determined in siRNA-nanoparticles obtained from lysine- (CK3) and arginine- (CR3) modified pBAEs, as cationic polymers, and glutamic acid- (CE3) and aspartic acid- (CD3) modified pBAEs, as anionic polymers, at a cationic/anionic ratio of 70:30 (Figure II-10).

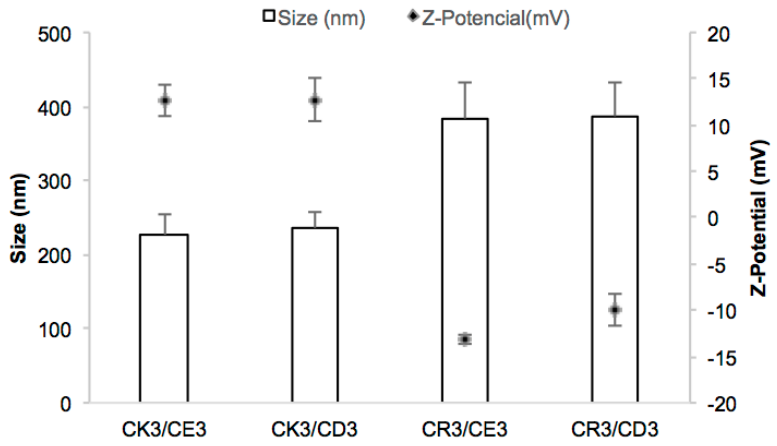

Figure II-10. Average hydrodynamic diameter and zeta-potential distributions of nanoparticles prepared from siGFP and cationic and anionic oligopeptide-modified pBAEs mixtures at a fixed cationic/anionic ratio of 70:30 (w/w). All complexes were prepared at a pBAE/siRNA ratio of 200:1 (w/w). Results are shown as mean and standard deviation of triplicates.

Results shown in Figure II-10 revealed that the chemical composition of the oligopeptide end-modifying groups had a dramatic effect on the physicochemical properties of the resulting nanoparticles. Polyplexes prepared with lysine-bearing oligopeptides, CK3/CE3 and CK3/CD3, presented particles with an average hydrodynamic radius of approximately 220 nm and a zeta potential greater than 12 mV. In contrast, polyplexes prepared with arginine-bearing oligopeptides, CR3/CE3 and CR3/CD3, resulted in larger nanoparticles with an average hydrodynamic radius of approximately 400 nm and negative zeta potentials.

2.3.3.2 Amino acid analysis of different polyplexes formulations

In order to ensure that the chemical composition of the formulation mixture was maintained upon complexation of siRNA, nanoparticles obtained from the different formulations were analysed by amino acid analysis (Table II-3).

Table II-3. Analysis of the amino acid composition of polyplexes prepared with different mixtures of poly(β-amino ester) polymers.

Poly(β-amino ester) polymer mixture	Theoretical ratio (weight percentage)	Experimental ratio (weight percentage)
R/H	50:50	51:49
K/H	50:50	55:45
R/K	50:50	58:42
R/D	70:30	70:30
K/D	70:30	77:23
R/E	70:30	71:29
K/E	70:30	69:31

Analysis of the chemical composition of the nanoparticles after purification revealed that the ratio of cationic and anionic poly(β-amino ester) polymers was maintained in the particles upon complexation. Therefore, these results suggest that the difference in zeta potential may necessarily derive from the different packing distribution of siRNA with cationic and anionic pBAE polymers. Since both cationic and anionic oligopeptide-modified poly(β-amino ester) polymers were obtained from the same diacrylate precursor, C32, the experimental differences in surface charge distribution are probably attributed to the chemical nature of the end-modifying amino acid residues and their different interactions with the phosphate groups of the siRNA backbone. It has been earlier described that guanidinium-phosphate interactions may be stronger and more directional than ammonium-phosphate interactions, suggesting that guanidinium groups may be more effective as phosphate complexing moieties [30]. Therefore, we hypothesize that when arginine-modified poly(β-amino ester) polymer is formulated with an anionic poly(β-amino ester) polymer to complex siRNA, the higher affinity of the guanidinium groups towards phosphate groups may affect the distribution of poly(β-amino ester) chains in the nanoparticle structure, leaving the amino acid residues of the anionic pBAE chains more exposed to the surface of the nanoparticle and resulting in lower zeta potential values. In contrast, in cationic/anionic mixtures of lysine- and glutamic acid- or aspartic acid-modified poly(β-amino ester) polymers, the ammonium groups of lysine residues may favour both cationic pBAE - anionic pBAE and cationic pBAE - siRNA interactions, resulting in a more random distribution of polymer chains, which may leave more lysine residues exposed on the nanoparticle surface, resulting in a greater zeta potential.

To conclude, our results indicate that formulation of mixtures of cationic and anionic poly(b-amino ester) polymers have the potential to tune the surface of the resultant RNAi polyplex formulation. We suggest that this tunability may be a powerful strategy to control electrostatic interactions between the polyplex formulation and physiological media, making them a promising vector for future therapeutic applications.

2.3.4 Silencing efficiency of siRNA delivered using mixed formulations of oligopeptide-modified pBAEs

In order to evaluate the influence of the amino acid nature of oligopeptide-modified poly(β-amino ester) polymers on gene silencing efficiency, two different cell lines stably expressing green fluorescent protein, MDA-MB-231/GFP and Hela-GFP cells, were transfected with anti-GFP siRNA (siGFP) using different pBAE formulations. Silencing efficiency was evaluated by measuring the decrease in cell fluorescence determined by flow cytometry. GFP silencing of different formulations of oligopeptide-modified poly(β-amino ester)s was compared to a commercially available transfection reagent, Polyplus Interferin®, as shown in Figure II-11.

A)

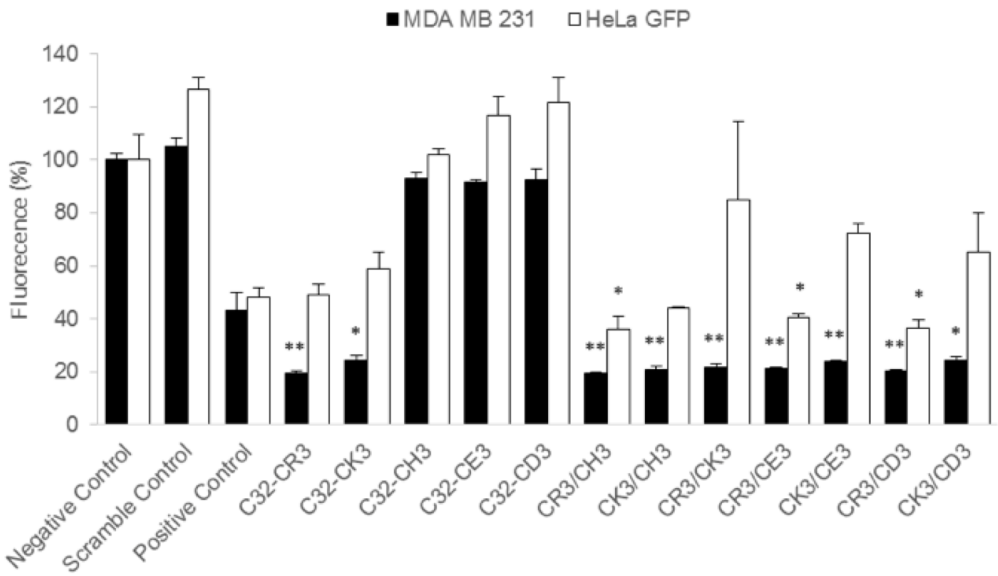

B)

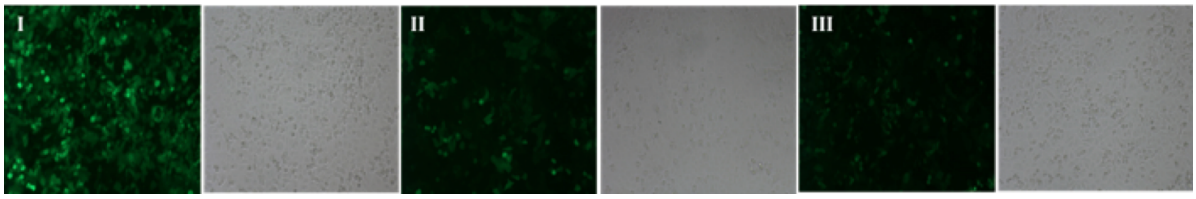

Figure II-11. Knockdown efficiency using different oligopeptide-modified pBAEs. (a) Gene silencing of MDA-MB-231-GFP and Hela cells transfected with different pBAE polymer nanoparticles. MDA-MB- 231-GFP and Hela-GFP cells were transfected with siGFP at a final concentration of 50 nM of siGFP/well and were determined after 48 h by flow cytometry. Results are shown as mean and standard deviation of triplicates. Statistical significance was determined using positive control cells as control group. *$p < 0.05$, ** $p < 0.01$, *** $p < 0.001$. (b) Light and confocal laser scanning microscopic images of MDA MB 231 cells: using arginine end-modified PBAEs carriers with siGFP at 50nM: (I) cells untreated, (II) cells transfected with Interferin (positive control) and (III) cells transfected using C32-CR3 polymer at a final concentration of 50 nM of siGFP.

Transfection of MDA cells with nanoparticles prepared from oligopeptide-modified poly(β-amino ester)s and siGFP resulted in efficient and specific silencing of green fluorescent proteins, when compared to negative and scrambled control. In general, oligopeptide-terminated poly(β-amino ester)s achieved a higher reduction in cell fluorescence than the commercially available control reagent, ~20% *vs.* ~40% respectively, except for polymers modified with oligopeptides containing histidine, aspartic acid or glutamic acid. These results correlate well with the low complexation efficacy observed in the gel retardation assays (Figure II-4), suggesting that these oligopeptide-modified poly(β-amino ester)s were not able to complex siRNA. Interestingly, formulations prepared from mixed oligopeptide-terminated poly(β-amino ester)s showed high gene silencing efficiency, approximately 80% reduction in cell fluorescence, even if one of the oligopeptide-terminated poly(β-amino ester) did not result in cell transfection per se. Interestingly, arginine-modified poly(β-amino ester)s with anionic modified poly(β-amino ester)s complex present a negative surface charge, as previously demonstrated, however this formulation present a high silencing efficiency.

In contrast to MDA cells, a greater silencing heterogeneity was observed when Hela cells, which is a hard to transfect cell line, were transfected with oligopeptide-modified poly(β-amino ester) formulations. Nanoparticles prepared from single oligopeptide-modified poly(β-amino ester) polymers did not promote greater GFP silencing than commercial positive control. However, when different oligopeptide-modified pBAE polymers were formulated with siGFP, significantly higher silencing efficiencies were achieved in some cases. In the case of cationic pBAE mixtures, formulations prepared with histidine- and either arginine- or lysine-bearing pBAE polymers showed superior GFP knockdown, when compared with commercially available transfection reagent, i.e. 35% (CR3/CH3) and 44% (CK3/CH3) *vs.* 49%. In contrast, formulations prepared with mixtures of arginine- and lysine-bearing pBAE polymers showed poor silencing efficiency in Hela cells. Interestingly, when mixtures of cationic and anionic pBAE polymers were used, only formulations that had arginine-modified pBAEs achieved significantly superior gene silencing than positive control, independently of the amino acid chemical nature of the anionic pBAE polymer. On the contrary, pBAE formulations containing lysine-modified pBAE as the cationic polymer were less efficient than the commercial control, resulting in a cell fluorescence decrease of approximately 30%.

2.3.4.1 Cellular uptake of siRNA delivered using mixed formulations of oligopeptide-modified pBAEs

In order to determine which polymer formulation was more efficient at delivering siRNA, cellular uptake of a fluorescently-labelled nucleic acid delivered using different formulations of poly(β-amino ester) polymers was quantified. Briefly, MDA MB 231 and HeLa-GFP cells were incubated with nanoparticles prepared from different pBAE formulations containing AlexaFluor 546 labelled siRNA and the fluorescence of cells resulting from nanoparticle uptake was determined by flow cytometry (Figure II-12).

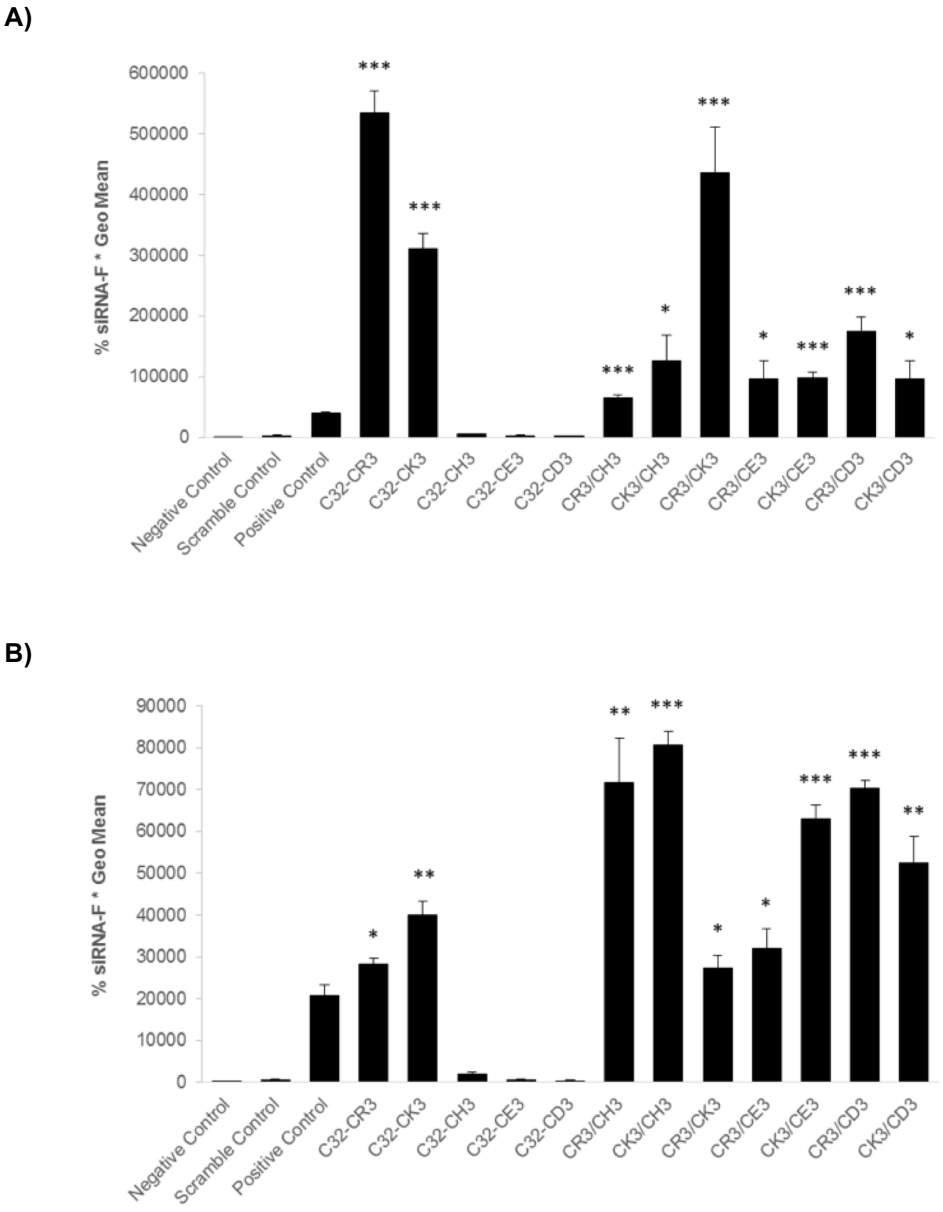

Figure II-12. Cellular uptake of fluorescently-labelled particles prepared from AF546-labeled siRNA and different oligopeptide-terminated poly(β-amino ester) formulations. a) MDA MB 231 cells and b) HeLa-GFP cells. Cells were transfected at siRNA-F (AlexaFluor 546) expression was determined after transfection by flow cytometry and plotted as percentage of positive cells multiplied by the GeoMean fluorescence of the positive population. Results are shown as mean and standard deviation of triplicates. Statistical significance was determined using positive control cells as control group. *$p < 0.05$, ** $p < 0.01$, *** $p < 0.001$.

Analysis of cells incubated with fluorescently-labelled complexes showed differential uptake depending on the poly(β-amino ester) formulation for both cell lines. In general, MDA MB 231 cells showed greater cell uptake when compared with HeLa-GFP cells, confirming that HeLa-GFP cells were more difficult to transfect. For MDA MB 231 cells, oligopeptide-terminated pBAEs showed higher levels of cellular uptake than Polyplus Interferin control, except for nanoparticles prepared from histidine-, glutamic acid- and aspartic acid-terminated polymers, which already showed no GFP silencing (Figure II-11). Complexes prepared with arginine- or lysine-modified poly(β-amino ester)s or

mixtures thereof showed the highest levels of cellular uptake, achieving a cell fluorescence up to 14 fold higher than cells transfected with the commercial control. Interestingly, cationic/cationic and cationic/anionic pBAE formulations resulted in more modest cellular uptake, ranging from 1.5 to 4-fold higher cellular fluorescence, when compared to the commercial transfection agent. These results suggest that despite showing better silencing efficiency (Figure II-12), mixtures of pBAE polymers resulted in lower cellular uptake, suggesting that probably endosomal escape or unpacking features was more efficient than in particles prepared from single pBAE polymers.

When the cell uptake of pBAE polymers was evaluated in HeLa-GFP cells, different cellular fluorescence was observed depending on the amino acid nature of the oligopeptides used for pBAE end-modification. As similarly observed in MDA MB 231 cells, nanoparticles prepared from histidine-, glutamic acid- and aspartic acid-modified pBAE polymers alone showed almost negligible cell uptake. Interestingly, cationic/cationic pBAE mixtures showed significantly greater cell uptake when histidine-modified pBAE was present in the formulation mixture, achieving 3.5 and 4-fold higher cell fluorescence for CR3/CH3 and CK3/CH3 mixtures respectively, when compared to the commercial control. Cationic/anionic poly(β-amino ester) mixtures showed greater cellular uptake than their constituting oligopeptide-modified polymers alone, reaching up to 3.4-fold higher cell fluorescence than commercial control.

Interestingly, our results do not suggest a clear trend between cellular uptake and the silencing efficiency and the zeta potential of nanoparticles in both cell lines, suggesting that charge balancing of the nanoparticles due to the introduction of anionic polymers may not necessarily result in fewer nanoparticle-cell membrane interactions. These results suggest that the chemical composition and the charge distribution rather than the zeta potential alone may have a deeper influence in cell uptake, as it naturally occurs in capsidated viruses, whose surfaces are decorated with different ionizable amino acids that are responsible for interactions between viruses and various structural components of the cell [31]. Our group and others have recently shown that appropriate choice of the end-modifying group of poly(β-amino ester) polymers or even mixtures of two or more differently terminated poly(β-amino ester)s may confer cell-specific gene delivery properties [25,32,33]. Other authors have described the coating of pre-fabricated polyplexes with anionic polymers or lipids to produce ternary polyplexes, as a way to engineer the surface charge of polyplexes and control the tissue specificity of the resulting particles [9,16,34]. However the use of mixtures of cationic and anionic poly(β-amino ester) polymers to form nanoparticles in the presence of siRNA, is in our opinion new and represents a more simple and attractive procedure to tailor the surface of the nanoparticles and control their silencing efficiency in a cell dependent manner.

2.3.5 Cell viability assessment of cells transfected with formulations of oligopeptide-modified pBAEs

The next step was to assess the biocompatibility of oligopeptide-modified pBAE polymers as delivery materials for gene silencing applications, the viability of MDA MB 231 and Hela cells was determined after transfection with different poly(β-amino ester) polymeric formulations. Cell viability was determined at 48 hours post-transfection using the MTS assay (Figure II-13).

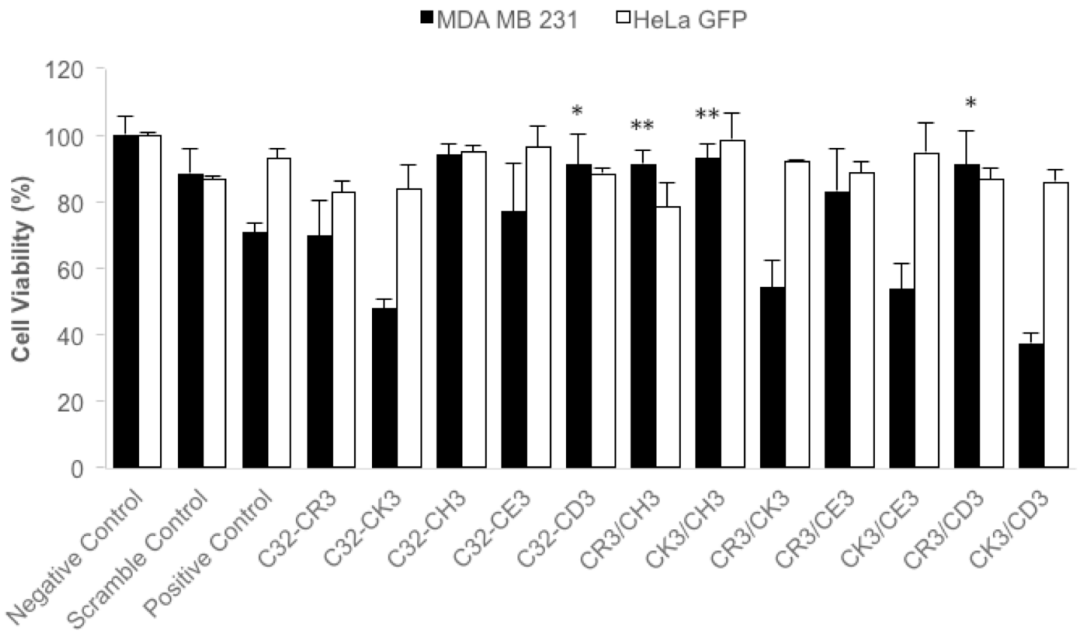

Figure II-13. Cell viability of MDA-MB231 and Hela cells transfected with siGFP and different poly(β-amino ester) formulations. Cell viability was determined at 48 hours by MTS assay and plotted as percentage of viable cells relative to a control of untreated cells. Negative control represents untreated cells; scramble control corresponds to an siRNA scrambled control delivered using C32-CR3 polymer; positive control is the commercial transfection agent Polyplus Interferin; CR3/CH3, CK3/CH3 and CR3/CK3 are mixtures of cationic polymers at 1:1 ratio (w/w); CR3/CE3, CK3/CE3, CR3/CD3 and CK3/CD3 are mixtures of cationic/anionic polymers at 7:3 ratio (w/w). Results are shown as the mean and standard deviation of triplicates. Statistical significance was determined using positive control cells, *$p < 0.05$, ** $p < 0.01$, *** $p < 0.001$.

Viability of MDA MB 231 and Hela cells transfected with nanoparticles prepared with oligopeptide-modified poly(β-amino ester) polymers was generally superior than cells treated with positive control, Interferin. In general, HeLa-GFP cells showed greater cell viability when compared to MDA MB 231 cells transfected with the same pBAE formulations, which probably reflects the fact that cellular uptake was lower in HeLa-GFP cells, as shown in Figure II-12. Similarly, nanoparticles prepared from poly(β-amino ester) polymers end-modified with histidine, glutamic acid or aspartic acid showed remarkably high cell viabilities, however these values were probably the result of the low transfection efficiencies shown by these polymers. Interestingly, some formulations of cationic/cationic polymers, such as CR3/CH3 and CK3/CH3, or cationic/anionic polymers, such as CR3/CE3 and CR3/CD3, which were highly efficient at silencing GFP expression, also showed remarkable cell viabilities greater than 80%, or even 95% in some cases, such as for mixtures of lysine- and histidine-modified

pBAE polymers (CK3/CH3). Despite these remarkably favourable cytocompatibility, exceptions of lower cell viabilities were also observed especially in complexes prepared with mixtures containing lysine-modified pBAE polymers, such as CR3/CK3, CK3/CE3 and CK3/CD3, which resulted in a cell viability comprised between 40 and 55% relative to commercial control.

Recent studies have shown that introduction of negative charges mitigate the toxicity commonly associated with the high density of positive charges of polyplexes [35,36]. Then, we have observed amino acid-related correlation between zeta potential and cell viability. As previously commented, mixtures of lysine-modified and negatively-charged pBAE polymers formed nanoparticles with positive zeta potential, which present lower cell viabilities. In contrast, particles having negative zeta potential, which were obtained from arginine-modified and negatively-charged pBAE polymers, CR3/CD3 and CR3/CE3 mixtures, resulted in excellent cell viability.

2.4 Concluding remarks

The results of this chapter show that RNAi polyplexes can be designed in a cell-specific way using different combinations of oligopeptides-end modified pBAE. We observed that surface charge of polyplexes can be tuned by varying their oligopeptide compositions, obtaining a powerful strategy to control their interaction with physiological media.

To reach this aim, in this chapter, different C32 polymer were modified using positive amino acids (arginine, lysine, and histidine) and negative amino acids (aspartic acid and glutamic acid). After that, newly oligopeptide-modified pBAE demonstrated to efficiently encapsulate nucleic acids as particles of nanometric size. Formulation of siRNA with pBAE polymers modified with positively-charged oligopeptides resulted in efficient siRNA complexation, as observed by gel retardation assay and dynamic light scattering. In addition, it was observed that mixtures of pBAE polymers resulted in complexes with tuneable features, indicating that polymer formulation may be a versatile strategy to control the properties of nanoparticles. However, RNAi complexation was not achieved when pBAE polymers modified solely with negatively-charged oligopeptides were used. Nevertheless, their mixtures with either arginine- or lysine-modified pBAE polymers resulted in discrete nanoparticle formation. We observed that accurate formulation of positively- and negatively-charged pBAE polymers allowed control of nanoparticle composition and features, especially zeta potential, which could be fine-tuned depending on the amino acid nature of pBAE polymers and their mixture composition.

Taking in account all the previously reported features, newly developed pBAEs were used to deliver a functional RNAi. *In vitro* experiments demonstrated that cationic- or mixtures of cationic- with cationic- or anionic- oligopeptides polyplexes achieved good GFP knockdown efficiencies comparable to a commercial transfection reagent in MDA MB 231 cells. In contrast, greater silencing heterogeneity was observed in HeLa-GFP cells, which formulations prepared with histidine- and either arginine- or lysine-bearing pBAE polymers showed superior GFP knockdown than positive control. In addition, highly GFP silencing was obtained using a mixture of arginine- and glutamic acid- bearing pBAE.

In contrast, a trend between cellular uptake and the silencing efficiency was not clearly observed. These results suggest that nanoparticle-cell membrane interactions could be controlled by controlling oligopeptide composition, modulating their cell uptake. However, high uptake is not related with silencing efficiency and therefore polyplexes have to be designed to obtain a modest cellular uptake with high silencing efficiencies, such as mixtures of cationic- / anionic- oligopeptide modified pBAEs.

Finally, we observed that the introduction of negative charges mitigates the toxicity commonly associated with the high density of positive charges of polyplexes, as previously discussed in the introduction. Nanoparticles with positive zeta potential present lower viability values compared to nanoparticles with slightly negative surface charge. Particularity, we observed amino acid-related correlation between zeta potential and cell viability, confirming these results.

In conclusion, we have developed a new strategy to design cell-specific and cell-efficient RNAi delivery vectors that differs from common methodologies using oligopeptide-modified pBAEs. Their easy manipulation and formulation using a combination of synthetic polymer and natural peptides, give them a promising potential inside of medical field. Therefore, in the next chapter, we are going to explore the use of newly developed polymers to carefully control gene expression of difficult-to-transfect and delicate cell line, such as stem cells.

2.5 References

[1] R. Titze-de-Almeida, C. David, S.S. Titze-de-Almeida, The Race of 10 Synthetic RNAi-Based Drugs to the Pharmaceutical Market, Pharm. Res. 34 (2017) 1339–1363. doi:10.1007/s11095-017-2134-2.

[2] K.A. Whitehead, R. Langer, D.G. Anderson, Knocking down barriers: advances in siRNA delivery, 8 (2009). doi:10.1038/nrd2742.

[3] G. Zuber, E. Dauty, M. Nothisen, P. Belguise, J.-P. Behr, Towards synthetic viruses, Adv. Drug Deliv. Rev. 52 (2001) 245–253. doi:http://dx.doi.org/10.1016/S0169-409X(01)00213-7.

[4] G. Jacobson, Biodegradable nanoparticles with sustained release of functional siRNA in skin, J. Pharm. Sci. 99 (2010) 4261–4266. doi:10.1002/jps.

[5] L.M. Ensign, C. Schneider, J.S. Suk, R. Cone, J. Hanes, Mucus Penetrating Nanoparticles: Biophysical Tool and Method of Drug and Gene Delivery, Adv. Mater. 24 (2012) 3887–3894. doi:10.1002/adma.201201800.

[6] M. de la Fuente, N. Csaba, M. Garcia-Fuentes, M.J. Alonso, Nanoparticles as protein and gene carriers to mucosal surfaces, Nanomedicine. 3 (2008) 845–857. doi:10.2217/17435889.3.6.845.

[7] L. Novo, L.Y. Rizzo, S.K. Golombek, G.R. Dakwar, B. Lou, K. Remaut, E. Mastrobattista, C.F. van Nostrum, W. Jahnen-Dechent, F. Kiessling, K. Braeckmans, T. Lammers, W.E. Hennink, Decationized polyplexes as stable and safe carrier systems for improved biodistribution in systemic gene therapy, J. Control. Release. (n.d.). doi:http://dx.doi.org/10.1016/j.jconrel.2014.08.028.

[8] Y. Wang, Z. Xu, R. Zhang, W. Li, L. Yang, Q. Hu, A facile approach to construct hyaluronic acid shielding polyplexes with improved stability and reduced cytotoxicity, Colloids Surfaces B Biointerfaces. 84 (2011) 259–266. doi:http://dx.doi.org/10.1016/j.colsurfb.2011.01.007.

[9] G. Jiang, S.-H. Min, E. Oh, S. Hahn, DNA/PEI/Alginate polyplex as an efficientin vivo gene delivery system, Biotechnol. Bioprocess Eng. 12 (2007) 684–689. doi:10.1007/BF02931086.

[10] M.C. Woodle, P. Scaria, S. Ganesh, K. Subramanian, R. Titmas, C. Cheng, J. Yang, Y. Pan, K. Weng, C. Gu, S. Torkelson, Sterically stabilized polyplex: ligand-mediated activity, J. Control. Release. 74 (2001) 309–311. doi:http://dx.doi.org/10.1016/S0168-3659(01)00339-X.

[11] J.H. van Steenis, E.M. van Maarseveen, F.J. Verbaan, R. Verrijk, D.J.A. Crommelin, G. Storm, W.E. Hennink, Preparation and characterization of folate-targeted pEG-coated pDMAEMA-based polyplexes, J. Control. Release. 87 (2003) 167–176. doi:http://dx.doi.org/10.1016/S0168-3659(02)00361-9.

[12] R.C. Carlisle, T. Etrych, S.S. Briggs, J.A. Preece, K. Ulbrich, L.W. Seymour, Polymer-coated polyethylenimine/DNA complexes designed for triggered activation by intracellular reduction, J. Gene Med. 6 (2004) 337–344. doi:10.1002/jgm.525.

[13] D. Oupicky, M. Ogris, K. a Howard, P.R. Dash, K. Ulbrich, L.W. Seymour, Importance of lateral and steric stabilization of polyelectrolyte gene delivery vectors for extended systemic circulation., Mol. Ther. 5 (2002) 463–72. doi:10.1006/mthe.2002.0568.

[14] A.L. Parker, K.D. Fisher, D. Oupicky, M.L. Read, S.A. Nicklin, A.H. Baker, L.W. Seymour, Enhanced gene transfer activity of peptide-targeted gene-delivery vectors, J. Drug Target. 13 (2005) 39–51. doi:10.1080/10611860400020449.

[15] Y. Wang, Z. Xu, R. Zhang, W. Li, L. Yang, Q. Hu, A facile approach to construct hyaluronic acid shielding polyplexes with improved stability and reduced cytotoxicity, Colloids Surfaces B Biointerfaces. 84 (2011) 259–266. doi:10.1016/j.colsurfb.2011.01.007.

[16] T.J. Harris, J.J. Green, P.W. Fung, R. Langer, D.G. Anderson, S.N. Bhatia, Tissue-specific gene delivery via nanoparticle coating, Biomaterials. 31 (2010) 998–1006. doi:10.1016/j.biomaterials.2009.10.012.

[17] J.J. Green, E. Chiu, E.S. Leshchiner, J. Shi, R. Langer, D.G. Anderson, Electrostatic ligand coatings of nanoparticles enable ligand-specific gene delivery to human primary cells., Nano Lett. 7 (2007) 874–9. doi:10.1021/nl062395b.

[18] D.M. Lynn, R. Langer, Degradable Poly(β-amino esters): Synthesis, Characterization, and Self-Assembly with Plasmid DNA, J. Am. Chem. Soc. 122 (2000) 10761–10768. doi:10.1021/ja0015388.

[19] D.G. Anderson, A. Akinc, N. Hossain, R. Langer, Structure/property studies of polymeric gene delivery using a library of poly(beta-amino esters)., Mol. Ther. 11 (2005) 426–34. doi:10.1016/j.ymthe.2004.11.015.

[20] A. Akinc, D.M. Lynn, D.G. Anderson, R. Langer, Parallel synthesis and biophysical characterization of a degradable polymer library for gene delivery., J. Am. Chem. Soc. 125 (2003) 5316–23. doi:10.1021/ja034429c.

[21] J.J. Green, R. Langer, D.G. Anderson, A Combinatorial Polymer Library Approach Yields Insight into Nonviral Gene Delivery, Acc. Chem. Res. 41 (2008) 749–759. doi:10.1021/ar7002336.

[22] S.Y. Tzeng, D.R. Wilson, S.K. Hansen, A. Quiñones-Hinojosa, J.J. Green, Polymeric nanoparticle-based delivery of TRAIL DNA for cancer-specific killing, Bioeng. Transl. Med. 1 (2016) 149–159. doi:10.1002/btm2.10019.

[23] C.H. Jones, M. Chen, A. Ravikrishnan, R. Reddinger, G. Zhang, A.P. Hakansson, B.A. Pfeifer, Mannosylated poly(beta-amino esters) for targeted antigen presenting cell immune modulation, Biomaterials. 37 (2015) 333–344. doi:10.1016/j.biomaterials.2014.10.037.

[24] S.Y. Tzeng, B.P. Hung, W.L. Grayson, J.J. Green, Cystamine-terminated poly(beta-amino ester)s for siRNA delivery to human mesenchymal stem cells and enhancement of osteogenic differentiation, Biomaterials. 33 (2012) 8142–8151. doi:10.1016/j.biomaterials.2012.07.036.

[25] N. Segovia, P. Dosta, A. Cascante, V. Ramos, S. Borrós, Oligopeptide-terminated poly(β-amino ester)s for highly efficient gene delivery and intracellular localization., Acta Biomater. 10 (2014) 2147–58. doi:10.1016/j.actbio.2013.12.054.

[26] G.T. Zugates, N.C. Tedford, A. Zumbuehl, S. Jhunjhunwala, C.S. Kang, L.G. Griffith, D. a Lauffenburger, R. Langer, D.G. Anderson, Gene delivery properties of end-modified poly(beta-amino ester)s., Bioconjug. Chem. 18 (2007) 1887–96. doi:10.1021/bc7002082.

[27] A. Akinc, D.G. Anderson, D.M. Lynn, R. Langer, Synthesis of poly(beta-amino ester)s optimized for highly effective gene delivery., Bioconjug. Chem. 14 (2003) 979–88. doi:10.1021/bc034067y.

[28] G.T. Zugates, W. Peng, A. Zumbuehl, S. Jhunjhunwala, Y.-H. Huang, R. Langer, J. a Sawicki, D.G. Anderson, Rapid Optimization of Gene Delivery by Parallel End-modification of Poly(β-amino ester)s, Mol. Ther. 15 (2007) 1306–1312. doi:10.1038/sj.mt.6300132.

[29] J. Behr, The Proton Sponge: a Trick to Enter Cells the Viruses Did Not Exploit, 2 (1997) 34–36.

[30] S.L. Hauser, E.W. Johanson, H.P. Green, P.J. Smith, Aryl Phosphate Complexation by Cationic Cyclodextrins. An Enthalpic Advantage for Guanidinium over Ammonium and Unusual Enthalpy−Entropy Compensation, Org. Lett. 2 (2000) 3575–3578. doi:10.1021/ol006503r.

[31] A. Lošdorfer Božič, A. Šiber, R. Podgornik, How simple can a model of an empty viral capsid be? Charge distributions in viral capsids, J. Biol. Phys. 38 (2012) 657–671. doi:10.1007/s10867-012-9278-4.

[32] K.L. Kozielski, S.Y. Tzeng, B.A. Hurtado De Mendoza, J.J. Green, Bioreducible Cationic Polymer-Based Nanoparticles for Efficient and Environmentally Triggered Cytoplasmic siRNA Delivery to Primary Human Brain Cancer Cells, ACS Nano. 8 (2014) 3232–3241. doi:10.1021/nn500704t.

[33] S.Y. Tzeng, L.J. Higgins, M.G. Pomper, J.J. Green, Student award winner in the Ph.D. category for the 2013 society for biomaterials annual meeting and exposition, april 10–13, 2013, Boston, Massachusetts , J. Biomed. Mater. Res. Part A. 101A (2013) 1837–1845. doi:10.1002/jbm.a.34616.

[34] M. Sanjoh, K. Miyata, R.J. Christie, T. Ishii, Y. Maeda, F. Pittella, S. Hiki, N. Nishiyama, K. Kataoka, Dual Environment-Responsive Polyplex Carriers for Enhanced Intracellular Delivery of Plasmid DNA, Biomacromolecules. 13 (2012) 3641–3649. doi:10.1021/bm301095a.

[35] D. Putnam, C.A. Gentry, D.W. Pack, R. Langer, Polymer-based gene delivery with low cytotoxicity by a unique balance of side-chain termini, Proc. Natl. Acad. Sci. . 98 (2001) 1200–1205. doi:10.1073/pnas.98.3.1200.

[36] C.J. Needham, A.K. Williams, S.A. Chew, F.K. Kasper, A.G. Mikos, Engineering a Polymeric Gene Delivery Vector Based on Poly(ethylenimine) and Hyaluronic Acid, Biomacromolecules. 13 (2012) 1429–1437. doi:10.1021/bm300145q.

This page left blank intentionally

Chapter III

In vitro applications of oligopeptide modified C32 poly(β-amino ester)s for controlling stem cells differentiation

Originally published as:

R. Núñez-Toldrà*, P. Dosta*, S. Montori, V. Ramos, M. Atari, and S. Borrós, "Improvement of osteogenesis in dental pulp pluripotent-like stem cells by oligopeptide-modified poly(ß-amino ester)s," Acta Biomater., Feb. 2017.

*Both authors contributed equally to this work

This page left blank intentionally

In vitro applications of oligopeptide modified C32 poly(β-amino ester)s for controlling stem cells differentiation

This chapter describes the usefulness of oligopeptide-modified C32 polymers in regenerative medicine, specifically to improve osteogenic differentiation. In this study, oligopeptide-modified pBAEs were used to simultaneously control different key osteogenic genes, such as OCT3/4, NANOG, and RUNX2 to cells from the dental pulp with pluripotent-like characteristics (DPPSC) in order to promote and accelerate their osteogenic differentiation. Results indicate that co-delivery strategy of different nucleic acids using a specific oligopeptide-moiety may be a safe and a quick option for the improvement of DPPSC osteogenic differentiation.

3.1 Introduction

As previously discussed in chapter II, oligopeptide-end modified C32 polymers present high transfection efficiencies, biodegradability and biocompatibility. In addition, playing with their oligopeptide composition, nanoparticles can be designed in a cell-specific manner [1]. Taking into account all of these proprieties, these newly developed polymers are attractive for a wide range of *in vitro* applications that currently present a powerful potential in the field of regenerative medicine. For instance, one of the major focus points is to generate healthy bone for the replacement of diseased or missing bone tissue [2,3].

Nowadays, many strategies have been developed to create bone constructs, including different cell-based techniques, bioactive materials [4–7] and various growth factors [3,8]. Cell-based therapies for bone repair based on differentiation of stem cells have experienced substantial advances in recent years and represent a promising approach for the generation of bone. For example, recombinant vectors derived from adenovirus, retrovirus and lentivirus were widely used for this purpose during the last years [9,10], obtaining several successful *in vitro*, *ex vivo* and *in vivo* strategies. However, bone regeneration is a proses where gene expression is continually changing. Then, the use of RNAi therapies may be required, which it is limiting viral delivery strategies due to RNAi therapies may require repeated administration regimens in order to maintain regulation of target gene expression. Consequently, polymeric vectors are taking a great advantage over viral vectors, as previously discussed in Chapter I. Recently, pBAEs have been used in different therapeutic applications, such as stem cell modification [11] or osteodifferentation [12].

Harnessing pBAE holds great promise to deliver RNAi in a safety way, we applied our previously designed polymers to improve and/or accelerate osteogenic differentiation using a new adult stem cell population from the human third molar dental pulp described by Atari et al. [13,14] (this work was carried out in colaboration with Maher Atari laboratory from Universitat Internacional de Catalunya).

These cells, called dental pulp pluripotent-like stem cells (DPPSC), express pluripotency markers, such as OCT3/4, LIN28, SOX2 and NANOG until late passages [15], as shown in Figure III-1. Moreover, DPPSCs show chromosomal stability and have the ability to differentiate into cells from the three embryonic layers [13].

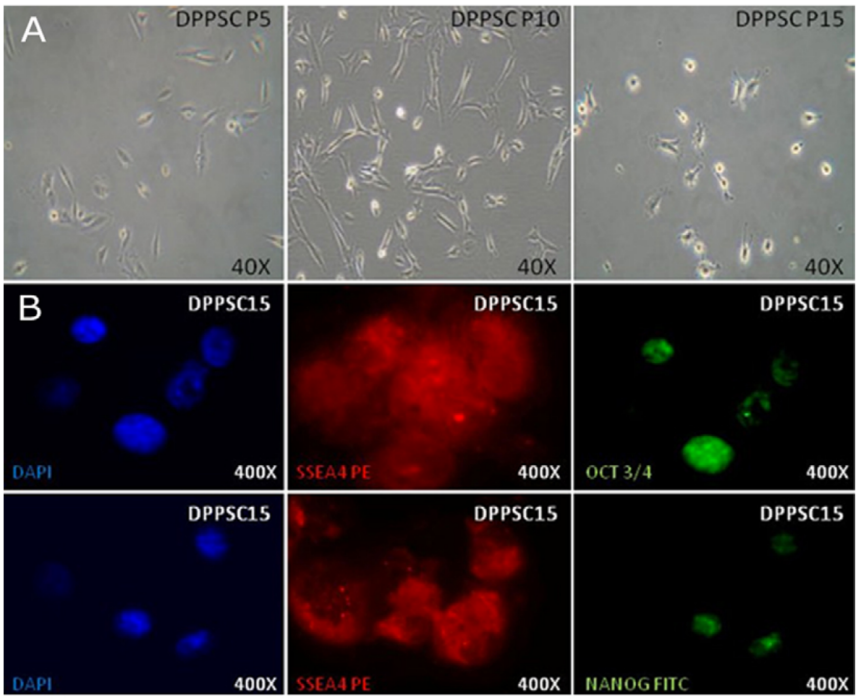

Figure III-1. Characterization and cellular morphology of (DPPSCs) by *in vitro* expansion. Morphology of DPPSCs at different passages (P5, P10 and P15). (B) Analysis of DPPSC immuno- phenotype by confocal microscopy shows the expression of SSEA4 PE together with OCT3/4 FITC or NANOG FITC [16].

It has been shown that DPPSC have higher capacity to differentiate into bone tissue than other dental pulp stem cells, and they are able to grow, attach and differentiate using different biomaterials [17] . Therefore, DPPSC may be a promising candidate cell population for bone tissue engineering approaches.

Despite their attractiveness, it has been demonstrated that, after osteogenic induction of stem cells, cultures retain an undifferentiated population of cells expressing OCT3/4 and NANOG transcription factors, which maintain their high proliferative potential [18,19]. Although the expression of pluripotency transcription factors, such as OCT3/4 and NANOG, is essential during cell differentiation [20], residual expression impedes complete differentiation into osteocytes [16,21]. This phenomenon

can limit their clinical applications. Therefore, a fine-regulation of pluripotent genes may be a powerful way to improve osteogenic differentiation.

Apart from pluripotent genes, there are a wide range factors that may play an important role to control the stem cell behaviour in bone regeneration. Osteogenic differentiation is modulated by the constitutive expression of certain transcription factors that are rapidly degraded and are strongly involved in the regulation of bone development, such as RUNX2, SOX9 and Osterix [22–25]. Specifically, RUNX2 is an essential regulator of bone development, controlling the expression of a number of key target genes and different pathways during the osteogenic differentiation [24]. It has been shown that forced expression of RUNX2 in non-osteoblastic cells induces expression of multiple osteoblast-specific genes and upregulates osteoblastic differentiation [26]. However, RUNX2 inhibits the late stage of osteoblast maturation, restricting their positive function to the early differentiation stage in the process of osteoblast development. Moreover, it has been reported that prolonged overexpression of RUNX2 may generate adverse effects, such as severe osteopenia and bone fractures [27,28].

It should be noted that efficient bone engineering may not be solely achieved by expression of a single transcription factor. However, the orchestrated expression of a selection of key proteins or transcription factors, which can specifically control gene expression, may result in clinically useful osteogenesis. In this sense, gene and RNAi therapy may be an alternative way to enhance bone healing. To achieve this, safe, efficient, and non-toxic delivery system is crucial in order to deliver therapeutic RNAi and plasmidic DNA without altering others gene pathways that can harm the differentiation process. Then, in this work our previously described pBAEs have been personalized playing with their oligopeptides formulation to deliver nucleic acids to DPPSCs in a safer and efficient way that current used delivery vectors.

Therefore, the main objective of this chapter is to design a safer way to accelerate the osteogenic differentiation process in a new pluripotent-like population of adult stem cells using pBAE polymers as RNAi and gene delivery method. After 7 days of osteogenic differentiation, DPPSC were transfected with poly(*β*-amino ester)s containing plasmid DNA vectors to induce transient overexpression of RUNX2 and, simultaneously, the cells were transfected with siRNAs to silence the OCTA3/4 and NANOG pluripotency genes. After that, osteogenic advanced markers, such as ALP, COL1 and OSN, and more bone functional activity were analyzed in order to corroborate their osteogenic improvement or acceleration.

In order to achieve this objective, the following tasks were proposed:

- Identification of top performing formulations of oligopeptide-modified pBAEs to efficiently deliver large and small nucleic acids to DPPSCs.
- Determine gene up- or downregulation after nucleic acid delivery using our previously selected oligopeptide formulation in undifferentiated and differentiated DPPSC.
- Determination of osteogenic key markers to corroborate DPPSC osteogenic acceleration

3.2 Materials and Methods

3.2.1 Materials

Reagents and solvents used for polymer synthesis were purchased from Sigma-Aldrich and Panreac. Oligopeptide moieties used on the polymer modification (H-Cys-Arg-Arg-Arg-NH2, H-Cys-Lys-Lys-Lys-NH2, H-Cys-His-His-His-NH2 and H-Cys-Asp-Asp-Asp-NH2) were obtained from GL Biochem (Shanghai) Ltd with a purity of at least 98%. Polyplus Interferin and Lipofectamine 2000 transfection reagents were purchased from VWR and used according to manufacturer instructions. ~~For~~ Knockdown of OCT3/4 was performed using ON-TARGETplus Human POU5F1siRNA SMART Pool (L-019591-00), knockdown of NANOG using ON-TARGETplus Human NANOG siRNA SMART Pool (L-014489-00) and scramble siRNA control using ON-TARGETplus Non-Targeting Control Pool (D-001810-10), all of them obtained from Thermo GE Dharmacon. Labelled siRNA (AllStars Neg. siRNA AF 546) for uptake experiments was purchased from Qiagen. For plasmid transfection, RUNX2 gene overexpression was obtained using RUNX2 plasmid ((Myc-DDK-tagged)-Human runt-related transcription factor 2) from OriGene and pmaxGPF from Amaxa was used as a scramble control. MTT assay kit (Sigma-Aldrich) was used for viability studies.

3.2.2 Synthesis of oligopeptide end-modified pBAEs (C32 polymer)

Poly(*β*-amino ester)s were synthesized following a two-step procedure, described in previous papers [29] and in Chapter II. Briefly, acrylate-terminated C32 intermediate polymer was obtained by conjugate addition of 5-amino-1-pentanol to 1,4-butanediol diacrylate during 24 h at 90ºC. Then, oligopeptide-modified pBAEs were obtained by end-capping modification of the resulting acrylate-terminated polymer with thiol-bearing oligopeptides at 1:2,5 molar ratios in dimethyl sulfoxide (DMSO) [1,30].

3.2.3 Patient selection

Healthy human third molars extracted for orthodontic and prophylactic reasons were selected from 3 different patients of different sexes and ages (14–20 years old). The extraction procedure was kept simple to prevent tooth damage. Dental pulp tissues used for these experiments were obtained with informed consent from donors. All experiments were performed in accordance with the guidelines on human stem cell research issued by the Committee on Bioethics of the *UIC Barcelona* with the study code: BIO-ELB-2013-03.

3.2.4 Isolation, culture and osteogenic induction of DPPSC

The teeth were cleaned using gauze soaked in 70% ethanol. The tissues from the dental pulp were disaggregated by digesting them with collagenase type I (3 mg/mL; Sigma) for 60 minutes in a bath at 37°C. Afterwards, cells were cultured in 150 mL flasks, which were coated one hour before seeding with 100 ng/mL fibronectin, in DPPSC medium at 37°C in a 5% CO^2 incubator. DPPSC medium consists of 60% Dulbecco's modified Eagle's medium (DMEM)-low glucose (Life Technologies) and 40% MCDB-201 (Sigma) supplemented with 1X selenium-insulin-transferrin-sethanolamine (SITE;

Sigma), 1X linoleic acid-bovine serum albumin (LA-BSA; Sigma), 10^{-4} M ascorbic acid 2-phosphate (Sigma), 100 units of penicillin/1000 units of streptomycin (PAA), 2% fetal bovine serum (FBS; Sigma), 10 ng/mL hPDGF-BB (R&D Systems) and 10 ng/mL EGF (R&D Systems). To propagate DPPSC, cells were detached at 30% confluence by adding 0.25% trypsin-EDTA (Life Technologies) and then reseeded at the proper density (100 cells/cm^2).

For the osteogenic induction, DPPSC from passage 6 were seeded on 24 well plates at 5×10^3 cells/cm^2 during 21 days with the following osteogenic medium: RPMI 1640 (Sigma) containing 10% FBS (Biochrom), 10 mM β-glycerol phosphate (Sigma-Aldrich), 50 μM L-ascorbic acid (Sigma-Aldrich), 0.01 μM dexamethasone and 1% penicillin/streptomycin solution. The medium was changed every 3 days.

3.2.5 Polymer formulation / oligopeptide moiety selection using pmaxGFP and labelled-siRNA in DPPSC

At 7 days of osteogenic induction, polymer screening of end-modified oligopeptide pBAEs was carried out using pmaxGFP plasmid and fluorescent siRNA (AF546). Plasmid transfection was performed with polyplexes prepared as described previously at 50:1 w:w ratio with AcONa buffer (25 mM, pH 5.0). Cells were washed with PBS 1x and pmaxGFP complexes were added at a final concentration 0.95 μg/mL working with serum-free medium. After 3 h of incubation, the remaining complexes were removed and replaced with osteogenic medium. GFP expression was analyzed at 48 hours post-transfection by flow cytometry. Lipofectamine 2000 was used as positive control of transfection following the manufacturer instructions, and untreated cells were used as negative control. siRNA uptake screening was carried out using polyplexes prepared at 200:1 w:w ratio with AcONa buffer (25 mM, pH 5.0). As before, cells were washed with PBS 1x and siRNA-labelled (AF546) complexes were added at a final concentration of 50 nM working with serum-free medium. After 2 h of incubation, the remaining complexes were removed and uptake fluorescence was analysed by flow cytometry. For siRNA particles, Polyplus Interferin was used as positive control of transfection following the manufacturer instructions and untreated cells were used as a negative control.

3.2.6 Transfection of DPPSC using siNANOG, siOCT3/4 and pRUNX2

As before, at day 7 of the osteogenic induction, transfections were carried out using the top-performing polymer formulation, C32-R/D. siRNA polyplexes were performed at 200:1 polymer/siRNA ratio and plasmid polyplexes were performed at 50:1 polymer/plasmid ratio using AcONa buffer (25mM, pH 5.5), as previously is explained (Supporting Data). Cells were washed with PBS 1x and polyplexes were added. siRNA transfection was performed working at a final concentration of 50 nM, plasmid transfection was carried out at 0.95 μg/mL and the co-transfection of siRNA-plasmid was performed at 25 nM and 0.48 μg/mL, respectively. At 3 h post-transfection, the remaining complexes were removed and replaced with osteogenic medium. Scramble siRNA and scramble plasmid were used as a negative control in all experimental conditions following the same procedure of transfection.

3.2.7 Immunocytochemical staining

The pluripotent state of DPPSC was studied before osteogenic induction and pBAE transfections. Cells were fixed with 4% paraformaldehyde (BD Biosciences) (1h at RT), incubated with 1% Tween 20 (20 min at RT) to increase permeability and then blocked with 6% FBS (45 min at RT). The slides were incubated overnight at +4°C with primary antibodies against NANOG (1:100, Abcam) and OCT3/4 (1:50, Santa Cruz Biotech.). After washes, both samples were treated with the secondary antibodies Alexa 568 anti-rabbit IgG (1:500, Life Technologies) and Alexa 488 anti-mouse IgG (1:500, Santa Cruz Biotech.) respectively for 60 min at 37°C. Between each step, the slides were washed with Perm/Wash 1X (1:200, BD Biosciences). The cells were examined by confocal fluorescence microscopy.

3.2.8 RNA isolation, RT-PCR and qRT-PCR

Total RNA was extracted by TRI Reagent® (Molecular Research Center, Inc.) from undifferentiated DPPSC (day 0) and differentiated DPPSC at day 9, 15 and 21 of osteogenic differentiation following the manufacturer's instructions. After RNA quantification, 2 µg of RNA aliquots were treated with DNase I (Life Technologies) and reverse-transcribed using Transcriptor First Strand cDNA Synthesis Kit (Roche) following the manufacturer's instructions. RT-PCRs were performed using the primers listed in Table III-1 for the amplification of OCT3/4, NANOG, ALP, COL1, OCN and GAPDH cDNAs. The resulting amplicons were resolved by agarose gel electrophoresis. Quantitative RT-PCR was performed using the CFX96 thermocycler (Bio-Rad). 50 ng of cDNA of undifferentiated DPPSC (day 0) and differentiated DPPSC at day 9, 15 and 21 of osteogenic differentiation were used. cDNA samples were amplified using specific primers (Table III-1) and SYBR Green Supermix (Bio-Rad Laboratories, Inc.). The expression levels of the genes of interest (OCT3/4, NANOG, RUNX2, ALP, COL1, OCN and OSN) were normalized against the housekeeping gene GAPDH. The relative expression levels were normalized to DPPSC at day 0 cDNAs, which was assigned as 1. All analyses were performed using the $2^{-\Delta\Delta CT}$ method [31] and 3 technical replicates.

Table III-1 Primers sequences used in this chapter for qPCR analysis. OCT-3/4, octamer-binding transcription factor 4; NANOG, NANOG homeobox; ALP, alkaline phosphatase; COL1, type I collagen; OCN, osteocalcin; OSN, osteonectin; RUNX2, Runt-related protein 2; GAPDH, glyceraldehyde-3-phosphate dehydrogenase.

Primer	Accession Number	Forward Sequence	Reverse Sequence
OCT 3/4	MM_002701	5'-GTGGAGAGCAACTCCGATG -3'	5'-TGCAGAGCTTTGATGTCCTG -3'
NANOG	MM_024865	5'-CAGAAGGCCTCAGCACCTAC -3'	5'-ATTGTTCCAGGTCTGGTTGC -3'
ALP	MM_000478	5'-CCGTGGCAACTCTATCTTTGG -3'	5'-GCCATACAGGATGGCAGTGA -3'
COL1	MM_000088	5'-CCCTGGAAAGAATGGAGATGAT -3'	5'-ACTGAAACCTCTGTGTCCCTTCA -3'
OCN	MM_199173	5'-AAGAGACCCAGGCGCTACCT -3'	5'-AACTCGTCACAGTCCGGATTG -3'
OSN	MM_001309444	5'-ATCTTCCCTGTACACTGGCAGTTC- 3'	5'- CTCGGTGTGGGAGAGGTACC-3'
RUNX2	MM_001146038	5'-AGCAAGGTTCAACGATCTGAGAT -3'	5'-TTTGTGAAGACGGTTATGGTCAA -3'
GAPDH	MM_002046	5'-CTGGTAAAGTGGATATTGTTGCCA-3'	5'-TGGAATCATATTGGAACATGTAAAC-3'

3.2.9 Bone functional assays: Alkaline phosphatase (ALP) and Alizarin Red S staining

Pre-transfected DPPSC at day 7 of osteogenic induction, and transfected DPPSC cultures at day 21 of osteogenic induction were fixed with 4% paraformaldehyde (BD Biosciences) for the ALP and Alizarin Red S staining's. Alkaline Phosphatase Staining Kit (CosmoBio) detects the ALP activity in blue, and Alizarin Red S staining (Sigma) stains the calcium minerals red. Both staining was used according to de manufacturer's instructions. The biomineralization staining's (ALP and Alizarin Red S) were quantified by Image J software.

3.2.10 Cell viability assay (MTT)

Polymer toxicity was measured using MTT assay (Sigma-Aldrich) at 48 hour post siRNAs transfection and 21 days after osteogenic differentiation according to the manufacturer's instructions. MTT assay measures the activity of living cells via mitochondrial dehydrogenase activity. Briefly, MTT stock solution (5 mg/mL) was added to each culture well, being assayed to equal one-tenth of the original culture volume and incubated for 3 h. After that, DMSO was added in an amount equal to the original culture volume. Finally, the cell viability was determined by measuring the absorbance at 570 nm, and subtracting background absorbance at 690 nm.

3.2.11 Short-comparative genomic hybridization (sCGH)

Undifferentiated DPPSC (day 0) and differentiated DPPSC at days 9, 15 and 21 of osteogenic differentiation (N=3) were analysed by sCGH as described in Rius M. et al. [32]. sCGH is an aneuploidy screening that allows the detection of chromosome imbalances generated by aberrant segregation and structural differences for fragments larger than 10–20 Mb. Briefly, 15-20 single cells from a homogeneous culture of each sample were collected and amplified using degenerate oligonucleotide-primed PCR (DOP-PCR). Then, whole genome amplification products were fluorescently labelled by nick translation. Test DPPSC DNA were labelled in Red-dUTP, whereas reference DNA (47, XXY) was labelled with Green-dUTP. After nick translation, reference and test DNA were mixed in equimolar proportions and ethanol precipitated. Finally, hybridization was performed on normal male (46,XY) metaphase spread. The capture of metaphases was performed with an epifluorescence microscope and an average of 12 metaphases per sample was captured and evaluated using Isis CGH software (MetaSystems). The ratio between red and green fluorescence is 1:1 when there is the same proportion of reference and test DNA. The thresholds used to diagnose losses and gains were 0.8 and 1.2, respectively. This procedure was performed by an external service (Universitat Autònoma de Barcelona).

3.2.12 Statistical analysis

Statistical analyses were performed with SPSS Statistics version 21.0 (IBM). All the quantitative data are presented as mean and standard deviation (SD). The results were analysed by applying the two-way analysis of variance test or ANOVA test for multiple factors. Confidence intervals were fixed at 95% ($P<0.05$).

3.3 Results and discussion

In order to enhance and accelerate osteo-differentiation in DPPSC, gene expression of key genes was regulated using an appropriate delivery vector. In this case, previously developed cell-specific oligopeptide end-modified pBAEs (C32 polymer) polymers were used [30]. C32 polymer synthesis and oligopeptide end-capping modification was carried out as previously discussed in Chapter II. Positive- and negative- oligopeptides were used to further modify C32 polymer. Then, oligopeptide-modified pBAEs were used to efficiently condense large and small nucleic acids, such as plasmid and siRNA's (Figure III-2).

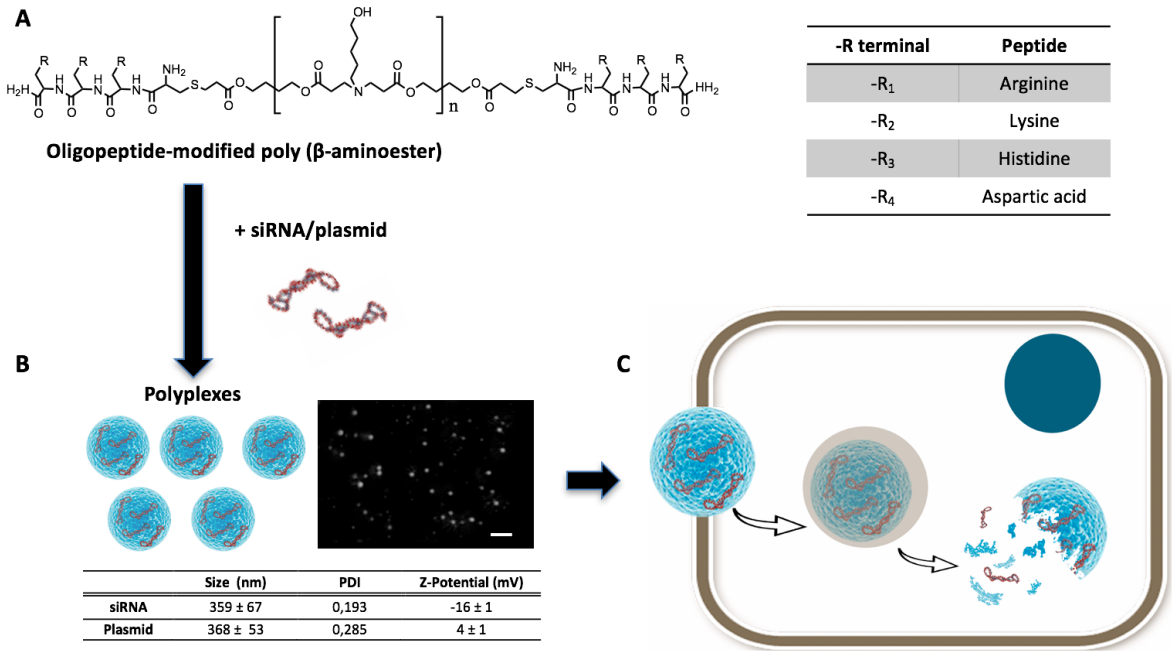

Figure III-2. Oligopeptides end-modified pBAEs were used to co-deliver siRNA and plasmids in DPPSCs. a) Chemical structure of new family of synthetized oligopeptide end-modified poly(β-amino ester)s. R terminal can be arginine-, lysine-, histidine- and aspartic acid- oligopeptide. b) Average hydrodynamic diameter and zeta-potential distributions of C32-R/D polymer using siRNA or plasmid as nucleic acids. Average size and zeta potential were determined by Dynamic Light Scattering and Nanoparticle Tracking Analysis. Scale bar: 100 nm. c) Surface composition of polyplexes play a crucial role in cell-specify interaction formed by electrostatic interactions between polymer and nucleic acids.

As is well known, oligopeptide composition plays an important role in the final polyplexes physicochemical properties, obtaining a wide family of polyplexes with different characteristics and behaviours. Therefore, hydrodynamic size and surface charge were analysed by DLS using plasmid or siRNA's as a nucleic acid, as shown in Table III-2.

Table III-2 Average hydrodynamic diameter and zeta potential of pBAE:plasmid and pBAE:siRNA nanoparticles by DLS. Results are shown as mean and standard deviation of triplicates analysed by intensity.

Polymer	Plasmid		siRNA	
	Size (nm)	Z-potential (mV)	Size (nm)	Z-potential (mV)
C32-CR3	195 ± 3	19 ± 1	323 ± 35	-0,3 ± 3
C32-CK3	146 ± 13	20 ± 1	211 ± 20	9,1 ± 1
C32-R/H	350 ± 38	10 ± 1	351 ± 55	-8 ± 1
C32-K/H	198 ± 2	22 ± 2	390 ± 60	10 ± 1
C32-R/K	127 ± 25	12 ± 6	279 ± 30	12 ± 1
C32-R/D	368 ± 53	4 ± 1	359 ± 67	-16 ± 1
C32-K/D	> 1000	-	235 ± 24	13 ± 3

As Table III-2 showed, the average hydrodynamic diameter of polyplexes obtained using siRNA or plasmid DNA as nucleic acid ranged from 200 to 400 nm and the surface charge of the resulting polyplexes ranged between -10 mV and +20 mV. Interestingly, more differences were observed when siRNA was used as nucleic acid in terms of surface charge. In contrast, when plasmid was used as nucleic acid, positive surface charge was observed in all the oligopeptide formulations. These results corroborate previous reported results, where C32 polymers were used to efficiently delivery plasmids [30] and siRNA [1].

3.3.1 C32-R/D polymer formulation shows the highest cell-specificity to DPPSC to delivery nucleic acids

Based on previous results, pBAE end-modification with different oligopeptides can confer cell-specificity in different cells types[1]. Then, an important step was focused on the identification of the top-performing polymer formulation in order to achieve optimal co-delivery of nucleic acids in DPPSC. Therefore, screening analysis of end-modified pBAEs was performed using GFP reporter plasmid and fluorescently-labelled siRNA. For plasmid screening, cells were incubated with nanoparticles containing pmaxGFP plasmid and GFP expression was analysed by flow cytometry and confocal laser scanning microscopy at 48hours post-transfection, as shown in Figure III-3-A and Figure III-3-C.

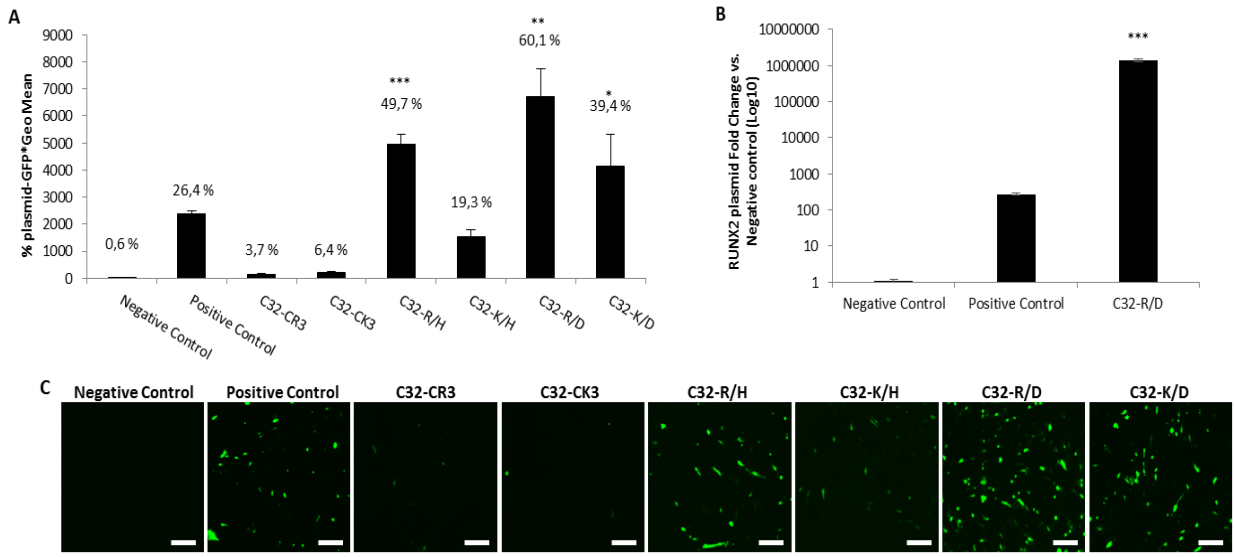

Figure III-3. Arginine/aspartic acid- modified pBAEs present the highest cell-specificity and transfection efficiency to DPPSCs in order to deliver plasmids. A) Screening of EGFP expression was evaluated in differentiated DPPSC using different oligopeptide-modified pBAE formulations and plasmid encoding GFP gene (pmaxGFP). GFP expression was determined after 48 h by flow cytometry and plotted as a percentage of GFP-positive cells multiplied by the GeoMean fluorescence of the positive population. Statistical significance was determined using positive control cells as control group. *P< 0.05, ** P < 0.01, *** P< 0.001. B) Top performing polymer formulation was used to transfect a functional plasmid encoding RUNX2 gene. RUNX2 expression was analysed at 48h post-transfection by qPCR. Statistical significance was determined using positive control cells as control group. *P< 0.05, ** P < 0.01, *** P< 0.001. C) Confocal laser scanning microscopic images of DPPSC cells using pmaxGFP plasmid and different oligopeptide end-modified PBAEs. Scale bars: 200 μm.

Transfection analysis using pmaxGFP plasmid showed differential GFP protein expression at 48-hour post-transfection depending on the oligopeptide termini (Figure III-3-A). In general, mixtures of arginine or lysine oligopeptides with aspartic acid or histidine presented a greater GFP expression than polyplexes prepared with either arginine- or lysine-modified pBAEs alone. Among all the tested formulations, the formulation composed by arginine- and aspartic acid-terminated polymer (C32-R/D) was identified as the top-performing formulation under these conditions. C32-R/D was able to transfect 60% of DPPSC, achieving a 2.3-fold increase in GFP expression, compared to commercial control (lipofectamine 2000). Furthermore, when this top-performing formulation was employed to transfect cells with functional RUNX2 plasmid, the levels of RUNX2 mRNA determined by RT-qPCR were more than 2000 times higher than cells transfected with lipofectamine 2000 (Figure III-3-B), confirming the great efficacy of this formulation for DPPSC cells.

Once C32-R/D seems to be a promising formulation for plasmid delivery, siRNA screening was carried out using AlexaFluor 546-labelled siRNA in DPPSCs in order to check if this polymer formulation is able to efficiently deliver small RNA. Firstly, cells were transfected at different siRNA doses in order to determine the optimal siRNA concentration, ranging from 25 nM to 100 nM, as shown in Figure III-4.

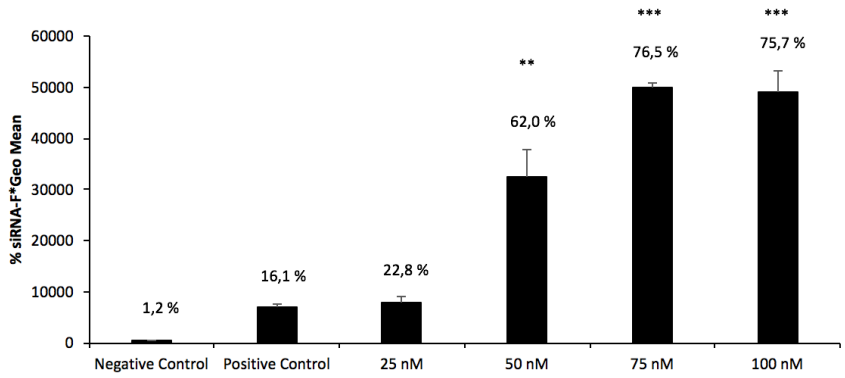

Figure III-4 Dose curve of siRNA concentration in DPPSC cells using C32-R/D polymer. DPPSC cells were transfected with siRNA-F at different concentrations, ranging from 25nM to 100nM. Fluorescence expression was determined 2 hours post-transfection by flow cytometry and plotted as percentage of positive cells multiplied by the GeoMean fluorescence. Statistical significance was determined using positive control cells as control group. *P< 0.05, ** P < 0.01, *** P< 0.001

Higher uptake fluorescence was observed at higher siRNA doses. Particularity, significant cell uptake working at siRNA concentrations of 50 nM or higher compared to commercial reagent. However, we have already described that some cytotoxic effects were noted at siRNA concentrations higher than 75 nM [1]. Then, 50 nM was selected to efficiently deliver siRNA's to DPPSCs.

After that, DPPSC were transfected using mixtures of different oligopeptide end-modified pBAEs in order to corroborate if arginine- / aspartic acid- mixture is still the top-performing formulation. Then, cells were transfected during 2 hours and fluorescence was analysed by flow cytometry, as shown in Figure III-5.

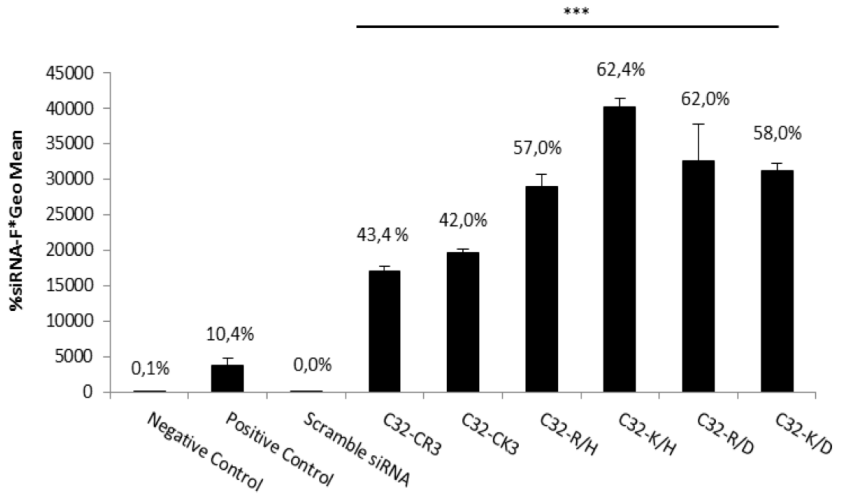

Figure III-5 Arginine/aspartic acid- modified pBAEs present the highest cell-specificity and transfection efficiency to DPPSCs in order to deliver siRNA. Uptake experiment using labelled siRNA was carried out in DPPSCs at final concentration of 50nM using different oligopeptide end-modified poly(β-amino ester)s. Fluorescence expression was determined 2 hours post-transfection by flow cytometry and plotted as percentage of positive cells multiplied by the GeoMean fluorescence. Statistical significance was determined using positive control cells as control group. *P< 0.05, ** P < 0.01, *** P< 0.001.

Interestingly, cellular uptake results using different oligopeptide-modified pBAE formulations showed less dependence on oligopeptide nature than for GFP transfection. Figure III-5 shows that all the tested polymer formulations presented more than 4-fold increase in cellular uptake than the commercial reagent, Polyplus Interferin. As for plasmid transfection, oligopeptide mixtures presented higher siRNA uptake than arginine- or lysine- pBAEs alone. Lysine-/histidine- and arginine-/aspartic acid-modified pBAE formulations were the top performing polymer formulations achieving a 62.4% and 62.0% of transfection, respectively. Therefore, C32-R/D was identified as the top performing formulation for the delivery of both siRNA and plasmid DNA.

Based on these results, it can be concluded that a mixture of positively- and negatively-charged oligopeptides promoted a preferential delivery both siRNAs and plasmids to DPPSC. This result corroborates with Chapter II data were mixtures of positively- and negatively-charged oligopeptides are one of the best formulations in terms of transfection efficiency. Moreover, the presence of negatively-charged oligopeptides (aspartic acid) decreases the overall charge of the polyplexes, thus decreasing their cytotoxicity [33].

3.3.2 Silencing of pluripotent genes improves the expression of osteogenic markers in DPPSC differentiation

In order to evaluate the effect of the pluripotent genes OCT3/4 and NANOG on the osteogenic differentiation of pluripotent-like adult stem cells, OCT3/4 and NANOG expression was silenced using C32-R/D polymer formulation in both undifferentiated and initial differentiated stage (day 7 of differentiation) DPPSC cells. Silencing efficiency was evaluated by measuring the decrease of the pluripotency markers at 48h post-transfection and at the end of the osteogenic induction.

3.3.2.1 Silencing the pluripotency in undifferentiated DPPSC

DPPSC showed expression of OCT3/4 and NANOG in their undifferentiated stage. To further characterize the change of the pluripotency markers during the osteogenic process, RNA was isolated at days 0, 7, 15 and 21 of the DPPSC osteogenic differentiation. qRT-PCR demonstrated a progressive decrease of OCT3/4 during the process and a rapid downregulation of the NANOG expression during the first week of differentiation, which was maintained throughout the differentiation process. However, at the end of the osteogenic process, low levels of these pluripotency markers still remained (Figure III-6).

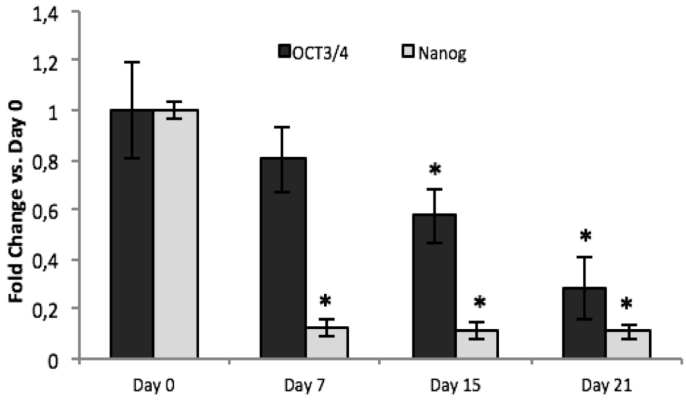

Figure III-6 Expression profile of pluripotent genes during osteogenic differentiation. Nanog and OCT3/4 expression were evaluated at days 7, 15, and 21 of osteoblast differentiation respect undifferentiated DPPSC (Day 0). The relative value for undifferentiated DPPSC (Day 0) was considered 1. *P <0.05 respect Day 0.

Figure III-6 indicates that the levels of OCT3/4 and NANOG decrease during the osteogenic differentiation of DPPSC. However, some expression of these markers still remains at the end of the differentiation process. It has been described that a potentially undifferentiated population of cells can be may remain, maintaining their high proliferative potential but impeding a complete differentiation into osteocytes [16,21].

To verify the silencing efficiency of the pluripotency genes by siRNAs, transfection with different combinations of siRNAs was performed to silence OCT3/4 and NANOG in undifferentiated DPPSC, as is shown in Figure III-7.

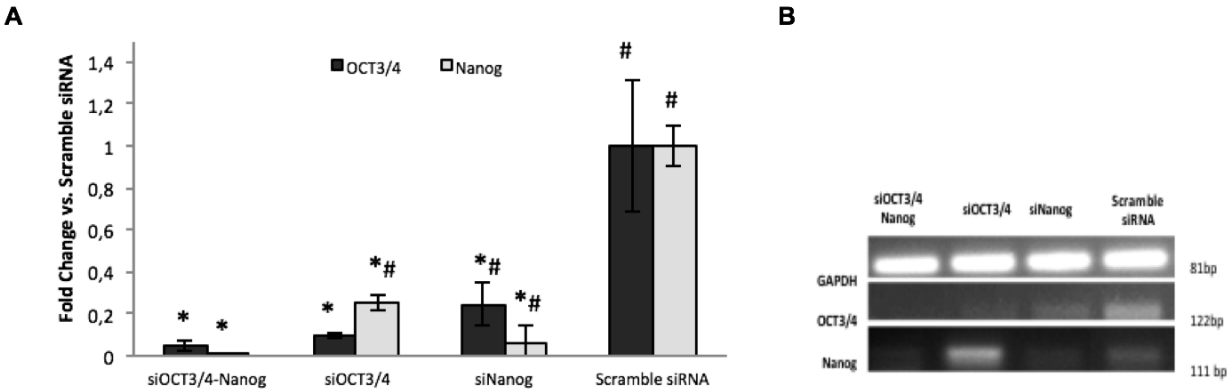

Figure III-7. Silencing the pluripotency genes in undifferentiated DPPSC.A) NANOG and OCT3/4 knockdown using siRNA-C32-R/D polyplexes in undifferentiated DPPSC at final concentration of 10nM. Results were evaluated by qRT-PCR at 48h post transfection respect Scramble siRNA. The relative value for Scramble siRNA was considered 1. *P <0.05 respect Scramble siRNA; #P <0.05 respect siOCT3/4-Nanog. B) Knockdown of OCTA3/4 and NANOG. Results were evaluated by RT-PCR at 48h post transfection and scramble siRNA control was used as negative control.

qRT-PCR analysis showed that OCT3/4 and NANOG expression decreased after 48h post-transfection when compared with the scramble siRNA control. In addition, the simultaneous silencing of OCT3/4 and NANOG reached the lowest levels of both pluripotency markers (Figure III-7). Interestingly, independently if the silencing was targeted at one or both pluripotent genes, a decrease in both genes was observed.

It have been described by Chambers et al. that NANOG is expressed in OCT3/4-deficient embryos, and NANOG overexpression does not revert the differentiation program of ESC triggered by OCT3/4 down-regulation [34]. They observed that NANOG is not just a downstream version of OCT3/4; indeed, NANOG and OCT3/4 work in concert to support stem cell potency and self-renewal [34,35]. Then, our results also confirmed that there is a co-expression and a genetic interaction between these two pluripotency markers in DPPSC.

3.3.2.2 Silencing the pluripotency in differentiated DPPSC

Once we corroborate that OCTA3/4 and NANOG could be modulated using our designed polyplexes in undifferentiated DPPSC, they are used to treated differentiated DPPSC into bone-like tissue during 21 days. At day 7 of the differentiation, cells were transfected with siRNAs to reduce the expression of the pluripotency genes and improve the osteogenic process. The silencing efficiency of OCT3/4 and NANOG genes was confirmed by RT-PCR at 48h post-transfection (Figure III-8).

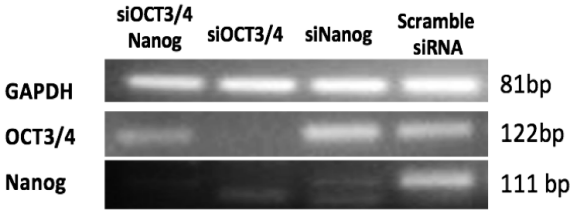

Figure III-8. NANOG and OCT3/4 knockdown using siRNA-C32-R/D polyplexes in differentiated DPPSC. Pluripotent OCT3/4 and Nanog gene expression were controlled by siOCT3/4 and/or siNanog delivery at 7 days of osteogenic differentiation in DPPSC. Pluripotency markers were analysed at gene level at 48h post-transfection. Scramble siRNA was used as negative control.

Results showed high silencing of NANOG gene using siOCT3/4 and/or siNANOG compared to scramble control. Moreover, OCT3/4 was reduced only after siOCT3/4 delivery, remaining stable after siNANOG delivery. These results further corroborate Chambers et al. results were NANOG gene may be a downstream version of OCT3/4.

In order to evaluate the enhancement of the osteogenic differentiation after silencing of pluripotent genes using the anti-OCT3/4 and anti-NANOG siRNA, RNA was isolated at day 21 of the osteogenic induction and key osteogenic markers, such as ALP, COL1 and OCN, were analysed (Figure III-9-A). In addition, a key osteogenic gene, RUNX2, was further analysed (Figure III-9-B).

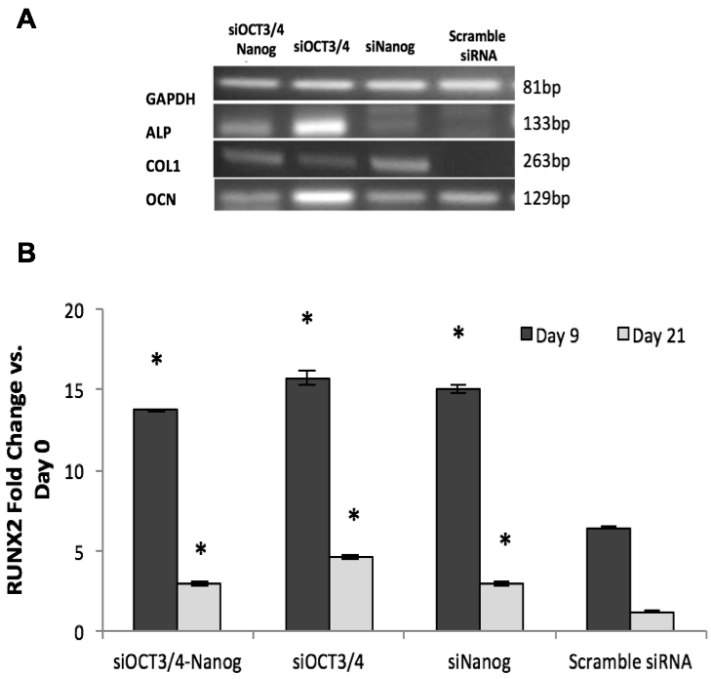

Figure III-9. OCT3/4 knockdown accelerates the expression of the osteogenic markers. A) RT-PCR of osteogenic markers ALP, COL1 and OCN at the end of the osteogenic differentiation (day 21) were analysed. B) After siRNA's delivery, RUNX2 expression was analysed at 48h post transfection (day 9) and at the end of the osteogenic differentiation (day 21) respect undifferentiated DPPSC (Day 0). The relative value for undifferentiated DPPSC (Day 0) was considered 1. *P <0.05 respect Scramble siRNA.

RT-PCR (Figure III-9-A) showed higher expression of the majority of the osteogenic markers in the siRNA-transfected cells than in the scramble siRNA control cells. Moreover, the levels of ALP and OCN were greater in the siOCT3/4 transfected cells. On the other hand, the relative expression of RUNX2 (Figure III-9-B) indicated that there was an up-regulation of this gene at 48h post-transfection (day 9 of osteogenic differentiation) in the cells with the silenced pluripotency genes. In fact, RUNX2 levels remained higher in these cells than in cells transfected with the scramble siRNA control. This phenomenon was maintained until the end of the osteogenic induction. Furthermore, the siOCT3/4 transfected cells achieved higher levels of RUNX2 than cells transfected with either siNANOG alone or both siOCT3/4 and NANOG. For this reason, we hypothesized that the silencing of OCT3/4 combined with the expression of RUNX2 may be promising strategy in order to further improve the osteogenic differentiation of DPPSC.

3.3.3 Co-delivery of siOCT3/4 and pRUNX2 accelerates the osteogenic differentiation of DPPSC while maintaining high cell viability

During the first week of the osteogenic induction, the proliferation and the first stages of stem cells differentiation occur. This process corresponds with an increase of some pluripotency markers that are later downregulated. A critical factor in osteogenic gene therapy is the timing of RUNX2 gene delivery into the cells. The early stage of the osteogenesis (pre-osteoblastic cells) is the most active

period of bone formation and it occurs during the first week of differentiation [36,37]. Some studies suggest that RUNX2 promotes the proliferation of osteoblasts in the early stage, but inhibits osteoblast differentiation and blocks osteoblast maturity in the late stage, leading to osteopenia and fragility [27,28]. Thus, the optimal time for delivery the exogenous RUNX2 plasmid and silencing OCT3/4 gene should be at day 7 of the osteogenic differentiation. Therefore, transient expression of both anti-OCT3/4 and pRUNX2 plasmid was conducted at day 7, because after 72 hours the plasmid and the siRNA are typically degraded.

3.3.3.1 Co-delivery of siOCT3/4 and pRUNX2

Thus, DPPSC were transfected with C32-R/D polymer using pRUNX2 plasmid and/or anti-OCT3/4 siRNA at day 7 of osteodifferentation. In these experiments, negative control was transfected with both scramble plasmid (i.e. pmaxGFP plasmid) and scramble siRNA, as shown in Figure III-10.

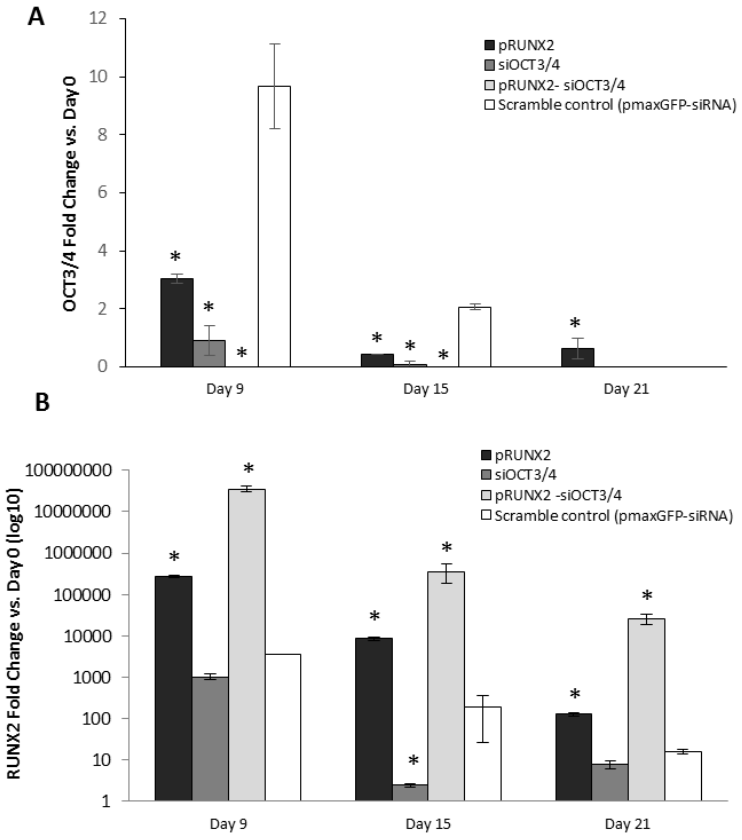

Figure III-10. Viability and efficiency of single and double transfections in DPPSC during the osteogenic differentiation. A-B) Relative expression of the pluripotency gene OCT3/4 and the osteogenic gene RUNX2 after pRunx2 and siOCT3/4 single and double transfections in DPPSSC at day 9 (48h post transfection), 15, and 21 of osteogenic differentiation respect undifferentiated DPPSC (Day 0). The relative value for undifferentiated DPPSC (Day 0) was considered 1. Scramble control (pMaxGFP-siRNA) was used as a negative control. *P<0.05 respect Scramble Control.

RNA was isolated at different osteodifferentiation time points, particularly at days 9, 15 and 21, observing a different OCT3/4 and RUNX2 expression during the bone induction in the transfected cells. Particularly, OCT3/4 levels decreased in all transfected cells along the differentiation progress.

However, pRUNX2-siOCT3/4 transfection had the lowest expression levels at each time point. Moreover, pRUNX2 transfected cells showed a rapidly OCT3/4 downregulation at day 15, but it was the only population with certain OCT3/4 expression at the end of the process (Figure III-10-A). On the other hand, RUNX2 expression was downregulated in OCTA3/4 knockdown cells and was over-expressed in the pRUNX2 and pRUNX2-siOCT3/4 transfected cells (Figure III-10-B).

3.3.3.1.1 OCT3/4 knockdown and pRUNX2 over-expression accelerates the osteogenic differentiation

Once efficient co-delivery of siOCTA3/4 and pRUNX2 was confirmed, different osteogenic markers, such as ALP, COL1 and OSN, were studied in order to evaluate the quality of osteogenic induction at day 9, 15, and 21 of cell differentiation (Figure III-11). In addition, functional osteogenic activity was evaluated at day 21of differentiation by ALP and Alizarin Red S staining (Figure III-11-E-F).

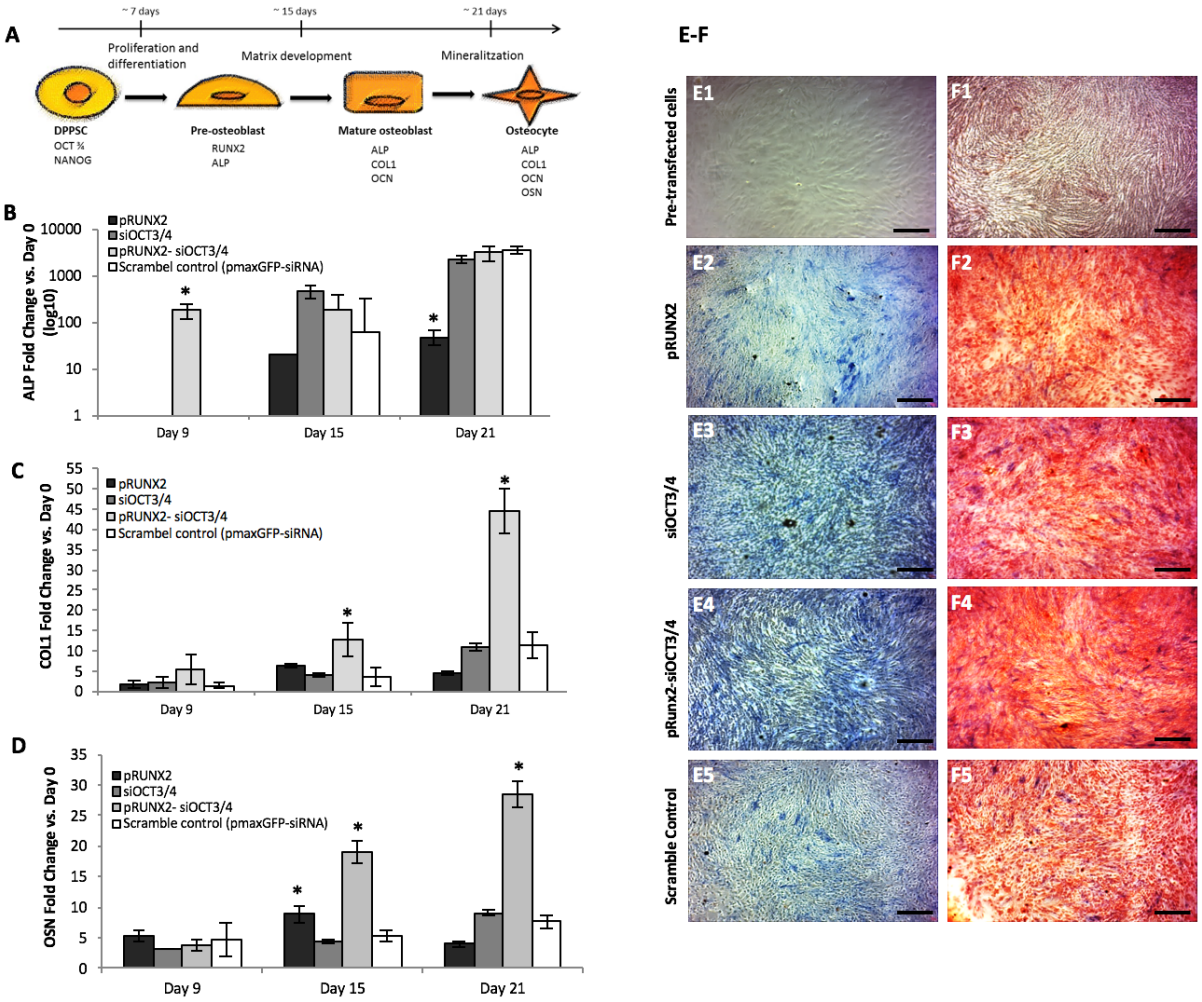

Figure III-11. Co-delivery of siOCT3/4 and pRUNX2 accelerates osteogenic differentiation of DPPSC. Scheme of the osteogenic process in DPPSC with recognizable stages of the osteogenic differentiation. B-D) Changes in the expression of osteogenic markers ALP, COL1 and OSN after DPPSC transfections respect undifferentiated DPPSC (Day 0) were analysed at days 9, 15, and 21 of osteogenic differentiation. The relative value for undifferentiated DPPSC (Day 0) was considered 1,

Scramble Control was used as a negative control. *P<0.05 respect Scramble Control. E) ALP activity observed in blue by an ALP staining before transfection, day 7 of osteogenic induction, (E1) and at the end of the osteogenic induction (E2-E5). F) Images of mineralization in red by Alizarin Red S staining before transfection, at day 7 of osteogenic induction, (F1) and after 21 days of osteogenic differentiation (F2-F5). Scale bars: 200 µm.

In general, raising levels of ALP were observed during the osteogenic differentiation in all transfected populations. However, pRUNX2-siOCT3/4-treated cells were the only condition with detectable ALP expression at 48 hours post transfection (day 9) (Figure III-11-B). In addition, similar behaviour was observed when COL1 and OSN levels were analysed. Cells transfected with pRUNX2-siOCT3/4 showed a significant increase of COL1 and OSN expression at day 15 and day 21 of osteo-differentation respect to other conditions (Figure III-11-C-D).

The functional osteogenic activity of the transfected cells after the osteogenic induction (day 21) was evaluated by ALP and Alizarin Red S staining's (Figure III-11-E-F). Representative images from bone-like transfected DPPSC showed that pRUNX2, siOCT3/4 and pRUNX2-siOCT3/4 transfected cells had more ALP activity and mineralization than the control cells transfected with pGFP plasmid and scramble siRNA. In addition, ALP and Alizarin Red quantification revealed that pRUNX2-siOCTA3/4 treated cells present more than 2-fold expression than scramble control.

Then, this results corroborate that RUNX2 upregulates osteoblastic gene expression and promotes osteogenesis[32]. It was demonstrated that pRUNX2 transfected cells exhibited increased osteoblastic gene expression and produced significantly higher quantities of mineralized matrix compared to the control cells. However, RUNX2 transfection alone was not sufficient to promote and accelerate the osteogenic process. Therefore, the co-transfection of DPPSC with pRUNX2 and siOCT3/4 showed a significantly higher expression of osteogenic markers (ALP, COL1 and OSN) and an earlier expression of some of these genes. Moreover, doubly transfected cells resulted in a higher matrix mineralization and ALP activity at the end of the differentiation process. Therefore, the administration of pRUNX2 and siOCT3/4 at day 7 of the osteogenic differentiation seems to allow the improvement and the acceleration of this process.

3.3.3.1.2 Cell viability and genetic stability study of DPPSC siOCTA 3/4 and/or pRUNX2 delivery

Transfection of cells using synthetic vectors could present some cell toxicity, which may limit their use for future therapeutic approaches. Furthermore, in regenerative medicine field is essential use a non-toxic delivery vectors because these can alter genetic behaviour of cells, altering their genetic stability. Therefore, viability of DPPSC cells after transfection with both pRUNX2 plasmid and/or anti-OCT3/4 siRNA was determined using the MTT assay, as shown Figure III-12.

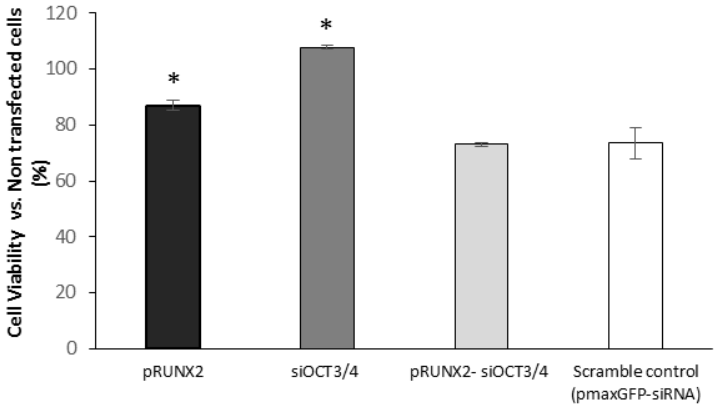

Figure III-12 Cell viability assay after siOCTA3/4 and/or pRUNX2 delivery using C32-R/D polymer. MTT assay was performed at day 21 of the osteogenic process. Scramble Control were used as negative control. *P<0.05 respect Scramble Control.

After 21 days of differentiation, cell viabilities greater than 70% were observed in all transfections. Transfection with both nucleic acids, pRUNX2-siOCT3/4, resulted in lower cell viability than cells transfected with either pRUNX2 plasmid or anti-OCT3/4 siRNA alone, 73% *vs* 87% *vs* 100% respectively. However, cell viability of double transfection was not statistically different than viability observed for cells transfected with the double control, i.e. pGFP and scramble siRNA. Similar cell viability values were observed for control cells transfected with pGFP plasmid and scramble siRNA, suggesting that the differences in cellular viability derived osteogenic differentiation process (Figure III-12). Previous results using the same oligopeptide-modified pBAEs showed cellular viabilities higher than 80%, and even 90%, in different cells types [1,30], proving themselves as excellent transfection agents. Therefore, these results may suggest that delivery vector is not altering the cellular viability.

However, stem cells are known to acquire genomic changes due to their genomic instability. Therefore, genomic integrity of stem cells before and after any treatment should be monitored carefully in basic research and clinical trials [38]. Then, to further characterize if delivery system or gene regulation can affect DPPSC behaviour, possible genetic alterations were studied. The short-CGH allowed the detection of all the characteristic aneuploidies in each sample analysed. We evaluated the genetic stability of DPPSC before the osteogenic differentiation (Day 0), 48h post double DPPSC transfection (Day 9) and during the osteogenic process of double transfected DPPSC (Days 15 and 21). 47, XXY control samples (labelled in green) and DPPSC samples (labelled in red) were co-hybridized onto 46, XY metaphases, as shown in figure Figure III-13.

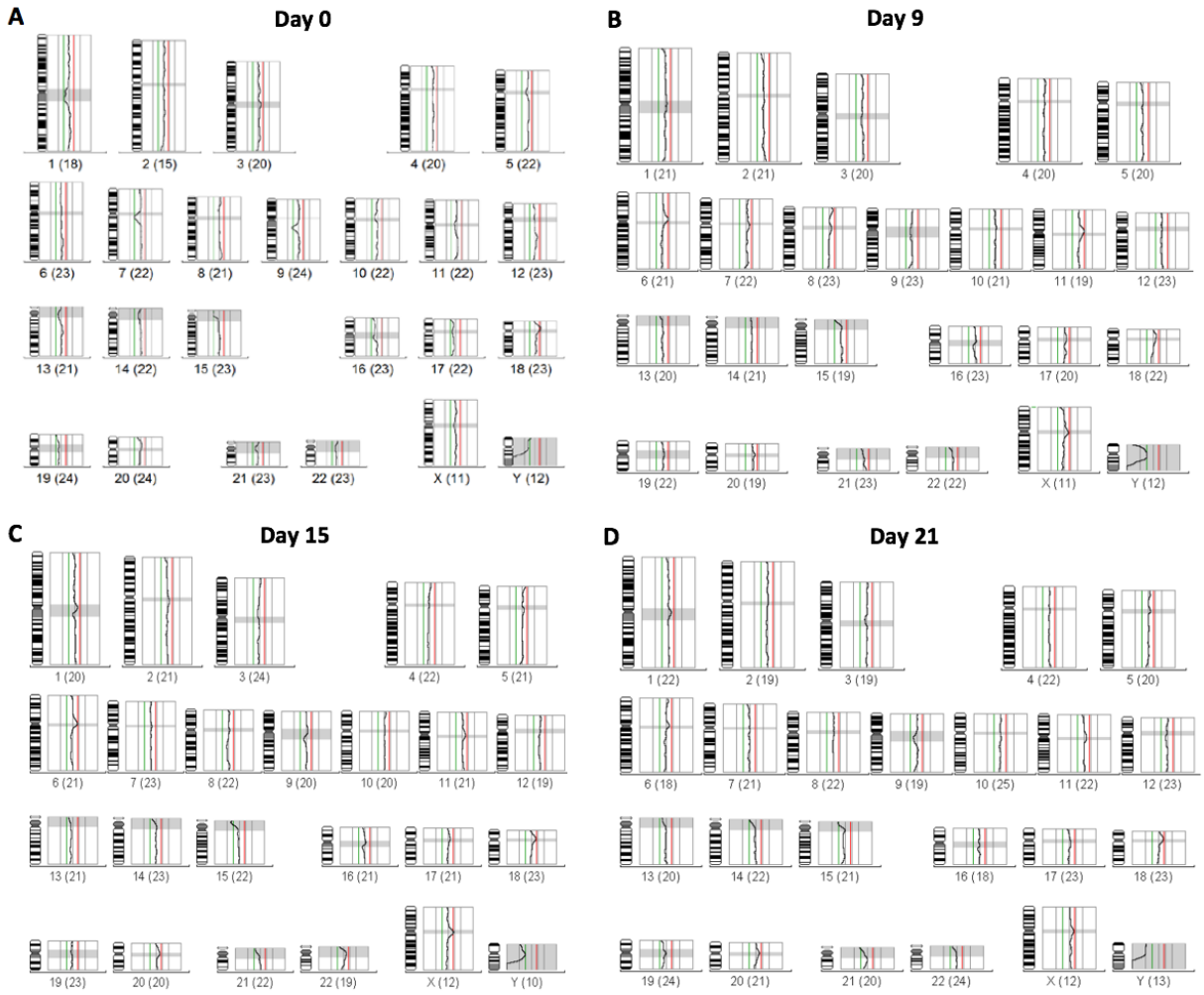

Figure III-13. pRunx2-siOCT3/4 transfections with modified-pBAEs do not induce genetic instability of DPPSCs during osteogenic differentiation Fixed limits summary of 47, XXY control samples (labelled in green) and pRunx2-siOCT3/4 DPPSC samples (labelled in red) co-hybridization onto 12 normal metaphases (46, XY) in triplicate. A) sCGH from undifferentiated DPPSC (day 0 of differentiation); B) sCGH from 48h post transfected DPPSC (day 9 of differentiation). C) sCGH from DPPSC at day 15 of differentiation. D) sCGH from DPPSC at day 21 of differentiation. Losses in the Y chromosome dosage were due to the female donors.

Transfection of DPPSC using oligopeptide-modified pBAEs did not show chromosome aneuploidies or imbalances in a summary of short-CGH with fixed limits (Figure III-13-A). Moreover, DPPSC maintained a normal chromosome dosage after transfection with pRUNX2-siOCT3/4 using modified-pBAEs at 48h post-transfection (Figure III-13-B) and until the end of the osteogenic induction (Figure III-13-C-D). There were only losses in the Y chromosome dosage (labelled in green) due to the female donors.

Therefore, these results suggest that previously developed carries are able to deliver therapeutic nucleic acids to challenging cells lines, such as stem cells, having a therapeutic effect without cytotoxic effects. Specifically, arginine- /aspartic acid- oligopeptide formulation was used due to their

efficient co-delivery of RNAi and plasmidic DNA. Moreover, as previously have been reported in chapter II and further corroborated in this chapter, arginine- /aspartic acid- oligopeptide mixture present slightly negative surface charge, which is able to avoid usual cytotoxic effects that high positive polyplexes present.

3.4 Concluding remarks

In this chapter, we have demonstrated the great potential of previously developed polymers inside of regenerative medicine. Taking in account all the oligopeptide-modified pBAEs features, we are able do co-deliver large and small nucleic acids to stem cell line in efficient and safety way, obtaining a promising therapeutic effect.

Due to the wide range of therapeutic applications, nanoparticle delivery systems have to be optimized for each study. As previously discussed in Chapter II, nanoparticle surface composition of pBAEs plays a key role and can be modulated varying with their oligopeptide composition. In this case, DPPSC polymer screening revealed that a mixture of positively- and negatively-charged oligopeptides promoted a preferential delivery both siRNAs and plasmids. Specifically, a mixture of arginine- /aspartic acid- oligopeptides at 70:30 weigh/weight ratio was identified as the top performing polymer formulation in terms of transfection efficiency and viability, obtaining more than 60% of transfection using both RNAi or plasmid and viabilities higher than 80-90%. Therefore, newly developed polymers are able to administrated high doses of therapeutics nucleic acids drugs in a safety way.

Once polymer formulation was selected, this was used to silencing undifferentiated population of cells expressing OCT3/4 and NANOG transcription factors that limits their osteogenic differentiation. Efficient OCTA3/4 and NANOG knockdown was observed in undifferentiated and differentiated DPPSC cells at 48 hour post-transfection. Consequently, ALP, COL1 and OCN osteogenic markers expression were increased in OCTA3/4 and/or NANOG knockdown DPPSC. Particularly, levels of ALP and OCN were greater in the siOCT3/4 transfected cells. In addition, it has been confirmed that RUNX2 expression, that is an essential regulator of bone development, was further enhanced in OCT3/4 knockdown DPPSC. Therefore, we hypothesized that the silencing of OCT3/4 combined with the expression of RUNX2 may be promising strategy in order to further improve and/or accelerate the osteogenic differentiation of DPPSC.

First of all, we confirmed that significant OCTA3/4 knockdown and RUNX2 overexpression was observed when pRUNX2 and siOCTA3/4 was delivered at day 7 of DPPSC osteodiffrentation. These results corroborate the potential of newly developed oligopeptide-modified pBAE, specifically C32-R/D, due to there are able to be therapeutically useful delivering different types of nucleic acids at the same time and in a simple administration.

Furthermore, a robustly osteogenic acceleration was observed in DPPSC after pRUNX2 and OCTA3/4 delivery, where a promising increase an earlier expression of osteogenic markers, such as ALP, COL1 and OSN, were obtained. In addition, higher matrix mineralization and ALP activity at the end of the differentiation process was observed.

Additionally, it has been confirmed that non-cytotoxic effect has been observed using our developed delivery vectors to enhance DPPSC differentiation. MTT assay demonstrated that delivery

vector is not altering the cellular viability and genetic stability analysis showed that transfection with modified pBAEs did not induce chromosomal instability.

Thus, we can conclude that, the combination of stem cells and biocompatible polymers to deliver/silencing specific genes may be a powerful technique to improve and accelerate bone tissue regeneration approaching them to different clinical applications. Moreover, these results confirm that newly developed delivery vectors could have a promising potential due to their biocompatibility and their easy manipulation to be designed for each therapeutic application.

Once they in vitro usability and compatibility were demonstrated, the next chapter goes and step further exploring oligopeptide-modified pBAEs stability having in mind their *in vivo* applications.

3.5 References

[1] P. Dosta, N. Segovia, A. Cascante, V. Ramos, S. Borrós, Surface charge tunability as a powerful strategy to control electrostatic interaction for high efficiency silencing, using tailored oligopeptide-modified poly(beta-amino ester)s (PBAEs), Acta Biomater. 20 (2015) 82–93. doi:http://dx.doi.org/10.1016/j.actbio.2015.03.029.

[2] M. Chimutengwende-Gordon, W.S. Khan, Advances in the use of stem cells and tissue engineering applications in bone repair., Curr. Stem Cell Res. Ther. 7 (2012) 122–6.

[3] A.S. Mistry, A.G. Mikos, Tissue Engineering Strategies for Bone Regeneration, in: 2005: pp. 1–22. doi:10.1007/b99997.

[4] P.B. Malafaya, G.A. Silva, R.L. Reis, Natural?origin polymers as carriers and scaffolds for biomolecules and cell delivery in tissue engineering applications, Adv. Drug Deliv. Rev. 59 (2007) 207–233. doi:10.1016/j.addr.2007.03.012.

[5] B. Chevallay, D. Herbage, Collagen-based biomaterials as 3D scaffold for cell cultures: applications for tissue engineering and gene therapy, Med. Biol. Eng. Comput. 38 (2000) 211–218. doi:10.1007/BF02344779.

[6] H. Kato, T. Nakamura, S. Nishiguchi, Y. Matsusue, M. Kobayashi, T. Miyazaki, H.M. Kim, T. Kokubo, Bonding of alkali- and heat-treated tantalum implants to bone., J. Biomed. Mater. Res. 53 (2000) 28–35.

[7] E. Ferraz, G. Freitas, M. Crovace, O. Peitl, E. Zanotto, P. Tambasco de Oliveira, M. Mateus Beloti, A. Rosa, Bioactive-glass ceramic with two crystalline phases (BioS-2P) for bone tissue engineering, Biomed. Mater. (2017). doi:10.1088/1748-605X/aa768e.

[8] A. Arthur, A. Zannettino, S. Gronthos, The therapeutic applications of multipotential mesenchymal/stromal stem cells in skeletal tissue repair, J. Cell. Physiol. 218 (2009) 237–245. doi:10.1002/jcp.21592.

[9] C.H. Evans, Gene delivery to bone, Adv. Drug Deliv. Rev. 64 (2012) 1331–1340. doi:10.1016/j.addr.2012.03.013.

[10] F. Wegman, F.C. Öner, W.J.A. Dhert, J. Alblas, Non-viral gene therapy for bone tissue engineering, Biotechnol. Genet. Eng. Rev. 29 (2013) 206–220. doi:10.1080/02648725.2013.801227.

[11] F. Yang, S. Cho, S. Mi, S.R. Bogatyrev, D. Singh, J.J. Green, Y. Mei, S.M. Son, S.R. Bogatyrev, D. Singh, J.J. Green, Y. Mei, S. Park, S.H. Bhang, B.-S. Kim, R. Langer, D.G. Anderson, Genetic engineering of human stem cells for enhanced angiogenesis using biodegradable polymeric nanoparticles, Proc. Natl. Acad. Sci. U. S. A. 107 (2010) 3317–22. doi:10.1073/pnas.0905432106.

[12] S.Y. Tzeng, B.P. Hung, W.L. Grayson, J.J. Green, Cystamine-terminated poly(beta-amino ester)s for siRNA delivery to human mesenchymal stem cells and enhancement of osteogenic differentiation, Biomaterials. 33 (2012) 8142–8151. doi:10.1016/j.biomaterials.2012.07.036.

[13] M. Atari, C. Gil-Recio, M. Fabregat, D. Garcia-Fernandez, M. Barajas, M.A. Carrasco, H.-S. Jung, F.H. Alfaro, N. Casals, F. Prosper, E. Ferres-Padro, L. Giner, Dental pulp of the third molar: a new source of pluripotent-like stem cells, J. Cell Sci. 125 (2012) 3343–3356. doi:10.1242/jcs.096537.

[14] M. Atari, M. Barajas, F. Hernández-Alfaro, C. Gil, M. Fabregat, E. Ferrés Padró, L. Giner, N. Casals, Isolation of pluripotent stem cells from human third molar dental pulp., Histol. Histopathol. 26 (2011) 1057–70.

[15] M.-S. E., Characterization of Dental Pulp Pluripotent-like Stem Cells (DPPSC) and their mesodermal differentiation potential., PhD. (2017).

[16] B.S. Kochupurakkal, R. Sarig, O. Fuchs, D. Piestun, G. Rechavi, D. Givol, Nanog inhibits the switch of myogenic cells towards the osteogenic lineage, Biochem. Biophys. Res. Commun. 365 (2008) 846–850. doi:10.1016/j.bbrc.2007.11.073.

[17] M. Atari, J. Caballé-Serrano, C. Gil-Recio, C. Giner-Delgado, E. Martínez-Sarrà, D.A. García-Fernández, M. Barajas, F. Hernández-Alfaro, E. Ferrés-Padró, L. Giner-Tarrida, The enhancement of osteogenesis through the use of dental pulp pluripotent stem cells in 3D, Bone. 50 (2012) 930–941. doi:10.1016/j.bone.2012.01.005.

[18] Y.-H. Loh, Q. Wu, J.-L. Chew, V.B. Vega, W. Zhang, X. Chen, G. Bourque, J. George, B. Leong, J. Liu, K.-Y. Wong, K.W. Sung, C.W.H. Lee, X.-D. Zhao, K.-P. Chiu, L. Lipovich, V.A. Kuznetsov, P. Robson, L.W. Stanton, C.-L. Wei, Y. Ruan, B. Lim, H.-H. Ng, The Oct4 and Nanog transcription network regulates pluripotency in mouse embryonic stem cells, Nat. Genet. 38 (2006) 431–440. doi:10.1038/ng1760.

[19] L. Liu, L. Wu, X. Wei, J. Ling, Induced Overexpression of Oct4A in Human Dental Pulp Cells Enhances Pluripotency and Multilineage Differentiation Capability, Stem Cells Dev. 24 (2015) 962–972. doi:10.1089/scd.2014.0388.

[20] J.-C. Yeo, H.-H. Ng, The transcriptional regulation of pluripotency, Cell Res. 23 (2013) 20–32. doi:10.1038/cr.2012.172.

[21] H. Darr, Overexpression of NANOG in human ES cells enables feeder-free growth while inducing primitive ectoderm features, Development. 133 (2006) 1193–1201. doi:10.1242/dev.02286.

[22] S. Park, K. Na, The transfection efficiency of photosensitizer-induced gene delivery to human MSCs and internalization rates of EGFP and Runx2 genes., Biomaterials. 33 (2012) 6485–94. doi:10.1016/j.biomaterials.2012.05.040.

[23] Y.-R. Yun, J.H. Jang, E. Jeon, W. Kang, S. Lee, J.-E. Won, H.W. Kim, I. Wall, Administration of growth factors for bone regeneration, Regen. Med. 7 (2012) 369–385. doi:10.2217/rme.12.1.

[24] Q.-G. Lai, K.-F. Yuan, X. Xu, D. Li, G.-J. Li, F.-L. Wei, Z.-J. Yang, S.-L. Luo, X.-P. Tang, S. Li, Transcription factor osterix modified bone marrow mesenchymal stem cells enhance callus formation during distraction osteogenesis, Oral Surgery, Oral Med. Oral Pathol. Oral Radiol. Endodontology. 111 (2011) 412–419. doi:10.1016/j.tripleo.2010.05.012.

[25] K. Pan, Q. Sun, J. Zhang, S. Ge, S. Li, Y. Zhao, P. Yang, Multilineage differentiation of dental follicle cells and the roles of Runx2 over-expression in enhancing osteoblast/cementoblast-related gene expression in dental follicle cells, Cell Prolif. 43 (2010) 219–228. doi:10.1111/j.1365-2184.2010.00670.x.

[26] P. Ducy, R. Zhang, V. Geoffroy, A.L. Ridall, G. Karsenty, Osf2/Cbfa1: A Transcriptional Activator of Osteoblast Differentiation, Cell. 89 (1997) 747–754. doi:10.1016/S0092-8674(00)80257-3.

[27] W. Liu, S. Toyosawa, T. Furuichi, N. Kanatani, C. Yoshida, Y. Liu, M. Himeno, S. Narai, A. Yamaguchi, T. Komori, Overexpression of Cbfa1 in osteoblasts inhibits osteoblast maturation and causes osteopenia with multiple fractures, J. Cell Biol. 155 (2001) 157–166. doi:10.1083/jcb.200105052.

[28] V. Geoffroy, M. Kneissel, B. Fournier, A. Boyde, P. Matthias, High Bone Resorption in Adult Aging Transgenic Mice Overexpressing Cbfa1/Runx2 in Cells of the Osteoblastic Lineage Vale, Mol. Cell. Biol. 17 (2013) 6222–6233. doi:10.1128/MCB.22.17.6222.

[29] D.M. Lynn, R. Langer, Degradable Poly(β-amino esters): Synthesis, Characterization, and Self-Assembly with Plasmid DNA, J. Am. Chem. Soc. 122 (2000) 10761–10768. doi:10.1021/ja0015388.

[30] N. Segovia, P. Dosta, A. Cascante, V. Ramos, S. Borrós, Oligopeptide-terminated poly(β-amino ester)s for highly efficient gene delivery and intracellular localization., Acta Biomater. 10 (2014) 2147–58. doi:10.1016/j.actbio.2013.12.054.

[31] K.J. Livak, T.D. Schmittgen, Analysis of Relative Gene Expression Data Using Real-Time Quantitative PCR and the 2−ΔΔCT Method, Methods. 25 (2001) 402–408. doi:10.1006/meth.2001.1262.

[32] M. Rius, A. Obradors, G. Daina, J. Cuzzi, L. Marques, G. Calderon, E. Velilla, O. Martinez-Passarell, M. Oliver-Bonet, J. Benet, J. Navarro, Reliability of short comparative genomic hybridization in fibroblasts and blastomeres for a comprehensive aneuploidy screening: first clinical application, Hum. Reprod. 25 (2010) 1824–1835. doi:10.1093/humrep/deq118.

[33] D. Putnam, C.A. Gentry, D.W. Pack, R. Langer, Polymer-based gene delivery with low cytotoxicity by a unique balance of side-chain termini, Proc. Natl. Acad. Sci. . 98 (2001) 1200–1205. doi:10.1073/pnas.98.3.1200.

[34] I. Chambers, D. Colby, M. Robertson, J. Nichols, S. Lee, S. Tweedie, a Smith, Functional expression cloning ot nanog, a pluripotency sustaining factor in embryonic stem cells, Cell. 113 (2003) 643–655.

[35] N.H. Foley, I. Bray, K.M. Watters, S. Das, T. Bernas, J.H.M. Prehn, R.L. Stallings, StemCellDB: The Human Pluripotent Stem Cell Database at the National Institutes of Health Barbara, Stem Cell. 18 (2012) 1089–1098. doi:10.1038/cdd.2010.172.MicroRNAs.

[36] E. Kärner, C.-M. Bäckesjö, J. Cedervall, R. V. Sugars, L. Ährlund-Richter, M. Wendel, Dynamics of gene expression during bone matrix formation in osteogenic cultures derived from human embryonic stem cells in vitro, Biochim. Biophys. Acta - Gen. Subj. 1790 (2009) 110–118. doi:10.1016/j.bbagen.2008.10.004.

[37] R.J. Miron, Y.F. Zhang, Osteoinduction: A Review of Old Concepts with New Standards, J. Dent. Res. 91 (2012) 736–744. doi:10.1177/0022034511435260.

[38] U. Ben-David, Analyzing the genomic integrity of stem cells, StemBook. (2014) 1–11. doi:10.3824/stembook.1.150.1.

Chapter IV

Development of stable polyplexes using poly(β-amino ester)s for efficient RNAi delivery

Submitted:

P. Dosta, V. Ramos, and S. Borrós, “Stable and efficient generation of poly(β-amino ester)s for RNAi delivery”, ACS Biomacromolecules, July 2017.

This page left blank intentionally

Development of stable polyplexes using poly(β-amino ester)s for efficient RNAi delivery

Despite their promising results in in vitro assays, their stability in physiological mediums represents one of the major historical limitations of these polymers. Then, in this chapter, different modifications in the pBAE structures have been explored to overcome stability limitation. Recent studies have demonstrated that hydrophobicity plays a key role to control electrostatic interactions of plasma proteins with nanoparticles, making them more stable and effective. Results show that a slight increase in the polymer hydrophobicity increases their siRNA packaging capacity, stability, and transfection efficiency. Therefore, newly designed hydrophobic polymers present great potential as RNAi delivery vectors.

4.1 Introduction

During the last year's greats efforts were focused to develop stable RNAi-based drugs using different chemical modifications in their structure, increasing their lifetime in plasma conditions [1–3]. However, as previously discussed in Chapter I, the use of naked nucleic acids is still limited because of they are rapidly degraded by RNases and basically eliminated by kidney [4]. Furthermore, if siRNA reaches target cells, it lacks the mechanism to enter to the cytoplasm. On the other hand, hydrophobic modifications using linear fatty acids, cholesterol or alkyl chains have been conjugated to RNAi in order to enhance delivery and endosome entrance [5]. However, this approach does not solve the lack of targeting. Furthermore different biomaterials have been used as delivery vectors, such as liposomes, cationic polymer, polymersomes, cell-penetrating peptide, and inorganic nanoparticles [6–10]. Typical synthetic vectors, such as poly(amido amine)s (PAA), polyethylenimine (PEI), chitosan or poly(l-lysine) (PLL) have been further improved to effectively deliver RNAi [11,12]. Despite their promising results *in vitro*, they are not efficient enough in order to obtain specific and efficient therapeutic delivery for *in vivo* applications.

In the previous chapters, a new strategy to deliver RNAi in a cell-specific manner using different oligopeptide-modified poly(β-amino ester)s has been developed. Results have showed that using a combination of natural oligopeptides during the polyplexes formation we are able to fine-tune polyplexes surface composition, designing a powerful mechanism to design highly cell-efficient and cell-specific polymeric carriers [13–15]. Promising results have been obtained using this newly developed approach in *in vitro* systems, however, they present low efficiency when are used in physiological media. Then, despite their attractiveness, they possess limited *in vivo* stability, which hampers their further development in clinical applications.

Taking into account the current status of delivery systems, this chapter describe an overview of different strategies in order to overcome oligopeptide-modified pBAEs stability limitations, obtaining a stable and cell-specific RNAi delivery vector.

For instance, recently it has been described that shielding the surface of pBAE-RNAi polyplexes using hydrogel matrix is a promising way to stabilize the resulting formulation [16]. For instance, oligopeptide-modified pBAEs were combined with a hydrogel scaffold based on polyamidoamine (PAMAM) dendrimer cross-linked with dextran aldehyde, which is able to protect them from degradation, obtaining a promising local delivery strategy to treated solid tumours [16]. However, this technique con not be used for systemic delivery, limiting their applicability in a wide range of therapeutic applications.

Alternatively, coating of polyplexes with reactive hydrophilic polymers has also shown both lateral and steric stabilization, resulting in nanoparticles with greater circulation times *in vivo* [17,18]. However, such strategies generate a shielding around the nanoparticle that hampers the formation of protein corona, which has lately shown to be beneficial for controlling uptake into specific cell types [19]. In order to exploit the benefits of protein corona, it is required to generate protein-resistant pBAE-siRNA nanoparticles capable of maintaining their physicochemical properties in complex media. In addition, nanoparticle surface composition is essential to describe their cell-entrance mechanism. It is already described that highly positive surface charge shown a different biodistribution than slightly negative nanoparticle surface charge. However, nowadays the potential of such protein-nanopaticle surfaces composition due to their protein corona interaction lacks of general method of characterization [20]. Furthermore, polymer modification of pBAEs has been widely explored and, as a result, controlled fine-tuning of the physicochemical properties of the nanoparticles has been reported [21]. In general, hydrophobization of polymers leads to increased stability of polyplexes, favouring the interactions between nanoparticles and the plasma proteins [22]. An increase of polymer hydrophobicity conduces to reduce or control protein absorption to polyplexes surface, making them more resistant to reach their final target or protect their RNAi-based drugs. Serum is one of the main causes that inhibit transfection efficiency of the resultant polyplex or limit their stability [23]. Recently, it is described that amphiphilic polycations, such as Pluronic, were combined to other polymers, making them capable of forming stable complexes in plasma conditions [24].

In addition, it is already described that an increase in the polyplex hydrophobicity is able to enhance packaging capacity of nucleic acids, reducing their nanometric size [12,23,25]. Besides electrostatic forces, hydrophobicity play a key role to the complex formation between pBAEs and RNAi-drug. Optimized hydrophilic/hydrophobic polymer are enough to condense higher RNA quantity increasing polyplex density. Furthermore, adding hydrophobic moieties to polymers formulations increase polyplex-cell affinity to biological lipid membranes, improving their transfection efficiency in different cells lines [26]. Cholesterol moieties are expected to enhance cellular transfection due to their high affinity with lipid parts of cell membrane[12]. As example, a higher binding affinity to bone

marrow stromal cells was observed when palmitic acid is added to PEI due to their hydrophobicity increment [27].

Therefore, in this chapter, we explored different poly(β-amino ester)s structures playing with their hydrophobicity in order to enhance their stability, packaging capacity and transfection efficiency. Mainly, previously described pBAEs (C32 polymer) [28] were further modified using different aliphatic amine chains, such as hexylamine, hexadecylamine, and cholesterol. As a result, we developed a wide range of stable natural-synthetic pBAE able to protect RNAi-drug from physiological media that maintain their cell-specificity proprieties. Then, their composition differs from traditional cationic polymers for their enough stability and functionality, making them closer for in vivo applications.

Therefore, the main objective of this chapter is to increase pBAE stability playing with their backbone structure in order to obtain stable and cell-specific polymer formulation taking in mind their *in vivo* applications.

In order to achieve this objective, the following tasks were proposed:

- Synthesis and biophysical characterization of a wide library of hydrophobic/hydrophilic pBAE.
- Stability study of newly synthetized pBAEs in physiological medium.
- Study of GFP knockdown efficiency and viability using stable polymer formulations, determining the effect of polymer hydrophobicity and oligopeptide composition.
- RNAi delivery study using the top-stable and efficient polymers modified with different oligopeptides in serum conditions.

4.2 Materials and Methods

4.2.1 Materials

Reagents and solvents used for polymer synthesis were purchased from Sigma-Aldrich and Panreac. Oligopeptide moieties used for polymer modification (H-Cys-Arg-Arg-Arg-NH_2, H-Cys-Lys-Lys-Lys-NH_2, H-Cys-His-His-His-NH_2, H-Cys-Glu-Glu-Glu-NH_2 and H-Cys-Asp-Asp-Asp-NH_2) were obtained from GL Biochem (Shanghai) Ltd with a purity higher than 98%. For in vitro studies, silencer GFP siRNA (AM4626) was used for EGFP knockdown and ON-TARGETplus non-targeting control pool (D-001810-10) as scramble siRNA control, all of them were obtained from Thermo GE Dharmacon. Labelled siRNA (AllStars Neg. siRNA AF 546) for uptake experiments was purchased from Qiagen. Polyplus Interferin reagent was purchased from VWR and used according to manufacturer instructions.

4.2.2 Synthesis of C32, C6, and C16 polymers

Acrylate-terminated polymers were synthesized by addition reaction of primary amines to 1,4-butanediol diacrylate (at 1:1.1 molar ratio of amine:diacrylate). C32 polymer was synthetized following a procedure described by Lynn et. al.[28]. Briefly, 5-amino-1- pentanol (3.44 g, 33 mmol) and 1,4-butanediol diacrylate (7.93 g, 40 mmol) were polymerized under magnetic stirring at 90 ºC for 24 h.

- C32 polymer

^{1}H-NMR(400MHz, DMSO-d_6, TMS) (ppm): δ =6,32 (d, C$\underline{H}_2$=CH-), 6,16 (d, CH_2=C$\underline{H}$-), 5,94 (d, C$\underline{H}_2$=CH-), 4.12 (br, C$\underline{H}_2$-O-C(=O)-CH=CH_2), 4.01 (t, -CH_2-C$\underline{H}_2$-O-), 3.35 (t, CH_2-C$\underline{H}_2$-OH), 2.65 (br, -CH_2-C$\underline{H}_2$-N-), 2.34 (br, -N-CH_2-C$\underline{H}_2$-C(=O)-O), 1.63 (br, -O-CH_2-C$\underline{H}_2$-C$\underline{H}_2$-CH_2-O), 1.35 (br, - C$\underline{H}_2$-CH2-C$\underline{H}_2$-CH_2-OH), 1.22 (br, N-$(CH_2)_2$-C$\underline{H}_2$-$(CH_2)_2$-OH).

C6 polymer was carried out by conjugate addition of different ratio of hexylamine / 5-amino-1-pentanol to 1,4-butanediol diacrylate using a slight excess of diacrylate (at 1:1.1 molar ratio of amine:diacrylate). Briefly, C6-100 polymerization was performed using hexylamine (0.845 g, 8.3 mmol) and 1,4-butanediol diacrylate (2.0 g, 9.1 mmol). C6-50 polymerization was performed using 5-amino-1-pentanol (0.426 g, 4.1 mmol), hexylamine (0.422 g, 4.1 mmol) and 1,4-butanediol diacrylate (2.0 g, 9.1 mmol). C6-25 polymerization was performed using 5-amino-1- pentanol (0.639 g, 6.2 mmol), hexylamine 0.232 g, 2.1 mmol) and 1,4-butanediol diacrylate (2.0 g, 9.1 mmol). All polymerizations were carried out under magnetic stirring at 90 ºC for 24 h. Polymers were characterized by ^{1}H-NMR using Chloroform-*d* as a solvent.

Table IV-1. Molar ratio of hexylamine/5-amino-1-pentanol of different C6 polymerizations.

Polymer	Molar Ratio (Hexylamine/5-amino-1-pentanol)	Molar Ratio (Amine/Diacrylate)	1,4-butanediol diacrylate	5-amino-1-pentanol	hexilamine
C6-100	1/0	1/1.1	9,1	-	8,3
C6-50	0.5/0.5	1/1.1	9,1	4,1	4,1
C6-25	0.25/0.75	1/1.1	9,1	6,2	2,1

- C6-100 polymer

^{1}H-NMR(400MHz, Chloroform-*d,* TMS) (ppm): δ =6,45 (d, C$\underline{H}_2$=CH-), 6,18 (d, CH_2=C$\underline{H}$-), 5,88 (d, C$\underline{H}_2$=CH-), 4.15 - 4.05 (br, C$\underline{H}_2$-O-C(=O)-CH=CH_2), 3,99 (t, -CH_2-C$\underline{H}_2$-O-), 2.62 (br, -CH_2-C$\underline{H}_2$-N-), 2.32 (br, -N-CH_2-C$\underline{H}_2$-C(=O)-O), 1.71 - 1.53 (br, -O-CH_2-C$\underline{H}_2$-C$\underline{H}_2$-CH_2-O), 1.36 - 1.12 (br, - C$\underline{H}_2$-CH2-C$\underline{H}_2$-CH_2-OH, N-$(CH_2)_2$-C$\underline{H}_2$-$(CH_2)_2$-OH), 0.83 (t, CH_2-CH_2-C$\underline{H}_3$).

- C6-50 polymer

^{1}H-NMR (400MHz, Chloroform-*d*, TMS) (ppm): δ =6,40 (d, C$\underline{H}_2$=CH-), 6,10 (d, CH_2=C$\underline{H}$-), 5,83 (d, C$\underline{H}_2$=CH-), 4.18 (br, C$\underline{H}_2$-O-C(=O)-CH=CH_2), 4,09 (t, -CH_2-C$\underline{H}_2$-O-), 3.62 (t, CH_2-C$\underline{H}_2$-OH), 2.78 (br, -CH_2-C$\underline{H}_2$-N-), 2.45 (br, -N-CH_2-C$\underline{H}_2$-C(=O)-O), 1.83 - 1.60 (br, -O-CH_2-C$\underline{H}_2$-C$\underline{H}_2$-CH_2-O), 1.40- 1.18 (br, - C$\underline{H}_2$-CH2-C$\underline{H}_2$-CH_2-OH, N-$(CH_2)_2$-C$\underline{H}_2$-$(CH_2)_2$-OH), 0.88 (t, CH_2-CH_2-C$\underline{H}_3$).

- C6-25 polymer

^{1}H-NMR(400MHz, Chloroform-*d*, TMS) (ppm): δ =6,40 (d, C$\underline{H}_2$=CH-), 6,12 (d, CH_2=C$\underline{H}$-), 5,83 (d, C$\underline{H}_2$=CH-), 4.19 (br, C$\underline{H}_2$-O-C(=O)-CH=CH_2), 4,09 (t, -CH_2-C$\underline{H}_2$-O-), 3.61 (t, CH_2-C$\underline{H}_2$-OH), 2.78 (br, -CH_2-C$\underline{H}_2$-N-), 2.45 (br, -N-CH_2-C$\underline{H}_2$-C(=O)-O), 1.80 – 1.57 (br, -O-CH_2-C$\underline{H}_2$-C$\underline{H}_2$-CH_2-O), 1.40- 1.18 (br, - C$\underline{H}_2$-CH2-C$\underline{H}_2$-CH_2-OH, N-$(CH_2)_2$-C$\underline{H}_2$-$(CH_2)_2$-OH), 0.88 (t, CH_2-CH_2-C$\underline{H}_3$).

C16 polymer was carried out by conjugate addition of different ratio of hexadecylamine / 5-amino-1-pentanol to 1,4-butanediol diacrylate using a slight excess of diacrylate (at 1:1.1 Molar ratio of amine:diacrylate). C16-50 polymerization was performed using 5-amino-1-pentanol (0.426 g, 4.1 mmol), hexadecylamine (1.1 g, 4.1 mmol) and 1,4-butanediol diacrylate (2.0 g, 9.1 mmol). C16-25 polymerization was performed using 5-amino-1- pentanol (0.639 g, 6.2 mmol), hexadecylamine (0.550 g, 2.1 mmol) and 1,4-butanediol diacrylate (2.0 g, 9.1 mmol). Polymerizations were carried out under magnetic stirring at 90 ºC for 24 h. Polymers were characterized by ^{1}H-NMR using Chloroform-*d* as a solvent.

Table IV-2. Molar ratio of hexadecylamine/5-amino-1-pentanol of different C16 polymerizations

Polymer	Molar Ratio (Hexylamine/ 5-amino-1-pentanol)	Molar Ratio (Amine/Diacrylate)	1,4-butanediol diacrylate	5-amino-1-pentanol	Hexadecylamine
C16-50	0.5/0.5	1/1.1	9,1	4,1	4,1
C16-25	0.25/0.75	1/1.1	9,1	6,2	2,1

- C16-50 polymer

^{1}H NMR (400 MHz, Chloroform-*d*, TMS) (ppm): δ =6,40 (d, C$\underline{H}_2$=CH-), 6,12 (d, CH$_2$=C$\underline{H}$-), 5,83 (d, C$\underline{H}_2$=CH-), 4.18 (br, C$\underline{H}_2$-O-C(=O)-CH=CH$_2$), 4,09 (t, -CH$_2$-C$\underline{H}_2$-O-), 3.61 (t, CH$_2$-C$\underline{H}_2$-OH), 2.74 (br, -CH$_2$-C$\underline{H}_2$-N-), 2.41 (br, -N-CH$_2$-C$\underline{H}_2$-C(=O)-O), 1.88- 1.15 (m, - C$\underline{H}_2$-CH2-C$\underline{H}_2$-CH$_2$-OH, N-(CH$_2$)$_2$-C$\underline{H}_2$-(CH$_2$)$_2$-OH, -O-CH$_2$-C$\underline{H}_2$-C$\underline{H}_2$-CH$_2$-O, -CH$_2$-(C$\underline{H}_2$)$_{14}$-CH$_3$), 0.85 (t, CH$_2$-CH$_2$-C$\underline{H}_3$).

- C16-25 polymer

^{1}H NMR (400 MHz, Chloroform-*d*, TMS) (ppm): δ =6,40 (d, C$\underline{H}_2$=CH-), 6,12 (d, CH$_2$=C$\underline{H}$-), 5,83 (d, C$\underline{H}_2$=CH-), 4.18 (br, C$\underline{H}_2$-O-C(=O)-CH=CH$_2$), 4,10 (t, -CH$_2$-C$\underline{H}_2$-O-), 3.62 (t, CH$_2$-C$\underline{H}_2$-OH), 2.76 (br, -CH$_2$-C$\underline{H}_2$-N-), 2.41 (br, -N-CH$_2$-C$\underline{H}_2$-C(=O)-O), 1.79- 1.18 (m, - C$\underline{H}_2$-CH2-C$\underline{H}_2$-CH$_2$-OH, N-(CH$_2$)$_2$-C$\underline{H}_2$-(CH$_2$)$_2$-OH, -O-CH$_2$-C$\underline{H}_2$-C$\underline{H}_2$-CH$_2$-O, -CH$_2$-(C$\underline{H}_2$)$_{14}$-CH$_3$), 0.83 (t, CH$_2$-CH$_2$-C$\underline{H}_3$).

4.2.3 Synthesis of Cchol polymers

Cchol polymers were synthetized by esterification of hydroxyl groups from C32 polymer with acid-modified cholesterol (cholesterol-COOH). However, firstly Cholesterol-COOH was synthetized by esterification of succinic anhydrous and cholesterol hydroxyl group. Briefly, Cholesterol (5g), succinic anhydride (5g), and a catalyst amount of 4-dimethylaminopyridine were dissolved in anhydrous pyridine (10 mL) and tetrahydrofuran (10 mL) and the resulting mixture was refluxes for 24 hours. After that, pH from the reaction was adjusted to 1-2 with hydrochloric acid solution (2 M) under ice cooling. Once pH was adjusted, the product was filtrated, collected and washed with distilled water until pH>5. The precipitate was recrystallized in ethyl acetate/ethanol system and dried under vacuum to obtain a pure white needle-like cholesterol succinate product, also called acid-modified cholesterol (Cholesterol-COOH). Figure IV-1 summarize Cholesterol-COOH chemical structure and synthesis. Final structure was corroborated by ^{1}H-RMN.

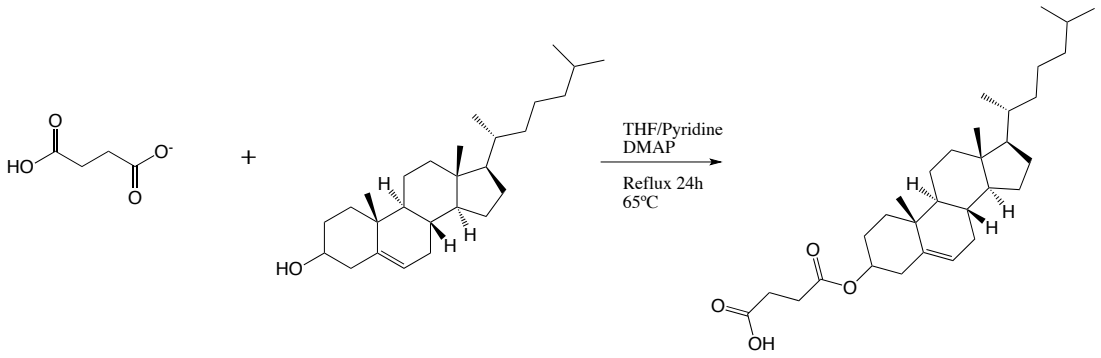

Figure IV-1. Cholesterol succinate synthesis.

Once Cholesterol-COOH was synthetized, Cchol-50 polymer was polymerized by esterification of 50% of hydroxyl groups mixing C32 polymer (0.3 g, 0.14 mmol) and Cholesterol-COOH (0.242 g, 0.49 mmol). Cchol-25 polymer was polymerized by esterification of 25% of hydroxyl groups mixing C32 (0.3 g, 0.14 mmol) and Cholesterol-COOH (0.121 g, 0.25 mmol). Cchol-12.5 polymer was

polymerized by esterification of 12.5 % of hydroxyl groups mixing C32 (0.3 g, 0.14 mmol) and Cholesterol-COOH (0.061 g, 0.12 mmol). All the polymerizations were carried out during 48 hours in tetrahydrofuran (THF). When esterification was completed, dicyclohexyl urea salt (DCU) were formed. Then, DCU salts were removed by filtration and THF was removed by rotavaporation. Finally, polymers were characterized by ^{1}H-NMR using Chloroform-*d* as a solvent.

Table IV-3. Different percentage of C32 polymer esterification using Cholesterol-COOH

Polymer	C32 (mmol)	Cholesterol-COOH (mmol)	C32 (g)	Cholesterol-COOH (g)
Cchol-50	0,14	0,49	0,3	0,242
Cchol-25	0,14	0,25	0,3	0,121
Cchol-12,5	0,14	0,12	0,3	0,061

- Cchol-50 polymer

^{1}H-NMR (400MHz, Chloroform-*d*, TMS) (ppm): δ =6,40 (d, C$\underline{H}_2$=CH-), 6,12 (d, CH$_2$=C$\underline{H}$-), 5,83 (d, C$\underline{H}_2$=CH-), 5.37(s, -C=C$\underline{H}$-C-), 4.69 – 4.55 (m, -O-C$\underline{H}$(-C-)$_2$) 4.19 (br, C$\underline{H}_2$-O-C(=O)-CH=CH$_2$), 4,09 (t, -CH$_2$-C$\underline{H}_2$-O-), 3.62 (t, CH$_2$-C$\underline{H}_2$-OH), 2.76 (br, -CH$_2$-C$\underline{H}_2$-N-), 2.60 (t, -O-C(=O)-C$\underline{H}_2$-C$\underline{H}_2$-C(=O)-O), 2.42 (br, -N-CH$_2$-C$\underline{H}_2$-C(=O)-O), 2.36 – 2.24, (m, from cholesterol), 2.09- 0.94 (m, - C$\underline{H}_2$-CH2-C$\underline{H}_2$-CH$_2$-OH, -O-CH$_2$-C$\underline{H}_2$-C$\underline{H}_2$-CH$_2$-O, N-(CH$_2$)$_2$-C$\underline{H}_2$-(CH$_2$)$_2$-OH, from cholesterol), 0.86 (dd, from cholesterol), 0.67 (s, -CH-(C$\underline{H}_2$)$_2$).

- Cchol-25 polymer

^{1}H NMR (400 MHz, Chloroform-d, TMS) (ppm): δ =6,40 (d, C$\underline{H}_2$=CH-), 6,12 (d, CH$_2$=C$\underline{H}$-), 5,83 (d, C$\underline{H}_2$=CH-), 5.37(s, -C=C$\underline{H}$-C-), 4.72 – 4.51 (m, -O-C$\underline{H}$(-C-)$_2$) 4.19 (br, C$\underline{H}_2$-O-C(=O)-CH=CH$_2$), 4,09 (t, -CH$_2$-C$\underline{H}_2$-O-), 3.62 (t, CH$_2$-C$\underline{H}_2$-OH), 2.76 (br, -CH$_2$-C$\underline{H}_2$-N-), 2.60 (t, -O-C(=O)-C$\underline{H}_2$-C$\underline{H}_2$-C(=O)-O), 2.43 (br, -N-CH$_2$-C$\underline{H}_2$-C(=O)-O), 2.35 – 2.22, (m, from cholesterol), 2.11- 0.89 (m, - C$\underline{H}_2$-CH2-C$\underline{H}_2$-CH$_2$-OH, -O-CH$_2$-C$\underline{H}_2$-C$\underline{H}_2$-CH$_2$-O, N-(CH$_2$)$_2$-C$\underline{H}_2$-(CH$_2$)$_2$-OH, from cholesterol), 0.86 (dd, from cholesterol), 0.67 (s, -CH-(C$\underline{H}_2$)$_2$).

- Cchol-12,5 polymer

^{1}H NMR (400 MHz, Chloroform-d, TMS) (ppm): δ =6,41 (d, C$\underline{H}_2$=CH-), 6,12 (d, CH$_2$=C$\underline{H}$-), 5,83 (d, C$\underline{H}_2$=CH-), 5.37(s, -C=C$\underline{H}$-C-), 4.66 – 4.55 (m, -O-C$\underline{H}$(-C-)$_2$) 4.18 (br, C$\underline{H}_2$-O-C(=O)-CH=CH$_2$), 4,09 (t, -CH$_2$-C$\underline{H}_2$-O-), 3.61 (t, CH$_2$-C$\underline{H}_2$-OH), 2.76 (br, -CH$_2$-C$\underline{H}_2$-N-), 2.60 (t, -O-C(=O)-C$\underline{H}_2$-C$\underline{H}_2$-C(=O)-O), 2.43 (br, -N-CH$_2$-C$\underline{H}_2$-C(=O)-O), 2.31, (m, from cholesterol), 2.09- 0.89 (m, - C$\underline{H}_2$-CH2-C$\underline{H}_2$-CH$_2$-OH, -O-CH$_2$-C$\underline{H}_2$-C$\underline{H}_2$-CH$_2$-O, N-(CH$_2$)$_2$-C$\underline{H}_2$-(CH$_2$)$_2$-OH, from cholesterol), 0.86 (dd, from cholesterol), 0.67 (s, -CH-(C$\underline{H}_2$)$_2$).

4.2.4 Synthesis of oligopeptide-modified pBAE polymers

In general, oligopeptide-modified pBAEs were obtained by end-modification of acrylate-terminated polymer with thiol-terminated oligopeptide at 1:2.5 molar ratio in dimethyl sulfoxide. The mixture was stirred overnight at room temperature, and the resulting polymer was obtained by precipitation in a mixture of diethyl ether and acetone (7:3 v/v).

All the polymerizations were modified using arginine as oligopeptide in order to study their stability/transfection efficiency. After that, the top performing polymer formulations (C6-50 and Cchol-50) were further modified using arginine, lysine, histidine, aspartic acid and glutamic acid peptides. The different oligopeptide modifications were confirmed by ^{1}H-RMN. C32 oligopeptide modifications have already described by Segovia et al. [14].

- C6-50-CR3

^{1}H-NMR(400MHz, Methanol-d_4, TMS) (ppm): δ = 4.41-4.33 (br, NH_2-C(=O)-C<u>H</u>-NH-C(=O)-C<u>H</u>-NH-C(=O)-C<u>H</u>-NH-C(=O)-C<u>H</u>-CH_2-, 4.11 (t, CH_2-C<u>H_2</u>-O), 3.55 (t, CH_2-C<u>H_2</u>-OH), 3.22 (br, NH_2-C(=NH)-NH-C<u>H_2</u>-, OH-$(CH_2)_4$-C<u>H_2</u>-N-), 3.04 (t, CH_2-C<u>H_2</u>-N-), 2.82 (dd, -C<u>H_2</u>-S-C<u>H_2</u>), 2.48 (br, -N-CH_2-C<u>H_2</u>-C(=O)-O), 1.90 (m, NH_2-C(=NH)-NH-$(CH_2)_2$-C<u>H_2</u>-CH-), 1.73 (br, -O-CH_2-C<u>H_2</u>-C<u>H_2</u>-CH_2-O), 1.69 (m, NH_2-C(=NH)-NH-CH_2-C<u>H_2</u>-CH_2-), 1.56 (br, -C<u>H_2</u>-CH2-C<u>H_2</u>-CH_2-OH), 1.39 (br, -N-$(CH_2)_2$-C<u>H_2</u>-$(CH_2)_2$-OH), 0.88 (t, CH_2-CH_2-C<u>H_3</u>).

- C6-50-CK3

^{1}H-NMR(400MHz, Methanol-d_4, TMS) (ppm): δ = 4.38-4.29 (br, NH_2-$(CH_2)_4$-C<u>H</u>-), 4.13 (t, CH_2-C<u>H_2</u>-O-), 3.73 (br, NH_2-C<u>H</u>-CH_2-S-), 3.55 (t, CH_2-C<u>H_2</u>-OH), 2.94 (br, CH_2-C<u>H_2</u>-N-, NH2-C<u>H_2</u>-$(CH_2)_3$-CH-), 2.81 (dd, -C<u>H_2</u>-S-C<u>H_2</u>), 2.57 (br, -N-CH_2-C<u>H_2</u>-C(=O)-O), 1.85 (m, NH_2-$(CH_2)_3$-C<u>H_2</u>-CH-), 1.74 (br, -O-CH_2-C<u>H_2</u>-C<u>H_2</u>-CH_2-O), 1.68 (m, NH_2-CH_2-C<u>H_2</u>-$(CH_2)_2$-CH-), 1.54 (br, - C<u>H_2</u>-CH2-C<u>H_2</u>-CH_2-OH), 1.37 (br, N-$(CH_2)_2$-C<u>H_2</u>-$(CH_2)_2$-OH), 0.88 (t, CH_2-CH_2-C<u>H_3</u>).

- C6-50-CH3

^{1}H-NMR(400MHz, Methanol-d_4, TMS) (ppm): δ = 8.0-7.0 (br -N(=C<u>H</u>)-NH-C(=C<u>H</u>)-), 4.61-4.36 (br, -CH_2-C<u>H</u>-), 4.16 (t, CH_2-C<u>H_2</u>-O-), 3.55 (t, CH_2-C<u>H_2</u>-OH), 3.18 (t, CH_2-C<u>H_2</u>-N-), 3.06 (dd, -C<u>H_2</u>-CH-), 2.88 (br, OH-$(CH_2)_4$-C<u>H_2</u>-N-), 2.82 (dd, -C<u>H_2</u>-S-C<u>H_2</u>-), 2.72 (br, -N-CH_2-C<u>H_2</u>-C(=O)-O), 1.75 (br, -O-CH_2-C<u>H_2</u>-C<u>H_2</u>-CH_2-O), 1.65 (m, NH_2-CH_2-C<u>H_2</u>-$(CH_2)_2$-CH-), 1.58 (br, -C<u>H_2</u>-CH2-C<u>H_2</u>-CH_2-OH), 1.40 (br, N-$(CH_2)_2$-C<u>H_2</u>-$(CH_2)_2$-OH), 0.88 (t, CH_2-CH_2-C<u>H_3</u>).

- C6-50-CD3

^{1}H-NMR(400MHz, DMSO-d_6, TMS) (ppm): δ = 4.56-4.44 (br, NH_2-C(=O)-C<u>H</u>-NH-C(=O)-C<u>H</u>-NH-C(=O)-C<u>H</u>-NH-C(=O)-C<u>H</u>-CH_2-), 4.19 (br,NH_2-C<u>H</u>-CH_2-S), 4.00 (t, CH_2-C<u>H_2</u>-O), 3.34 (t, CH_2-C<u>H_2</u>-OH), 2.98 (dd, -C<u>H_2</u>-S-C<u>H_2</u>), 2.57-2.48 (t, -CH-C<u>H_2</u>-COO-), 2.40 (br, -N-CH_2-C<u>H_2</u>-C(=O)-O), 1.60 (br, -O-

CH_2-C<u>H</u>$_2$-C<u>H</u>$_2$-CH_2-O), 1.38 (br, -C<u>H</u>$_2$-CH_2-C<u>H</u>$_2$-CH_2-OH), 1.20 (br, -N-$(CH_2)_2$-C<u>H</u>$_2$-(CH2)$_2$-OH), 0.88 (t, CH_2-CH_2-C<u>H</u>$_3$).

- <u>Cchol-50-CR3</u>

^{1}H NMR (400 MHz, Methanol-*d*$_4$, TMS): δ = 5.40(s, -C=C<u>H</u>-C-), 4.54 – 4.33 (m, -O-C<u>H</u>(-C-)$_2$, NH_2-C(=O)-C<u>H</u>-NH-C(=O)-C<u>H</u>-NH-C(=O)-C<u>H</u>-NH-C(=O)-C<u>H</u>-CH_2-), 4.29-4.09 (br, C<u>H</u>$_2$-O-C(=O)-CH=CH_2), 4,09 (t, -CH_2-C<u>H</u>$_2$-O-), 3.60 (t, CH_2-C<u>H</u>$_2$-OH), 3.40-2.76 (m, -CH_2-C<u>H</u>$_2$-N-, NH_2-C(=NH)-NH-C<u>H</u>$_2$-, -C<u>H</u>$_2$-S-C<u>H</u>$_2$, from cholesterol and peptide), 2.63 (t, -O-C(=O)-C<u>H</u>$_2$-C<u>H</u>$_2$-C(=O)-O), 2.38 – 2.25, (m, from cholesterol), 2.12- 0.99 (m, - C<u>H</u>$_2$-CH_2-C<u>H</u>$_2$-CH_2-OH, -O-CH_2-C<u>H</u>$_2$-C<u>H</u>$_2$-CH_2-O, N-$(CH_2)_2$-C<u>H</u>$_2$-$(CH_2)_2$-OH, from cholesterol and peptide), 0.90 (dd, from cholesterol), 0.74 (s, -CH-(C<u>H</u>$_2$)$_2$.

- <u>Cchol-50-CK3</u>

^{1}H NMR (400 MHz, Methanol-*d*$_4$, TMS): δ = 5.40(s, -C=C<u>H</u>-C-), 4.42 – 4.30 (m, -O-C<u>H</u>(-C-)$_2$, from peptide), 4,25-4.05 (m, C<u>H</u>$_2$-O-C(=O)-CH=CH_2, -CH_2-C<u>H</u>$_2$-O-), 3.60 (t, CH_2-C<u>H</u>$_2$-OH), 3.55-2.75 (m, -C<u>H</u>$_2$-S-C<u>H</u>$_2$, CH_2-C<u>H</u>$_2$-N-, NH2-C<u>H</u>$_2$-$(CH_2)_3$-CH-, from cholesterol and peptide), 2.62 (t, -O-C(=O)-C<u>H</u>$_2$-C<u>H</u>$_2$-C(=O)-O), 2.36 – 2.24, (m, from cholesterol), 2.10- 0.99 (m, - C<u>H</u>$_2$-CH_2-C<u>H</u>$_2$-CH_2-OH, -O-CH_2-C<u>H</u>$_2$-C<u>H</u>$_2$-CH_2-O, N-$(CH_2)_2$-C<u>H</u>$_2$-$(CH_2)_2$-OH, from cholesterol and peptide), 0.90 (dd, from cholesterol), 0.74 (s, -CH-(C<u>H</u>$_2$)$_2$.

- <u>Cchol-50-CH3</u>

^{1}H NMR (400 MHz, Methanol-*d*$_4$, TMS): δ = 8.6-7.0 (m -N(=C<u>H</u>)-NH-C(=C<u>H</u>)-), 5.41(s, -C=C<u>H</u>-C-), 4.75 – 4.49 (m, -O-C<u>H</u>(-C-)$_2$, from peptide), 4.20-4.08 (m, C<u>H</u>$_2$-O-C(=O)-CH=CH_2, -CH_2-C<u>H</u>$_2$-O-), 3.60 (t, CH_2-C<u>H</u>$_2$-OH), 3.55-2.70 (m, -C<u>H</u>$_2$-S-C<u>H</u>$_2$, CH_2-C<u>H</u>$_2$-N-, from cholesterol and peptide), 2.62 (t, -O-C(=O)-C<u>H</u>$_2$-C<u>H</u>$_2$-C(=O)-O), 2.32, (m, from cholesterol), 2.19- 0.93 (m, - C<u>H</u>$_2$-CH_2-C<u>H</u>$_2$-CH_2-OH, -O-CH_2-C<u>H</u>$_2$-C<u>H</u>$_2$-CH_2-O, N-$(CH_2)_2$-C<u>H</u>$_2$-$(CH_2)_2$-OH, from cholesterol), 0.93-0.86 (dd, from cholesterol), 0.74 (s, -CH-(C<u>H</u>$_2$)$_2$.

- <u>Cchol-50-CD3</u>

^{1}H NMR (400 MHz, DMSO-*d*$_6$, TMS): δ = 5.33(s, -C=C<u>H</u>-C-), 4.42 – 4.05 (m, -O-C<u>H</u>(-C-)$_2$, C<u>H</u>$_2$-O-C(=O)-CH=CH_2, -CH_2-C<u>H</u>$_2$-O-, from peptide), 3.63 (t, CH_2-C<u>H</u>$_2$-OH), 3.51-2.63 (m, -C<u>H</u>$_2$-S-C<u>H</u>$_2$, CH_2-C<u>H</u>$_2$-N-, -O-C(=O)-C<u>H</u>$_2$-C<u>H</u>$_2$-C(=O)-O, from cholesterol and peptide), 2.28 – 2.19, (m, from cholesterol), 2.05- 0.89 (m, - C<u>H</u>$_2$-CH_2-C<u>H</u>$_2$-CH_2-OH, -O-CH_2-C<u>H</u>$_2$-C<u>H</u>$_2$-CH_2-O, N-$(CH_2)_2$-C<u>H</u>$_2$-$(CH_2)_2$-OH, from cholesterol), 0.84 (dd, from cholesterol), 0.65 (s, -CH-(C<u>H</u>$_2$)$_2$.

- <u>Cchol-50-CE3</u>

^{1}H NMR (400 MHz, DMSO-*d*$_6$, TMS): ^{1}H NMR (400 MHz, DMSO-*d*$_6$, TMS): δ = 5.33(s, -C=C<u>H</u>-C-), 4.44 – 4.06 (m, -O-C<u>H</u>(-C-)$_2$, C<u>H</u>$_2$-O-C(=O)-CH=CH_2, -CH_2-C<u>H</u>$_2$-O-, from peptide), 3.63 (t, CH_2-C<u>H</u>$_2$-OH), 3.50-2.62 (m, -C<u>H</u>$_2$-S-C<u>H</u>$_2$, CH_2-C<u>H</u>$_2$-N-, -O-C(=O)-C<u>H</u>$_2$-C<u>H</u>$_2$-C(=O)-O, from cholesterol and

peptide), 2.27 – 2.18, (m, from cholesterol), 2.05- 0.89 (m, - C$\underline{H}_2$-CH_2-C$\underline{H}_2$-CH_2-OH, -O-CH_2-C$\underline{H}_2$-C$\underline{H}_2$-CH_2-O, N-$(CH_2)_2$-C$\underline{H}_2$-$(CH_2)_2$-OH, from cholesterol), 0.84 (dd, from cholesterol), 0.65 (s, -CH-(C$\underline{H}_2$)$_2$.

4.2.5 Biophysical characterization of oligopeptide end-modified pBAEs

Polyplexes were performed mixing equal volume of pBAEs and nucleic acids in acetate buffer at their appropriate concentration. For C32 polyplexes 25 mM AcONa buffer was used, for C6 polyplexes 12.5 mM AcONa buffer was used, and for Cchol polyplexes 8.3 mM AcONa buffer was used. Briefly, pBAE stock solutions in DMSO (100 mg mL^{-1}) were diluted at proper concentration to obtain the desired polymer–RNAi weight/weight ratio. pBAE was added to a solution of RNAi, mixed with pipetting for a few seconds and incubated at room temperature for 10 min. Then, the resulting nanoparticles were characterized by agarose retardation assay and Dynamic Light Scattering (DLS).

To assess RNAi retardation, different RNA-to-polymer ratios (w/w) between 10:1 until 400:1 were studied. pBAE-RNA complexes were freshly prepared and added to wells of agarose gel (2.5 %, containing 1 µg ml^{-1} ethidium bromide). Samples were run at 80 V for 45 min (Apelex PS 305, France) and visualized by UV illumination.

Size and surface charge were determined by DLS (Malvern Instruments Ltd, United Kingdom, 4-mW laser). Polyplexes were performed as previously described. After 10 min of incubation at room temperature, 100 µL of nanoparticles were diluted with 900 µL of PBS 1x for further hydrodynamic size and Z-potential analysis.

4.2.6 Polymer stability study

Arginine-modified polyplexes using C32, C6-100, C6-50, C6-25, C16-50, C16-25, Cchol-50, Cchol-25, and Cchol-12.5 backbone were prepared as previously described and used for stability studies. 100 µL of polyplexes were precipitated in 900 µL of PBS 1X. Then, size and polydispersity were determined using Dynamic Light Scattering (DLS) at different time points. In contrast, Z-potential were analyzed at the beginning and the end of the stability study. C32-CR3 polymer was used as a control group.

4.2.7 In vitro screening of newly developed hydrophilic/hydrophobic polymer using MDA MB 231

EGFP silencing screening using siRNA against GFP was performed using newly hydrophilic/hydrophobic polymer formulations (C32, C6-100, C6-50, C6-25, C16-50, C16-25, Cchol-50, Cchol-25, and Cchol-12.5) in MDA MB 231 cell line. siRNA transfection was performed with polyplexes prepared as previously described, using AcONa buffer (25-8.3 mM, pH 5.0). Briefly, MDA MB 231cells were seeded on 96-well plates at 10000 cells/well (DMEM, containing 10 % fetal bovine serum, 100 units mL^{-1} penicillin, 100 µg mL^{-1} streptomycin, 0.1mM MEM Non-Essential Amino Acids (NEAA), 2mM glutamine) and incubated overnight to roughly 80% confluence prior to performing the transfection experiments. Firstly, screening of polyplexes were performed at different polymer:siRNA w/w ratios using serum-free medium and added to cells at a final RNAi concentration of 50 nM. After

that, a different siRNA concentrations, ranging from 50 nM to 12.5 nM, were studied using all the polymeric formulations at 50:1 polymer:siRNA ratio. In both case, cells were incubated with nanoparticles during 2 h at 37 ºC in 5% CO_2 atmosphere. After that, polyplexes were removed and replaced with completed medium. GFP expression was analyzed at 48-hour post-transfection by flow cytometry (BD LSRFortessa cell analyzer). Polyplus Interferin was used as a transfection reagent control and untreated cells as a negative control.

4.2.8 Cellular uptake assay

siRNA labelled with AF555 was used for siRNA uptake experiment. MDA-MB 231 cells were seeded in 96 well plate at 10000 cell/ well. After 24 hours, uptake experiment was carried using different arginine-modified hydrophilic/hydrophobic polymer formulations. Briefly, polyplexes were performed as previously described using fluorescent siRNA. Then, cells were incubated with polyplexes at 50:1 ratio and final siRNA concentration of 50 nM during 2 h using serum free medium. After that, nanoparticles were removed, cells were washed twice with PBS 1X and collected according to the standard protocols (fixed using 1 % of paraformaldehyde) for flow cytometry analysis. Polyplus Interferin was conducted following manufacturer instructions and used as a positive control.

4.2.9 Cell viability assay

Immortalized MDA MB 231 cells were grown in 96-well plates at an initial seeding density of 10000 cells/well in 200 µL growth medium. Cells were grown for 24 h, transfected with different polymer formulations at final concentration of 50 nM (at 50:1 polymer:siRNA ratio) during 2h using serum free medium. Then, nanoparticles were removed, cells were washed once with PBS 1X and completed medium was added. 48 h post-transfection, the medium was removed, cells were washed with PBS, and complete medium supplemented with 20% MTS reagent (v/v) was added. Cells were incubated at 37 ºC, and absorbance was measured at 490 nm using a microplate reader (Elx808 Biotek Instrument Ltd, USA). Cell viability was expressed as a relative percentage compared with untreated cells.

4.2.10 In vitro screening of oligopeptide-modified C6-50 and Cchol-50 polymers in presence of serum

Transfection efficiency of our new oligopeptide end-modified C6-50 and Cchol-50 were studied in presence of serum. Briefly, MDA MB 231 cells were grown in 96-well plates at an initial seeding density of 10000 cells/well in 200 µL of growth medium, obtaining 80% of confluence prior to transfection. Then, cells were transfected using different oligopeptide end-modified pBAE at final siRNA concentration of 50 nM (at 100:1 polymer :siRNA w/w ratio). Polyplexes were incubated during 48 h. Then, the medium was removed, cells were washed with PBS 1X, cells were fixed using 1% of paraformaldehyde and analyzed by flow cytometry. Polyplus Interferin was conducted following manufacturer instructions and used as a positive control. Non-transfected cells and scramble siRNA were used as a negative control.

4.2.11 Transfection efficiency of stable polymers at different time points

Transfection efficiency of C32-CR3, C6-50-CR3, and Cchol-50-CR3 at different time points (0, 24, 48, and 120h) in presence or absence of FBS were determined in MDA MB 231 cells. Briefly, 100 µL of nanoparticles condensing siGFP were performed at different time points and incubated in completed or serum free medium at 37 ºC. After that, polyplexes were used to knockdown GFP expression using MDA MB 231 cells. Cells were seeded in 96 well plate at initial seeding density of 10000 cells/well in order to obtain an 80% of confluence prior to perform the transfection. Then, cells were transfected using different polyplexes in completed medium and 48 h post-transfection GFP expression was analyzed by flow cytometry.

4.2.12 Statistical analysis

Statistical analyses were carried out with Graph-Pad Prism (GraphPad Software). All error bars reported are SD unless otherwise indicated. Pairwise comparisons were performed using one-way Student *t*-tests. Differences between groups were considered significant at *p* values below 0.05 (* $p < 0.05$, ** $p < 0.01$, *** $p < 0.001$).

4.3 Results and discussion

Efficient RNAi delivery is one of the major historical limitations inside of RNAi therapy. As it has been introduced in Chapter I, different strategies to deliver RNAi-based drugs have been employed, however most of them are not effective enough for *in vivo* applications.

In chapter II, we observed that we are able to design cell-specific nanoparticles playing with their oligopeptide formulation resulting in fine tuning of their superficial composition. Moreover, we showed a direct effect between their oligopeptide composition, transfection efficiency, and viability. Specifically, we observed that by mixing positive and negative oligopeptides (C32-R/D) it was possible to obtain less cytotoxic polyplexes, maintaining their transfection efficiency. In addition, playing with their oligopeptide formulation, polyplexes with different surface charge have been obtained. Taking into account all of these proprieties, we hypothesized that controlling the nanoparticle surface composition could be a promising strategy to control their protein corona, increasing their stability for *in vivo* applications.

To assess if new pBAE formulations are stable in the presence of serum (FBS), the silencing efficiency of different oligopeptide-modified pBAE formulations was compared at different serum percentages, ranging from 0% to 10%, in MDA MB 231 cells. Silencing efficiency was evaluated by measuring the decrease in cell fluorescence by flow cytometry, as previously explained in materials and methods (Figure IV-2).

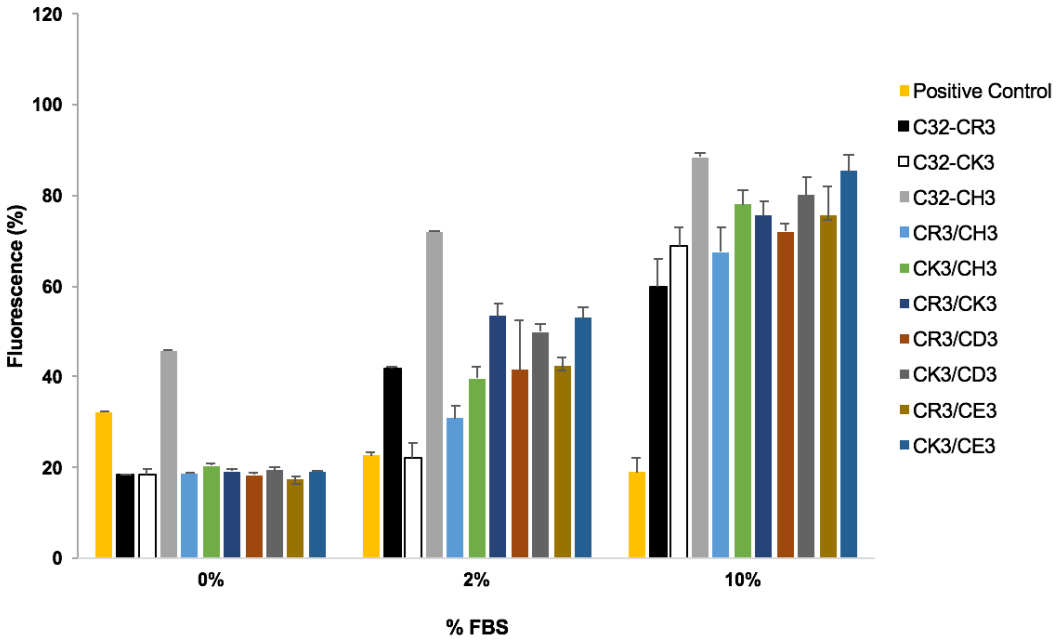

Figure IV-2 Gene silencing of MDA-MB-231-GFP cells transfected with different pBAE polymer nanoparticles. Cells were transfected with siGFP at a final concentration of 50 nM of siGFP/well at different percentatge of FBS. Their fluorescence was determined after 48 h by flow cytometry. Results are shown as mean and standard deviation of triplicates.

As previously observed in Chapter II, oligopeptide-modified pBAE polymers present greater GFP knockdown than positive control (commercial reagent) when serum free medium was used. However, it can be observed that the overall efficiency of pBAE formulations was decreased in the presence of serum proteins. Arginine-modified pBAE obtain the best silencing efficiency, reaching 40% of GFP knockdown. In contrast, when serum free medium was used, at least an 80% of GPF knockdown was observed. In addition, results demonstrated that siRNA particles prepared from mixtures of cationic and anionic or cationic and cationic pBAE polymers were not able to increase silencing efficiency compared to single cationic pBAEs formulations, suggesting that serum proteins interact or destabilize polyplexes formulations making them less efficient.

These preliminary results indicate that although formulation of cationic and anionic pBAEs may be a powerful strategy to identify cell-specific formulations, further stabilization may be required for *in vivo* applications. Thus, in this chapter, we were focused on enhancing the previously described poly(β-amino ester)s making them more efficient for *in vivo* applications. Therefore, different polymer backbone structures have been studied.

4.3.1 Synthesis and Biophysical characterization of newly stable oligopeptide end-modified pBAEs

Polymer backbone structure plays a key role to control polyplexes behavior in terms of stability and transfection efficiency [23]. Then, poly(β-amino ester)s with different hydrophobicity were synthesized and biophysically characterized. Polymerization of newly stable pBAE was performed following the same methodology previously described [28]. However, in this study, pBAE polymers with different hydrophobicity were obtained combining three different monomers: 1,4-butanediol diacrylate, two different hydrophobic alkylamines, hexylamine or hexadecylamine, and 5-amino-1-pentanol, which was used as the hydrophilic amine (Figure IV-3). The hydrophobicity of the resulting polymer (C6 and C16) was controlled by molar stoichiometry of hydrophilic/hydrophobic amine, as shown Figure IV-3(i).

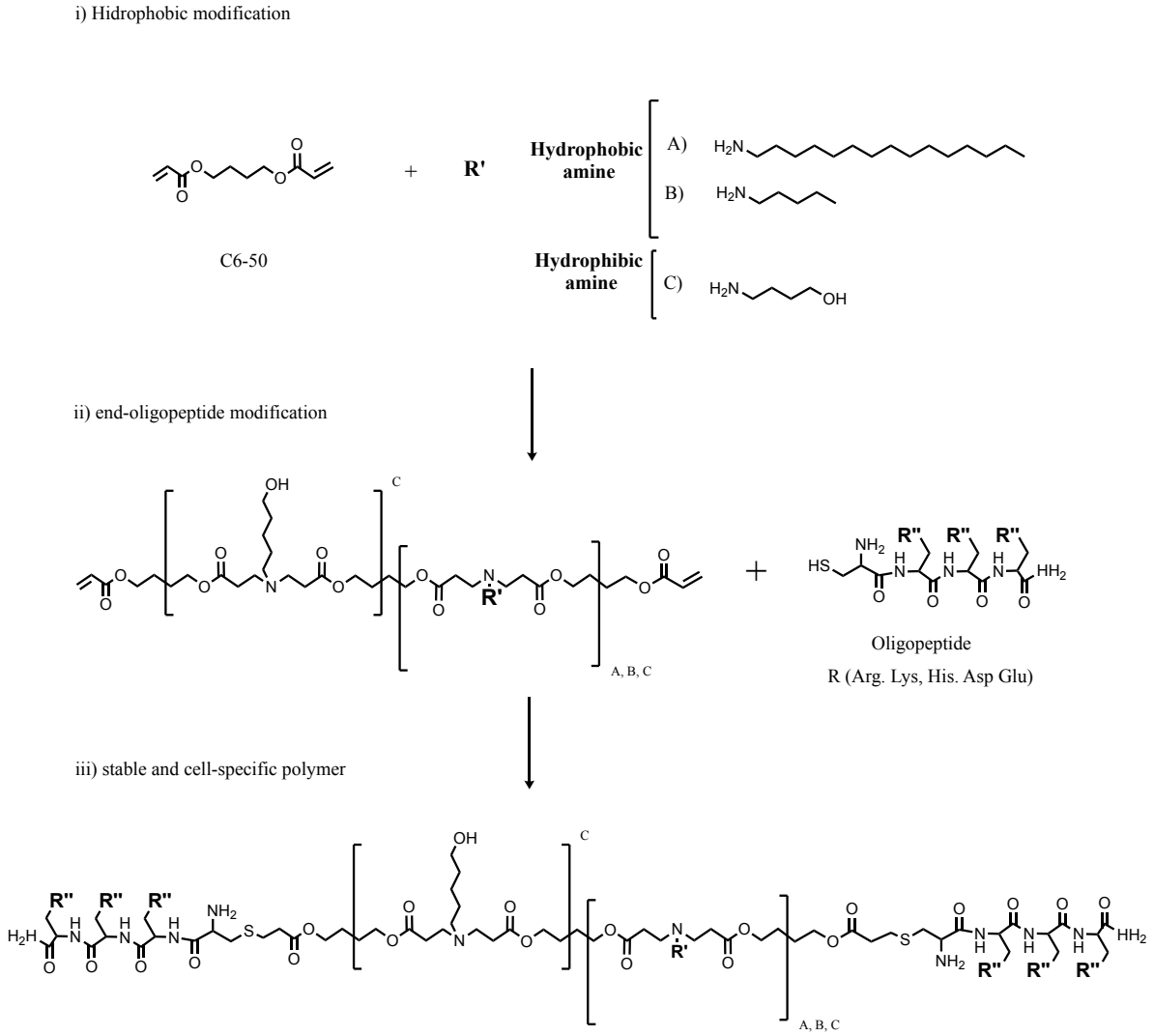

Figure IV-3. Synthesis of hydrophobic pBAE polymers. i) A combination of different hydrophobic amines (A and B) with a hydrophilic amine (C) were used for the synthesis of new family of pBAEs. Different stequiometry of hydrophobic/hydrophilic amine was used in combination with diacrylate at 1:1.1 ratio, obtaining a wide range of various polymer hydrophobicity. ii) PBAEs were further modified with different oligopeptide moieties. R'' terminal can be arginine-, lysine-, histidine-, glutamic acid- and aspartic acid-oligopeptide. iii) Different oligopeptide-end modified pBAEs were obtained.

An acrylate-terminated polymer intermediate was obtained by conjugate addition of hydrophilic/hydrophobic amine to 1,4-butanediol diacrylate using a slight excess of diacrylate. C32 polymer was synthetized as previously described by Lynn *et. al* [28]. Briefly, acrylate-terminated C32 intermediate polymer was obtained by addition of 5-amino-1-pentanol to 1,4-butanediol diacrylate. In contrast, a new family of hydrophobic polymers (C6-100, C6-50, C6-25, C16-50, and C16-25) was polymerized by combining different ratios of 5-amino-1-pentanol and hydrophobic amines, as previously explained in materials and methods. The hydrophobicity of the resulting polymer (C6 and C16) was controlled by the molar stoichiometry of hydrophilic and hydrophobic amines, as shown Figure IV-3-i. For example, C6-50 polymer was obtained using a stoichiometric proportion of 5-amino-1-pentanol/hexylamine and a slight excess of 1,4-butanediol. The resulting polymers were characterized in terms of molecular structure by ^{1}H-NMR. The chemical structure of C6- or C16-

containing polymers were confirmed by the decrease of –$\underline{CH_2}$-OH signals from the 5-amino-1-pentanol monomer and the presence of signals typically associated with the methyl group (-$\underline{CH_3}$) from hexylamine or hexadecylamine. At higher percentage of hydrophobic amine, during pBAE polymerization, methyl signal increased and –$\underline{CH_2}$-OH signals decreased. Moreover, molecular weight was determined using HPLC-SEC obtaining an average molecular weight of 2000-2500 g/mol (relative to polystyrene standards).

On the other hand, hydrophobicity of C32 polymer was further enhanced conjugating carboxylic acid-modified cholesterol (Chol-COOH). Cchol polymers were obtained by esterification of previously synthetized C32 polymer with carboxylic acid-modified cholesterol at different molar ratios, as shown Figure IV-4. As previously, the resulting polymers were characterized in terms of molecular structure by ^{1}H-NMR.

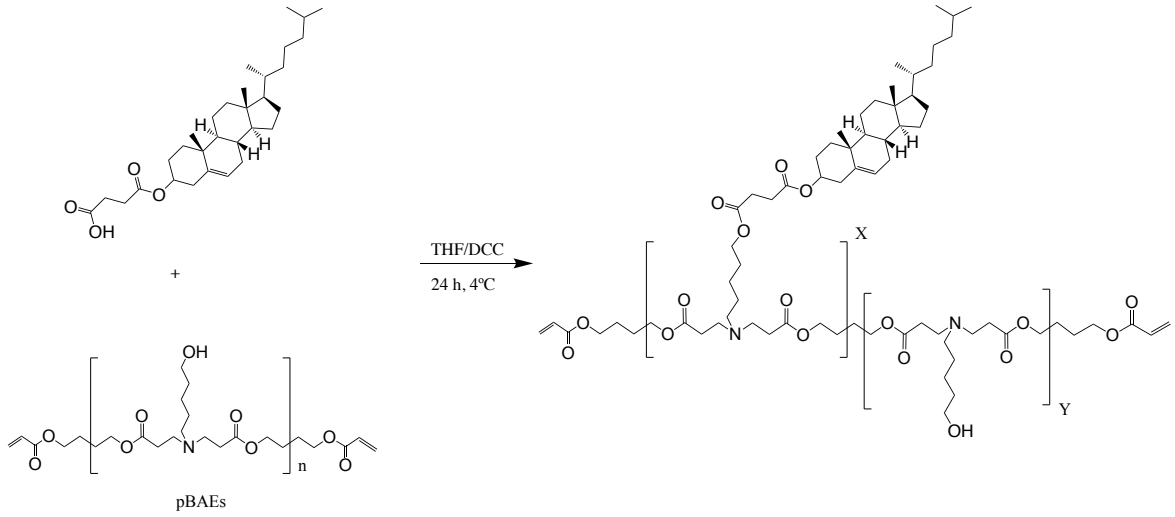

Figure IV-4. Synthesis of Cchol polymer. C32 polymer was esterified using succinic modified cholesterol. Different ratios of Chol-COOH were added to C32 polymer in order to obtain a wide range of hydrophobic/hydrophilic Cchol polymer. Esterification was carried out during 24 hours in THF at 4ªC.

Then, cholesterol percentage in the Cchol polymeric backbone was confirmed by the decrease of –$\underline{CH_2}$-OH signals from the 5-amino-1-pentanol monomer and the presence of signals typically associated with cholesterol, such as terminal methyl from aliphatic chain –CH-$(CH_3)_2$, C3 from Chol-COOH, and C6 from Chol-COOH. At higher percentage of cholesterol in pBAE backbone –$\underline{CH_2}$-OH signals were decreased and cholesterol signals were increased. Moreover, molecular weight was determined using HPLC-SEC obtaining an average molecular weight of 2000-3000 g/mol (relative to polystyrene standards).

Once the different backbone polymers were synthetized and characterized, the end-acrylate groups of the different newly synthetized polymers (C32, C6-100, C6-50, C6-25, Cchol-50, Cchol-25, Cchol-12.5, C16-50, and C16-25) were further modified using different oligopeptide moieties, such as arginine-, lysine-, histidine-, aspartic acid- or glutamic acid-oligopeptides. Oligopeptide modification

was carried out using thiol-end reaction with cysteine-ended oligopeptides (Figure IV-3). Finally, polymer modifications were analysed by ^{1}H-NMR. The chemical structures of new oligopeptide-modified pBAEs were confirmed by the disappearance of typical acrylate signals and the presence of signals associated with amino acid moieties. ^{1}H-NMR spectrum of end-oligopeptide modified C32 polymer was in agreement with previously published data[14].

4.3.2 Biophysical characterization of oligopeptide end-modified pBAEs

Once a new family of polymers have been synthetized, their ability to condense RNAi-drugs into discrete nanoparticles was studied. Firstly, polymer - nucleic acid binding capability was analyzed by gel retardation assay working at different polymer/nucleic acid weight ratios, ranging from 10:1 to 400:1. Polymers obtained by stoichiometric ratios of hydrophobic/hydrophilic amine and further end-modified with arginine were analyzed by gel retardation assay as a representative formulation of each hydrophobic modifications. Moreover, previously described C32-CR3 polymer was used as a control (Figure IV-5).

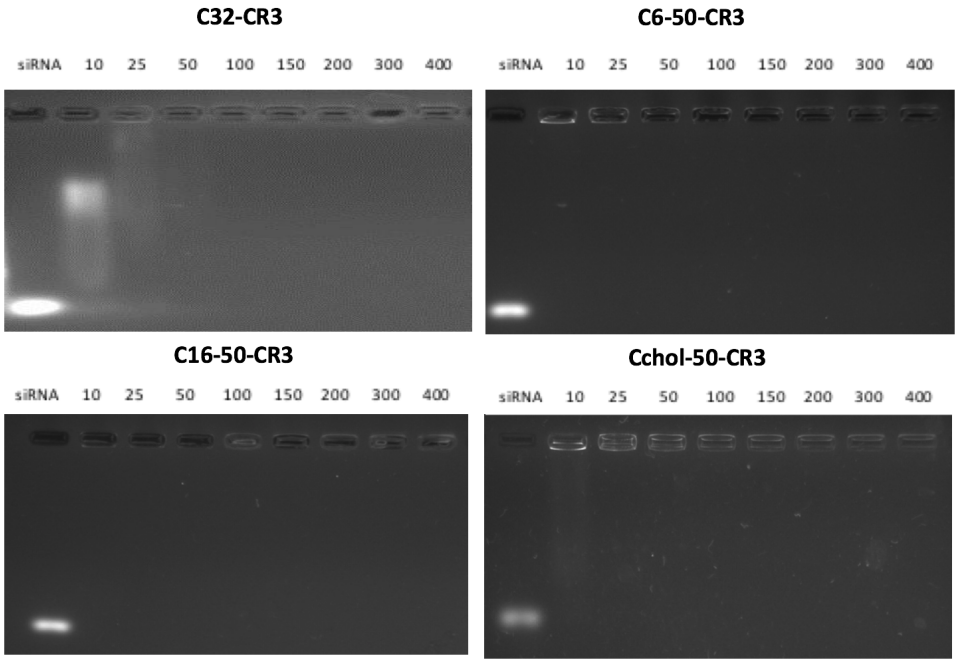

Figure IV-5. Agarose gel retardation assay of newly hydrophobic pBAEs using siGFP siRNA at various weight ratios. Polymer:siRNA complexes were prepared at different ratios (w/w) ranging from 1:10 to 1:400. An intermediate hydrophobicity range, stequiometry hydrophobic/hydrophilic ratio, of different alkyl side chains was selected. Polymers were compared with previously well characterized C32 polymer. Polyplexes were freshly prepared prior the assay and agarose gel containing ethidium bromide loaded into 2,5% and was run 1 h at 80 V.

Polyplexes formed with C32-CR3 polymer revealed complete siRNA encapsulation at ratios higher than 50:1, while at ratios lower than 50:1 free siRNA was observed, as previously reported [13]. In contrast, newly synthetized hydrophobic pBAEs presented siRNA retardation at lower ratios than C32-CR3 polymer. C6-50-CR3 and C16-50-CR3 polymers showed full siRNA retardation at ratios

higher than 10:1. In addition, Cchol-50-CR3 polymer, a slight fluorescence was observed at ratios lower than 25:1, suggesting that RNA complexation was not fully completed. However, for ratios higher than 25:1, Cchol-50-CR3 polymer is able to fully condense RNAi. These results suggest that polymers modified with hydrophobic chains present higher complexation capacity, making them a good candidate for furthers studies.

Once polymer/siRNA ratios were determined, polyplexes were further characterized using DLS. Hydrodynamic size and zeta potential of the resulting polyplexes were determined and summarized in the Table IV-4. For this study, polyplexes were prepared at 100:1 polymer:siRNA ratio and, as before, arginine moiety was used as the oligopeptide end-modifying moiety. Nevertheless, C32 polymer was formulated at 200:1 polymer:siRNA ratio, since this formulation required higher polymer:siRNA ratio to condense siRNA, as previously it has been described in Chapter II [13].

Table IV-4. Characterization of arginine-modified hydrophobic PBAE polymers using siRNA. Size, Z-Potential, and Polydispersity were determined using dynamic light scattering (DLS). Results are shown as mean and standard deviation of triplicates.

Pendant groups	Percentage of modification	Hydrophobicity	Size	Z-Potential	PDI
Cholesterol	50	+++	112 ± 11	15,7 ± 2,4	0,154 ± 0,023
	25	++	59 ± 3	16,9 ± 1,6	0,166 ± 0,042
	12,5	+	113 ± 9	17,1 ± 2,1	0,184 ± 0,008
Hexadecylamine	50	+++	267± 21	17,9 ± 0,9	0,201 ± 0,076
	25	++	289± 37	15,1 ± 1,8	0,232 ± 0,074
Hexylamine	100	+++	184± 10	18,2 ± 1,3	0,111 ± 0,012
	50	++	111± 6	17,2 ± 2,2	0,156 ± 0,017
	25	+	68 ± 7	19,1 ± 0,5	0,266 ± 0,041
5-amino-1-pentanol	100	-	222 ± 19	18,5 ± 1,8	0,202 ± 0,038

Polyplexes obtained using C32-CR3 as a polymer (5-amino-1-pentanol amine) showed a particle average size of 220 nm with positive zeta potential, +18.5 mV. In general, dynamic light scattering analyses showed that some of newly developed polymers were able to achieve smaller nanoparticles than C32 polymer. while maintaining their positive surface charge. For example, the most promising formulations were able to perform nanoparticles with hydrodynamic size ranging from 60 to 120 nm. In addition, low polydispersity indexes were observed in the resulting polyplexes were observed. However, polyplexes obtained using hexadecylamine pBAE presented considerably greater size, around 300 nm, maintaining a positive surface charge. Therefore, an increase of hydrophobicity due to the modification of backbone polymer is able to reduce the size of the resultant nanoparticle, with exception of hexadecilamine modification, maintaining their positive surface charge, which has been classically associated with higher packaging capacity[23].

4.3.3 Stability effect of different hydrophobic modifications

Prior to transfection efficiency analysis, the influence of the modifying hydrophobic group on the stability of the resulting nanoparticles was evaluated in order to select the most stable polymer formulation. Stability of different hydrophobic modifications was determined using arginine as oligopeptide. Briefly, nanoparticles were freshly prepared using hydrophobized pBAEs and siRNA and their size was evaluated as a function of time. Size of siRNA nanoparticles was determined using DLS over the course of 24 hours. Moreover, initial and final nanoparticles surface charge was determined, as shown Figure IV-6.

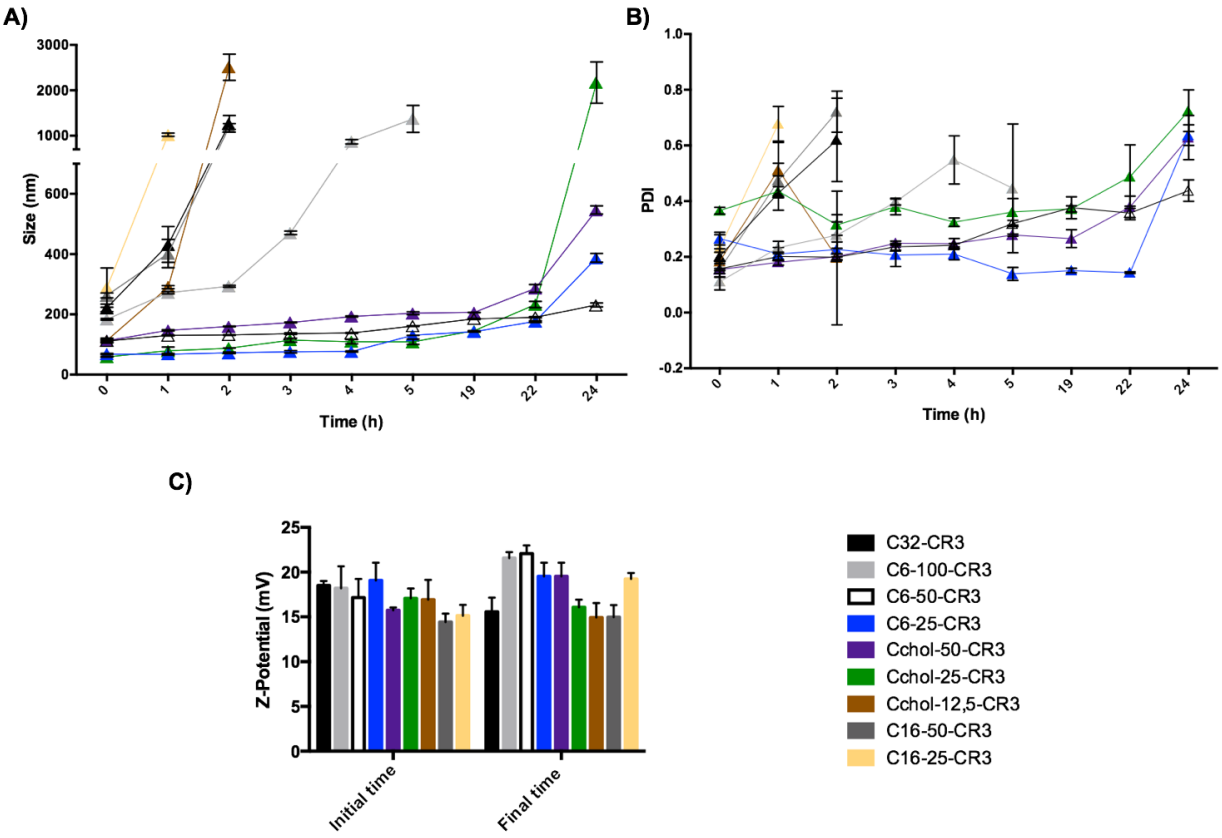

Figure IV-6. Effect of hydrophobic/hydrophilic ratio side chains on polyplex stability. Freshly polymer:siRNA complexes were prepared at 100:1 w/w ratios using siRNA. Arginine oligopeptide madification was used in order to compare the different polymers. Polyplexes were prepared in acetate buffer and incubated with PBS 1X. Size (A), polydispersity(B), and Z-potential (C) were determined using Dynamic Light Scattering at different time points.

Results showed that basic poly(β-amino ester), C32 polymer, described by Lynn et al. and further end-modified with arginine oligopeptides exhibited low stability, reaching a size greater than 1000 nm, revealing a high degree of nanoparticle aggregation, i.e. average hydrodynamic diameter greater than 1000 nm, after a 2 hour incubation in PBS. However, an increase in particle diameter did not affect nanoparticle surface charge. This result indicated that this polymeric formulation is able to completely condense the nucleic acids inside of the polyplex, but it is not sufficiently to maintain its nanometric proprieties. In order to solve this limitation, an increase in polymer hydrophobicity was studied using

our hydrophobized polymers. Interestingly, results show that a slight increase in polymer hydrophobicity yields an important enhancement in nanoparticle stability. Results showed that C6 polymer modified with 25% of hexylamine (C6-25) was able to maintain the size of the resulting nanoparticles below 250 nm up to 22 hours. Moreover, particles prepared with C6 polymer modified 50% of hexylamine (C6-50) were able to maintain a discrete nanometric size and a positive surface charge for more than 24 h in PBS. In contrast, nanoparticles obtained from 100 % hexylamine-modified polymer (C6-100) presented greater stability than C32 polymer, but lower than 25% and 50% modified C6 polymer. C6-100 polyplexes were stable for approximately 2 hours, maintaining a particle size of 200 nm. Therefore, these results suggest that the hydrophobicity of polymer backbone plays a major role in the stability of the resulting nanoparticle. Similarly to hexylamine modification, poly(β-amino ester)s were modified using cholesterol (Cchol polymer). As previously discussed, Cchol polymer was synthesized with different degrees of esterification using carboxylic acid- modified cholesterol, at 50% (Cchol-50), 25% (Cchol-25), 12.5% (Cchol-12.5), and 0% (C32). Results showed that 25% and 50% of cholesterol modification presented greater stability than 12.5%, maintaining particle size below 300 nm for up to 22 h. In addition, nanoparticles containing 50 % of cholesterol remained smaller than polyplexes with 25 % of cholesterol after of incubation in physiological medium for 22 hours. Moreover, formulations with lower percentage of cholesterol than 25% did not present a significant improvement in their stability. Finally, modification of hexadecylamine at 50% and 25% was not able to further increase the stability of polyplexes in PBS. However, their surface charge remained positive due to their ability to efficiently condense siRNA.

Taking into account the different biophysical proprieties, it can be observed that such nanoparticles that presented a smaller initial size are more stable than larger nanoparticles. Their ability to condense nucleic acids in smaller nanoparticles in more efficient manner than previously developed C32 polymer, suggests that new hydrophobic polymers may exhibit higher stability in physiological conditions. In addition, these results suggest that nanoparticle composition plays a key role in nanoparticle-medium interactions. It is well described that hydrophilic polyplexes present larger number of protein interactions than hydrophobic formulations. For instance, studies using n-iso-Propylacrylamide/ n-tert-Butylacrylamide copolymer nanoparticles has shown a well described correlation between nanoparticle core hydrophilicity and protein absorption, which describes their final protein corona [29]. Therefore, it can be concluded that a similar correlation was observed here, showing that an increase in hydrophobicity is sufficient to dramatically improve polyplexes packaging capacity and stability in physiological medium.

4.3.4 Slightly hydrophobic polyplexes increase siRNA delivery

In order to study the hydrophobicity contribution in different pBAEs formulations, EGFP knockdown was determined using anti-GFP siRNA in GFP-expressing MDA MB 213 cells. Silencing efficiency was evaluated by measuring the decrease in cell fluorescence by flow cytometry. GFP knockdown of different hydrophobic/hydrophilic poly(b-amino ester)s was compared to previously described C32 polymer and commercial reagent, Polyplus Interferin, as shown in Figure IV-7.

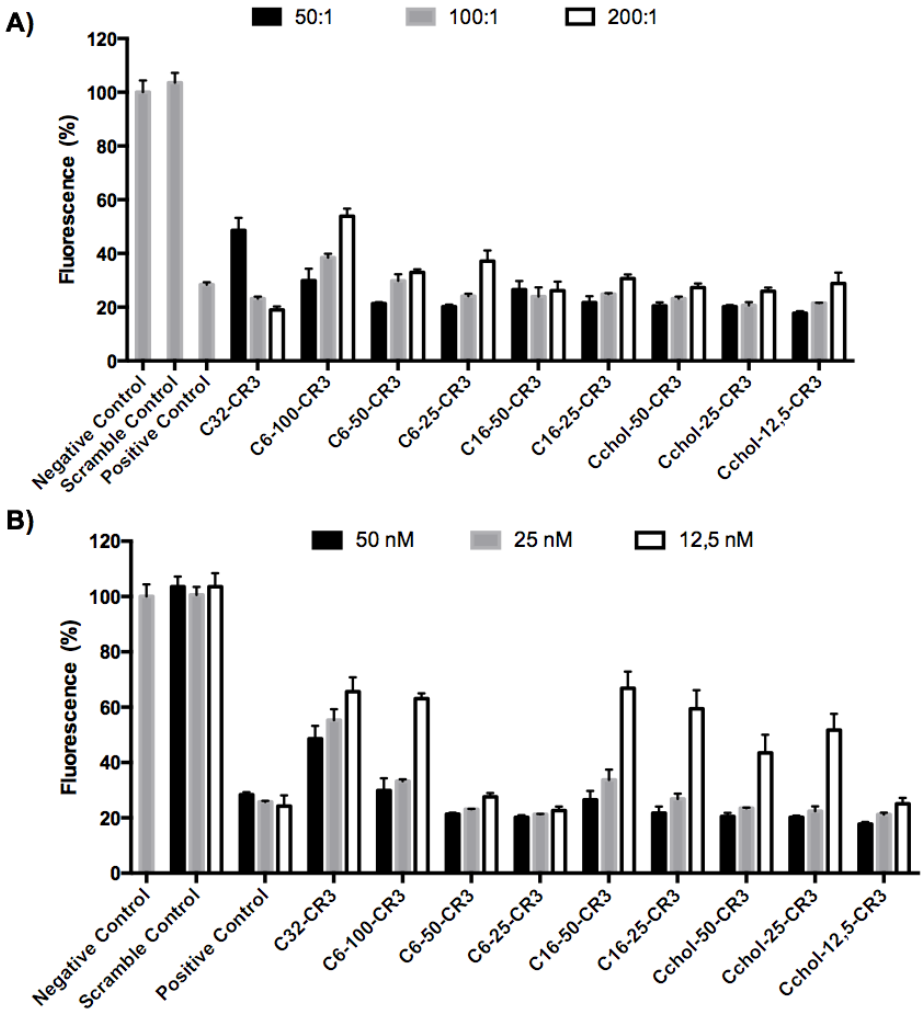

Figure IV-7. GFP silencing efficiency is increased using slightly hydrophobic polymer formulations. MDA MB 231 cells were transfected with siRNA against GFP protein using polymers with different degree of hydrophobicity (C32, C6-100, c6-50, C6-25, C16-50, C16-25, Cchol-50, Cchol-25, and Cchol-12,5). Transfection were carried out in serum free medium and GFP expression was determined at 48-hour post-transfection by flow cytometry. Different polymer:siRNA ratios (A) and siRNA concentration at 50:1 ratio were studied (B). Results are shown as mean and standard deviation of triplicates. Statistical significance was determined using positive control cells as control group. *p < 0.05, **p < 0.01, ***p < 0.001.

As it has been already described, an increase in polyplex hydrophobicity results in an increase of packaging capacity and transfection efficiency[23]. In this report, transfection efficiency of different polymer:siRNA ratios was tested (Figure IV-7-A). As is expected using C32-CR3 polymer, at lower

polymer:siRNA ratio (50:1) transfection efficiency is reduced, remarking that optimal C32 polymer:siRNA ratio is 200:1[13]. In contrast, the opposite behavior was observed using hydrophobized polymers. Hexylamine-, hexadecylamine- or cholesterol- modified pBAEs achieved the highest reduction in cell fluorescence at low polymer:siRNA ratios, as is shown in Figure IV-7-A. Incorporation of hydrophobic moieties on the pBAE structure may increase nanoparticle interaction with cell membrane and subsequent entry into the cytoplasm [30]. It is well known, that amphiphilic or hydrophobic compounds show a high affinity for biological lipid membranes. In the case of polyplexes, their interaction should enhance polyplexes abortion on the cell membrane, which may ultimately favor cellular uptake. For example, it has been described that the addition of palmitic acid, oleic acid, cholesterol, pendant hexyl or dodecyl chains to the polyplexes formulations enhances endocytosis and, in consequence, increase the transfection efficiency[31,32]

Once the most effective polymer/RNAi ratio was confirmed, a siRNA dose curve was performed (Figure IV-7-B) in order to determine the most efficient polymer formulation. As is expected, knockdown efficiency of C32-CR3 polymer is limited at 50 nM. Then, when siRNA concentration was decreased, C32-CR3 polyplexes were not able to silence GFP expression in MDA MB 231 cells. In contrast, C6-50 and C6-25 polymers are capable of maintaining reduced GFP expression at a siGFP concentration as low as 12,5 nM. Fully hexylamine-modified pBAEs presents a limited transfection efficiency, showing a similar behavior than C32-CR3 polymer. On the other hand, polyplexes prepared with C16 polymers showed limited GFP knockdown when siRNA concentration is reduced. Finally, slight modification of pBAE backbone with cholesterol was able to silence more than 70% of GFP expression at 12,5 nM. However, silencing efficiency using highly modified pBAE-cholesterol (Cchol-50 and Cchol-25) is limited at 25 nM.

We can conclude that slightly hydrophobized polymers are capable of condensing siRNA more efficiently using lower polymer:RNAi ratios and their hydrophobic component is able to efficiently interact with cell membrane promoting their cellular entrance. Specifically, stoichiometric mixture of 5-amino-1-pentanol/hexylamine (C6-50 polymer) is the most promising candidate in terms of transfection efficiency/stability.

4.3.5 siRNA uptake using different synthetized hydrophobic/hydrophilic polymers

siRNA uptake was carried out in order to determine which polymer formulation is able to deliver more efficiently nucleic acids into the cells. For this study, different arginine-modified hydrophobic/hydrophilic polymers were tested. Briefly, polyplexes were obtained using different polymers and AF555-labeled siRNA at 50:1 ratio. MDA MB 231 cells were incubated with nanoparticles during 2 hours and the resulting cellular fluorescence was determined by flow cytometry.

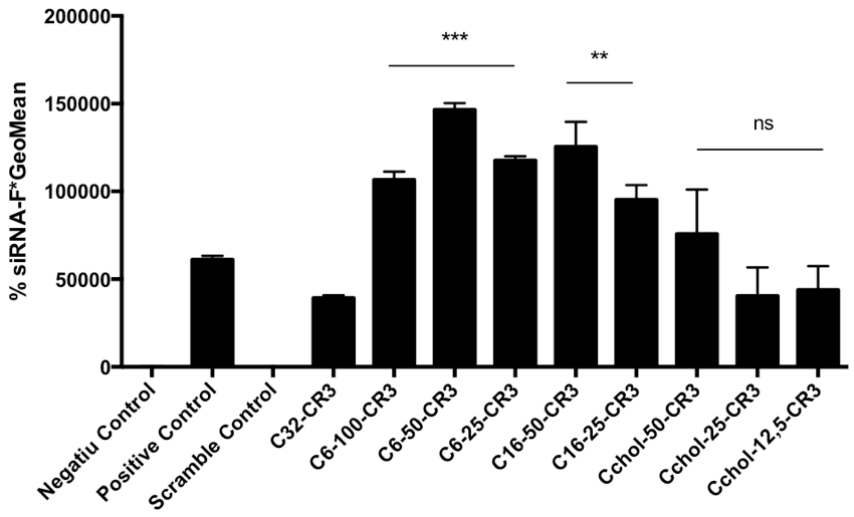

Figure IV-8. Cellular uptake of newly developed hydrophobic polymers using labeled siRNA. MDA MB 231 cells were transfected using siRNA-F (AlexaFluor 555) at 50 nM. 2 hours after transfection, fluorescence was determined by flow cytometry and plotted as percentage of positive cells multiplied by the GeoMean fluorescence of the positive population. Results are shown as mean and standard deviation of triplicates. Statistical significance was determined using positive control cells as control group. *p < 0.05, **p < 0.01, ***p < 0.001.

Uptake analysis of cells incubated with fluorescent polyplexes showed differential behavior depending on the hydrophobic/hydrophilic amine used for poly(β-amino ester) polymerization. Polyplexes prepared using C32-CR3 polymer at 50:1 ratio show lower siRNA uptake than commercial reagent, which is in agreement with the observed knockdown. However, it has been previously reported that polyplexes make at 200:1 polymer:siRNA ratio present higher uptake than commercial control [13]. Thus, we can conclude than 50:1 polymer:siRNA ratio is not able to fully condense nucleic acids using C32 polymer. Polymer formulations containing hexylamine or hexadecylamine in their backbone showed the highest levels of cellular uptake, achieving a 2 to 3-fold higher fluorescence than previously described C32 polymer and positive control. These results corroborated that hydrophobic groups enhance cellular entrance.

In contrast, cholesterol-modified polymers showed a lower siRNA uptake than hexylamine and hexadecylamine polymers, obtaining a similar cellular uptake than C32-CR3 polymer and Polyplus Interferin. These results suggested that cholesterol-modified polyplexes were able to efficiently escape from endosome after endocytosis due to their high levels of GFP knockdown. Consequently, cholesterol-containing polyplexes may interact with the endosome membrane and promote their endosomal escape. Therefore, we can conclude that polyplex uptake efficiency could be controlled playing with their hydrophobic modification.

4.3.6 Cytotoxicity of newly stable polymers

Highly efficient polymer formulations present some degree of cell toxicity due to their large capacity to cell-entry, which may limit their further use as RNAi delivery vehicle [33]. Then, different polymer formulation factors have to be considered in order to avoid cytotoxicity problems. A polymeric formulation capable of delivering nucleic acids without changing the cell behavior is required. In this work, we evaluated the influence of hydrophobized pBAE formulations in cell viability. To determine the toxicity, silencing assay using siRNA was carried out in MDA MB 231 cells and viability was analyzed at 48-hour post-transfection by MTS assay. Polyplexes were freshly prepared at 50:1 polymer:siRNA ratio and cells were transfected at 50 nM siRNA concentration.

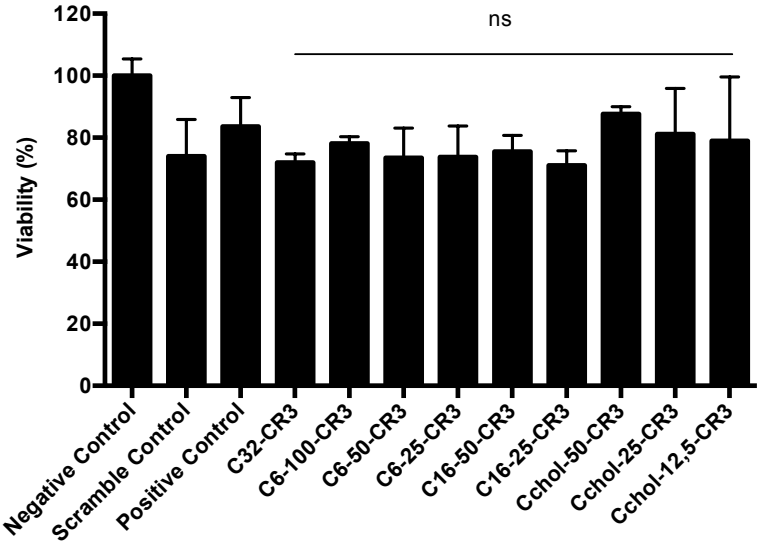

Figure 6. Cell viability study of effect of different hydrophobic/hydrophilic formulations, measured using the MTS assay. Viability was determined at 48 h post-transfection and plotted as percentage of viable cells relative to a control of untreated cells. Results are shown as mean and standard deviation of triplicates. Statistical significance was determined against Polyplus Interferein as control group. *p < 0.05, **p < 0.01, ***p < 0.001.

Cell viability results did not show any non-significant differences between the hydrophobized pBAEs and C32-CR3 polymer and commercial Polyplus Interferin polymer. Results showed that all the formulations were able to efficiently knockdown GFP expression with cell viabilities greater than 80%. Moreover, scramble control showed the same behavior than hydrophobic modified pBAE. These results suggest that hydrophobized PBAEs have low toxicity effects, maintaining a high transfection efficiency.

4.3.7 Oligopeptide-end modification of C6-50 and Cchol-50 polymers

Based on the previous results, stoichiometric hexylamine / 5-amino-1-pentanol amine (C6-50) and Cholesterol/5-amino-1-pentanol (Cchol-50) polymers were chosen as the most promising polymers due to their high silencing efficiency, stability in physiological medium, and low cytotoxicity. Consequently, C6-50 and Cchol-50 were further modified with different oligopeptide moieties. Tailoring the oligopeptide composition allows to obtain polyplexes with controlled surface properties,

which has been shown to confer cell-specificity in different cells lines, as previously demonstrated in Chapter II. Therefore, the next step is to confirm if cell-specific proprieties can be incorporated to our newly stable polymers.

To reach this aim, C6-50 and Cchol-50 polymers were further modified using positive and negative oligopeptides and biophysically characterized by DLS, as shown Figure IV-9.

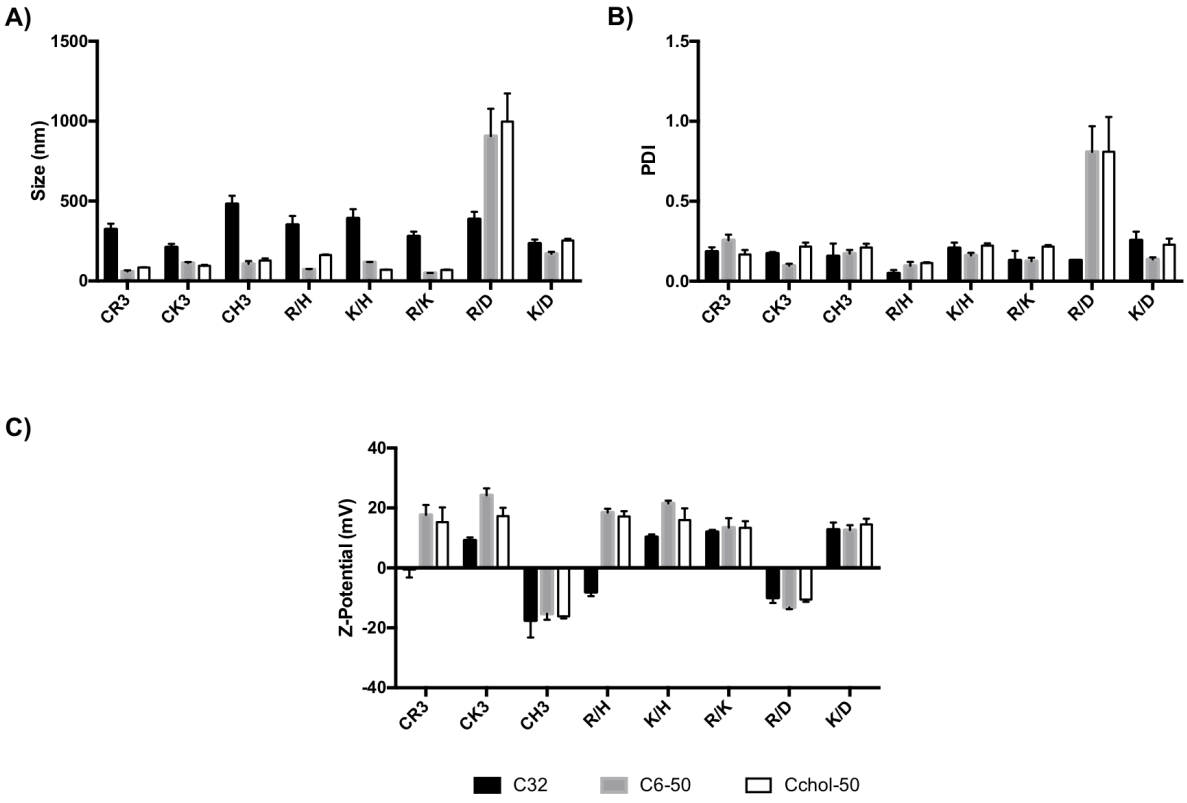

Figure IV-9. Biophysical characterization of oligopeptide end-modified C6-50 and Cchol-50 polymers. A) Average size, B) polydispersity, C) and zeta potential were determined by dynamic light scattering (DLS). Polyplexes were prepared using siRNA and different end-modified pBAE C6-50 and Cchol-50 polymers at 100:1 w/w ratio. 200:1 w/w ratio was used for C32 polymer. Results are shown as mean and standard deviation of triplicates.

As previously observed in Table IV-4, hydrodynamic size of most of the oligopeptide modified C6-50 and Ccho-50 polymers present smaller size than previously C32 polymers. In addition, in all the cases where C6-50 and Cchol-50 polyplexes size is smaller than C32 polymers, they present a positive surface charge. However, we observed that arginine- /aspartic acid- mixture is not able to form nanometric nanoparticles. We supposed that an increase of polymer hydrophobicity may reorganize the final polyplexes surface oligopeptide composition, obtaining a non-stable formulation.

As before, these results suggest that newly developed polymers present high capacity to condense RNAi-based drugs, making them a promising delivery vector for RNAi therapy, where loading capacity is a key to be pharmacologically useful.

4.3.8 EGFP silencing in MDA MB231 using new hydrophobic polymers in FBS conditions

To assess conditions in complex media, transfection screening was performed in medium supplemented with FBS. In order to evaluate their behavior and efficiency, freshly prepared nanoparticles using different oligopeptide moieties combinations were compared with previously characterized C32 polymer using MDA MB 231 as a cell line. GFP fluorescence was determined at 48 hour post-transfection by flow cytometry, as shown in Figure IV-10.

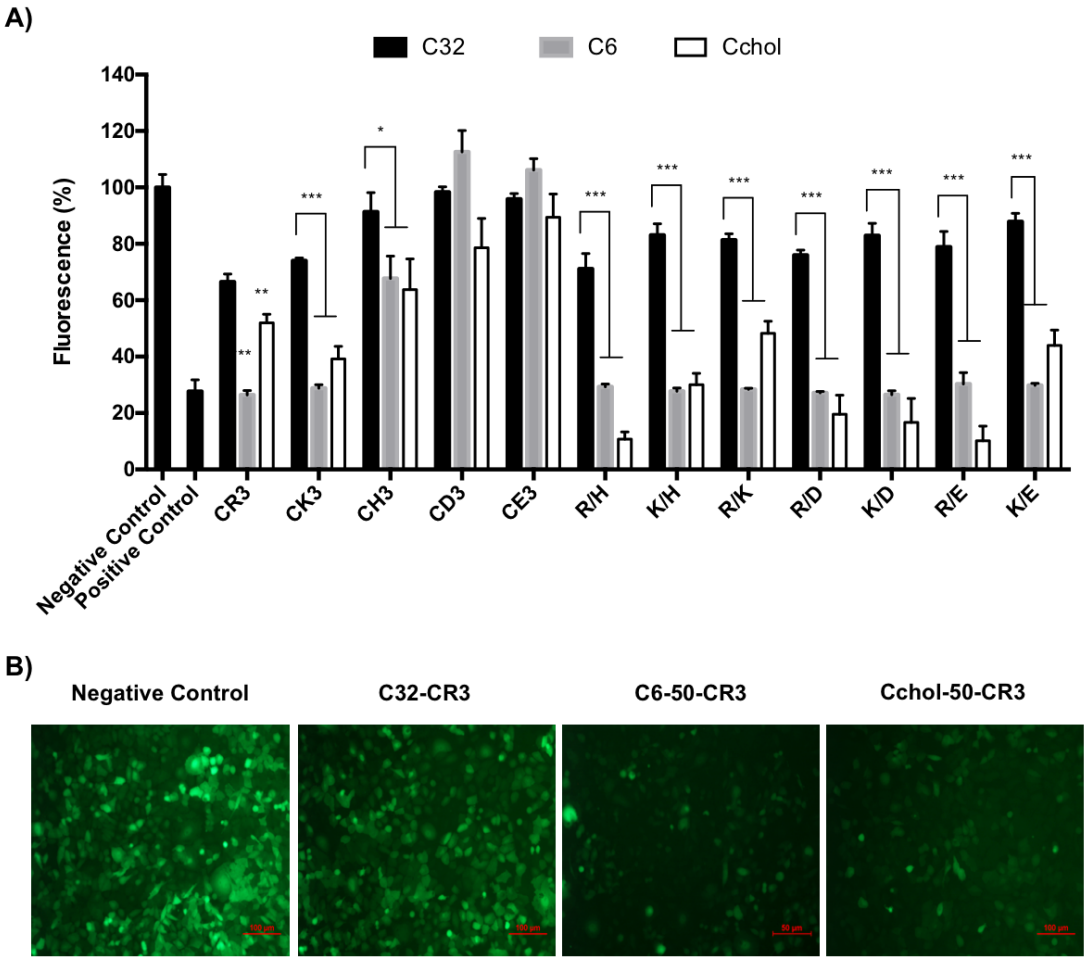

Figure IV-10. EGFP silencing efficiency was determined using different stable end-modified oligopeptide pBAEs (C32, C6-50 and Cchol-50) in MDA MB 231 cell line. A) Cells were transfected with siGFP at a final concentration of 50 nM of siGFP/well using completed medium. Fluorescence was analysed 48h post-transfection by flow cytometry. Results are shown as mean and standard deviation of triplicates. Statistical significance was determined using different oligopeptide-modified C32 polymer as control group. * p<0.05, ** p<0.01, *** p<0.001. B) Fluorescent images silenced MDA MB 231 cells using different polymer formulations (C32-CR3, C6-50-CR3, Cchol-50-CR3) at 50 nM. Fluorescence was analyzed at 48-hour post-transfection.

Different silencing behavior of GFP knockdown using the different oligopeptide-modified C32, C6-50, and Cchol-50 polymers was observed. As previously noticed, C32 transfection efficiency in serum conditions is limited, obtaining low levels of GFP knockdown due to their low stability in serum conditions. C32-CR3 polymer showed the highest efficiency, obtaining a 30% of GFP silencing

compared with negative control. However, hydrophobized polymers, such as C6-50, showed higher levels of GFP silencing than C32 polymer. 80% of silencing was observed in all the oligopeptide formulations, with the exception of nanoparticles solely formulated with histidine-, aspartic acid- and glutamic acid-modified pBAEs. In addition, oligopeptide-modified C6-50 achieved a similar reduction in cell fluorescence than commercial reagent polymer, achieving 80% of fluorescence reduction. Furthermore, all siRNA complexes prepared with different oligopeptide end-modified Cchol-50 polymers showed a high GFP silencing, with the exception of histidine-, aspartic acid- and glutamic acid- oligopeptides. In addition, oligopeptide mixtures of arginine- with histidine- or glutamic acid- presented the highest GFP silencing in MDA MB213 cells, reaching 85-90% of GFP knockdown.

In addition, GFP knockdown was determined by confocal microscopy analysis using arginine-modified polymers, as shown Figure IV-10-B. Results showed a direct concordance with previous data, showing the highest levels of GFP knockdown when cells are transfected with C6-50, C6-25 and Cchol-50 polymers. In contrast, previously developed C32 polymer showed lower silencing effect than hydrophobic formulations. Therefore, these results indicate that C6-50 and Cchol-50 polymers might be a promising vector to be used as a nucleic acid carrier in presence of plasma-proteins, making them an interesting candidate for *in vivo* delivery.

4.3.9 Stability/transfection efficiency study of C32, C6-50, and Cchol-50 in presence or absence of serum

Finally, in order to further confirm the transfection efficiency in the presence of plasma proteins of formulations containing C6-50, Cchol-50 and C32 polymers, a dual experiment was performed where stability and transfection efficiency were compared. Polyplexes were incubated in either serum-free or serum-containing medium for different time points. The resulting polyplexes were used to knockdown GFP expression in MDA MB 231 cells, as shown in Figure IV-11.

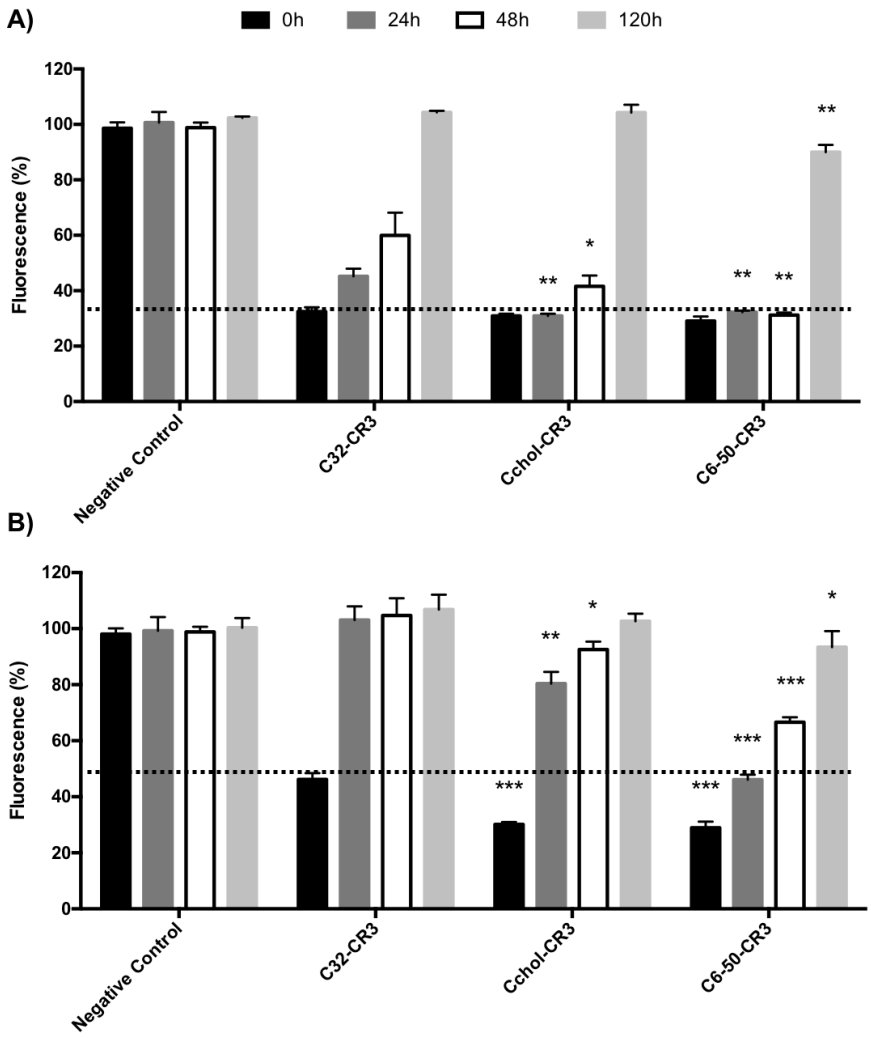

Figure IV-11. Transfection/Stability study of C32, C6-50 and Cchol polymer at different time points. Polyplexes were freshly prepared at different time points (120h, 48h, 24h, and 0h) and incubated without (A) or with serum (B). Polyplex efficiency were analyzed for their capacity to knockdown GFP expression in MDA MB 231 cells. Fluorescence was analyzed 48h post-transfection by flow cytometry. Results are shown as median and standard deviation of triplicates. Statistical significance was determined using C32 polymer as control group. * p<0.05, ** p<0.01, *** p<0.001

Serum free stability experiment (Figure IV-11-A) showed an efficient EGFP silencing of polyplexes prepared with C32, Cchol-50 and C6-50 polymers, and at least a 70% knockdown effect was achieved, when polyplexes were freshly prepared and readily used for cell transfection (time point 0h). In addition, polyplexes were incubated during 24h, 48h and 120 h in serum free medium. Results showed that knockdown effect of C32 nanoparticles was reduced, showing a 50 % silencing effect at 24 hours, 40% at 48 hours and no silencing after pre-incubation for 120 hours. In contrast, C6-50 polyplexes incubated in serum free medium were able to maintain an 70% of GFP silencing at 48 hours. On the other hand, Cchol-50 polyplexes showed a 70% of GFP silencing at 24 hours, remaining at 60% of silencing after pre-incubating for 48 hours. However, in all the cases, polyplexes efficiency was dramatically decreased after 120 hours of incubation in serum free medium, obtaining a moderate 15% of knockdown using C6-50 polymer.

Different stability/transfection behavior was observed when polyplexes were incubated in the presence of serum proteins. As previously demonstrated, hydrophobized pBAEs present higher transfection efficiency than C32 polymer, reaching more than 70% GFP silencing compared to 50% obtined with C32 polymer. As previously demonstrated, C32 polyplexes presented a limited stability, then C32 silencing efficiency is dramatically decreased when polyplexes are incubated with medium containing serum proteins (figure 8-B). In contrast, hexylamine modified polymers showed a significant GFP knockdown when nanoparticles were incubated in complete medium, obtaining a 50% of silencing at 24 hours, 40% of silencing at 48 hours, and 10 % of decrease at 120 hours. Lower stability/transfection was observed using cholesterol modified pBAE. Cchol-50 polymer is able to efficiently deliver siRNA in the presence of serum, but when nanoparticles were incubated in serum proteins their efficiency was reduced, showing only a 20% of GFP knockdown after 24 hours and a 10% of silencing at 48 hours. As previously discussed, intrinsic polyplexes formulation could control protein corona absorption, making a C6-50-CR3 a good candidate to protect and efficiently deliver siRNA in in vivo applications.

4.4 Concluding remarks

Previously in Chapter II and III, it has been described that playing with the oligopeptide formulations, cell-specifics delivery vectors can be designed. We observed that a mixture of arginine-/aspartic acid- oligopeptide present a preferential delivery over DPPSCs in an efficient and safety way, obtaining a promising therapeutic effect. Nevertheless, their usability in *in vivo* systems is limited due to their limited stability. Consequently, this chapter was focused to enhance polymer stability of our previously designed polymers maintaining their cell-specificity proprieties. To reach this aim, not all the strategies that are been used to stabilize nanoparticle formulations can be used. In our case, we studied how the stability can be modulated playing with polyplexes hydrophobicity.

Different pBAEs were synthetized using different hydrophobic structures, such as hexylamine, hexadecilamine, and cholesterol, and further modified using oligopeptide formulations. New developed polymers are able to condense RNAi into discrete nanoparticles maintaining their positive surface charge, presenting smaller hydrodynamic size than previously C32 polymer, in exception of hexadecilamine hydrophobic modification. In addition, gel retardation assay demonstrated that slightly increase of polymer hydrophobicity increase nucleic acid packaging capacity. These results suggest that biophysical proprieties of the resultant polyplexes formulations can be modulated playing with pBAEs hydrophobicity, promoting higher packaging capacity, which is required in order to design a pharmacological useful delivery system.

In addition, stability experiments demonstrated that polyplexes formulated with hexylamine (C6-50 and C6-25) or cholesterol (Cchol-50 and Cchol-25) exhibited higher stability in physiological conditions, remaining stable more than 24 hours. We observed that the most stable polyplexes correspond with the polyplexes with smaller hydrodynamic size and high packaging capacity.

Once stable polymer formulations have synthetized, their functionality was checked at *in vitro* level. Higher GFP knockdown was observed using our newly developed polymers than previously described C32 formulation. For instance, C6-50 polymer is able to knockdown GFP gene expression at the same level than C32 polymer, working at 12,5 nM instead of 50 nM and using less quantity of polymer. These results corroborates previous biophysical results, where newly hydrophobic polymers present higher RNAi packaging capacity than C32 polymers.

Taking account all the previously reported features, hexylamine/5-amino-1-pentanol amine (C6-50) and cholesterol/5-amino-1-pentanol (Cchol-50) polymers were chosen as the most promising in terms of silencing efficiency, stability in physiological medium, and cytotoxicity.

After that, C6-50 and Cchol-50 polymers were tested in *in vitro* assays using completed medium (10% FBS). Results demonstrated that newly developed formulations are able to efficiently deliver RNAi to MDA MB 231 cells in serum containing medium, obtaining around 70-90% of GFP knockdown in most of the oligopeptide formulations. However, a clear cell-specificity was observed

between the different oligopeptides formulations, confirming that previously cell-specificity observed in Chapter II, remain in our newly developed C6-50 and Cchol-50 polymers.

Furthermore, stability/transfection efficiency study using arginine- as oligopeptide moiety demonstrated that C6-50-CR3 polymer is able to protect and efficiently deliver RNAi-drugs after 48 hours of incubation in physiological medium (without FBS), achieving an 80 % of GFP knockdown. Moreover, a 50 % of GFP knockdown was observed when C6-50 polyplexes were incubated 24 h in serum supplemented medium (with FBS). In contrast, less transfection efficiency was observed when arginine-modified Cchol-50 polymer was used.

Then, we can conclude that newly developed polymers present higher transfection efficiency, packaging capacity and stability than previous developed pBAEs. Specifically, C6-50 polymer seems to be a promising delivery systems that can be used for *in vivo* applications. Therefore, in the next Chapter, oligopeptide composition of C6-50 polymer have been optimized in order to preferentially deliver RNAi to endothelial cells from mice vasculature.

4.5 References

[1] G.R. Rettig, M.A. Behlke, Progress Toward In Vivo Use of siRNAs-II, Mol. Ther. 20 (2012) 483–512. doi:10.1038/mt.2011.263.

[2] Y. Chiu, T.M. Rana, siRNA function in RNAi : A chemical modification analysis, RNA Soc. 9 (2003) 1034–1048. doi:10.1261/rna.5103703.2000.

[3] N.M. Snead, J.R. Escamilla-Powers, J.J. Rossi, A.P. McCaffrey, 5′ Unlocked Nucleic Acid Modification Improves siRNA Targeting, Mol. Ther. - Nucleic Acids. 2 (2013) e103. doi:10.1038/mtna.2013.36.

[4] H.J. Kim, A. Kim, K. Miyata, K. Kataoka, Recent progress in development of siRNA delivery vehicles for cancer therapy, Adv. Drug Deliv. Rev. 104 (2016) 61–77. doi:10.1016/j.addr.2016.06.011.

[5] C. Wolfrum, S. Shi, K.N. Jayaprakash, M. Jayaraman, G. Wang, R.K. Pandey, K.G. Rajeev, T. Nakayama, K. Charrise, E.M. Ndungo, T. Zimmermann, V. Koteliansky, M. Manoharan, M. Stoffel, Mechanisms and optimization of in vivo delivery of lipophilic siRNAs, Nat. Biotechnol. 25 (2007) 1149–1157. doi:10.1038/nbt1339.

[6] W. Li, F.C. Szoka, Lipid-based Nanoparticles for Nucleic Acid Delivery, Pharm. Res. 24 (2007) 438–449. doi:10.1007/s11095-006-9180-5.

[7] M. Thomas, A.M. Klibanov, Non-viral gene therapy: polycation-mediated DNA delivery, Appl. Microbiol. Biotechnol. 62 (2003) 27–34. doi:10.1007/s00253-003-1321-8.

[8] M.E. Martin, K.G. Rice, Peptide-guided gene delivery, AAPS J. 9 (2007) E18–E29. doi:10.1208/aapsj0901003.

[9] D.E. Discher, F. Ahmed, POLYMERSOMES, Annu. Rev. Biomed. Eng. 8 (2006) 323–341. doi:10.1146/annurev.bioeng.8.061505.095838.

[10] H. Yin, R.L. Kanasty, A.A. Eltoukhy, A.J. Vegas, J.R. Dorkin, D.G. Anderson, Non-viral vectors for gene-based therapy, Nat. Rev. Genet. 15 (2014) 541–555. doi:10.1038/nrg3763.

[11] T. PARK, J. JEONG, S. KIM, Current status of polymeric gene delivery systems☆, Adv. Drug Deliv. Rev. 58 (2006) 467–486. doi:10.1016/j.addr.2006.03.007.

[12] C.-J. Chen, J.-C. Wang, E.-Y. Zhao, L.-Y. Gao, Q. Feng, X.-Y. Liu, Z.-X. Zhao, X.-F. Ma, W.-J. Hou, L.-R. Zhang, W.-L. Lu, Q. Zhang, Self-assembly cationic nanoparticles based on cholesterol-grafted bioreducible poly(amidoamine) for siRNA delivery, Biomaterials. 34 (2013) 5303–5316. doi:10.1016/j.biomaterials.2013.03.056.

[13] P. Dosta, N. Segovia, A. Cascante, V. Ramos, S. Borrós, Surface charge tunability as a powerful strategy to control electrostatic interaction for high efficiency silencing, using tailored oligopeptide-modified poly(beta-amino ester)s (PBAEs), Acta Biomater. 20 (2015) 82–93. doi:http://dx.doi.org/10.1016/j.actbio.2015.03.029.

[14] N. Segovia, P. Dosta, A. Cascante, V. Ramos, S. Borrós, Oligopeptide-terminated poly(β-amino ester)s for highly efficient gene delivery and intracellular localization., Acta Biomater. 10 (2014) 2147–58. doi:10.1016/j.actbio.2013.12.054.

[15] R. Núñez-Toldrà, P. Dosta, S. Montori, V. Ramos, M. Atari, S. Borrós, Improvement of osteogenesis in dental pulp pluripotent-like stem cells by oligopeptide-modified poly(β-amino ester)s, Acta Biomater. 53 (2017) 152–164. doi:10.1016/j.actbio.2017.01.077.

[16] N. Segovia, M. Pont, N. Oliva, V. Ramos, S. Borrós, N. Artzi, Hydrogel Doped with Nanoparticles for Local Sustained Release of siRNA in Breast Cancer, Adv. Healthc. Mater. 4 (2015) 271–280. doi:10.1002/adhm.201400235.

[17] D. Oupicky, M. Ogris, K. a Howard, P.R. Dash, K. Ulbrich, L.W. Seymour, Importance of lateral and steric stabilization of polyelectrolyte gene delivery vectors for extended systemic circulation., Mol. Ther. 5 (2002) 463–72. doi:10.1006/mthe.2002.0568.

[18] R.C. Carlisle, T. Etrych, S.S. Briggs, J.A. Preece, K. Ulbrich, L.W. Seymour, Polymer-coated polyethylenimine/DNA complexes designed for triggered activation by intracellular reduction, J. Gene Med. 6 (2004) 337–344. doi:10.1002/jgm.525.

[19] G. Caracciolo, L. Callipo, S.C. De Sanctis, C. Cavaliere, D. Pozzi, A. Laganà, Surface adsorption of protein corona controls the cell internalization mechanism of DC-Chol–DOPE/DNA lipoplexes in serum, Biochim. Biophys. Acta - Biomembr. 1798 (2010) 536–543. doi:10.1016/j.bbamem.2009.11.007.

[20] R. Weissleder, K. Kelly, E.Y. Sun, T. Shtatland, L. Josephson, Cell-specific targeting of nanoparticles by multivalent attachment of small molecules, Nat. Biotechnol. 23 (2005) 1418–1423. doi:10.1038/nbt1159.

[21] A. a. Eltoukhy, D. Chen, C. a. Alabi, R. Langer, D.G. Anderson, Degradable Terpolymers with Alkyl Side Chains Demonstrate Enhanced Gene Delivery Potency and Nanoparticle Stability, Adv. Mater. 25 (2013) 1487–1493. doi:10.1002/adma.201204346.

[22] S.Y. Wong, J.M. Pelet, D. Putnam, Polymer systems for gene delivery—Past, present, and future, Prog. Polym. Sci. 32 (2007) 799–837. doi:10.1016/j.progpolymsci.2007.05.007.

[23] Z. Liu, Z. Zhang, C. Zhou, Y. Jiao, Hydrophobic modifications of cationic polymers for gene delivery, Prog. Polym. Sci. 35 (2010) 1144–1162. doi:10.1016/j.progpolymsci.2010.04.007.

[24] J.S. Kuo, Effect of Pluronic-block copolymers on the reduction of serum-mediated inhibition of gene transfer of polyethyleneimine – DNA complexes, 271 (2003) 267–271.

[25] A. Alshamsan, A. Haddadi, V. Incani, J. Samuel, A. Lavasanifar, H. Uludag, Formulation and Delivery of siRNA by Oleic Acid and, Mol. Pharm. 6 (2008) 188–200.

[26] D. Wang, A.S. Narang, M. Kotb, A.O. Gaber, D.D. Miller, S.W. Kim, R.I. Mahato, Novel branched poly(ethylenimine)-cholesterol water-soluble lipopolymers for gene delivery., Biomacromolecules. 3 (2002) 1197–207. doi:10.1021/bm025563c.

[27] Vanessa Incani, Emily Tunis, Basak Acan Clements, Cori Olson, Cezary Kucharski, H.U. Afsaneh Lavasanifar, Palmitic acid substitution on cationic polymers for effective delivery of plasmid DNA to bone marrow stromal cells, J. Biomed. Mater. Res. Part A. 81A (2007) 493–504. doi:10.1002/jbm.a.31031.

[28] D.M. Lynn, R. Langer, Degradable Poly(β-amino esters): Synthesis, Characterization, and Self-Assembly with Plasmid DNA, J. Am. Chem. Soc. 122 (2000) 10761–10768. doi:10.1021/ja0015388.

[29] S. Lindman, I. Lynch, E. Thulin, H. Nilsson, K.A. Dawson, S. Linse, Systematic investigation of the thermodynamics of HSA adsorption to N-iso-propylacrylamide/N-tert-butylacrylamide copolymer nanoparticles. Effects of particle size and hydrophobicity., Nano Lett. 7 (2007) 914–20. doi:10.1021/nl062743+.

[30] V. Incani, A. Lavasanifar, H. Uludağ, Lipid and hydrophobic modification of cationic carriers on route to superior gene vectors, Soft Matter. 6 (2010) 2124. doi:10.1039/b916362j.

[31] I. a Khalil, S. Futaki, M. Niwa, Y. Baba, N. Kaji, H. Kamiya, H. Harashima, Mechanism of improved gene transfer by the N-terminal stearylation of octaarginine: enhanced cellular association by hydrophobic core formation, Gene Ther. 11 (2004) 636–644. doi:10.1038/sj.gt.3302128.

[32] D.Y. Takigawa, D.A. Tirrell, Phospholipid Packing by Branched Poly(ethy1enimine) Derivatives?, (1985) 338–342.

[33] D. Fischer, Y. Li, B. Ahlemeyer, J. Krieglstein, T. Kissel, In vitro cytotoxicity testing of polycations: influence of polymer structure on cell viability and hemolysis., Biomaterials. 24 (2003) 1121–31. doi:S0142961202004453 [pii].

Chapter V

Lysine/histidine oligopeptide-modified pBAEs preferentially deliver siRNA to endothelial cells of vasculature

Prepared for submission:

P. Dosta, V. Ramos, M. Mahmoud, H. Jo* and S. Borrós*, "Lysine/histidine oligopeptide-modified pBAEs preferentially deliver siRNA to endothelial cells of vasculature", ACS Nano.

This page left blank intentionally

Lysine/histidine oligopeptide-modified pBAEs preferentially deliver siRNA to endothelial cells of vasculature

Once polymer stability limitation has been solved, C6-50 polymer have used to drive a therapeutic siRNA dose to endothelial cells from vasculature. Results showed that using a combination of stable vector with a fine-design oligopeptide formulations we were able to selectively deliver siRNA to endothelial cells avoiding off-target effects. Lysine- / histidine- oligopeptide mixture (C6-50-K/H) was identified as a top performing polymer from *in vitro* screening and C6-50-K/H was used to deliver siICAM-2 to vasculature in C57BL/6 mice. Results demonstrated that we designed a new strategy to deliver RNAi-based nucleic acids in a cell-specific-manner that differs from current used mechanisms.

5.1 Introduction

In the previous chapter, it was demonstrated that incorporation of hydrophobic moieties during pBAE polymerization is an effective strategy to overcome nanoparticle stability limitations. Particularly, pBAE backbone composition have been improved playing with their hydrophobicity/hydrophilicity ratio during their polymerization. The lead candidate from this screening (C6-50 polymer) demonstrated to remain effective after more than 48 hours of serum proteins incubation, making them a promising candidate for *in vivo* applications. Moreover, newly designed C6-50 polymer present higher packaging efficiency, cell delivery and endosome entrance, than previously reported C32 polymers [1–3]. Nevertheless, the *in vivo* RNAi delivery using pBAEs nanoparticles needs to be studied in order to evaluate the applicability of this novel family of stable pBAEs. In this project, a first proof of concept was carried out using this new generation of polymers in collaboration with Biomedical Engineering Department (BME) at Georgia Institute of Technology and Emory University (Atlanta, USA). We were focus to specifically and efficiently deliver a therapeutically dose of RNAi-based nucleic acids to endothelial cells (ECs) from the vasculature, which is well-known that plays an important role in wide ranges of diseases[4–6].

Currently, at least 30 RNAi-vascular drugs have been tried in clinical trials, using different delivery systems or naked siRNA [7,8]. However, current RNAi therapies are limited due to endothelial cells are difficult to be transfect due to their functionality [9,10]. Furthermore, their distribution around all the organism makes RNAi-based nucleic acids delivery more challenging.

Current bibliography showed different approaches in order to deliver siRNA drugs to endothelial cells, using chemically modified RNAi, cationic lipids or polyplexes [11–13]. As it has been explained in Chapter I, improvements in RNAi synthesis makes them more stable and resistant to external degradation[14]. However, they are not able to overcome intracellular barriers. On the other hand, cationic lipids are widely used in this field. However, periodic administration at high doses (7-8 mg/kg) are required in order to obtain a therapeutic effect [11,15–18]. To our knowledge, only a low molecular weight 7C1 lipid-polymer hybrid, described by Dahlman et al., has been reported to efficiently deliver siRNA to endothelial cells[19]. Others studies have demonstrated that some lipidoids are able to reduce hepatic gene expression after siRNA administration, while they present low knockdown efficiency over other tissues[20–22]. However, it has been described that lipidic/lipidoids nanoparticles can produce several toxicity after successive administrations, limiting their therapeutic effect [23,24]. They present high affinity to deregulate certain cell populations of the immune system, such as macrophages and T lymphocytes, after intravenous administration [25]. Lipid-like particles interact with critical enzymes, such as inhibition of protein kinase C (PKC), which may be associated elicit cytokine response. It is already described that high levels of IL6 (interleukin-6), CXCL2 (C-X-C motif chemokine ligand 2), and CCL2 (chemokine (C-C motif) ligand 2) cytokines were observed in lung, spleen or liver after lipoparticles administration [24]. Moreover, lipoplexes can alter or modify cellular behaviour, which include transmembrane pores and cell dysfunction [23,26]. In addition, is already described that when lipidic formulation reach the target cells, their lack of efficient scape delivery. Recent studies demonstrated that 70% cytoplasm internalized liposomes containing RNAi-drug are not able to disrupt and scape from the endosome, driving the resultant RNAi-drugs to exosome/lysosome pathways. Therefore, less than 30% of therapeutic RNAi become therapeutic [27].

To overcome these limitations, the use of our newly design oligopeptide-modified C6-50 polymer formulations could be a promising way due to their attractiveness in terms of biodegradability, biocompatibility, and endosomal scape efficiency [2,3,28]. Unpublished results have been showed lower cytokine response of our oligopeptide-modified pBAEs in comparison with different lipidic nanoparticle, making them a safer candidate for RNAi-drug delivery. Furthermore, as previously commented in Chapter I and II, playing with pBAEs oligopeptide composition and backbone structure, endosomal scape limitations can be reduced or avoid. Polymers with tertiary amines in their structure have been shown to facilitated the proton effect phenomena, showing a buffering effect at the endosomal pH range between 5.0 and 7.5, which causes an increase in osmotic pressure that results in disruption of the endosome [29]. Previously, published results have demonstrated that using pBAE oligopeptide composition knowledge we are able to design an efficient polyplex in terms of cellular uptake and endosomal scape [2,3].

In addition, the easy adaptability and flexibility to design a pBAEs with different oligopeptide compositions can be used to target pBAEs nanoparticles due to it is still a challenge to be address. Nowadays, nanovectors have been modified with cell-targeting ligands to enhance their preferentiality to specific cell-line. Targeting has been achieved by adding antibodies or peptides to the nanoparticle surface [30–32]. However, this methodology shows some limitations in *in vivo* applications due to their

cost, limited time life, and potential immunogenicity. However, recent studies have shown that small-molecule modifications or specific peptide composition may change the nanoparticle properties, showing a preferential link mechanism with the cell membrane making them tissue-specific [32]. Nanoparticles become internalized into cells by energy-dependent mechanisms [33] due to their surface composition and their protein corona. When nanoparticles are placed in plasma, biological proteins show a constant interaction with proteins, forming a protein corona, which plays an important role in nanoparticle biodistribution [34]. Then, understand the protein corona behaviour could be a promising way to further control of our developed nanoformulations. In our group, we have already described that is possible to control the passive rates of DNA payloads by varying the protein corona composition [35]. Moreover, preliminary data demonstrated that playing with the nature of the nanoparticle in terms of size and chemical composition, we can preferentially control the type of proteins that are adsorbed on the nanocarrier surface, obtaining a clear relation between the particle chemical composition and the type of corona formed. For example, using lipidic formulations it has described that preferential tissue distribution can be accomplished by the synthesis of lipophilic-siRNA conjugates synthetized using different chain fatty acids through modulating their interaction with high-density lipoprotein (HDL) or with low density lipoprotein (LDP), obtaining a preferential distribution to specifics organs [36]. In addition, global surface can also be modified to promote cell-specificity. For example, high positive nanoparticles, such as PEI polymers, can exhibit unfavorable interaction with erythrocytes and activate adaptive immune responses [37,38]. Recently, it has been demonstrated that the protein corona composition can be controlled by natural functionalization of nanomaterials, optimizing their rational design and improving their cell –specific preferential delivery [39].

Taking in account previous results obtained in Chapter II and III, we hypothesized that using our developed oligopeptide-end-modified pBAEs is possible to design tissue-specific nanoparticles for *in vivo* applications playing with their oligopeptide formulations [1]. Therefore, controlling their oligopeptide composition by combining different cationic or cationic and anionic peptides, could be a promising strategy to define a specific protein corona to lead them to precise cell lines.

Thus, the main objective of this chapter is the proof of concept of our newly developed deliver polymers for *in vivo* applications. Particularly, we designed a cell-specific polymer formulation able to condense high quantity of RNAi-drug to obtain a final therapeutic effect over endothelial cells from the mice vasculature.

In order to achieve this objective, the following tasks were proposed:

- *In vitro* design of polyplexes oligopeptide composition in order to achieve a preferential delivery to endothelial cell line form vasculature
- *Ex-vivo* RNAi-drug delivery to abdominal aorta in C57BL/6 mice using top-performing polymer formulation and labelled siRNA in order to corroborate polyplexes endothelial-specificity.

- *In vivo* siICAM2 delivery using endothelial-specific polyplexes. ICAM2 expression was determined in endothelial and in smooth muscle cells from vasculature.

- Biodistrubution study of siICAM-2 using C6-50-K/H polymer after IV administration.

5.2 Materials and Methods

5.2.1 Materials

Reagents and solvents used for polymer synthesis were purchased from Sigma-Aldrich and Panreac. Oligopeptide moieties used on the polymer modification (H-Cys-Arg-Arg-Arg-NH2, H-Cys-Lys-Lys-Lys-NH2, H-Cys-His-His-His-NH2 and H-Cys-Asp-Asp-Asp-NH2) were obtained from GL Biochem (Shanghai) Ltd with a purity of at least 98%. For *in vitro* studies, labelled siRNA (AllStars Neg. siRNA AF 546) for uptake experiments was purchased from Qiagen. ON-TARGETplus Non-targeting Control Pool (D-001810-10) used as scrambled siRNA control was obtained from Thermo GE Dharmacon. Polyplus Interferin reagent was purchased from VWR and used according to manufacturer instructions. For *in vivo* studies, siRNA against ICAM-2 with forward sequence 5'-AGGACGGUCUCAACUUUUC-3' and reverse sequence 5'-GAAAAGUUGAGACCGUCCU-3' and siRNA luciferace negative control were used, all of them were obtained from AXOlabs. All, the *in vivo* studies were performed using C57BL/6 mice. RNA extraction was carried out using Directzol RNA kit from Genesee Scientific, cDNA reaction was performed using Applied Biosystems cDNA kit and cDNA quantification was analyzed using SYBER green from Affymetrix.

5.2.2 Synthesis of oligopeptide-modified C6 polymer

Synthesis of newly stable poly(β-amino ester)s was performed via a two-step procedure, as similarly described in chapter III. C6 polymer was synthesized using a stoichiometric mixture of 5-amino-1-pentanol and hexylamine with slightly excess of 1.4-butanodiol diacrylate at 1:1.1 molar ratio. Briefly, C6-50 polymerization was performed mixing 5-amino-1- pentanol (0.426 g, 4.1 mmol), hexylamine (0.422 g, 4.1 mmol) and 1,4-butanediol diacrylate (2.0 g, 9.1 mmol) under magnetic stirring at 90 ºC for 24 h. Chemical structure of resulting acrylate-terminated polymers C6-50 polymer was evaluated by 1H-NMR and IR, as previously reported [1].

Oligopeptide-modified pBAE were obtained by end-modification of acrylate-terminated polymer (C6-50) with thiol-terminated oligopeptide at 1:2.1 molar ratio in dimethyl sulfoxide. The mixture was stirred overnight at room temperature, and the resulting polymer was obtained by precipitation in a mixture of diethyl ether and acetone (7:3). C32 and C6 polymer were modified using arginine, lysine, histidine, aspartic acid and glutamic acid peptides. The different oligopeptide modifications were confirmed by 1H-RMN, as previously reported [1].

5.2.3 Endothelial cell-specific polymer formulation screening

Polymer screening of end-modified oligopeptide C6-50 polymer was carried out using fluorescent siRNA (AF555) in endothelial, smooth muscle cells, and immune cells. 80000 cells were seeded onto 12 well plate 24 hours prior transfection. RNAi polyplexes were performed as described previously, at 100:1 w:w ratio with AcONa buffer (12.5 mM, pH 5.0). Uptake analysis of immortalized mouse endothelial cells (iMAEC) and smooth muscle cells (SMC) were carried out following the same

procedure. Adherent cells were transfected with polyplexes during 2 hours. Then, polyplexes were washed twice using PBS 1x and harvest using trypsin. Finally, trypsin was removed by centrifugation and cells were resuspended using PFA at 1% for flow cytometry analysis. Cells in suspension, such as immune cells (THP-1), were collected by centrifugation during 5 min at 1000 rpm after polyplex transfection. Then, cells were resuspended and washed twice using PBS 1x. Finally, cells were resuspended with PFA 1% for flow cytometry analysis. Untreated cells were used as a negative control of cell fluorescence.

5.2.4 In vitro delivery of siICAM-2

iMAECs cells were grown in 12-well plates at a seeding density of 80000 cells/well in 1000 µL growth medium (DMEM, containing 10% fetal bovine serum, 100 units mL^{-1} penicillin, 100 µg mL^{-1} streptomycin, 0.1mM MEM Non-Essential Amino Acids (NEAA), 2mM glutamine, and 50 µg mL^{-1} ECGS (bovine brain extract 1%)). Cells were grown until 80-90% of confluence prior to siICAM-2 delivery. Cells were transfected using C6-K/H polymer and siICAM-2 at different siRNA concentrations, ranging from 10nM until 100nM. At 48 hour post-transfection, the medium was removed, cells were washed with PBS, and collected for qPCR analysis. Scrambled siRNA was used as a negative control of ICAM-2 knockdown at 50 nM. ICAM-2 expression was normalized to scrambled control and plotted as percentage of gene silencing.

5.2.5 Inflammatory markers remain constant after siICAM-2 delivery

VCAM-1, TNF-alpha, and MCP-1 inflammatory markers were analysed at gene level in iMAECs after siICAM-2 delivery. As previously described, cells were seeded at initial density of 80000 cells/wells and cultured until 80% of confluence. Then, cells were transfected using C6-K/H and siICAM-2 at different siRNA concentrations. At 48-hour post-transfection, cells were collected, RNA was extracted, and inflammatory markers were analysed by qPCR. 18S gene was used as a housekeeping gene. Results were normalized to non-treated cells.

5.2.6 Preparation of nanoparticles solution for in vivo IV injection

siRNA polyplexes were performed mixing equal volume of siRNA at 0,5 µg/µL with poly(β-amino ester)s at 37.5 µg/µL in AcONa buffer solution (12.5 mM, pH 5.5). Mixture was mixed by pipetting during few seconds. After 10 min of incubation at room temperature, 200 µL of nanoparticles were precipitated in 1800 µL of HEPES at 10 mM with 5.4 mg/mL of sucrose. After that, the nanoparticles were lyophilized and resuspended with 120 µL of RNA/DNA free water in order to be injected by tail vein injection according to the IACUC protocol.

5.2.7 In vivo animal experiments

Five-week-old female C57BL/6 mice were used for each condition. All procedures used in animal studies were conducted at Emory University and they were approved by the Institutional Animal Care and Use Committee (IACUC).

5.2.8 Ex vivo delivery of labelled siRNA to vasculature

Abdominal aorta was extracted from C57BL/6 mice following the Institutional Animal Care and Use Committee (IACUC) protocol. Mice were sacrificed using CO_2 camber and perfused with saline containing heparin (10 U/mL) via the cava vein. Abdominal aorta was isolated and carefully cleaned of periadventitial fat. Aortas were maintained in PBS 1X at 4ºC until their use.

Labelled nanoparticles were prepared as previously described in AcONa buffer and concentrated by lyophilization. Then, 0.3 mL of lyophilized nanoparticles at 200 nM were injected through the abdominal aorta. After that, aorta was incubated with the remaining nanoparticles during 1 hour at 37ºC and 5% CO_2. Then, abdominal aorta was washed twice using PBS flushing and fixed in 4% paraformaldehyde. After that, samples were opened for *en-face* microscopy analysis. Finally, samples were counter-stained using DAPI and mounted on glass slides using fluorescence mounting medium (Dako). Samples were imaged using a Zeiss-LSM 510 META confocal microscope (Carl Zeiss).

For histology staining, PFA fixed samples were placed in OCT medium and frozen at -80ºC. Histology sections at 8 µm was carried out using Leica Cryostat CM3050S. Then, samples were cleaned twice using PBS 1x and were counter-stained using DAPI. Finally, samples were mounted on coverslip using fluorescence mounting medium (Dako). Samples were imaged using a Zeiss-LSM 510 META confocal microscope (Carl Zeiss).

5.2.9 Isolation of endothelial enriched RNA

At 48-hour post-injection endothelial enriched RNA from the carotids was extracted as described by Nam et. al. [40]. Briefly, mice were killed by CO_2 inhalation according to Emory University's IACUC protocol and perfused with saline containing heparin (10 U/mL) via the left ventricle after severing the inferior abdominal aorta. LCA and the right common carotid artery (RCA) were then isolated and carefully cleaned of periadventitial fat. Then, the carotid lumen was quickly flushed with 150 µL of QIAzol lysis reagent using a 29-gauge insulin syringe in Eppendorf tube. The eluate was snap-frozen in liquid nitrogen for posterior RNA extraction. Moreover, media and adventitia was snap-frozen in liquid nitrogen, pulverized by mortar and pestle, and lysed with QIAzol lysis reagent (300 µL).

5.2.10 siICAM-2 biodistribution study

At 48-hour post-injection, ICAM-2 expression was analysed in lung, liver, spleen, thymus, heard, and kidney. Briefly, 120 µL of polyplexes condensing siICAM-2 or siCONTROL were injected to C57BL/6 mice by tail vein injection at 2 mg/kg. At 48-hour post-injection, mice were killed by CO_2 inhalation according to Emory University's IACUC protocol and perfused with saline solution. Organs were collected and snap-frozen in liquid nitrogen. After that, organs were crashed and lysed with QUIzol for posterior RNA extraction and qPCR analysis. ICAM-2, PECAM-1, CD45, and 18S genes were analyzed by qPCR. 18S was used as a housekeeping gene.

5.2.11 RNA isolation and qPCR analysis

Total RNA obtained from carotids and organs were extracted and purified using Direct-zol™ RNA Kits according to the manufacturer's instructions. Briefly, RNA with QiaZol were mixed with equal volume of Ethanol and the mixture was loaded to a column of silica filters. The RNA binds selectively to the silica matrix and can be washed before eluting in RNase-free water. Before eluting the RNA, DNase digestion was performed during 15 minutes at room temperature, and then the filter was washed three times before elution of the desired RNA. The amount and purity of RNA was determined by NanoDrop 1000 Spectrophotometer following the manufacturer's instructions. Then, RNA was reverse-transcribed using High-Capacity cDNA Reverse Transcription Kit (Applied Biosystems) following the manufacturer's instructions. Finally, gene expression was determined by RT-PCR using the primers listed in Table V-1 for the amplification of ICAM-2, 18S, CD45, PECAM-1 and SM22a cDNAs. Genes of interest were normalized against the 18S housekeeping gene. All analyses were performed using the 2-ΔΔCT method and 3 technical replicates.

Table V-1. Primers sequences used for qPCR analysis.

Primer	**Forward Sequence**	**Reverse Sequence**
18S	5'-AGGAATTGACGGAAGGGCACCA-3'	5'-GTGCAGCCCCGGACATCTAAG-3'
mPECAM1	5'-GCTGGTGCTCTATGCAAGC-3'	5'-ATGGATGCTGTTGATGGTGA-3'
mSM22a	5'-CCTTCCAGTCCACAAACGAC-3'	5'-GTAGGATGGACCCTTGTTGG-3'
mCD45	5'-CTTCAGTGGTCCCATTGTGGTG-3'	5'-TCAGACACCTCTGTCGCCTTAG-3'
mICAM2	5'-GACGGTCTCAACTTTTCCTGCC-3'	5'-CCATTTGGTTGTCCTGCATCGG-3'
mMCP-1	5'- GTGCTGACCCCAATAAGGAA-3'	5'- TGAGGTGGTTGTGAAAAGA-3'
mVCAM1	5'-ACTTGTGCAGCCACCTGAGATC-3'	5'-GCTATGAGGATGGAAGACTCTGG-3'
mTNF-alpha	5'-CGAATTTTGAGAAGATGATCCTG-3'	5'-TGCTGGGAAGCCTAAAAG-3'

5.2.12 Statistical analysis

Statistical analyses were carried out to assess significant differences between experimental groups. Pairwise comparisons were performed using one-way Student t-tests. Differences between groups were considered significant at P values below 0.05 (* $p < 0.05$, ** $p < 0.01$, *** $p < 0.001$)

5.3 Results and discussion

Natural-synthetic polymers designed in Chapter III have been used to efficiently deliver RNAi-drugs to endothelial cells. C6-50 polymer formulation was selected due to their promising results based on transfection/stability ratio, from a large family of synthetized hydrophobic/hydrophilic pBAEs [1]. Previously, we have been reported that C6-50 polymer is an improve version of C32 polymer, where a slightly hydrophobic modification to pBAEs backbone structure was carried out. This modification demonstrated to avoid destabilization of the resulting nanoparticles in physiological conditions, obtaining a stable polymeric formulation. Then, an improvement in stability is translated in an increase in blood circulation time and reduce their non-specific interactions with circulating proteins or blood cells, making these nanoparticles more efficient to reach their target tissue. In addition, the incorporation of hydrophobic moieties in gene delivery carriers has been described to increase nanoparticle interaction with cell membrane and subsequent entry into the cytoplasm [41]. Furthermore, previously published data demonstrated that nanoparticles with appropriate oligopeptide composition is a key factor to obtain a cell-efficient transfection [3,2,42]. It is already described that nanoparticle surface composition is the main factor to predict or control their protein corona, that is the responsible of cell or tissue targeting. Then, in this chapter hypothesize that playing with different oligopeptide combinations could be a promising strategy to control their final nanoparticle specificity, as shown in Figure V-1.

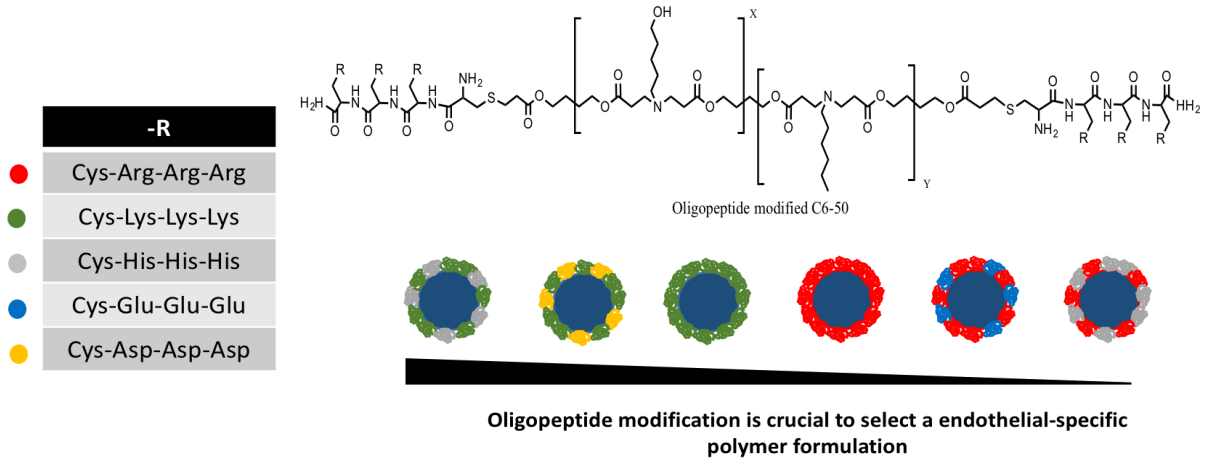

Figure V-1. Structure and synthetic scheme of new stable oligopeptide-modified poly(β-amino ester) polymers. C6-50 synthesis was carried out by stoichiometric reaction of 5-amino-1-pentanol/hexylamine to 1,4-butanediol diacrylate using a slight excess of diacrylate. Further oligopeptide modifications of end-modified C6-50 polymer was performed by thiol reaction. R terminal can be arginine-, lysine-, histidine-, glutamic acid- and aspartic acid-oligopeptide. Polyplexes with different surface proprieties were obtained combining different oligopeptide-moieties.

Then, different polymers formulations were performed combining different oligopeptide moieties. Hydrodynamic size and surface charge of the resulting polyplexes using single oligopeptide-moiety or mixtures of different cationic- / cationic- and cationic-/anionic- oligopeptide were characterized using siICAM2 as a nucleic acid. Nanometric size (below 200 nm) and positive surface charge was observed using positively or mixtures of different positively-charged oligopeptides moieties. In

contrast, bigger polyplexes size were observed using mixtures of positively- and negatively-charged oligopeptides, limiting their stability. However, positive zeta potential was observed, indicating efficient condensation of RNAi. The obtained average size and zeta potential are in good agreement with the results achieved in Chapter IV, when siGFP was used as nucleic acid.

5.3.1 Lysine- / histidine- modified C6-50 polymer formulation shows preferential endothelial cell delivery

As stated before, previous results revealed that the chemical composition of oligopeptides has a dramatic effect on the features of the resulting polyplexes, which ultimately determines cell specificity [2,3]. In order to select endothelial-specific polymer formulation, screening of different oligopeptide-modified poly(β-amino ester) polymers was performed using labelled siRNA in different cell lines. Particularly, endothelial cells (iMAECs), smooth muscle cells (SMC), and immune cells (THP-1) were used for this study. Cells were transfected using different oligopeptide-modified pBAE containing fluorescent siRNA. Finally, fluorescence was determined by flow cytometry as shown in Figure V-2.

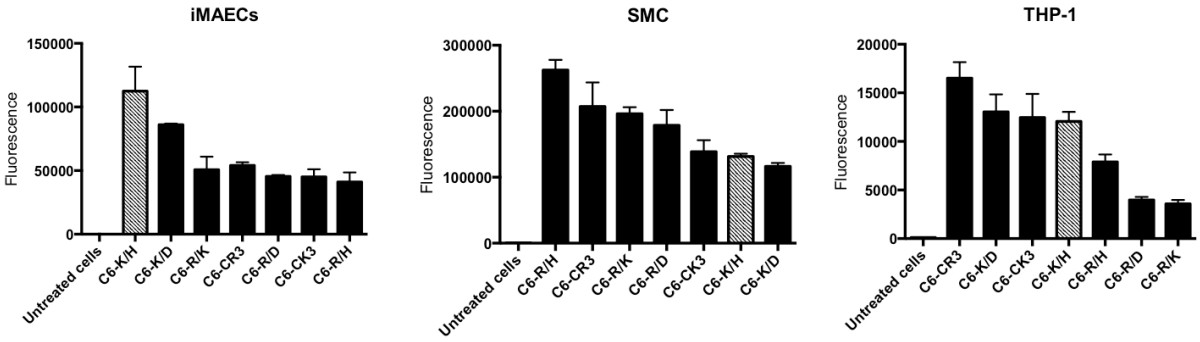

Figure V-2. Cellular uptake of fluorescently-labelled particles prepared from AF555-labelled siRNA in iMAEC, SMC and THP-1 cells. These cells were transfected with siRNA-F at final concentration of 20 nM using different oligopeptide-modified poly(β-amino ester)s in order to select the top performing polymer formulation. Fluorescence expression was determined after transfection by flow cytometry and determined as a percentage of positive cells multiplied by the Median fluorescence.

Uptake analysis showed differential specificity profiles for each cell line depending on the poly(β-amino ester) oligopeptide formulation. Lysine containing polyplexes present a preferential uptake into mouse endothelial cells (iMAECs). Mixtures of lysine with histidine or aspartic acid end-modified pBAE showed the highest levels of cellular uptake, achieving up to 2-fold increase respect to arginine-containing formulations. In general, SMC present a greater cellular uptake compared to endothelial or immune cell line, confirming that SMC cell line was more permissive. Arginine-modified pBAE showed higher uptake on SMC than formulations containing lysine, achieving the highest cellular transfection using arginine/histidine mixture. Finally, immune cells (THP-1) present lower cellular uptake than iMAECs and SMC. Interestingly, the results shown that the highest uptake for immune cells corresponds to arginine-modified polymers. Is already described that nanoparticles with relative high surface charge present a preferential delivery to endothelial or smooth muscle cells due to their interaction of cationic polymer with proteoglycans of the cell membrane [43]. In contrast, negative

charged particles, such as siRNAs, are highly recognized by phagocytic cells. Oligopeptide-modified pBAEs surface charge range from 10 mV to 20 mV, making them less efficient to transfect THP-1 cells. Therefore, THP-1 presented a low or insignificant uptake transfection efficiency compared to iMAECs or SMC using any of oligopeptide combinations, validating that pBAE are not recognized by cells from immune system.

Therefore, we can conclude that lysine-/histidine- or lysine-/aspartic acid- end-modified poly(β-amino ester)s present a preferential transfection efficiency of iMEACs over SMC and THP-1 cells. However, we have chosen lysine- / histidine- modified C6-50 polymer formulation due to the stability concerns previously detected using lysine- / aspartic acid- modified C6-50 polymer formulation.

In order to confirm preferential endothelial specificity, *ex vivo* uptake was performed using different cationic oligopeptide mixture of lysine-, arginine-, and histidine- modified pBAE. Polyplexes were performed using labelled siRNA and injected through the abdominal aorta from C57BL/6 mice at 200 nM. After that, aorta was incubated with the remaining nanoparticles during 1 hour. Aorta histology was performed and the fluorescence was determined by confocal microscopy (Figure V-3).

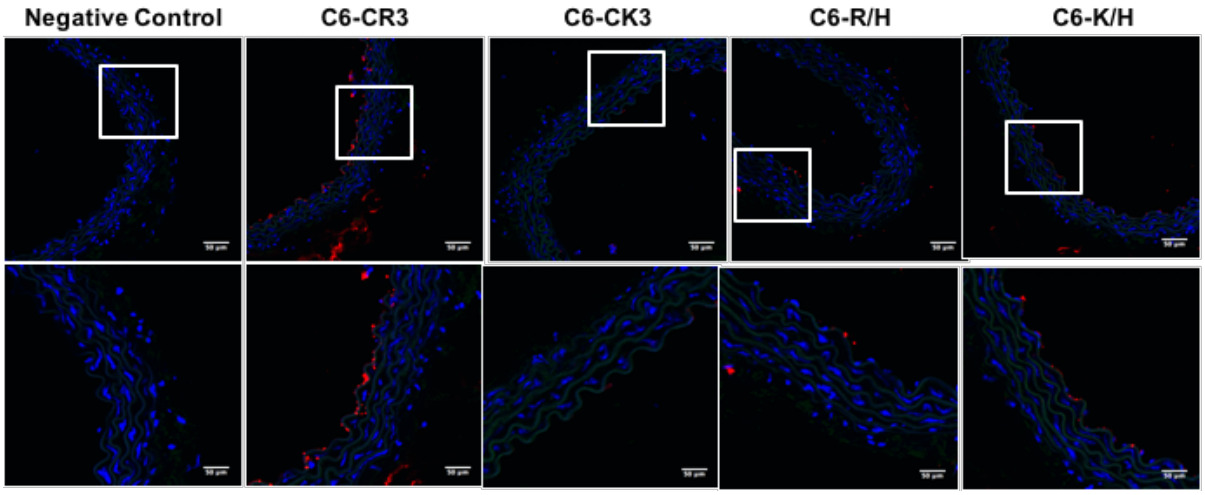

Figure V-3. *Ex vivo* screening of different polymer formulations were carried out in abdominal aorta using labelled siRNA at 200nM. Aorta histology technique allow to observe C6polyplex localization at higher resolution. Images were taken using confocal microscopy.

Aorta histology was carried out in order to specifically study nanoparticle localization. As Figure V-3 showed, arginine-containing formulation had the highest fluorescent uptake in the abdominal aorta, but this formulation not present endothelial specificity, as previously observed in Figure V-2. High fluorescence levels were observed in endothelial and smooth muscle cells. Furthermore, lysine- or arginine- and histidine-modified pBAEs mixture rendered lower uptake *ex vivo* than the cellular uptake observed in *in vitro* assays. Interestingly, these oligopeptide formulations correspond to the less efficient to transfect endothelial cells (Figure V-2), this can suggest that the polyplexes were not able to cross the endothelial cell layer. Then, they are not able to reach smooth muscle cells, where these

polymers present high transfection efficiency. In contrast, as previously observed in *in vitro* polymer screening, lysine-/histidine- modified polymers showed a preferential delivery to endothelial cells compared to SMC. In addition, labelled siRNA administrated without carrier (negative control) is not able to transfect any cell line, corroborating that nanovector is needed to obtain an efficient cell transfection. Thus, we conclude that we have developed lysine- / histidine- modified C6-50 polymer formulation which shows preferential endothelial cell delivery.

In order to further characterized their endothelial specificity *en-face* analysis was carried out using C6-50-K/H polymer, as shown in Figure V-4.

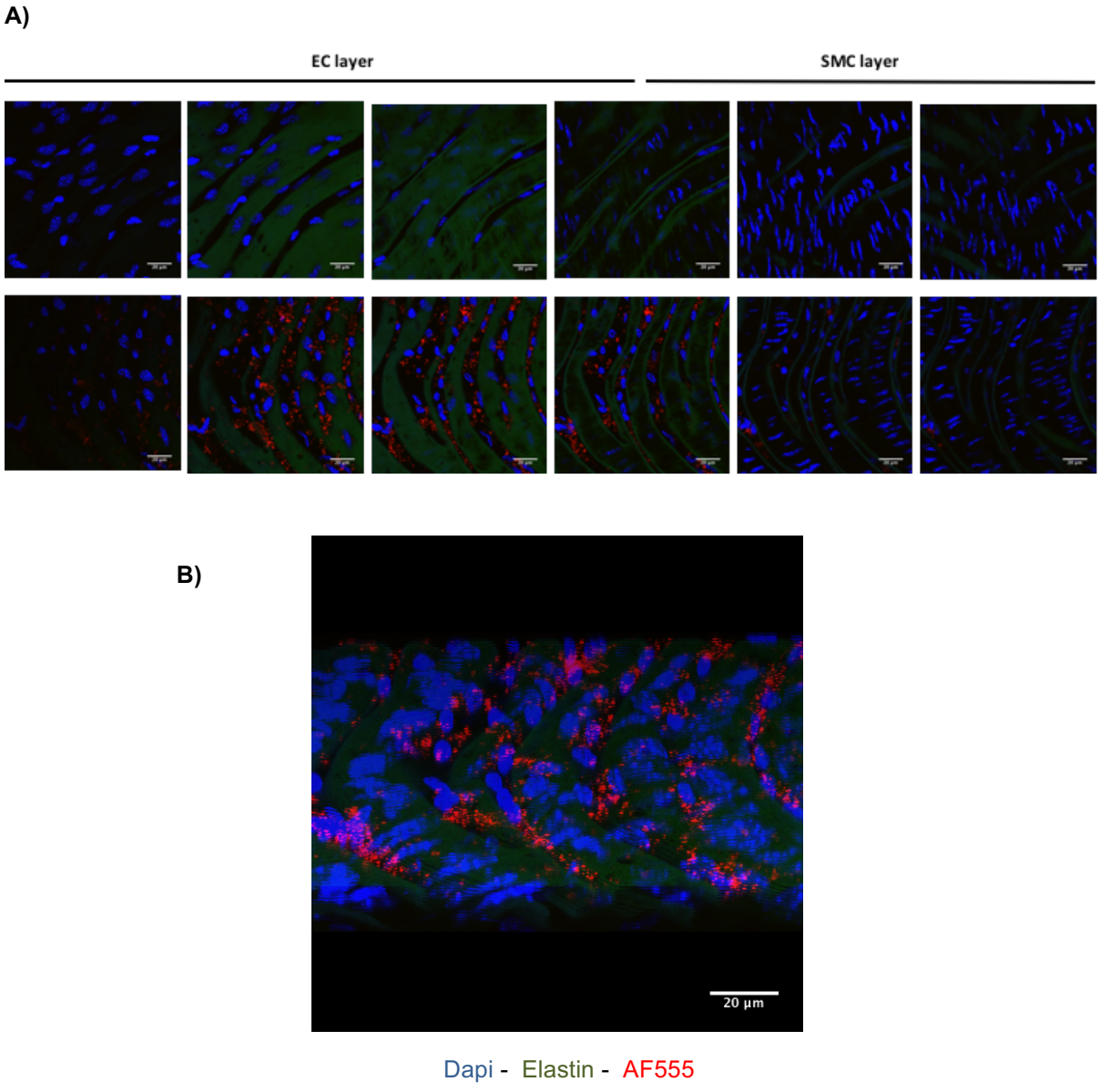

Figure V-4 Labeled siRNA delivery using C6-K/H polyplexes in aorta *ex vivo* C57/BL6 mice. A) *En face* imaging studies shown preferential endothelial delivery using C6-K/H polymer. Nanoparticles were administrated through the abdominal aorta at 200 nM. Images were taken using Confocal microscopy. Labelled siRNA alone was used as a negative control. B) 3D reconstruction of abdominal aorta after labelled siRNA injection using C6-K/H polymer.

One hour after C6-K/H polyplex injection, *en-face* confocal imaging of abdominal aorta endothelium showed significant fluorescence signals from fluorescent siRNA, as shown in Figure V-4-A. Z-stack images showed a preferential delivery to endothelial cells, avoiding the transfection of SMC, demonstrating EC-specific delivery. Therefore, this strategy of passive targeting reduces non-specific side effects to non-desired tissues. Then, we can conclude that playing with oligopeptide formulation we are able to control their protein corona interaction, designing a personalized polymer formulation in function their final target.

5.3.2 C6-K/H polymers efficiently deliver siICAM-2 in iMAECs without cytotoxic effects.

We demonstrated preferential endothelial cell-specificity using lysine- / histidine- modified C6-50, to test the application of this polymer to deliver functional RNAi. We carried out a gene silencing assay using a siRNA targeted towards the EC-specific gene marker ICAM-2 (siICAM-2) in iMAECs. Briefly, cells were incubated with C6-50-K/H polymer at different siICAM-2 or siSCR (scrambled non-targeting siRNA) concentrations, ranging from 10 nM to 100 nM. ICAM-2 expression was determined at the mRNA level by qPCR at 48-hour post-transfection (Figure V-5).

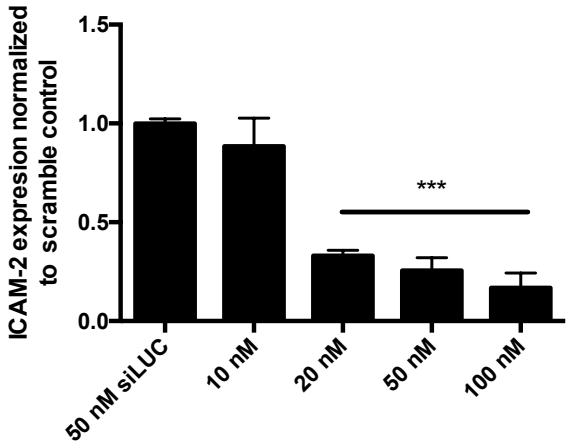

Figure V-5 Efficient and safety siRNA delivery in iMAECs. siICAM-2 dose curve using C6-K/H polymer formulation in iMAECs. ICAM-2 expression was determined 48 h post-transfection by qPCR. Statistical significance was determined using siLUC control as control group. *p < 0.05, **p < 0.01, ***p < 0.001.

A depended dose curve response of ICAM-2 expression was obtained, reaching a 70% of ICAM2 knockdown at siICAM-2 concentrations of 20 nM or higher. ICAM-2 silencing was compared using siSCR at 50nM (scrambled control).

However, most of the delivery vectors used to vascular diseases produce side-effects, such as inflammation. Consequently, cellular behaviour is altered changing their phenotype or compromising their function after gene delivery treatment. Usually, when inflammation occurs in the vasculature is usually observed by the infiltration of leukocytes in the tissue[5,44]. Therefore, delivery vehicles capable of minimizing inflammatory effects are crucial to treat vascular diseases. *In vitro* level,

different inflammatory markers, such as vascular cell adhesion molecule 1 (VCAM-1), tumor necrosis factor alpha (TNF-alpha) and monocyte chemoattractant protein-1 (MCP-1), were analysed in response to different siICAM-2 concentrations.

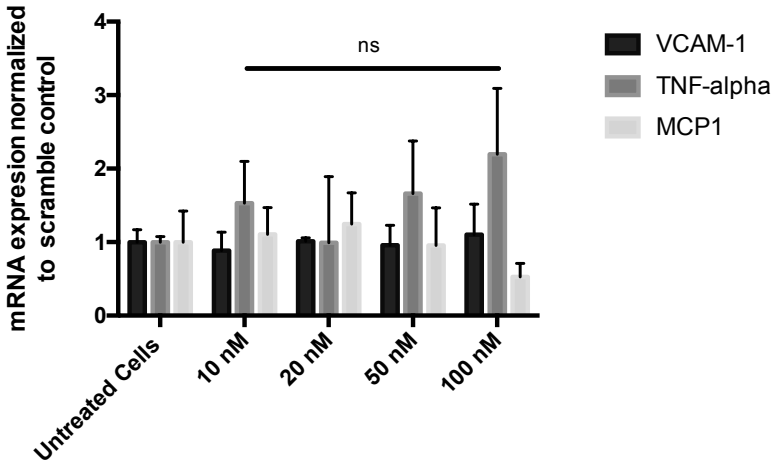

Figure V-6 Efficient and safety siRNA delivery in iMAECs. Different inflammatory expression markers (VCAM-1, TNF-alpha and MCP1) were analysed by qPCR at different polymer:siRNA concentrations. Statistical significance was determined using untreated cells as control group. *p < 0.05, **p < 0.01, ***p < 0.001.

Figure V-6 reveals that no significant differences of early inflammatory markers (VCAM-1 and TNF-alpha) were observed. Moreover, late inflammatory markers, such asMCP1, remained stable. Furthermore, cell morphology remained stable working at high siRNA doses.

At this point, we could conclude that C6-50-K/H polymer demonstrated efficient and safer gene knockdown in iMAECs cell line using siICAM-2 as a RNAi-drug. Firstly, C6-50-K/H polymer was able to reduce 70% of ICAM-2 expression at 20 nM in presence of serum, suggesting that C6-50-K/H-siICAM-2 are able to enter by endocytosis and scape from endosomal pathway, giving them a high therapeutic value. Furthermore, results showed that inflammatory markers, such as VCAM-1, TNF-alpha and MCP1, remain stable after ICAM-2 knockdown. Therefore, results suggest that newly natural-synthetic delivery vectors are able to present efficient nucleic acid delivery with low cell cytotoxicity.

5.3.3 C6-K/H polymers efficiently deliver siICAM-2 to endothelial cells in vivo.

Once *in vitro* and *ex vivo* studies demonstrated efficient cell-specificity and delivery of siRNA using C6-50-K/H nanoparticles, animal studies were performed to determine the effectiveness of this formulation for *in vivo* gene silencing. In this case, siICAM-2 was used [45] in order to downregulate ICAM-2 gene, which plays an important role in endothelial cells and immune system [46,47]. C6-50-K/H polymer formulation was used as a vehicle to selectively deliver siICAM-2 in endothelial cells, avoiding its delivery to other cells types.

Nanoparticles of siICAM-2 or siCONTROL (2mg/kg) were injected by intravenous administration in C57BL/6 mice as a single dose. At 48-hour post-injection, ICAM-2 levels from vasculature, such as carotids, were analysed by qPCR. siCONTROL was used as a negative control of silencing as shown in Figure V-7.

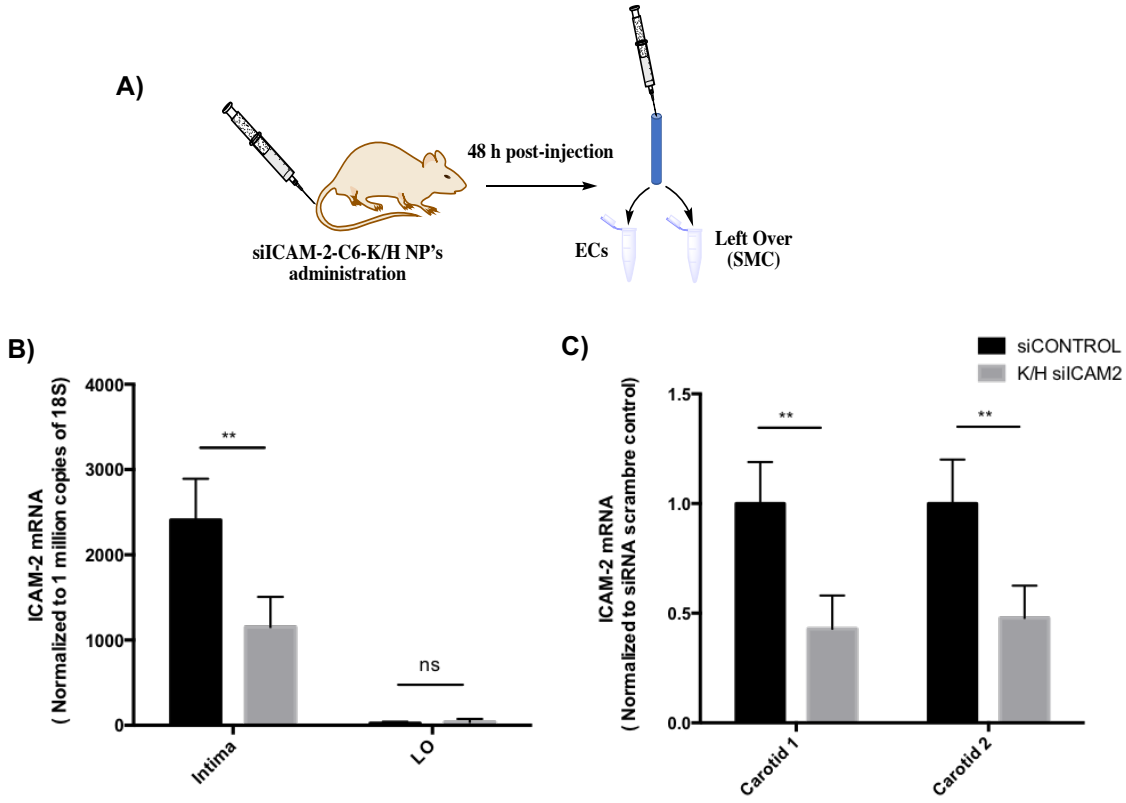

Figure V-7. C6-50-K/H polymer formulation present preferential siICAM-2 delivery to endothelium cell line. A) siICAM-2 and siCONTROL were administrated at 2mg/kg by intravenous injection using C6-K/H polymer in mice, which were sacrifed after 2 days post-injection. 48 hours post-injection endothelial enriched fraction (intima) and SMC enriched fraction (leftover) were extracted and analyzed by qPCR. B) ICAM-2 expression level was analysed in carotids, comparing the endothelial layer (rich in endothelial cells) with the leftover (rich in SMC). Statistical significance was determined using respective scramble controls as control group. *p < 0.05, **p < 0.01, ***p < 0.001.C) Expression of ICAM-2 was determined by qPCR in left carotid (Carotid 1) and in right carotid (Carotid 2). Statistical significance was determined using respective scramble controls as control group. *p < 0.05, **p < 0.01, ***p < 0.001.

ICAM-2 expression from endothelial cell layer and smooth muscle cells was evaluated. To obtain either EC-specific or SMC-specific lysates, at 48h post-injection, right and left carotids were isolated and were flushed with Qiazol to isolate the media lysate (EC-enriched) followed by the isolation of

SMC-specific lysates (the remaining adventitia). ICAM-2 expression in the intima (EC-enriched) and leftover (SMC-enriched) were analysed at gene level (Figure V-7-A). The results showed a significant 55% knockdown of ICAM-2 expression in EC-enriched fraction, whilst no significant reduction was observed in SMC-enriched samples. Moreover, SMC-enriched samples presented lower ICAM-2 expression than EC-enriched samples, confirming that the ICAM-2 is overexpressed in endothelial cells (Figure V-7-C). Thus, these results confirm the therapeutic use of newly developed polymers, which are able to efficiently decrease ICAM-2 expression in a simple dose of 2 mg/kg. Moreover, results showed a similar silencing in both the RCA and LCA (more than 50 %), corroborating efficient gene knockdown in endothelial cells from the main arteria's (Figure V-7-D). These results suggest that nanoparticles are distributed around all the organism, decreasing ICAM2 expression of ECs.

Finally, to further corroborate these results, quality controls of endothelial elution using cell-type markers were analysed. Endothelial marker (PECAM-1), smooth muscle cells marker (SM22a) and immune marker (CD45) were determined.

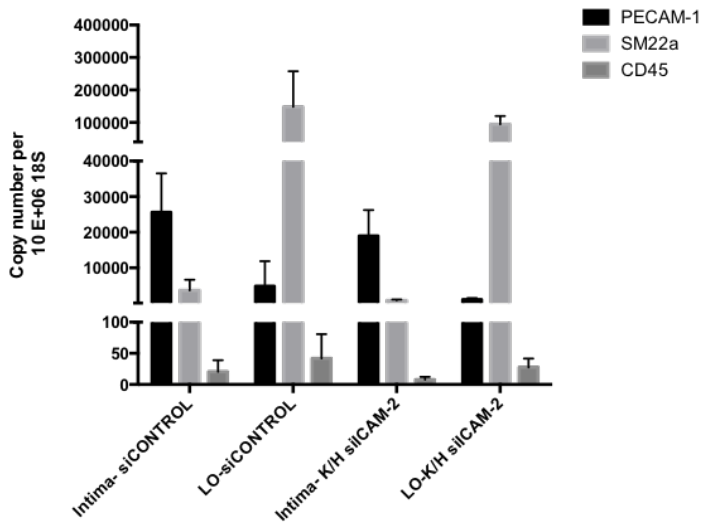

Figure V-8 Quality criteria of endothelial enriched layer was determined analysing PECAM-1 as endothelial marker, SM22a as a smooth muscle cell marker and CD45 as immune marker.

As shown in Figure V-8, high PECAm-1 levels and low SM22-a levels in endothelial enriched samples were found (Intima). In contrast, low PECAM-1 levels and high SM22-a were observed in SMC enriched samples (LO). In addition, low CD45 levels were observed in all conditions due to non-lymphoid infiltration after 48h post-injection, confirming the purity of our EC-rich and SMC-rich samples.

5.3.4 Reduction of ICAM-2 expression was detected in highly vascularized organs

There is a wide range of factors that play an important role in order to determine nanoparticle distribution. These include polyplex biophysical proprieties properties such as size, shape, and surface charge, the route of administration or the final protein corona. The last one, polyplex – protein interactions, is one of the most important factors that compromise their biodistribution [48–50].Thus, biodistribution of EC–specific C6-50- K/H polymer formulation was studied. As previously described, a single dose of nanoparticles containing siICAM-2 or siCONTROL were injected at 2 mg/kg and ICAM-2 levels were determined at 48 hours post-injection in lung, spleen, thymus, kidney, heart and liver.

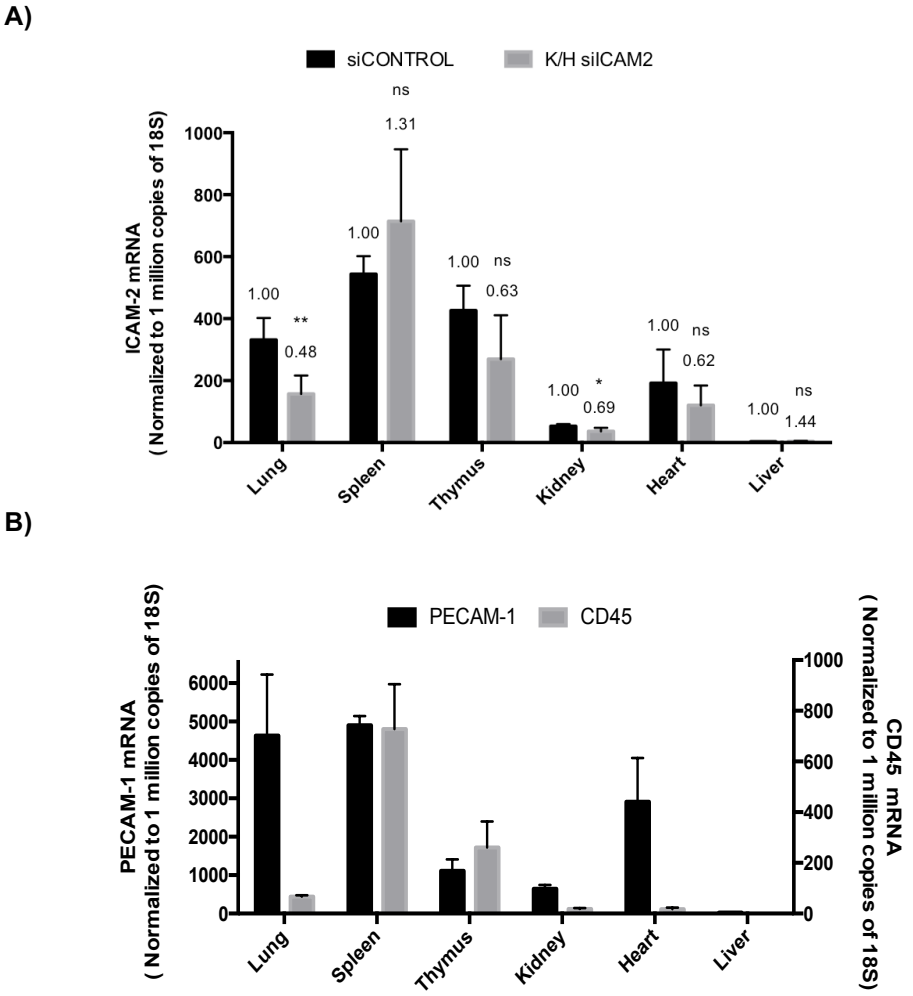

Figure V-9. ICAM-2 organ biodistribution. A) ICAM-2 mRNA levels in different organs at 48 h post-injection of siICAM-2 after IV administration at 2 mg/kg (n=5). Statistical significance was determined using respective scramble controls as control group. *p < 0.05, **p < 0.01, ***p < 0.001. B) Endothelial marker (PECAM-1) and immune marker (CD45) mRNA expression in different organ.

After IV administration, endothelial-specific polyplexes are distributed around all the tissues and organs. Curiously, polyplexes were strongly taken up by the vascular endothelium from the lung, heard, and kidney, which they are high vascularized organs. Results demonstrated that at 48-hour post-injection, ICAM-2 expression was reduced in these organs. In contrast, no significant ICAM-2 reduction was observed in spleen and thymus, which ICAM-2 is also highly expressed (Figure V-9-A).

ICAM-2 gene also play an important role in in lymphocyte recirculation by blocking LFA-1-dependent cell adhesion [51], which are highly expressed in these organs. To further understand these results, PECAM-1 (endothelial marker) and CD45 (immune cell marker) were analysed in different organs (Figure V-9-B). Interestingly, significant ICAM-2 silencing was observed in endothelial rich and low CD45 organs, such as lung or kidney. However, no significant ICAM-2 reduction was observed in CD45 rich and low PECAM-1 organs, such as thymus or spleen. Then, these results suggest that C6-50-K/H formulation present a selective delivery to endothelial cell line, while avoiding recognition by immune system.

Therefore, in this chapter we demonstrated that lysine- / histidine- oligopeptide mixture present a preferential RNAi delivery to endothelial from mice vasculature. Resultant positive surface charge and oligopeptide composition of siICAM2-polyplexes are able to transfect vascular ECs, deliver their nucleic acids, and have therapeutic effect.

5.4 Concluding remarks

In the previous chapters the efforts were focused to developed a stable, efficient, and tissue-specific delivery system based on poly(β-amino ester)s. In this chapter, all of these proprieties were used to evaluate the applicability of this novel family of polymers in *in vivo* applications. At this point, we were focus to specifically and efficiently deliver a therapeutically dose of RNAi-drug to endothelial cells from the vasculature.

In order to design a endothelial-specific polymer formulation, screening of different oligopeptide-modified poly(β-amino ester) polymers were performed using iMAECs. Results demonstrated that lysine/histidine oligopeptide mixture preferential delivers siRNA to ECs, avoiding others cells lines such as SMC and immune cells. To further confirm they endothelial specificity, *ex vivo* delivery was carried out using aorta arteria form C56BL/6 mice. Results corroborate previous *in vitro* results, obtaining a preferential delivery to endothelial cells, avoiding the transfection of SMC.

After that, lysine- / histidine- modified C6-50 polymer (C6-50-K/H) was used to deliver a functional siRNA (siICAM2) at *in vitro* and *in vivo* level. C6-50-K/H polymer was able to efficiently knockdown ICAM-2 expression in iMAECs without cytotoxic effects. This result suggests that previously formulated polyplexes are able to enter by endocytosis and efficiently scape. Once efficient ICAM-2 knockdown was observed *in vitro* studies, polyplexes were tested in C56/BL6 mice. *In vivo* results demonstrated a significant ICAM-2 knockdown effect, reducing more than 55% of gene expression, in endothelial cells from carotids compared to negative control. In contrast, no significant reduction of ICAM-2 was observed in leftover samples (SMC), confirming the endothelial preferentiality of our newly designed polymer formulation.

In addition, biodistrubution studies demonstrated that C6-50-K/H formulation present a selective delivery to endothelial cell line, while avoiding recognition by immune system. Curiously, ICAM-2 reduction was observed in high vascularized organs, such as lung, heard, and kidney. In contrast, not significant ICAM2 silencing was observed in thymus and spleen, which ICAM-2 is also highly expressed due to their role in immunity system.

We can conclude that newly synthetized polymers are a promising delivery strategy to specifically deliver RNAi to specific tissue. In this chapter, we demonstrate that controlling polyplexes surface composition, we are able to define a specific protein corona, which plays a key role in order to design a cell-specific delivery vector. As a proof of concept, in this chapter, we observed that lysine-/histidine oligopeptide mixture seems to present the optimal proprieties to target endothelial cells from the vasculature obtaining low off-target effects over others cells lines.

Therefore, current developed nanoparticles can have a potential therapeutic use for preventive treatments. However, in order to only treat disease cells, the current developed nanoparticles have to

be further improve. In the next chapter, targeted nanoparticles have been designed in order to specifically deliver RNAi to diseased cells o tissues.

5.5 References

[1] P. Dosta, V. Ramos, S. Borrós, Stable and efficient generation of poly(β-amino ester)s for RNAi delivery, Unpubl. Manuscr. (n.d.).

[2] N. Segovia, P. Dosta, A. Cascante, V. Ramos, S. Borrós, Oligopeptide-terminated poly(β-amino ester)s for highly efficient gene delivery and intracellular localization., Acta Biomater. 10 (2014) 2147–58. doi:10.1016/j.actbio.2013.12.054.

[3] P. Dosta, N. Segovia, A. Cascante, V. Ramos, S. Borrós, Surface charge tunability as a powerful strategy to control electrostatic interaction for high efficiency silencing, using tailored oligopeptide-modified poly(beta-amino ester)s (PBAEs), Acta Biomater. 20 (2015) 82–93. doi:http://dx.doi.org/10.1016/j.actbio.2015.03.029.

[4] J.-M. Li, Endothelial cell superoxide generation: regulation and relevance for cardiovascular pathophysiology, AJP Regul. Integr. Comp. Physiol. 287 (2004) R1014–R1030. doi:10.1152/ajpregu.00124.2004.

[5] J.S. Pober, W.C. Sessa, Evolving functions of endothelial cells in inflammation, Nat. Rev. Immunol. 7 (2007) 803–815. doi:10.1038/nri2171.

[6] P.F. Davies, Hemodynamic shear stress and the endothelium in cardiovascular pathophysiology, Nat Clin Pr. Cardiovasc Med. 6 (2009) 16–26. doi:10.1038/ncpcardio1397.

[7] R. Kanasty, J.R. Dorkin, A. Vegas, D. Anderson, Delivery materials for siRNA therapeutics, Nat. Mater. 12 (2013) 967–977. doi:10.1038/nmat3765.

[8] M. Foldvari, D.W. Chen, N. Nafissi, D. Calderon, L. Narsineni, A. Rafiee, Non-viral gene therapy: Gains and challenges of non-invasive administration methods, J. Control. Release. 240 (2016) 165–190. doi:10.1016/j.jconrel.2015.12.012.

[9] M. Merkerova, H. Klamova, R. Brdicka, H. Bruchova, Targeting of gene expression by siRNA in CML primary cells, Mol. Biol. Rep. 34 (2007) 27–33. doi:10.1007/s11033-006-9006-x.

[10] M. Zumbansen, L.M. Altrogge, N.U. Spottke, S. Spicker, S.M. Offizier, S.B. Domzalski, A.L. St Amand, A. Toell, D. Leake, H. a Mueller-Hartmann, First siRNA library screening in hard-to-transfect HUVEC cells., J. RNAi Gene Silencing. 6 (2009) 354–60. http://www.ncbi.nlm.nih.gov/pubmed/20628494.

[11] a Santel, M. Aleku, O. Keil, J. Endruschat, V. Esche, G. Fisch, S. Dames, K. Löffler, M. Fechtner, W. Arnold, K. Giese, A. Klippel, J. Kaufmann, A novel siRNA-lipoplex technology for RNA interference in the mouse vascular endothelium., Gene Ther. 13 (2006) 1222–34. doi:10.1038/sj.gt.3302777.

[12] J. Kaufmann, K. Ahrens, A. Santel, RNA interference for therapy in the vascular endothelium, Microvasc. Res. 80 (2010) 286–293. doi:10.1016/j.mvr.2010.02.002.

[13] H. Yin, R.L. Kanasty, A.A. Eltoukhy, A.J. Vegas, J.R. Dorkin, D.G. Anderson, Non-viral vectors for gene-based therapy, Nat. Rev. Genet. 15 (2014) 541–555. doi:10.1038/nrg3763.

[14] Y. Chiu, T.M. Rana, siRNA function in RNAi : A chemical modification analysis, RNA Soc. 9 (2003) 1034–1048. doi:10.1261/rna.5103703.2000.

[15] M. Breunig, U. Lungwitz, R. Liebl, A. Goepferich, Breaking up the correlation between efficacy and toxicity for nonviral gene delivery., Proc. Natl. Acad. Sci. U. S. A. 104 (2007) 14454–14459. doi:10.1073/pnas.0703882104.

[16] M. Aleku, G. Fisch, K. Möpert, O. Keil, W. Arnold, J. Kaufmann, A. Santel, Intracellular localization of lipoplexed siRNA in vascular endothelial cells of different mouse tissues, Microvasc. Res. 76 (2008) 31–41. doi:10.1016/j.mvr.2008.02.004.

[17] G. Thurston, J.W. McLean, M. Rizen, P. Baluk, A. Haskell, T.J. Murphy, D. Hanahan, D.M. McDonald, Cationic liposomes target angiogenic endothelial cells in tumors and chronic inflammation in mice., J. Clin. Invest. 101 (1998) 1401–1413. doi:10.1172/JCI965.

[18] a Santel, M. Aleku, O. Keil, J. Endruschat, V. Esche, B. Durieux, K. Löffler, M. Fechtner, T. Röhl, G. Fisch, S. Dames, W. Arnold, K. Giese, a Klippel, J. Kaufmann, RNA interference in the mouse vascular endothelium by systemic administration of siRNA-lipoplexes for cancer therapy., Gene Ther. 13 (2006) 1360–70. doi:10.1038/sj.gt.3302778.

[19] J.E. Dahlman, C. Barnes, O.F. Khan, A. Thiriot, S. Jhunjunwala, T.E. Shaw, Y. Xing, H.B. Sager, G. Sahay, L. Speciner, A. Bader, R.L. Bogorad, H. Yin, T. Racie, Y. Dong, S. Jiang, D. Seedorf, A. Dave, K. Singh Sandhu, M.J. Webber, T. Novobrantseva, V.M. Ruda, A.K.R. Lytton-Jean, C.G. Levins, B. Kalish, D.K. Mudge, M. Perez, L. Abezgauz, P. Dutta, L. Smith, K. Charisse, M.W. Kieran, K. Fitzgerald, M. Nahrendorf, D. Danino, R.M. Tuder, U.H. von Andrian, A. Akinc, D. Panigrahy, A. Schroeder, V. Koteliansky, R. Langer, D.G. Anderson, In vivo endothelial siRNA delivery using polymeric nanoparticles with low molecular weight, Nat. Nanotechnol. 9 (2014) 648–655. doi:10.1038/nnano.2014.84.

[20] K.T. Love, K.P. Mahon, G. Christopher, K.A. Whitehead, W. Querbes, J. Robert, J. Qin, W. Cantley, L.L. Qin, M. Frank-kamenetsky, K.N. Yip, R. Alvarez, D.W.Y. Sah, A. De Fougerolles, K. Fitzgerald, V. Koteliansky, A. Akinc, R. Langer, G. Daniel, K.T. Love, K.P. Mahon, C.G. Levins, K.A. Whitehead, W. Querbes, J. Robert, Correction for Love et al., Lipid-like materials for low-dose, in vivo gene silencing, Proc. Natl. Acad. Sci. 107 (2010) 9915–9915. doi:10.1073/pnas.1005136107.

[21] S.C. Semple, A. Akinc, J. Chen, A.P. Sandhu, B.L. Mui, C.K. Cho, D.W.Y. Sah, D. Stebbing, E.J. Crosley, E. Yaworski, I.M. Hafez, J.R. Dorkin, J. Qin, K. Lam, K.G. Rajeev, K.F. Wong, L.B. Jeffs, L. Nechev, M.L. Eisenhardt, M. Jayaraman, M. Kazem, M.A. Maier, M. Srinivasulu, M.J. Weinstein, Q. Chen, R. Alvarez, S.A. Barros, S. De, S.K. Klimuk, T. Borland, V. Kosovrasti, W.L. Cantley, Y.K. Tam, M. Manoharan, M.A. Ciufolini, M.A. Tracy, A. de Fougerolles, I. MacLachlan, P.R. Cullis, T.D. Madden, M.J. Hope, Rational design of cationic lipids for siRNA delivery., Nat. Biotechnol. 28 (2010) 172–6. doi:10.1038/nbt.1602.

[22] J.K. Nair, J.L.S. Willoughby, A. Chan, K. Charisse, M.R. Alam, Q. Wang, M. Hoekstra, P. Kandasamy, A. V. Kel'in, S. Milstein, N. Taneja, J. O'Shea, S. Shaikh, L. Zhang, R.J. van der Sluis, M.E. Jung, A. Akinc, R. Hutabarat, S. Kuchimanchi, K. Fitzgerald, T. Zimmermann, T.J.C. van Berkel, M.A. Maier, K.G. Rajeev, M. Manoharan, Multivalent N -Acetylgalactosamine-Conjugated siRNA Localizes in Hepatocytes and Elicits Robust RNAi-Mediated Gene Silencing, J. Am. Chem. Soc. 136 (2014) 16958–16961. doi:10.1021/ja505986a.

[23] H. Lv, S. Zhang, B. Wang, S. Cui, J. Yan, Toxicity of cationic lipids and cationic polymers in gene delivery, J. Control. Release. 114 (2006) 100–109. doi:http://dx.doi.org/10.1016/j.jconrel.2006.04.014.

[24] K.B. Knudsen, H. Northeved, P. Kumar EK, A. Permin, T. Gjetting, T.L. Andresen, S. Larsen, K.M. Wegener, J. Lykkesfeldt, K. Jantzen, S. Loft, P. Møller, M. Roursgaard, In vivo toxicity of cationic micelles and liposomes, Nanomedicine Nanotechnology, Biol. Med. 11 (2015) 467–477. doi:10.1016/j.nano.2014.08.004.

[25] M.C. Filion, N.C. Phillips, Toxicity and immunomodulatory activity of liposomal vectors formulated with cationic lipids toward immune effector cells., Biochim. Biophys. Acta. 1329 (1997) 345–56. doi:10.1016/S0005-2736(97)00126-0.

[26] A.M. Aberle, F. Tablin, J. Zhu, N.J. Walker, D.C. Gruenert, M.H. Nantz, A Novel Tetraester Construct That Reduces Cationic Lipid-Associated Cytotoxicity. Implications for the Onset of Cytotoxicity †, Biochemistry. 37 (1998) 6533–6540. doi:10.1021/bi9801154.

[27] G. Sahay, W. Querbes, C. Alabi, A. Eltoukhy, S. Sarkar, C. Zurenko, E. Karagiannis, K. Love, D. Chen, R. Zoncu, Y. Buganim, A. Schroeder, R. Langer, D.G. Anderson, Efficiency of siRNA delivery by lipid nanoparticles is limited by endocytic recycling, Nat. Biotechnol. 31 (2013) 653–658. doi:10.1038/nbt.2614.

[28] D.M. Lynn, R. Langer, Degradable Poly(β-amino esters): Synthesis, Characterization, and Self-Assembly with Plasmid DNA, J. Am. Chem. Soc. 122 (2000) 10761–10768. doi:10.1021/ja0015388.

[29] J. Behr, The Proton Sponge: a Trick to Enter Cells the Viruses Did Not Exploit, 2 (1997) 34–36.

[30] H.W. Kang, L. Josephson, A. Petrovsky, R. Weissleder, A. Bogdanov, M.G. Hospital, Magnetic Resonance Imaging of Inducible E-Selectin Expression in Human Endothelial Cell Culture, (2002) 122–127.

[31] K.A. Kelly, J.R. Allport, A. Tsourkas, V.R. Shinde-patil, L. Josephson, R. Weissleder, Detection of vascular adhesion molecule-1 expression using a novel multimodal nanoparticle, Circ. Res. 96 (2005) 327–336. doi:10.1161/01.RES.0000155722.17881.dd.

[32] R. Weissleder, K. Kelly, E.Y. Sun, T. Shtatland, L. Josephson, Cell-specific targeting of nanoparticles by multivalent attachment of small molecules, Nat. Biotechnol. 23 (2005) 1418–1423. doi:10.1038/nbt1159.

[33] A. Salvati, C. Aberg, T. dos Santos, J. Varela, P. Pinto, I. Lynch, K.A. Dawson, Experimental and theoretical comparison of intracellular import of polymeric nanoparticles and small molecules: toward models of uptake kinetics., Nanomedicine. 7 (2011) 818–26. doi:10.1016/j.nano.2011.03.005.

[34] P. Aggarwal, J.B. Hall, C.B. McLeland, M.A. Dobrovolskaia, S.E. McNeil, Nanoparticle interaction with plasma proteins as it relates to particle biodistribution, biocompatibility and therapeutic efficacy, Adv. Drug Deliv. Rev. 61 (2009) 428–437. doi:10.1016/j.addr.2009.03.009.

[35] A. Cifuentes-Rius, H. de Puig, J.C.Y. Kah, S. Borros, K. Hamad-Schifferli, Optimizing the Properties of the Protein Corona Surrounding Nanoparticles for Tuning Payload Release, ACS Nano. 7 (2013) 10066–10074. doi:10.1021/nn404166q.

[36] C. Wolfrum, S. Shi, K.N. Jayaprakash, M. Jayaraman, G. Wang, R.K. Pandey, K.G. Rajeev, T. Nakayama, K. Charrise, E.M. Ndungo, T. Zimmermann, V. Koteliansky, M. Manoharan, M. Stoffel, Mechanisms and optimization of in vivo delivery of lipophilic siRNAs, Nat. Biotechnol. 25 (2007) 1149–1157. doi:10.1038/nbt1339.

[37] A. Malek, O. Merkel, L. Fink, F. Czubayko, T. Kissel, A. Aigner, In vivo pharmacokinetics, tissue distribution and underlying mechanisms of various PEI(–PEG)/siRNA complexes, Toxicol. Appl. Pharmacol. 236 (2009) 97–108. doi:10.1016/j.taap.2009.01.014.

[38] K. Regnström, E.G.E. Ragnarsson, M. Köping-Höggård, E. Torstensson, H. Nyblom, P. Artursson, PEI – a potent, but not harmless, mucosal immuno-stimulator of mixed T-helper cell response and FasL-mediated cell death in mice, Gene Ther. 10 (2003) 1575–1583. doi:10.1038/sj.gt.3302054.

[39] S. Tenzer, D. Docter, J. Kuharev, A. Musyanovych, V. Fetz, R. Hecht, F. Schlenk, D. Fischer, K. Kiouptsi, C. Reinhardt, K. Landfester, H. Schild, M. Maskos, S.K. Knauer, R.H. Stauber, Rapid formation of plasma protein corona critically affects nanoparticle pathophysiology., Nat. Nanotechnol. 8 (2013) 772–81. doi:10.1038/nnano.2013.181.

[40] D. Nam, C.-W.C.-W. Ni, A. Rezvan, J. Suo, K. Budzyn, A. Llanos, D. Harrison, D. Giddens, H. Jo, Partial carotid ligation is a model of acutely induced disturbed flow, leading to rapid endothelial dysfunction and atherosclerosis, AJP Hear. Circ. Physiol. 297 (2009) H1535–H1543. doi:10.1152/ajpheart.00510.2009.

[41] V. Incani, A. Lavasanifar, H. Uludağ, Lipid and hydrophobic modification of cationic carriers on route to superior gene vectors, Soft Matter. 6 (2010) 2124. doi:10.1039/b916362j.

[42] R. Núñez-Toldrà, P. Dosta, S. Montori, V. Ramos, M. Atari, S. Borrós, Improvement of osteogenesis in dental pulp pluripotent-like stem cells by oligopeptide-modified poly(β-amino ester)s, Acta Biomater. 53 (2017) 152–164. doi:10.1016/j.actbio.2017.01.077.

[43] E. Fröhlich, The role of surface charge in cellular uptake and cytotoxicity of medical nanoparticles, Int. J. Nanomedicine. 7 (2012) 5577. doi:10.2147/IJN.S36111.

[44] A. Kadl, N. Leitinger, The Role of Endothelial Cells in the Resolution of Acute Inflammation, Antioxid. Redox Signal. 7 (2005) 1744–1754. doi:10.1089/ars.2005.7.1744.

[45] J.E. Dahlman, C. Barnes, O.F. Khan, A. Thiriot, S. Jhunjunwala, T.E. Shaw, Y. Xing, H.B. Sager, G. Sahay, L. Speciner, A. Bader, R.L. Bogorad, H. Yin, T. Racie, Y. Dong, S. Jiang, D. Seedorf, A. Dave, K. Singh Sandhu, M.J. Webber, T. Novobrantseva, V.M. Ruda, A.K.R. Lytton-Jean, C.G. Levins, B. Kalish, D.K. Mudge, M. Perez, L. Abezgauz, P. Dutta, L. Smith, K. Charisse, M.W. Kieran, K. Fitzgerald, M. Nahrendorf, D. Danino, R.M. Tuder, U.H. von Andrian, A. Akinc, D. Panigrahy, A. Schroeder, V. Koteliansky, R. Langer, D.G. Anderson, In vivo endothelial siRNA delivery using polymeric nanoparticles with low molecular weight., Nat. Nanotechnol. 9 (2014) 648–55. doi:10.1038/nnano.2014.84.

[46] A.J. Thomson, Expression of intercellular adhesion molecules ICAM-1 and ICAM-2 in human endometrium: regulation by interferon-gamma, Mol. Hum. Reprod. 5 (1999) 64–70. doi:10.1093/molehr/5.1.64.

[47] Y. Reiss, B. Engelhardt, T cell interaction with ICAM-1-deficient endothelium in vitro: transendothelial migration of different T cell populations is mediated by endothelial ICAM-1 and ICAM-2, Int. Immunol. 11 (1999) 1527–1539. doi:10.1093/intimm/11.9.1527.

[48] D. Dutta, S.K. Sundaram, J.G. Teeguarden, B.J. Riley, L.S. Fifield, J.M. Jacobs, S.R. Addleman, G.A. Kaysen, B.M. Moudgil, T.J. Weber, Adsorbed Proteins Influence the Biological Activity and Molecular Targeting of Nanomaterials, Toxicol. Sci. 100 (2007) 303–315.

doi:10.1093/toxsci/kfm217.

[49] A. Gessner, A. Lieske, B.R. Paulke, R.H. Mu, Influence of surface charge density on protein adsorption on polymeric nanoparticles : analysis by two-dimensional electrophoresis, Eur. J. Pharm. Biopharm. 54 (2002) 165–170.

[50] W.H. De Jong, W.I. Hagens, P. Krystek, M.C. Burger, A.J.A.M. Sips, R.E. Geertsma, Particle size-dependent organ distribution of gold nanoparticles after intravenous administration, Biomaterials. 29 (2008) 1912–1919. doi:10.1016/j.biomaterials.2007.12.037.

[51] J.M. Casasnovas, C. Pieroni, T. a Springer, Lymphocyte function-associated antigen-1 binding residues in intercellular adhesion molecule-2 (ICAM-2) and the integrin binding surface in the ICAM subfamily, Proc. Natl. Acad. Sci. 96 (1999) 3017–3022. doi:10.1073/pnas.96.6.3017.

Chapter VI

Targeted delivery to inflamed endothelium using VHKP-decorated poly(β-amino ester)s

Prepared for submission:

P. Dosta, V. Ramos, M. Mahmoud, H.Jo*, S. Borrós*, “Targeted delivery to inflamed endothelium using VHKP-decorated poly(β-amino ester)s”, Biomaterials.

This page left blank intentionally

Targeted delivery to inflamed endothelium using VHKP-decorated poly(β-amino ester)s

Nanoparticle engineering for efficient delivery and specific of RNAi-drugs to diseased tissue is currently a vital research area, which may ultimately catalyse the translation of these systems into clinical evaluation. Here, we have developed a new methodology to incorporate targeting moieties to our previously developed pBAEs in order to deliver therapeutic RNAi in a receptor-mediated manner. Newly decorated pBAEs vectors present a simple design and manipulation, making them excellent candidates for gene therapy assays that can be used for a wide range of applications. In collaboration with Biomedical Engineering Department (BME) at Georgia Institute of Technology and Emory University (Atlanta, USA) we have designed a targeted formulation capable of achieving preferential delivery of RNAi-drugs to inflamed endothelial cells (ECs). Specifically, we have successfully demonstrated the potential of this approach using an atherosclerosis disease model.

6.1 Introduction

In Chapter II, it has been demonstrated that polyplexes functionalization using different oligopeptides moieties has a direct effect in their cellular specificity and delivery efficiency. Furthermore, pBAEs chemical structure combining an optimal ratio of hydrophilic / hydrophobic amines present a clear outcome in their loading capacity, stability and cellular entrance efficiency. Then, when previously developed stable and cell-specific polyplexes are administered into systemic circulation, these are distributed in the organism and specific cell lines are preferentially targeted, as previously demonstrated in Chapter V. Although important advances in the preferential cell-specificity or biodistribution of polyplexes have been solved, there are some drawbacks that are currently out of our capabilities. For example, some diseases occur only in certain cell subpopulations or in specific localizations. In these scenarios, delivery systems have to be further optimized to selectively deliver RNAi-drugs to diseased cells, while bypassing healthy cells and tissues to avoid off-target effects. A common early manifestation in diseased cells and tissues, which may be exploited to differentiate diseased cells from healthy cells, is inflammation. Targeting to inflamed tissues can be potentially achieved using delivery systems that exploit specific features of the diseased cells. Inflammation-targeted delivery of RNAi should achieve high drug concentration locally at the site of inflammation with minimal exposure to of healthy tissues. To demonstrate the potential of such inflammation-responsive vectors, a suitable model for inflammation is needed. Atherosclerosis is a suitable model to study preferential targeting to inflamed cells, since only a subpopulation of cells suffer

inflammation, inflammation occurs in the endothelial layer of the vasculature, which is easily accessible for systemically administered RNAi vectors, and the molecular mechanisms of inflammation are well known.

In this chapter, we have focused in the development of an inflamed-specific RNAi delivery vector in an atherosclerotic model in collaboration with Prof. Hanjoong Jo from Biomedical Engineering Department (BME). As previously commented, atherosclerosis only occurs in certain regions of the vasculature. Hence, polyplexes have to be designed to specifically deliver therapeutic RNA-drugs to atherosclerotic areas.

Atherosclerosis is a vascular inflammatory disease affecting arterial blood vessels due to a chronic inflammatory response. In its early stage, it involves the overexpression of cellular adhesion molecules, which are expressed on the vascular endothelium. Specifically, intercellular adhesion molecules (ICAMs) and vascular cell adhesion molecules (VCAM-1) induce adhesion and transendothelial migration of different inflammatory cells, such as monocytes and T lymphocytes, to the endothelium cell layer of vasculature[1]–[3]. Infiltration leads to recruitment of monocytes-macrophages, which are transformed to foam cells. Finally, the formation plaque occurs, which is essentially composed by fibrous tissue containing smooth muscle cells. Over time plaque gradually impinge on the arterial vessel lumen and impede blood flow, as is shown in Figure VI-1.

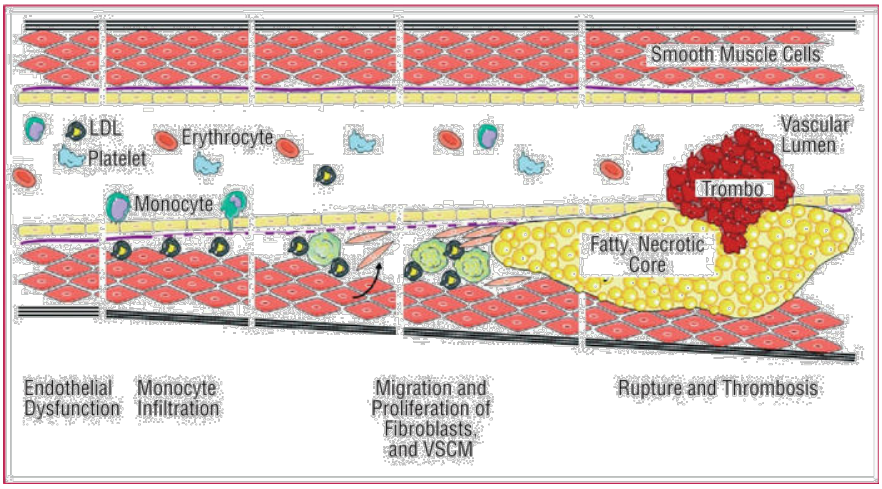

Figure VI-1 Stages of Atherosclerosis disease [4].

Different causes have been correlated to endothelial dysfunction, which it is the first manifestation of this disease. For example, hypertension [4] [5], hypercholesterolemia [7], low HDL-cholesterol [8], and diabetic patients [9] have been associated as the main cardiovascular risk factors. Additionally, the vasculature is exposed to a large number of biomechanical stimuli from blood flow profiles, which have demonstrated to contribute to atherosclerosis disease. Regions of disturbed flow (d-flow), such as arterial branches, bifurcations and curvatures are well-known to form atherosclerotic plaques due

to endothelial cell inflammation, while regions with stable flow (s-flow) are associated with regions where atherosclerosis rarely occurs [10], as shown Figure VI-2.

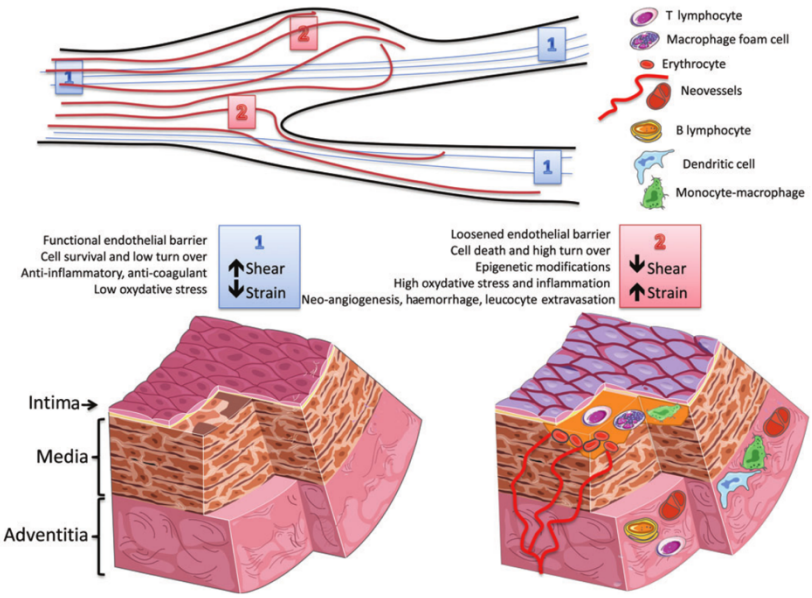

Figure VI-2. Effects of shear stress on the arterial wall. Schematic representation of how biomechanical forces can modify ECs phenotype. (1) Correspond to stable flow and (2) correspond to disturbed flow. (1) contribute to maintenance of the physiological properties of the ECs and (2) contribute to endothelial dysfunction, causing EC death and reducing their physiological functions [11]

Shear stress can influence to endothelial cell behavior by inducing different signaling pathways that can modify their phenotype, losing their functionality, as shown Figure VI-2. It is well known that dysfunctional ECs have a different gene expression profile compared to quiescent, healthy ECs, these genetic changes include an increase in inflammatory and pro-atherogenic genes. Different *in vitro* and *in vivo* models have been characterized to examine the relationship between shear stress and gene expression profile of ECs (Figure VI-3) [12], [13].

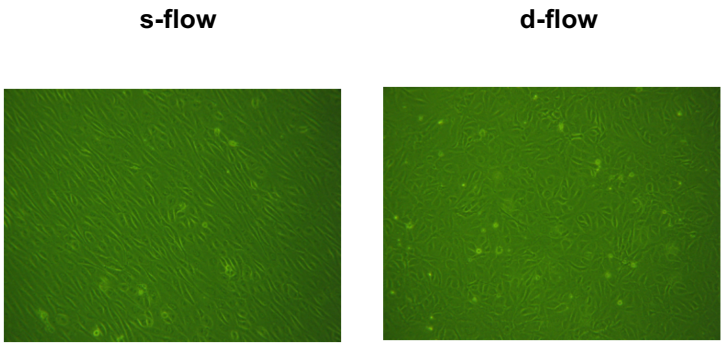

Figure VI-3. *In vitro* model of shear stress in EC using cone-and-plate viscometer. S-flow contribute to maintain ECs phenotype (ECs are lined to flow direction) and d-flow induce ECs dysfunction (ECs are disorganized).

When ECs are exposed to *d-flow*, these activate a different cell-signaling pathway that rapidly modify gene and protein expression. Firstly, shear stress produces a physical deformation of endothelium cell surface and consequently the cell cytoskeleton. Then, the mechanotransduction is produced by the conversion of mechanical force to biochemical signalling modifying different cell pathway behaviours [11], [14]. Therefore, different mechanosensitive genes could be a promising target to design artheroprotective therapies. For example, s-flow upregulates some antiatherogenic genes, such as Klf2, Klf4 and eNOS, while *d-flow* is responsible of proatherogenic genes, such as VCAM-1 and matrix metalloproteinases [15]–[17].

Emerging evidence indicates that similar behaviour was observed at RNAi (microRNA, siRNA, anti-miRNA) level, which are able to efficiently regulate gene expression, showing another potential way to design efficient atherosclerosis treatments. Recently, different studies have demonstrated this potential and a wide range of mechano-sensitive miRNA, which are upregulated or downregulated in flow-dependent conditions, have been characterized. miR-10, miR-19a, miR23b, and miR-101 are antiatherogenic microRNAs, which are further increased in s-flow or decreased by d-flow in endothelial cells. In contrast, miR-17-92, miR-92a, miR-663, miR-712, and miR-205 are proatherogenic miRNAs, which are increased in d-flow and decreased in s-flow conditions [18]. Recently, miR-712 has demonstrated to inhibit atherosclerosis in *in vitro* and *in vivo* assays. miR-712 is increased in d-flow areas, decreasing TIMP3 gene, which plays a key role in endothelial inflammation and atherosclerosis. Moreover, it has been demonstrated that anti-miR-712 is able to target and decrease miR712 levels, making it a promising RNAi approach to be used as a therapeutic treatment [19].

Previous studies have shown that naked anti-miR-712 delivered via subcutaneous injection (at 5 mg/kg, twice a week) reduced miR712 levels and increased TIMP3 target gene [19], obtaining a promising therapeutic effect. Nevertheless, high off-targets effects were observed in healthy tissues due to anti-miR712 is distributed throughout the entire body. Therefore, in order to address these limitations, our novel pBAEs were used to selectively drive RNAi-drugs to diseased ECs.

Recently, pBAEs have been used to deliver plasmid DNA and/or siRNA in a specific cell manner in *in vitro* and *in vivo* assays [20]–[24], as previously have been reported in Chapter III and Chapter V. We have described that oligopeptide composition can modulate nanoparticle protein corona, controlling their biodistribution and cell specificity. Furthermore, pBAE oligopeptide formulations were designed to increase cell-entrance and endosomal scape efficiency [24], [25]. However, oligopeptide-modified pBAEs cannot differentiate between dysfunctional and healthy ECs per se, and preferential delivery to *d-flow* arteries while avoiding the *s-flow* areas is difficult to achieve by just adjusting the oligopeptide composition of the vectors. For this reason, a more specific mechanism that may exploit a specific feature in dysfunctional ECs is required.

Nowadays, targeted delivery represents a promising way to overcome this limitation. Peptides, proteins or chemical ligands have been link to nanoparticle surface in order to increase their selectivity [12], [26]–[28]. Therefore, the combination of an active cell targeting against diseased ECs

using well-studied ligands and an efficient pBAE formulation could be an excellent strategy to drive specifically RNAi-based drugs to diseased cells, specifically to *d-flow* areas. To take advantage of both approaches, we hypothesized that targeted delivery using targeting peptides could drive pBAE polyplexes to dysfunctional ECs and an optimized oligopeptide pBAE composition could enhance their endosomal delivery once the target cell is reached.

However, design or selection a cell-specific targeting peptide is still challenging. In endothelial dysfunction, it has been reported that a wide range of cell surface target molecules are overexpressed in d-flow conditions, such as VCAM-1 protein. Specifically, VCAM-1 protein is an inflammatory marker that is widely used as cellular receptor due to its easy accessibility and well-designed ligands [29]. For example, VHPK peptide is an optimized protein sequence that shows high affinity to VCAM-1 membrane receptor [30], [31]. Therefore, VHPK targeting peptide was selected and incorporated into our previously developed pBAE formulation.

Considerable efforts have been directed toward rational surface modifications and coatings to link targeting peptides. Commonly, poly (ethylene glycol) (PEG) has become the most widely-used approach in clinical applications due to its safety and biocompatible profile, versatility, low inmunogenicity, and its present low non-specific toxicity. However, alternative polymers to control polyplex pharmacokinetics have been described, such as poly [N -(2-hydroxypropyl)methacrylamide] (pHPAM) [32], [33], poly(vinylpyrrolidone) (PVP) [34] or styrene-co-maleic acid/anhydride [35], shown in Figure VI-4.

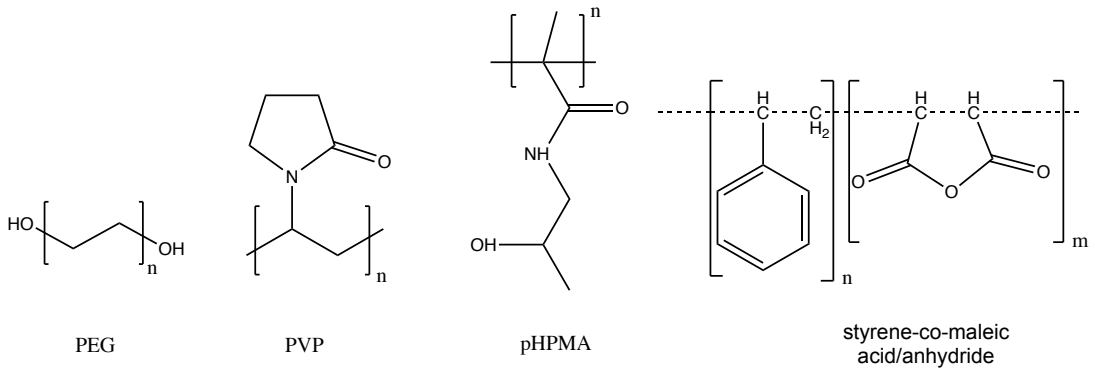

Figure VI-4 Different coating strategies can be used to shield the polyplexes surface. A) poly (ethylene glycol) (PEG), B) poly(vinylpyrrolidone) (PVP), C) Poly [N -(2-hydroxypropyl)methacrylamide] (pHPAM), and D) styrene-co-maleic acid/anhydride.

All of them possess several specific proprieties. In this work, we have selected pHPMA polymer as a coating due to its simple formulation and adaptability to our final application. pHPMA have been formulated using amino-reactive groups, which are used to bind the coating with polyplex structure by covalently bonds [33], [36]. In addition, amine-reactive groups can be modified to selective bind targeting peptides. For example, in this study, 1-(2-Aminoethyl)maleimide was used to link VHKP peptide to pHPMA coating formulation. Then, pHPAM coating played a dual role decreasing protein

interaction with polyplex formulation, making them more stable and minimizing their cell non-specificity, and as a linker of pBAE formulation and VHPK peptide.

Therefore, the main objective of this chapter is to develop a targeted-delivery to inflamed endothelial cells using VHPK-targeted pBAEs. Where the therapeutic anti-miRNA, called anti-miR-712, is used in order to design a promising atherosclerosis treatment.

In order to achieve this objective, the following tasks were proposed:

- Design and characterize VHPK targeted nanoparticles based on pBAEs.
- Therapeutic anti-miR712 delivery to inflamed endothelial cells by ligand-receptor mechanism using VHPK targeted polyplexes.
- *In vivo* determination of miR712 knockdown and TIMP3 gene recovery, in atherosclerosis mice model, using VHPK targeted polyplexes.
- Biodistribution study of VHPK targeted polyplexes after IV administration.

6.2 Materials and Methods

6.2.1 Materials

Reagents and solvents used for polymer synthesis were purchased from Sigma-Aldrich and Panreac. Oligopeptide moieties used on the polymer modification (H-Cys-Arg-Arg-Arg-NH2, H-Cys-Lys-Lys-Lys-NH2, H-Cys-His-His-His-NH2 and H-Cys-Asp-Asp-Asp-NH2) were obtained from GL Biochem (Shanghai) Ltd with a purity of at least 98%. VHPK peptide (VHPKQHRGGSKGC) was obtained from GenScript with a purity of at least 98%.

For *in vitro* studies, labelled anti-miR (Cy3™ Dye-Labeled Anti-miR™ Negative Control #; AM17011) and Anti-miR™ miRNA Inhibitor Negative Control #1 (AM17010) were used for uptake experiments and they were purchased from ThermoFisher. In addition, anti-miR-712 and pre-miR-712 were purchased from Qiagen and used to knockdown or overexpress miR712 expression. Oligofectamine™ Transfection Reagent was purchased from Invitrogen and used according to manufacturer instructions.

For *in vivo* studies, anti-miR 712 was used as a therapeutic gene and anti-miR-SCR was used as scramble control. All, the *in vivo* studies were performed using C57BL/6 mice obtained from Jackson Lab.

6.2.2 Synthesis of oligopeptide-modified C6-50 polymer

As previously reported, C6-50 polymer was synthesized using a stequiometric mixture of 5-amino-1-pentanol and hexylamine with slightly excess of 1.4-butanodiol diacrylate at 1:1.1 molar ratio [23]. Reaction was carried out under magnetic stirring at 90ºC for 24h and the resulting chemical structure was analysed by ^{1}H-NMR and IR. As previously have been determined, C6-50 polymer average molecular weight range between 2000-2500 g/mol (relative to polystyrene standards) by HPLC-SEC.

After that, oligopeptide-modified C6-50 polymer were obtained by end-modification of acrylate-terminated polymer at 1:2.1 molar ratio. Arginine-, lysine-, histidine-, aspartic acid-, and glutamic acid- were used as oligopeptides. The mixture was stirred overnight at room temperature, and the resulting polymer was obtained by precipitation in a mixture of diethyl ether and acetone (7:3). The different oligopeptide modifications were confirmed by ^{1}H-NMR and IR [23].

6.2.3 Synthesis of pHPMA-TT copolymer

pHPMA-TT co-polymer was carried out by free radical polymerization using N-(2-hydroxypropyl)methacrylamide (HPMA) [37] and (Ma-acap-TT) [38] as monomers.

6.2.3.1 HPMA monomer

N-(2-hydroxypropyl)methacrylamide (HPMA) monomer was synthesized by acylation of 1-aminopropan-2-ol with methacryloyl chloride using anhydrous sodium hydrogen carbonate

(NaHCO3). Na HCO3 was used as a base to quench HCl byproduct obtained during the HPMA synthesis. The reaction was stirred in order to ensure that two phases formed by NaHCO3 and organic DCM solvent were vigoroused mixed. The reaction was carried out at -20ºC and the final product was recrystallized from Et2O:MeOH (3:1). Chemical structure analysed by ^{1}H-RMN was in concordance with previously described HPMA structure by Ulbrich et al. [37].

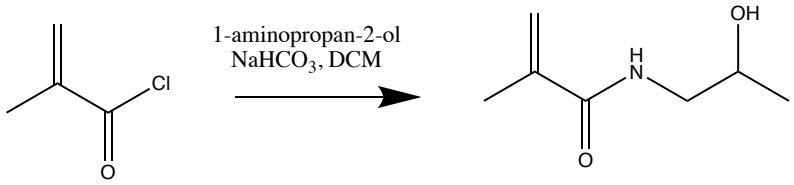

Figure VI-5. Synthesis of HPMA monomer.

^{1}H-NMR (200 MHz, CDCl3, TMS) (ppm): δ = 6.63 (s, 1H, NH), 5.71 (s, 1H, H- 3ii), 5.32 (t, 1H, H-3i), 3.91 (m, 1H, H-6), 3.70 (d, 1H, OH), 3.46 (dq, 1H), 3.13 (m, 1H),1.94 (s, 3H, H-1), 1.16 (d, 3H, H-7)

IR (ATIR) ν = 659, 824, 845, 914, 1001, 1053, 1088, 1117, 1142, 1232, 1263, 1331, 1427, 1553, 1614, 1653, 2933, 2976, 3275, 3306 cm^{-1}

6.2.3.2 Ma-acap-TT monomer

Ma-acap-TT monomer was synthesized in two steps. Firstly, Ma-acap-OH intermediated was obtained by acylation of aminocaproic acid with methacryloyl chloride in aqueous NaOH, in a procedure known as the Schotten-Baumann reaction (highly exothermic reaction). Then, Ma-acap-OH was recrystallized twice using EtOAc:Et_2O. The intermediated Ma-acap-OH chemical composition was confirmed by 1H-RMN and the results were in concordance with with previously described Ma-acap-OH structure by Subr et al. [38].

Once Ma-acap-OH intermediated was synthetized, Ma-acap-TT was obtained by acylation of 2-thiazoline-2-thiol (TT) with the free carboxylic group of Ma-acap-OH using dicyclohexylcarbodiimide (DCC) and a catalytic amount of 4-dimethyl-aminopyridine (DMAP) in THF, as shown Figure VI-6. The reaction was confirmed by the formation of white crystalline precipitate N,N'-dicyclohexylurea salt (DCU). Then, DCU salt was removed by filtration and the final product was recrystallized using Et2O. Chemical structure analysed by ^{1}H-RMN was in concordance with previously described HPMA structure by Subr et al.

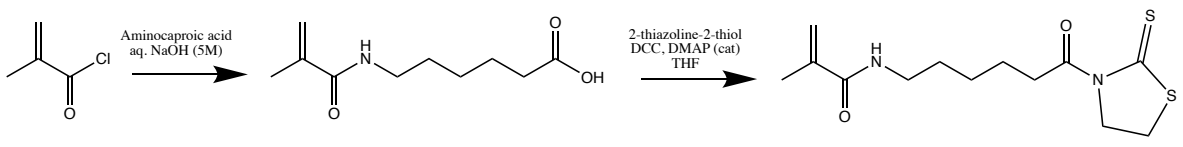

Figure VI-6 Synthesis of Ma-acap-TT monomer.

^{1}H-NMR (200 MHz, CDCl3, TMS) (ppm): δ = 5.86 (s, 1H, NH), 5.67 (s, 1H, H-3ii), 5.31 (t, 1H, H-3i), 4.58 (t, 2H, H-13), 3.29 (m, 6H, H-5, H-9, H-12), 1.97 (s, 3H, H-1), 1.80 – 1.30 (m, 6H, H-6 H-7 H-8)

IR (ATIR) ν = 677, 717, 878, 933, 1005, 1039, 1150, 1232, 1279, 1356, 1387, 1549, 1605, 1651, 1697, 2855, 2930, 3284 cm^{-1}

Once monomers have been synthetized, pHPMA-TT copolymer have been polymerized by Reversible Addition-Fragmentation Chain Transfer (RAFT) reaction [39]. Briefly, HPMA (3.0 g, 20.9 mmol), Ma-acap-TT (0.7 g, 2.3 mmol) and AIBN (0.59 g, 3.6 mmol) were dissolved in dry DMSO (25.3 g, 17.1 mL) and the resulting solution was placed in a reaction vessel. The reaction mixture was purged with Ar, sealed and placed in a water-bath. The polymerization was carried out at 60 ºC for 6h. The copolymer was isolated by precipitation in a mixture of acetone:Et_2O (3:1) and dried under vacuum until constant weight, yielding 2.9 g of a pale yellow solid (polymerization yield of 78%). Chemical structure and molecular weight was determined by ^{1}H-RMN The content of TT groups in the copolymers was determined from the absorption values at λ = 305 nm, resulting a 9 % molar. .

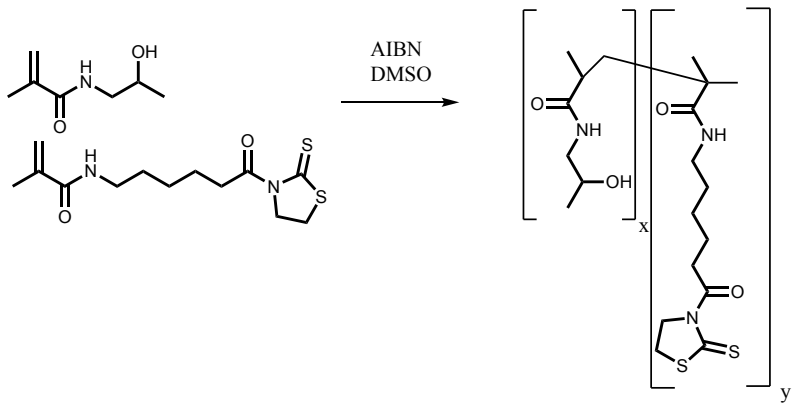

Figure VI-7 Synthesis of hydrophilic co-polymer coating containing amine-reactive groups.

6.2.4 Synthesis of 1-(2-Aminoethyl)maleimide modified pHPM-TT copolymer

(0.25 g, 1.59 mmol) pHPMA-TT co-polymer, (15.57 mg, 0.057 mmol) 1-(2-Aminoethyl)maleimide, and (0,017g, 0.17 mmol) trimethylamine were dissolved in DMSO and the reaction was carried out during 12 hours at room temperature. Polymer was precipitated in acetone:Et_2O (1:1) and dried under vacuum. Maleimide modification was corroborated and characterized by ^{1}H-RMN. The 1-(2-Aminoethyl) maleimide modified TT groups in the polymers was determined from the absorption values at λ = 305 nm.

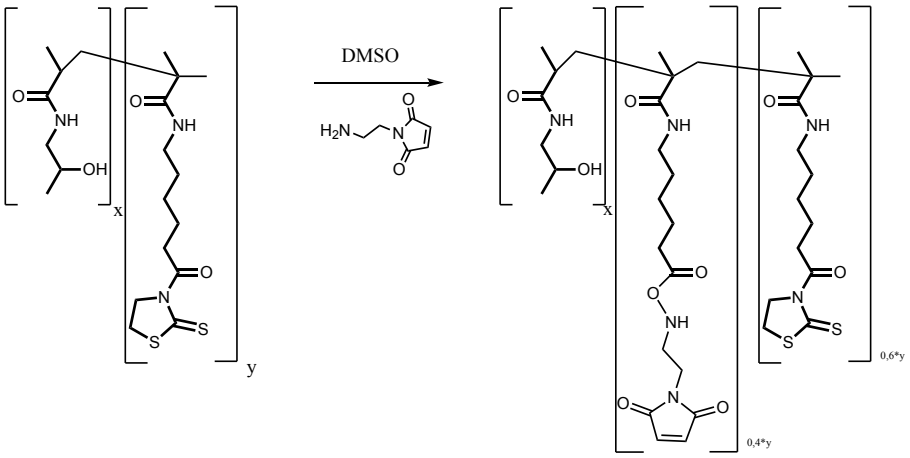

Figure VI-8 Modification of TT-group of pHPMA-TT copolymer using amino-maleimide.

6.2.5 VHPK-targeted nanoparticles formation and biophysical characterization

VHPK targeted polyplex were performed following a three-step procedure. Firstly, C6-50 polyplexes were carried out as previously have been described in the literature [23]. Briefly, polyplexes were formulated mixing equal volume of polymer and nucleic acids in acetate buffer (12.5 mM, pH 5.5) at 100:1 w/w ratio. Polyplexes were mixed by pipetting for a few seconds and incubated at room temperature for 10 min. After that, polyplexes nanoprecipitation were performed adding the polyplexes to PBS 1x at 1:2 ratio. Secondly, hydrophilic-coating was carried out using pHPMA-TT or maleimide-modified pHPMA-TT co-polymers. Where, HPMA-TT polymer was used as a coating and amino-maleimide-modified pHPMA-TT was used also as a linker of polyplexes and VHPK peptide. Then, in both cases maleimide-modified pHPMA-TT or pHPMA-TT co-polymers at 100 mg/mL were added directly to previous polyplexes at final percentage weight of 6,25%. The resulting formulation was mixed by pipetting and incubated at room temperature for 30 minutes. Finally, VHPK peptide was conjugate to maleimide-modified pHPMA coated polyplexes at 1:10 maleimide:VHPK ratio. The resultant formulation was incubated during 30 minutes at room temperature.

Size and surface charge were determined by Zetasizer Nano ZS (Malvern Instruments Ltd, United Kingdom, 4-mW laser). Polyplexes characterization were performed after each nanoparticle formation step.

6.2.6 Oligopeptide formulation screening in endothelial cell line (iMAECs) using C6-50 polymer

Polymer screening of different oligopeptide end-modified pBAEs using labelled anti-miR was carried out in iMAECs. 80000 iMAEC cells were seeded in 12 well plate 24 hours prior uptake screening to obtain a 80% of cell confluency. Briefly, polyplexes formation were performed as previously have been described, using AcONa buffer (12.5 mM, pH 5.0). Then, iMAEC cells were transfected at final labelled anti-miR concentration of 200 nM during 2 h. Transfections were carried out using serum containing medium. After that, polyplexes were washed twice using PBS 1x and cells

were fixed using PFA 1% for flow cytometry analysis. Untreated cells and labelled anti-miR without carrier conditions were used as a negative control and oligofectamine reagent was used as a positive control following the manufacture instructions.

6.2.7 In vitro miR-712 knockdown efficiency using C6-K/H polymer

Mouse TNF-alpha treatment was used to obtain inflamed endothelium model in iMAECs and miR712 expression was regulated by anti-miR 712 delivery using C6-K/H polymer formulation. Briefly, 80.000 cells were seeded 24 hours to anti-miR transfection to obtain an 80% of confluence prior to transfection. Then. iMAECs were pre-treated using mouse TNF-alpha during 2 hours (before anti-miR transfection) in order to overexpress VCAM-1 receptor. Anti-miR-712 was delivered using C6-K/H polymer at different concentrations, ranging from 50 nM to 200 nM. Transfections were carried out with and without serum proteins. 48 hours post-transfection, miR712 and miR15a levels were analyzed by qPCR. Scramble anti-miR were used as a negative control. Statistical significance was determined using scramble control as control group. *p < 0.05, **p < 0.01, ***p < 0.001.

6.2.8 Cellular uptake of labelled anti-miR using VHPK nanoparticles

Cellular uptake was realized using labelled anti-miR-Cy3 in iMAECs. Previously, cells were pre-treated with 3 ng/mL of mouse TNF-α during 2 hours to overexpress VCAM-1 membrane-receptor, obtaining a well-described inflamed cell model.

Nanoparticle formulation was performed in the same manner than previous explain. Different pHPMA co-polymer quantities were combined to C6-K/H polyplex in order to determine the optimal pHPMA proportion, ranging from 3.12 % to 200 %. Similarly, different VHPK peptide:C6-K/H-pHMPA ratios were studied, ranging from 1:1 to 100:1. Polyplexes formation were carried out as previously have been explained and incubated during 2 hours in iMAECs. After 2 h, the remaining complexes were removed and cells were trypsinized with 100ul of trypsin and fixed with 200 µL of paraformaldehyde (PFA) at 1% and 200 µL of completed medium for flow cytometry analysis. Oligofectamine was used as a positive transfection control and anti-miR-SCR was used as negative control. Statistical significance was determined using scramble control as control group. *p < 0.05, **p < 0.01, ***p < 0.001.

6.2.9 In vitro miRNA Knockdown using VHPK nanoparticles

In vitro therapeutic anti-miR study was developed using TNF-alpha treated iMAEC cells. VHPK peptide dependent delivery was determined using VHPK- targeted or non-targeted nanoparticles at gene level. For this study, C6-K/H, C6-K/H-pHPAM, and C6-K/H-pHPAM-VHPK nanoparticles were used to deliver anti-miR-712. miR712 and their target gene (TIMP3) expression were determined at 48 hours post transfection at gene level by qPCR. Anti-miR-SCR was used as scramble control. Statistical significance was determined using scramble control as control group. *p < 0.05, **p < 0.01, ***p < 0.001.

6.2.10 In vivo animal experiments using atherosclerosis mouse model

More than five-week-old female C57BL/6 mice were used for each condition. All procedures used in animal studies were conducted at Emory University and they were approved by the Institutional Animal Care and Use Committee (IACUC).

Mouse Partial Carotid Ligation (PCL) Surgery technique was used to obtain a well-described *in vivo* atherosclerosis model. PCL is a model of acutely induced disturbed flow, leading to rapid endothelial dysfunction and atherosclerosis [12]. Briefly, anaesthesia was induced by intraperitoneal injection to C57BL/6 mice. Then, surgery area was disinfected. LCA was exposed by blunt dissection. Three of four caudal branches of LCA (left external carotid, internal carotid, and occipital artery) were ligated, as shown Figure VI-9. The incision was then closed. Finally, mice were monitored until recovery in a chamber[12].

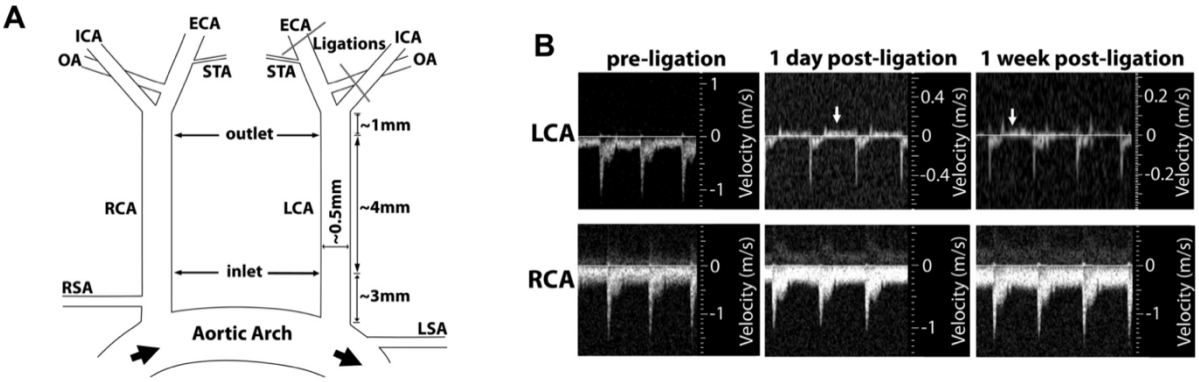

Figure VI-9. Partial ligation of left common carotid artery (LCA) reduce and induce oscillatory blood flow. A) Three of the four branches were ligated, while leaving the superior thyroid artery open. B) Ultrasound technique was used to determine flow velocity profiles, revealing that partial ligation induces flow reversal in LCA during diastole. (Adapted from Nam et. al.)[12]

Once PCL was conducted to induce disturbed flow in LCA, flow velocity and direction of LCA and RCA were determined by high resolution ultrasonography. Results showed in Figure VI-9 demonstrated that blood flow velocity during systole is decreased. In addition, reverse blood flow was observed during diastole in LCA, However, flow in the right common carotid artery (RCA) remains unchanged after ligation. These results are in concordance with previously described PCL model by Nam et. al.[12].

6.2.11 Preparation of nanoparticles solution for in vivo IV injection

Anti-miR polyplexes were performed following a three-step procedure previously explained. In order to administrate 1 mg/kg of anti-miR by tail vein injection, 100 µL of anti-miR at 0,5 µg/µL were mixed with 100 µL of C6-K/H polymer at 25 µg/µL in AcONa buffer solution (12,5mM, pH 5.5). After 10 min of incubation at room temperature, 200 µL of nanoparticles were precipitated in 2 mL of HEPES at 10mM with 5,4 mg/mL of sucrose.

Finally, nanoparticles were lyophilized overnight. Prior to systemic administration, lyophilized nanoparticles were resuspended with 120ul of RNA/DNA free water in order to be injected by tail vein injection according to the IACUC protocol.

6.2.12 Isolation of endothelial enriched RNA from carotids

As previously have been described [12], 48 hours post-injection endothelial enriched RNA from the carotids was extracted. Briefly, mice were killed by CO2 inhalation according to Emory University's IACUC protocol and perfused with saline containing heparin (10 U/mL). Left common carotid artery (LCA) and the right common carotid artery (RCA) were rapidly isolated and cleaned. Immediately, the carotid lumen was quickly flushed with 150 µL of QIAzol lysis reagent. The eluate was snap-frozen in liquid nitrogen for posterior RNA extraction. Moreover, media and adventitia was snap-frozen in liquid nitrogen, pulverized by mortar and pestle, and lysed with QIAzol lysis reagent (300 µL).

6.2.13 Anti-miR-712 biodistribution study

48 hours post-injection mice were killed by CO2 inhalation according to Emory University's IACUC protocol and perfused with saline solution. Immediately, organs were collected and snap-frozen in liquid nitrogen. Prior to RNA extraction, the organs were crashed and lysed with QUIzol for subsequent RNA extraction. miR712, miR15, TIMP3, PECAM-1, and CD45 genes expression were analyzed in lung, liver, spleen, thymus, heard, and kidney.

6.2.14 RNA isolation and qPCR analysis

Total RNA was extracted and purified using Direct-zol™ RNA Kits according to the manufacturer's instructions. Briefly, RNA with QiaZol was mixed with equal volume of ethanol and the mixture was loaded to a column of silica filters. The RNA binds selectively to the silica matrix and can be washed before eluting in RNase-free water. Before eluting the RNA, DNase digestion was performed during 15 minutes at room temperature, and then filter was washed three times before to eluted desired RNA. RNA quantity was determined by NanoDrop 1000 Spectrophotometer following the manufacturer's instructions. After that, 10 µL of total RNA obtained from carotids or 500 ng of RNA from different organs were reverse-transcribed using High-Capacity cDNA Reverse Transcription Kit (Applied Biosystems) following the manufacturer's instructions. Finally, qPCR using SYBR was performed to determine mRNA expression of TIMP3 gene from different organs. In addition, TIMP3, PECAM-1, SM22-alpha, and CD45 were analysed from carotids. Analysis study of the genes of interest were normalized against the 18S housekeeping gene. All analyses were performed using the 2-ΔΔCT method and 3 technical replicates.

Moreover, 10 µL of total RNA obtained from carotids or 500 ng of RNA from different organs were reverse-transcribed using miScript II RT Kit following the manufacturer's instructions. Finally, qPCR using SYBR was performed to determine miR712 and miR15a from different organs and carotids. As previously, fold change between LCA and RCA were determined. U6 miRNA was used as a

housekeeping gene and the specific miRNA primers were purchased from Qiagen. All analyses were performed using the 2-ΔΔCT method and 3 technical replicates.

Table VI-1 Primers sequences used for qPCR analysis.

Primer	Forward Sequence	Reverse Sequence
18S	5'-AGGAATTGACGGAAGGGCACCA-3'	5'-GTGCAGCCCCGGACATCTAAG-3'
mPECAM1	5'-GCTGGTGCTCTATGCAAGC-3'	5'-ATGGATGCTGTTGATGGTGA-3'
mSM22a	5'-CCTTCCAGTCCACAAACGAC-3'	5'-GTAGGATGGACCCTTGTTGG-3'
mCD45	5'-CTTCAGTGGTCCCATTGTGGTG-3'	5'-TCAGACACCTCTGTCGCCTTAG-3'
mTIMP3	5'-TCCCACCTCTCCACAAAGTT-3'	5'-CACGGAAGCCTCTGAAAGTC-3''
mVCAM1	5'-ACTTGTGCAGCCACCTGAGATC-3'	5'-GCTATGAGGATGGAAGACTCTGG-3'
mTNF-alpha	5'-CGAATTTTGAGAAGATGATCCTG-3'	5'-TGCTGGGAAGCCTAAAAG-3'

6.2.15 TIMP3 immunochemistry

48 hours post anti-miR-712 administration, mice were euthanized using CO2 inhalation according to Emory University's IACUC protocol and perfused with saline containing heparin. Not deeper perfusion was carried out in order to obtain a completely lung perfusion. After that, lungs were collected, washed twice in PBS 1x, and fixed using PFA 4% during more than 4 hours. Then, tissue was embedded in optimal cutting temperature (OCT) compound and was quick frozen in liquid nitrogen. Finally, resultant sample was stored at -80 ºC until immunochemistry analysis.

Histology of OCT lung samples were performed using a thickness of 10 µm for TIMP3 immunochemistry. Then, sections were washed using PBS 1x for 10 min, permeabilization buffer (0.25 % TritonX in PBS) was added during 20 min, samples were washed with PBS 1X, and 10% Donkey Serum in PBS 1X was added during 45 – 60 min. Immunohistochemical staining was carried out using anti-TIMP3 antibody (ab39185) at 1:100 dilution in Donkey Serum in PBS 1X overnight at 4 ºC. After that, primary antibody was removed, samples were washed twice with PBS 1X, and goat anti-rabbit secondary antibody (sc-2004 from Santa Cruz) was added and incubated during 2-3 hours at 4ºC. Finally, secondary antibody was removed, washed twice with PBS 1x, and samples were imaged using a Zeiss LSM 510 META confocal microscope (Carl Zeiss).

6.2.16 Western blot

Western blotting was carried out over lung protein. Briefly, after lung completely perfusion, it was collected and incubated with RIPA buffer. Tissue was disrupted using TissueLyser LT from Qiagen. Then, samples were centrifuged during 10 min at 10000 rpm at 4ºC and the supernatant was collected and used for posterior western blotting analysis.

Cell lysates (20 µg of protein) were loaded in 10% SDS-PAGE for protein separation. Then, proteins were transferred to a polyvinylidene difluoride membrane (Millipore) and probed using primary antibody following the standard western blotting method. TIMP3 (ab39185) and β-actin

(A5316; Sigma-Aldrich) were used as primary antibodies and there were diluted at 1:1.000 using TBST 1X with 5 % of milk. Goat anti-rabbit antibody (sc-2004 from Santa Cruz) were used as secondary antibodies, and the membrane was developed using chemiluminescence detection. The intensities of the immunoreactive bands in the Western blots were quantified using the NIH IMAGE program.

6.2.17 Statistical analysis

Statistical analyses were carried out with Graph-Pad Prism (GraphPad Software). All error bars reported are SD unless otherwise indicated. Pairwise comparisons were performed using one-way Student t-tests. Differences between groups were considered significant at P values below 0.05 (* $p < 0.05$, ** $p < 0.01$, *** $p < 0.001$)

6.3 Results and discussion

Nanoparticle engineering to efficiently deliver RNAi-drugs to specific tissues is currently an emerging research area, which may overcome off-target limitations that have typically hampered clinical translation. In this chapter, we developed a new methodology that can be used for a wide range of therapeutic applications. We demonstrated that combining the proprieties of our previously described pBAEs (C6-50 family) [23] with a well described targeting peptide, it is possible to preferentially drive therapeutic RNAi-drugs to specific cell lines or tissues. In this project, C6-50 polymer combined with VHPK targeting peptide were used to efficiently deliver therapeutic anti-miRNA to inflamed endothelial cells, designing an efficient atherosclerosis treatment.

To reach this aim C6-50 synthesis was carried out as previously reported in chapter III [24]. After that, C6-50 polymer was end-capped using our previously described oligopeptides moieties, obtaining a combination of artificial-natural carrier. As previously described, cell-efficient vectors may be modulated by tuning their oligopeptide composition. Therefore, prior to target our polyplexes, their oligopeptide composition was selected in order to design efficient polyplexes in terms of RNAi unpackaging and endosomal scape once their reach the target cells. Then, in order to determine this specific oligopeptide composition, polymer uptake screening using labelled anti-miRNA (anti-miR-Cy3) was conducted in inflamed mouse endothelial cells (iMAECs), as shown in Figure VI-10.

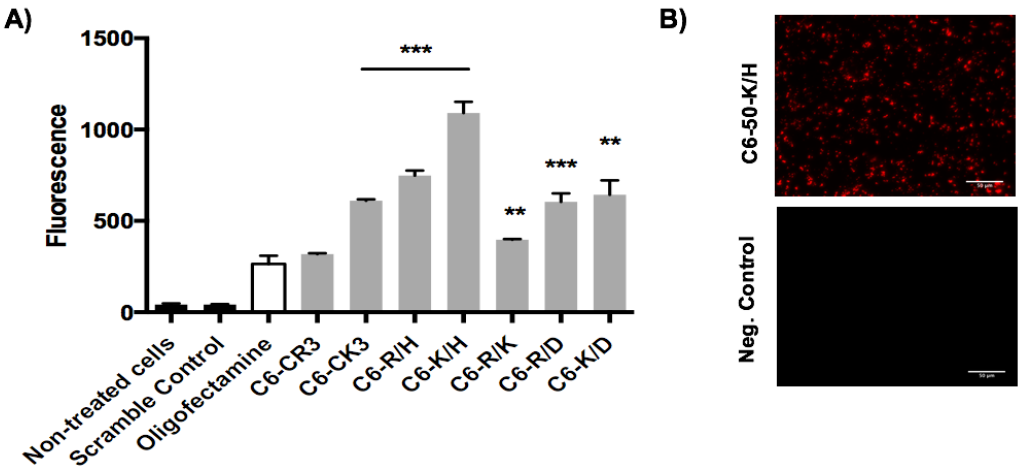

Figure VI-10 Cellular uptake of fluorescently-labeled particles prepared from AF555-labeled anti-miR in iMAECs. iMAECs were transfected with anti-miR-AF555 at final concentration of 200nM using different oligopeptide-modified poly(β-amino ester)s in order to select the top performing polymer formulation. Transfection was performed with complete medium. Fluorescence expression was determined 2 hours post-transfection by flow cytometry. Statistical significance was determined using positive control (oligofectamine) as control group. *p < 0.05, **p < 0.01, ***p < 0.001.

Oligopeptide-modified polyplexes showed notable cellular uptake compared with Oligofectamine, indicating that newly designed pBAE presented higher cell-entrance capacity than commercial reagents. Lysine- / histidine- oligopeptide moiety at 1:1 ratio presented the highest cellular uptake in iMAECs, obtaining a 4-fold increase compared to commercial reagent (Figure VI-10). This data is in

concordance with previously polyplex screening using endothelial cell line, where siRNA was used as a nucleic acid (Chapter V) [24]. Therefore, these results suggest that lysine-/histidine- polyplexes exhibit an excellent cell-entrance and endosomal-scape when their reach inflamed endothelial cells.

6.3.1 Formulation and biophysical characterization of VHPK targeted polyplexes

Once lysine-/histidine- mixture was selected as top-performing oligopeptide composition, polyplexes were targeted using VHPK peptide in order to achieved a preferential delivery to inflamed endothelial cells, avoiding healthy ECs targeting. To reach this goal, polyplexes were fine-formulated in a three-step procedure and characterized by dynamic light scattering (DLS). Briefly, C6-50-K/H polyplexes were carried out mixing equal volume of polymer and anti-miRNA in acetate buffer, incubated 30 min at 25ºC, and nanoprecipitated in PBS, as previously explained in materials and methods section. In general, oligopeptide-modified C6-50 polymers present a discrete nanometric size, ranging from 60 to 250 nm, with a positive surface charge (Chapter III). For example, C6-50-K/H polyplexes present average size around 100 nm with a positive surface charge, 19.4 ± 1.0, when anti-miRNA was used as nucleic acids (Figure VI-11).

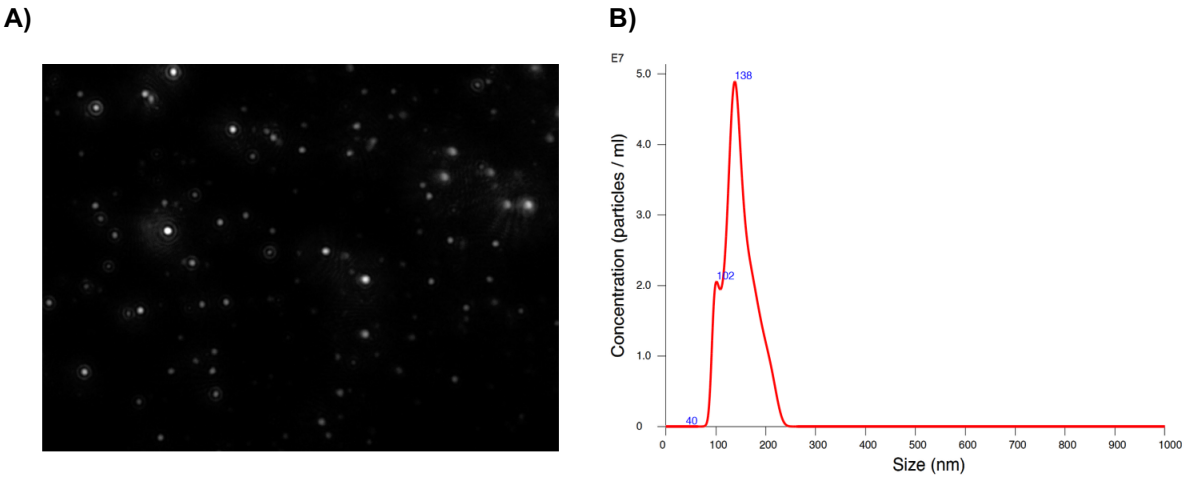

Figure VI-11. Biophysical characterization of anti-miRNA nanoparticles by Nanoparticle Tracking Analysis (NTA). A) Nanoparticle image using NTA. B) Nanoparticle concentration vs size distribution of C6-K/H-anti-miR polyplexes using NTA.

Once anti-miRNA was condensed using C6-50-K/H polyplexes, these were coated using hydrophilic polymer (pHPMA-TT), which was further used as a linker between C6-50-K/H polyplexes and VHPK peptide, as is showed in Figure VI-12.

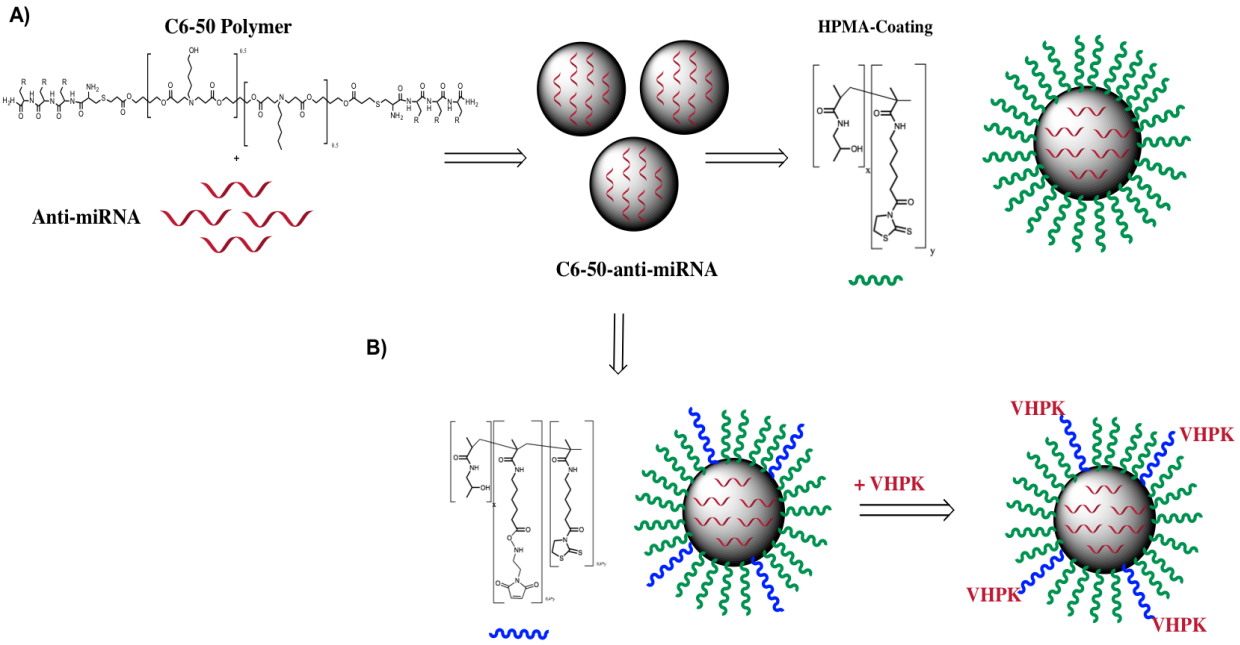

Figure VI-12: Preparation of targeted poly(b-amino ester) polymers. A)C6-50-K/H polyplexes were coated using a hydrophilic coating, pHPMA-TT. TT group from pHPMA-TT copolymer is able to react with amine group from polyplexes. B) C6-50-K/H polyplexes were coated using amino-maleimide modified pHPM-TT copolymer. TT group from amino-maleimide modified pHPMA-TT copolymer are able to react with amine group from polyplexes. Then, maleimide groups from amino-maleimide modified pHPMA-TT copolymer are able to react with thiol group from VHPK peptide.

pHPMA-TT polymers present 2-thiazoline-2-thiol group (TT group) able to react with amine group from polyplexes, coating their surface (Figure VI-12-A). However, when targeting peptide was added, 40% of TT groups from pHPMA-TT were further modified using 1-(2-Aminoethyl) maleimide, which was used as a linker of anti-miRNA-polyplexes with targeting peptides. Then, peptides containing cysteine amino acid can be linked to the surface of pHPMA-TT coated polyplexes via maleimide-thiol coupling reaction and the rest of TT groups (60 %) were used to react with amine group from polyplexes (previously explained in materials and methods). For polyplex –VHPK peptide reaction, slight excess of peptide was added to polyplexes solution in order to ensure a fully modification of maleimide reactive groups (Figure VI-12-B).

Polyplex pHPMA-TT coating and VHPK targeting were corroborated using DLS, as is shown in Table VI-2.

Table VI-2. Characterization of targeted poly(b-amino ester) polymers. Hydrodynamic size and zeta-potential of coated and non-coated C6-50-K/H polyplexes and targeted and non-targeted coated C6-50-K/H were determined by Dynamic Light Scattering. Results are shown as mean and standard deviation of triplicates

Polymer Formulation	Size (nm)	Z-Potential (mV)	PDI
C6-50-K/H	91.4 ± 1.3	19.4 ± 1.0	0.286 ± 0.013
C6-50-K/H-pHPMA-TT	93.4 ± 3.8	6.0 ± 1.0	0.392 ± 0.018
C6-50-K/H-pHPMA-TT-VHPK	92.8 ± 8.6	8.1 ± 0.9	0.342 ± 0.007

Results showed that neutral average charge from pHPAM-TT polymer is able to decrease the positive surface charge of our polyplexes formulations from 19.4 mV to 6.0 mV, corroborating a successful polyplex coating. However, when VHPK peptide is added to coated C6-50-K/H polyplexes, surface charge of the resultant formulation is slightly increase from 6.0 mV to 8.1 mV. In contrast, polyplexes hydrodynamic size remain stable when pHPMA-TT coating or VHPK peptide were added, confirming the integrity of our polyplexes.

6.3.2 VCAM-1 depended in vitro delivery using VHPK targeted nanoparticles

Once VHPK targeted pBAE have been formulated and characterized, polyplexes were used to deliver RNAi-based drugs to turbulent blood flow areas, where endothelial cells are inflamed. Before to test our polymer formulations to *in vivo* mouse model, *in vitro* studies using immortalized mouse aorta endothelial cells (iMAECs) were carried out. Then, to overexpress endothelial inflammatory markers, such as VCAM-1, iMAECs were pre-treated using TNF-alpha at 3 ng/μL during 2 hours, as previously has explained in materials and methods and Figure VI-13 shown.

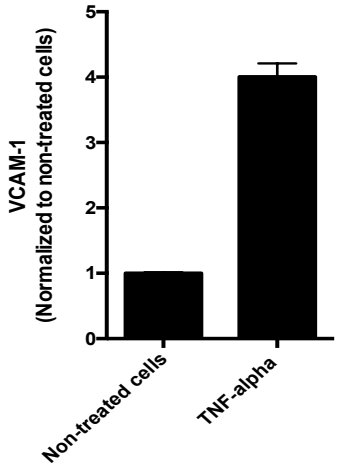

Figure VI-13. VCAM-1 expression of TNF-alpha treated iMAECs. Cells were pretreated with 3 ng/mL of mouse TNF-alpha during 2 hours and VCAM-1 expression was analyzed by qPCR at 48 hours post-treatment.

After TNF-alpha treatment, VCAM-1 inflammatory marker expression was increased in iMAECs. Results showed 4-fold increase of VCAM-1 marker compered to non-treated cells, corroborating that TNF-alpha is a well-known inducer of different inflammatory markers (Figure VI-13).

Once VCAM-1 was induced, polyplexes were tested for their ability to specifically deliver anti-miRNA to inflamed endothelial cells. Then, polyplexes condensing labelled anti-miRNA were used to study their VHPK receptor-mediated specificity in *in vitro* assays using inflamed iMAECs. Uptake experiment was carried out testing the behaviour of polyplexes with or without hydrophilic coating (pHPMA-TT) and polyplexes with or without VHPK targeting peptides, as is shown in Figure VI-14.

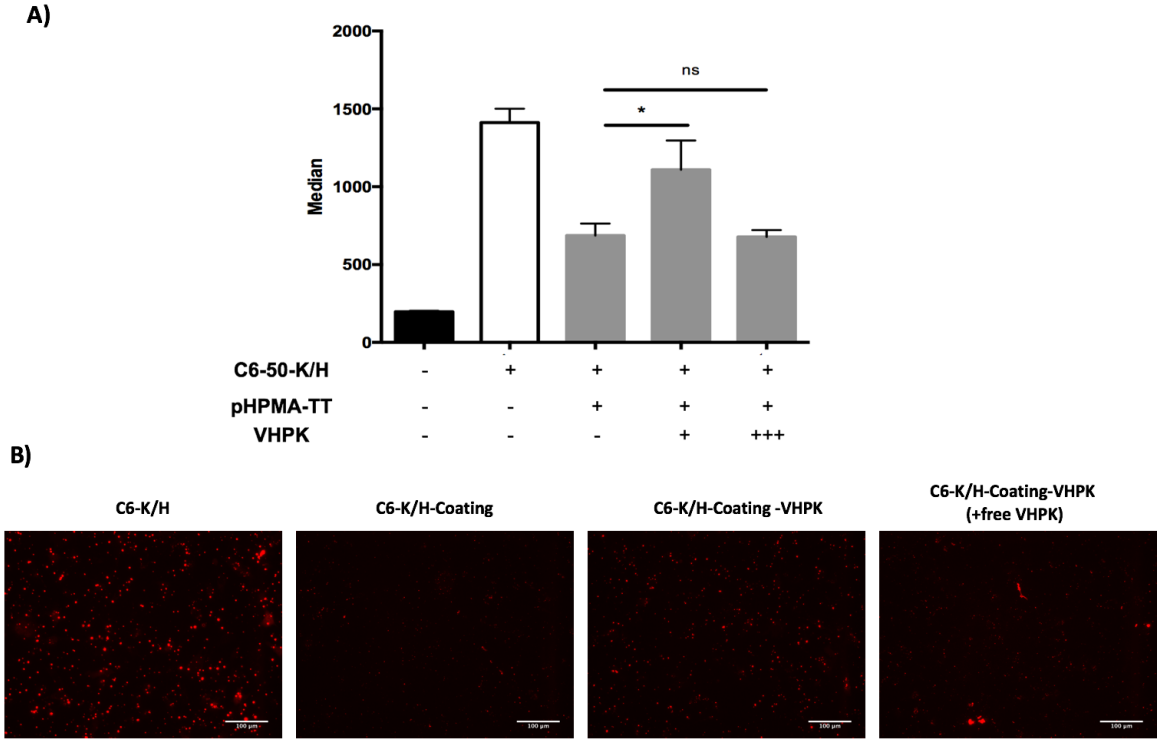

Figure VI-14 VHPK dependent delivery using Cy3-anti-miRNA in TNF-alpha treated iMAECs. A) Uptake delivery assay was performed using labelled anti-miR at 200nM and the results were analysed at 2h post transfection using flow cytometry. (-) mean absence of polymer, coating or VHPK peptide. (+) mean presence of polymer, coating or VHPK peptide. (+++) mean a high excess of VHPK peptide (competing peptide). Statistical significance was determined comparing coated nanoparticle as control group. *p < 0.05, **p < 0.01, ***p < 0.001. B) Confocal microscopy images were carried out over previous uptake experiment.

Results showed that anti-miRNA alone is able to cross cell membrane, however in order to obtain a therapeutic effect high anti-miRNA doses are needed. Then, VHPK-dependent delivery assay was performed using C6-50-K/H polymer. Results demonstrated that non-coated nanoparticles (anti-miRNA-C6-50-K/H polyplexes) present the highest uptake efficiency over iMAECs due to their ability to enter by endocytosis. Lysine- / histidine- formulations were previously designed to efficiently transfect endothelial cells, showing a promising cellular entrance and endosomal scape. As expected, when pHPMA-TT coating was added, polyplexes uptake decreased. However, when VHPK peptide

was added to pHPMA-TT coated polyplexes a significant uptake increase was observed, reaching a similar uptake values obtained by non-coated polyplexes. Then, these results seem to suggest that VHPK targeted polyplexes are able to enter by receptor-mediated endocytosis. Furthermore, to corroborate this hypothesis, a receptor-peptide competitive assay was carried out using an excess of VHPK peptide, incubating iMAECs with VHPK targeted nanoparticles and high excess of free VHPK. Results demonstrated a decrease of uptake efficiency due to in this case the entrance competition is between VHPK linked to nanoparticles and free VHPK in the medium.

6.3.3 Anti-miR-712 delivery using VHPK nanoparticles to inflamed endothelial cells

Once receptor-mediated endocytosis delivery of VHPK-coated-nanoparticles using labelled anti-miRNA was observed, targeted polyplexes were used to deliver therapeutic anti-miRNA, such as anti-miR-712.

Firstly, anti-miR-712 dose curve was carried out, ranging from 50 nM to 200 nM, in order to optimize anti-miR712 concentration in *in vitro* assays. Screening was performed using non-coated and non-targeted polyplexes (C6-50-K/H polymer) in TNF-alpha pre-treated iMAECs. 48 hours post-transfection, functional miR712 and control miR15a were analysed at gene level by qPCR (Figure VI-15).

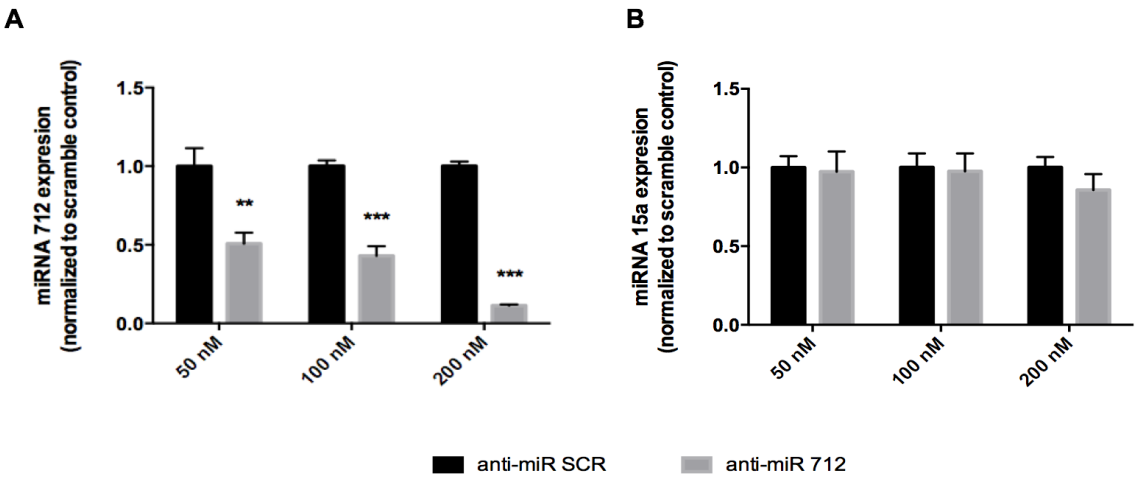

Figure VI-15. iMAECs were transfected with therapeutic anti-miR712 at different concentrations, ranging from 50nM to 200nM. A) miR712 expression was determined at 48 hours post-transfection by qPCR. B) miR712 expression was determined at 48 hours post-transfection by qPCR. Statistical significance was determined using scramble control as control group. *p < 0.05, **p < 0.01, ***p < 0.001.

A well-defined dose curve response was observed when anti-miR-712 concentration was increased, reaching a 90 % of miR712 knockdown efficiency working at 200 nM. In addition, non-significant miR15a (control miRNA) knockdown effect was observed when anti-miR712 was delivered at different anti-miR712 concentrations, confirming the anti-miR712 specificity. Therefore, in order to obtain an efficient therapeutic response, anti-miR712 final concentration of 200 nM was selected.

After that, VHPK-depended delivery was analysed using anti-miR712 as nucleic acid. miR712 and TIMP3 levels were determined in iMAECs after anti-miR712 delivery using targeted and non-targeted-polyplexes. In addition, non-coated polyplexes (C6-50-K/H polymer) was used as a positive control of transfection and scramble anti-miRNA delivered using VHPK targeted polyplexes was used as a negative control of silencing. miR712 and TIMP3 expression was analysed at 48 hours post-transfection by qPCR, as Figure VI-16-A-B shown.

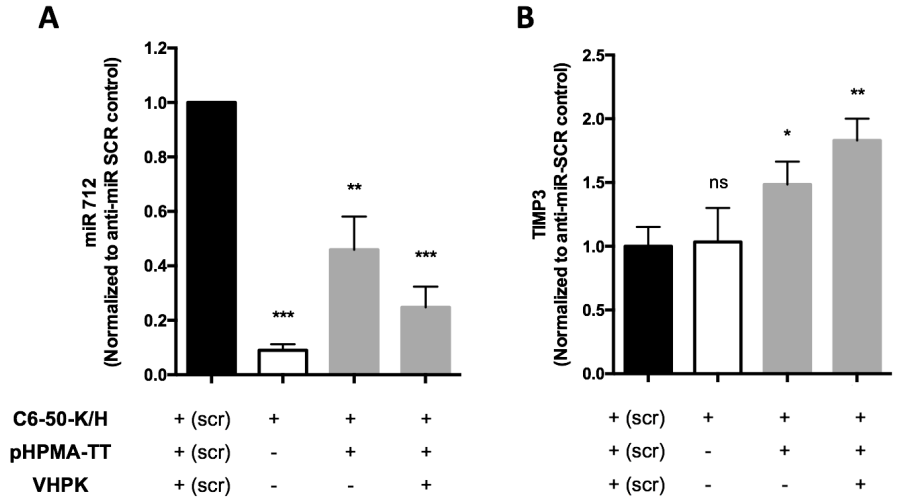

Figure VI-16. VHPK dependent delivery using therapeutic anti-miR712 as a nucleic acid. A) miR712 levels were determined after 48 hours of anti-miR712 delivery using C6-50-K/H polymer (white bar) and coated C6-50-K/H with or without VHPK (gray bar). Anti-miR-SCR was delivered using VHPK targeted polymer and used as a negative control (black bar). Statistical significance was determined using scramble control as control group. *p < 0.05, **p < 0.01, ***p < 0.001. B) TIMP3 levels were determined after 48 hours of anti-miR712 delivery using C6-50-K/H polymer (white bar) and coated C6-50-K/H with or without VHPK (gray bar). Anti-miR-SCR was delivered using VHPK targeted polymer and used as a negative control (black bar). Statistical significance was determined using scramble control as control group. *p < 0.05, **p < 0.01, ***p < 0.001.

Results from Figure VI-16-A further demonstrated receptor-mediated delivery using VHPK targeted polyplexes using anti-miR-712 as a therapeutic RNAi. C6-50-K/H polymers present high transfection efficiency due to their superficial oligopeptide composition, confirming previous uptake results (Figure VI-14). In contrast, when pHPMA-TT coating was added, polyplexes presented lower silencing efficiency than non-coated ones. However, when VHPK peptide was linked to pHPMA-TT coated polyplexes an increase of miR-712 knockdown was observed compared to non-targeted polyplexes. Then, we can confirm that targeted polyplexes enter by receptor-mediated endocytosis, avoiding unspecific cellular entrance that could compromise cell behavior.

Once a significant reduction of miR712 levels was observed, TIMP3 gene expression was further analysed. As is expected, the basal level of TIMP3 gene was rescued when anti-miR-712 was delivered using VHPK targeted polyplexes, reaching at 2-fold increase compared to scramble control (Figure VI-16-B). In addition, a significant 1.5-fold increase was observed when anti-miR-712 was

delivered without VHPK, confirming that the small quantity of anti-miR-712 that enter by non-receptor mediated endocytosis have a therapeutic effect over iMAECs. However, no correlation was observed when anti-miR-712 was delivered using non-coated polyplexes (C6-50-K/H polymer), where TIMP3 upregulation was not observed. These results are in concordance with previously reported data, where it was observed that high transfections efficiencies could compromise cells viabilities. Then, even through efficient miR712 knockdown was achieved, TIMP3 expression was not increased due to they play a key role in different cell inflammation pathways [40]. Then, these results confirm that the combination of therapeutic anti-miR-712 drug with well-designed VHPK targeted polyplexes is essential to obtain a powerful *in vitro* and *in vivo* arthrosclerosis treatment.

6.3.4 VHPK-CCL-anti-miR-712 delivery to inflamed endothelium in d-flow regions in in vivo atherosclerotic mice model

Once VCAM1-dependent delivery of anti-miR-712 was confirmed in *in vitro* model, the next step was to use VHPK-targeted-polyplexes to deliver anti-miR-712 to atherosclerosis *in vivo* model. Firstly, VCAM-1 inflammatory marker was overexpressed in left carotid from C57BL/6 mice by Partial Carotid Ligation (PCL), as previously explained in materials and methods. PCL surgery induce disturbed flow (d-flow) in the left carotid artery (LCA), while in the right carotid artery stable flow (s-flow) is present. In addition, VCAM-1 inflammatory marker is significantly expressed in *d-flow* naturally curved arteries. For example, the typical naturally pro-artherogenic zone is located in the aortic arch region, where VCAM-1 marker is significantly overexpressed in the lesser curvature (LC) region compared to greater curvature (GC) region[41].

Briefly, PCL was conducted in 5-week-old 18 C57BL/6 mice following the IACUC protocol. 72 hours post-surgery, therapeutic anti-miR-712 was administrated by IV injection using pBAEs as carrier at 1 mg/kg. Therapeutic anti-miR-712 was delivered using VHPK targeted and non-targeted polyplexes in order to determine their ligand-receptor specificity at *in vivo* level. Moreover, anti-miR-SCR was delivered using VHPK targeted polyplexes and used as a negative control. 48 hours post-administration, miR712 levels and TIMP3 gene expression were determined in LCA and RCA by qPCR, as shown in Figure VI-17.

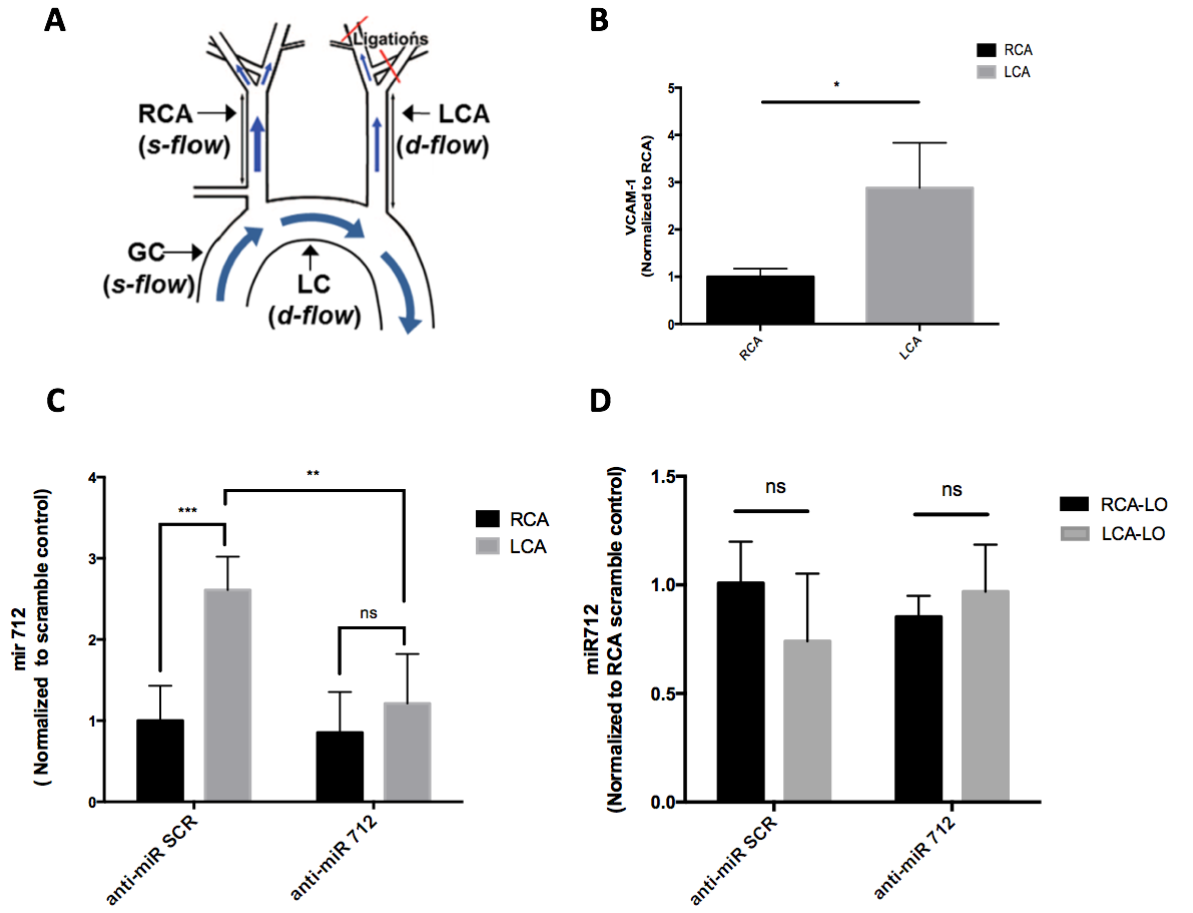

Figure VI-17. Selective and efficient anti-miR-712 delivery using VHPK targeted polyplexes to inflamed endothelium in d-flow regions of mice. At 3 days following partial carotid ligation, C56BL/6 mice were tail-vein injected with VHPK targeted polyplexes using anti-miR-712 (therapeutic RNAi) and anti-miR-SCR (control RNA) at 1 mg/kg. 48 hours post-injection mice were sacrificed and endothelial enriched RNA and was extracted from the RCA and LCA. Expression of miR-712 and its target gene TIMP3 were determined by qPCR in endothelial and smooth muscle cells enriched samples. A) PCL model. B) VCAM-1 expression in PCL model mouse. Statistical significance was determined using RCA as control group. *p < 0.05, **p < 0.01, ***p < 0.001. C) miR712 expression was analysed in endothelial enriched samples from RCA and LCA at 48 hours post-injection in PCL mice model. Statistical significance was determined using anti-miR-SCR/RCA or anti-miR-SCR/LCA samples as control group. *p < 0.05, **p < 0.01, ***p < 0.001. D) miR712 expression was analysed in smooth muscle cells enriched samples from RCA and LCA at 48 hours post-injection in PCL mice model. Statistical significance was determined using RCA as control group. *p < 0.05, **p < 0.01, ***p < 0.001.

First of all, VCAM-1 gene level was analysed at 48 hours post-ligation, obtaining a 3-fold increase in LCA compared to RCA (Figure VI-17-B). Results are in concordance with previously described data, where VCAM-1 expression was analysed at gene and protein level [31], [42], [43].

Once anti-miRNA was systemic administrated, miR712 levels were determined at 48 hours post-injection in endothelial and smooth muscle cell enriched RNA samples from RCA and LCA. Based on gene level analysis, a 2.5-fold increase of miR712 expression was observed in the LCA compared to RCA enriched-endothelium when control anti-mir-SCR was injected (Figure VI-17-C). In contrast, a

non-significant increase of miR712 was observed in the leftover samples (SMC) from RCA and LCA (Figure VI-17-D). However, when anti-miR-712 was delivered using VHPK targeted polyplexes, a significant decrease of miR712 levels was observed in LCA endothelial-enriched samples compared to anti-miR-SCR injected mice, obtaining a similar miR712 expression levels than s-flow regions (RCA) (Figure VI-17-C). As previously noticed, non-significant reduction of miR712 level was observed between the leftover samples. Thus, these results could suggest that novel VHPK polyplexes are able to deliver anti-miR712 in a receptor-specific manner without affecting gene expression of others cells lines, such as smooth muscle cells.

After that, TIMP3 gene levels was further studied in endothelial enriched and leftover samples, as is showed in Figure VI-18.

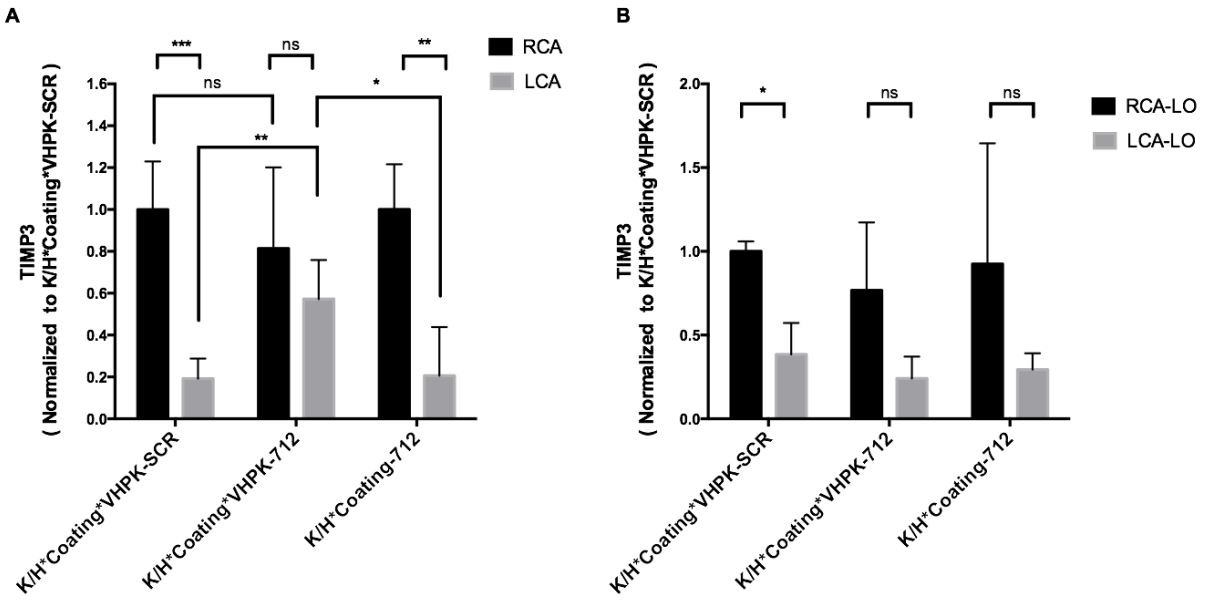

Figure VI-18. Selective and efficient anti-miR-712 delivery using VHPK targeted polyplexes to inflamed endothelium in d-flow regions of mice. A) TIMP3 expression was analysed in endothelial enriched samples from RCA and LCA at 48 hours post-injection in PCL mice model. Statistical significance was determined using different conditions as control group. *p < 0.05, **p < 0.01, ***p < 0.001. B) TIMP3 expression was analysed in smooth muscle cells enriched samples from RCA and LCA at 48 hours post-injection in PCL mice model. Statistical significance was determined using RCA as control group. *p < 0.05, **p < 0.01, ***p < 0.001.

In order to recover TIMP-3 expression in *d-flow* regions, anti-miR-712 was delivered using VHPK targeted nanoparticles. In addition, VCAM-1 targeting was corroborated comparing anti-miR-712 delivery using targeted or non-targeted polyplexes. As is expected, TIMP-3 expression was significantly reduced in LCA compared to RCA after PCL treatment when control anti-miR was injected, confirming the atherosclerosis *in vivo* model (Figure VI-18-A). In contrast, when anti-miR-712 was delivered using VHPK targeted nanoparticles a 2-fold TIMP3 expression increase was observed compared to control anti-miRNA in LCA. Furthermore, results demonstrated that only the polymer

formulation targeted with VHPK peptide is able to recover TIMP-3 expression. In addition, similar TIMP3 levels were observed using anti-miR712 or anti-miR-SCR in RCA (Figure VI-18-A). Finally, TIMP-3 was not increased in LCA leftover samples compared to RCA using our promising VHPK targeted polyplexes. These results confirm that newly developed polyplexes present a preferential affinity to endothelial cells over other cells lines (Figure VI-18-B).

To further corroborate these results, quality controls of endothelial elution using cell-type markers were performed. Endothelial marker (PECAM-1), smooth muscle cells marker (SM22a) and immune marker (CD45) were determined (Figure VI-19).

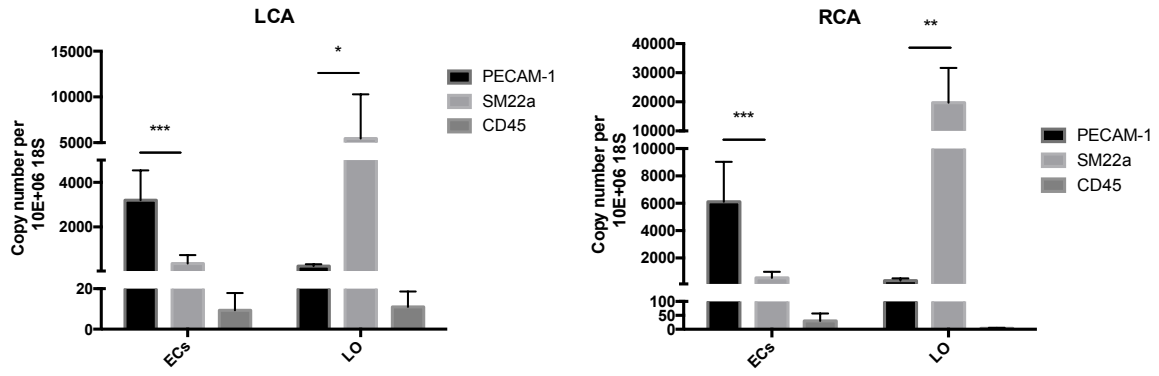

Figure VI-19. Quality criteria of endothelial enriched layer was determined analysing PECAM-1 as a endothelial marker, SM22a as a smooth muscle cell marker and CD45 as immune marker. Statistical significance was performed between PCAM-1 and SM22a markers. *p < 0.05, **p < 0.01, ***p < 0.001.

High PECAm-1 levels and low SM22-a levels in endothelial enriched samples were found. In contrast, low PECAM-1 levels and high SM22-a were observed in media and adventitia samples (LO). In addition, low CD45 levels were observed in all conditions due to non-lymphoid infiltration after 120h post PCL surgery, confirming the purity of our EC-rich and SMC-rich samples. These results are in concordance with previously published data and with Chapter V [12].

6.3.5 VHPK-CCL-anti-miR-712 biodistribution profile

After systemic administration polyplexes were distributed abroad of the organs. However, we hypothesized that our newly designed polyplexes preferably targets inflamed endothelial cells, avoiding off-targets effects over other tissue. For this study, VHPK targeted polyplexes were used to deliver therapeutic anti-miR712 and scramble anti-miRNA, which is used as a negative control, at 1 mg/kg. 48 hours post-administration, miR712, miR15a (control gene) and TIMP3 expression were analysed from different organs in order to determine their biodistribution, as shown in Figure VI-20 and Figure VI-21.

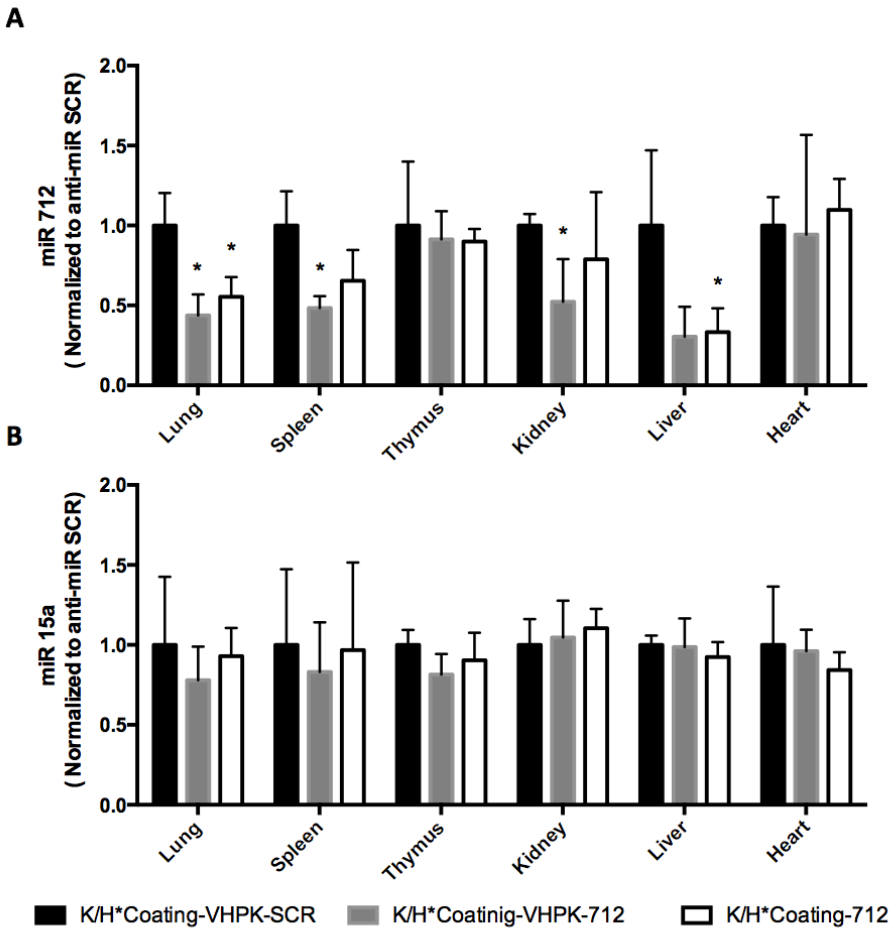

Figure VI-20. anti-miR712 biodistribution was analysed determining the A) miR712 expression and B) miR15a expression in lungs, spleen, thymus, kidney, liver and heart by qPCR. Statistical significance was determined using respective scramble controls as control group (n=4-6 mice). *p < 0.05, **p < 0.01, ***p < 0.001.

Data from Figure VI-20-A showed significant differences in miR712 expression comparing therapeutic and scramble anti-miRNA. Particularly, lung tissue present the highest miR712 knockdown after anti-miR-712 administration compared to anti-miR-SCR control, obtaining a 55% of miRNA silencing using VHPK targeted nanoparticles. In addition, VHPK targeted polyplexes carrying

anti-miR-712 significantly decrease miR712 expression in spleen and kidney. In contrast, non-relevant miR712 up- or downregulation was observed in thymus and heard using. Curiously, high variability of miR712 levels was observed in the liver, observing a non-significant difference between samples. In contrast, when anti-miR-712 was delivered using non-targeted polyplexes, non-significant miR712 downregulation was observed in spleen, kidney, thymus, liver and heart. However, miR712 levels were slightly decreased in the lung, obtaining a 45% of miR712 silencing.

To further corroborate these results, miR15a (control miRNA, non-targeted anti-miR712 gene) was analysed (Figure VI-20-B). Gene level analysis revel non-significant differences after 48h of anti-miR712 administration compared to scramble anti-miRNA control. As previously have been observed in Figure VI-15, these results corroborated the anti-miR712 specificity.

Once different miR712 expression profiles were observed, TIMP3 target gene expression was determined, as shown Figure VI-21.

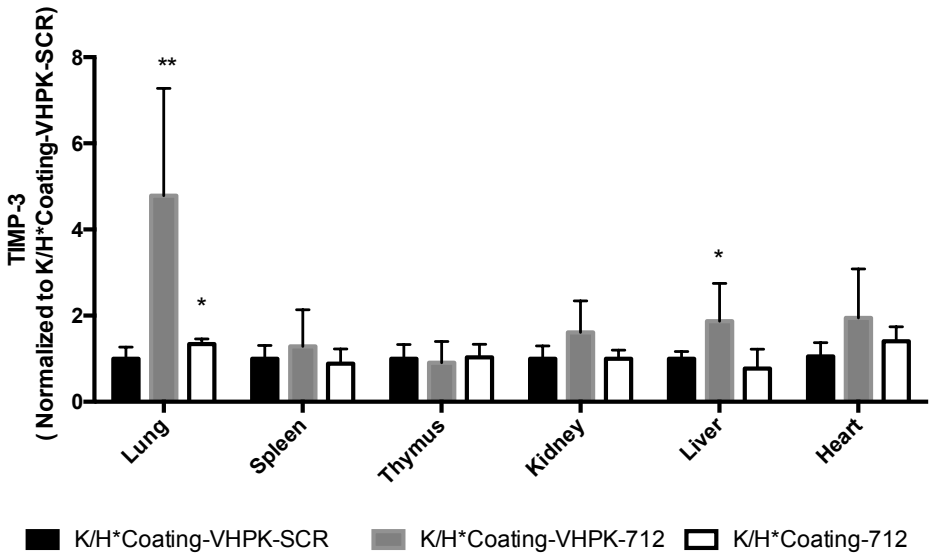

Figure VI-21. TIMP3 expression was determined after 48 hours post-administration of anti-miRNA712 in lungs, spleen, thymus, kidney, liver and heart by qPCR. Statistical significance was determined using respective scramble controls as control group (n=4-6 mice). *p < 0.05, **p < 0.01, ***p < 0.001.

Results did not show upregulation of TIMP3 after anti-miR-712 administration using targeted polyplexes in spleen, thymus, and heard. However, a slight increase in TIMP3 was observed in kidney and liver. Interestingly, more than 4-fold increase was observed in lung tissue after anti-miR-712 delivery using VHPK targeted polyplexes. In contrast, non-significant TIMP3 increase was observed when anti-miR712 was delivered non-targeted polyplexes. Therefore, these results suggest that our targeted polyplexes present a preferential delivery to lung tissue, that is well described to present high percentage of d-flow arteries.

6.3.6 TIMP3 expression is increased in lung tissue

To confirm that TIMP3 overexpression was caused by the successful delivery of anti-miR712, TIMP3 gene expression profile in the lung was further supported at protein level by a Western blotting assay and Immunofluorescence. Briefly, VHPK targeted polyplexes condensing anti-miR-712 or anti-miR-SCR were injected to five-week-old C57BL/6 mice by tail vein injection. 48 hours post injection mice were sacrificed using CO_2 and left lung was collected for protein analysis by western blot and immunofluorescence, as is showed in Figure VI-22.

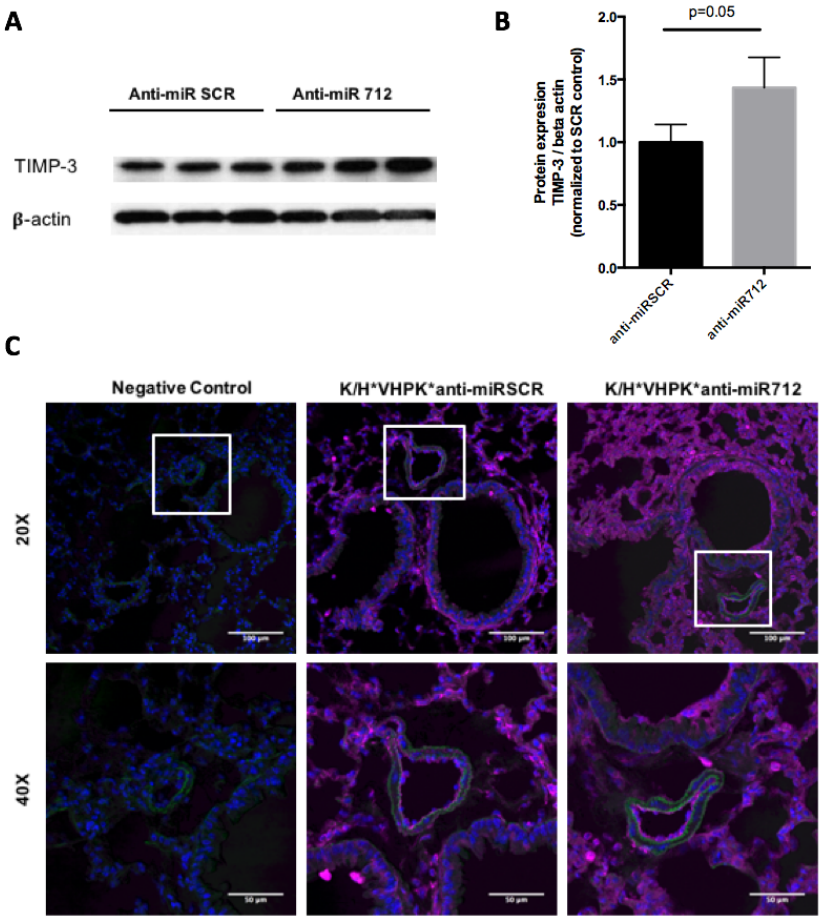

Figure VI-22. Anti-miR-712 silences miR-712 and restores TIMP3 protein expression in lungs. A-B) Representative western blots show modulation of TIMP3 expression after 48h post-injection of anti-miR712 in lungs. Statistical significance was determined using respective scramble controls as control group (n=3 mice). *p < 0.05, **p < 0.01, ***p < 0.001. C) C57bl/6 mice were injected using K/H*VHPK*anti-miR712 or K/H*VHPK*anti-miR-SCR nanoparticles. Lung frozen sections obtained from these mice were used for immunofluorescence staining with antibody specific to TIMP3 shown in purple (n=3 mice). Negative control staining was performed without primary TIMP3 antibody.

As predicted, western blot analysis showed that after anti-miR-712 delivery, TIMP3 protein level was significantly increased, compared to scramble anti-miRNA injected mice (Figure VI-22-A). To quantify TIMP3 protein expression ImageJ software was used, obtaining a 1.5-fold change once anti-miR712 was delivered. For this study, beta-actin antibody was used to normalized TIMP3 expression.

In addition, TIMP3 immunofluorescence in lung arteries was carried out using TIMP-3 antibody. Results showed a slightly increase of fluorescence when anti-miR-712 was delivered compared to scramble anti-miRNA, agreeing with western blot analysis. To confirm immune assay specificity, a negative control using secondary antibody was carried out, where no fluorescence was observed. Therefore, these results suggest that anti-miR712 delivery using VHPK targeted polyplexes may rescue TIMP3 expression from d-flow endothelial cells.

We can conclude that biodistribution studies are in concordance with previously observed data, which miR712 or TIMP3 expression are up- or downregulated when anti-miR712 is delivered using only VHPK targeted polyplexes. Particularly, miR712 is downregulated in lung, spleen, and kidney. However, only TIMP3 upregulation was observed in the lungs, obtaining a 4-fold increase at gene level and a significant 1.5-fold increase at protein level compared to scramble anti-miRNA control (Figure VI-21 and Figure VI-22). Lungs present a physiological function based on the fluid movement between the air space and the vascular system, witch's plays an important role in wide range of diseases. Therefore, osmotic water permeability is especially high across the alveolar epithelia and endothelial cells[44], [45]. Then, endothelial cell layer from lung vasculature is constantly involved in a high shear stress atmosphere. Thus, we hypothesized that certain endothelial cell layer overexpress some inflammatory markers, such as VCAM-1. Consequently, miR712 level is downregulated and TIMP3 expression is upregulated when anti-miR712 was delivered using VHPK targeted polyplexes.

6.4 Concluding remarks

We have formulated a simple design and efficient cationic polymer formulation based on poly(β-amino ester)s to deliver RNAi-drugs in a cell-specific-manner in *in vitro* and *in vivo* systems. Previously cell-efficient pBAEs were further decorated using targeting peptides to improve their cell specificity in diseased cells. We observed that combining a well described RNAi-drug with a well-described targeting peptide, our newly developed polyplexes shown a potential therapeutic effect in atherosclerosis disease.

As discussed in previous chapters, endothelial efficient oligopeptide formulation was selected by *in vitro* screening, obtaining that lysine/histidine oligopeptide composition preferentiality delivers anti-miRNA to endothelial cells, corroborating the results obtained in Chapter V. Lysine/histidine oligopeptide composition confer efficient cellular entrance and endosomal scape of anti-miRNA, making them efficient once polyplexes reach the target cells.

Once lysine/histidine oligopeptide formulation was selected, VHPK targeted polymers were synthetized and corroborated using DLS. Results showed that neutral average charge from pHPAM-TT polymer is able to decrease the positive surface charge of C6-50-K/H polyplexes from 19.4 mV to 6.0 mV, corroborating a successful polyplex coating. However, when VHPK peptide is added to coated C6-50-K/H polyplexes, surface charge of the resultant formulation is slightly increased, from 6.0 mV to 8.1 mV. Furthermore, hydrodynamic size remains stable when pHPMA-TT coating or VHPK peptide were added to C6-50-K/H polyplexes, confirming their structure integrity.

After that, VHPK targeted polyplexes were used to deliver RNAi-based drugs to inflamed endothelial cells from the vasculature. Firstly, *in vitro* assay using inflamed endothelial cells demonstrated that polyplexes enter by receptor-mediated endocytosis when VHPK peptide was added to pHPMA-TT coated C6-50-K/H polyplexes. Results were confirmed at uptake level using labelled anti-miR and at functional level, using anti-miR712.

Once inflamed endothelial specificity was observed at *in vitro* level, targeted nanoparticles were used in *in vivo* atherosclerotic mouse. When therapeutic anti-miR712 was delivered using VHPK targeted C6-50-K/H polyplexes, miR712 expression was decreased in d-flow areas (inflamed ECs), while miR712 levels in s-flow areas (healthy ECs) remain stable. Interestingly, no therapeutic effect was observed when anti-miR712 was delivered without VHPK targeting peptide, corroborating their receptor-mediated targeting pathway. Furthermore, results demonstrated that miR712 target genes, such as TIMP3, are upregulated after anti-miR712 treatment in in vitro.

Finally, biodistribution studies are in concordance with previously observed data, which miR712 is up- or downregulated when anti-miR712 is delivered using only VHPK targeted polyplexes. Particularly, miR712 is downregulated in lung, spleen, and kidney. However, only TIMP3 upregulation was observed in the lungs, obtaining a 4-fold increase at gene level and a significant 1.5-fold increase at protein level.

These results suggest that we have developed efficient vectors based in poly(β-amino ester)s with promising characteristics to treated a wide range of diseases, such as atherosclerosis. Showing that active targeting and efficient release of RNAi-drug are a key factor to obtain a successful therapeutic advance.

6.5 References

[1] Timothy A. Springer, “Adhesion receptors of immune system,” *Nat. Rev.*, vol. 346, no. 1, pp. 425–434, 1990.

[2] S. Blankenberg, S. Barbaux, and L. Tiret, “Adhesion molecules and atherosclerosis,” *Atherosclerosis*, vol. 170, no. 2, pp. 191–203, Oct. 2003.

[3] K. D. O’Brien, M. D. Allen, T. O. McDonald, A. Chait, J. M. Harlan, D. Fishbein, J. McCarty, M. Ferguson, K. Hudkins, and C. D. Benjamin, “Vascular cell adhesion molecule-1 is expressed in human coronary atherosclerotic plaques. Implications for the mode of progression of advanced coronary atherosclerosis.,” *J. Clin. Invest.*, vol. 92, no. 2, pp. 945–951, Aug. 1993.

[4] J. a Rodríguez, J. Orbe, and J. a Páramo, “[Metalloproteases, vascular remodeling and atherothrombotic syndromes].,” *Rev. Esp. Cardiol.*, vol. 60, no. 9, pp. 959–67, Sep. 2007.

[5] R. A. Preston, M. Ledford, B. J. Materson, N. M. Baltodano, A. Memon, and A. Alonso, “Effects of severe, uncontrolled hypertension on endothelial activation: soluble vascular cell adhesion molecule-1, soluble intercellular adhesion molecule-1 and von Willebrand factor,” *J Hypertens J. Hypertens.*, vol. 20, no. 20, pp. 871–877, 2002.

[6] J. T. Parissis, K. F. Venetsanou, D. G. Mentzikof, M. V Kalantzi, M. V Georgopoulou, N. Chrisopoulos, and S. M. Karas, “Plasma levels of soluble cellular adhesion molecules in patients with arterial hypertension. Correlations with plasma endothelin-1.,” *Eur. J. Intern. Med.*, vol. 12, no. 4, pp. 350–356, Jul. 2001.

[7] G. Lupattelli, R. Lombardini, G. Schillaci, G. Ciuffetti, S. Marchesi, D. Siepi, and E. Mannarino, “Flow-mediated vasoactivity and circulating adhesion molecules in hypertriglyceridemia: Association with small, dense LDL cholesterol particles,” *Am. Heart J.*, vol. 140, no. 3, pp. 521–526, Sep. 2000.

[8] L. Calabresi, “Elevated Soluble Cellular Adhesion Molecules in Subjects With Low HDL-Cholesterol,” *Arterioscler. Thromb. Vasc. Biol.*, vol. 22, no. 4, pp. 656–661, Apr. 2002.

[9] P. Clausen, P. Jacobsen, K. Rossing, J. S. Jensen, H. H. Parving, and B. Feldt-Rasmussen, “Plasma concentrations of VCAM-1 and ICAM-1 are elevated in patients with Type 1 diabetes mellitus with microalbuminuria and overt nephropathy,” *Diabet. Med.*, vol. 17, no. 9, pp. 644–649, Sep. 2000.

[10] P. F. Davies, “Endothelial Mechanisms of Flow-Mediated Athero-Protection and Susceptibility,” *Circ. Res.*, vol. 101, no. 1, pp. 10–12, May 2007.

[11] B. R. Kwak, M. Bäck, M.-L. Bochaton-Piallat, G. Caligiuri, M. J. A. P. Daemen, P. F. Davies, I. E. Hoefer, P. Holvoet, H. Jo, R. Krams, S. Lehoux, C. Monaco, S. Steffens, R. Virmani, C. Weber, J. J. Wentzel, and P. C. Evans, "Biomechanical factors in atherosclerosis: mechanisms and clinical implications," *Eur. Heart J.*, vol. 35, no. 43, pp. 3013–3020, Nov. 2014.

[12] D. Nam, C.-W. C.-W. Ni, A. Rezvan, J. Suo, K. Budzyn, A. Llanos, D. Harrison, D. Giddens, and H. Jo, "Partial carotid ligation is a model of acutely induced disturbed flow, leading to rapid endothelial dysfunction and atherosclerosis," *AJP Hear. Circ. Physiol.*, vol. 297, no. 4, pp. H1535–H1543, Oct. 2009.

[13] A. Magnin and J. M. Piau, "Cone-and-Plate Rheometry of Yield Stress Fluids. Study of an aqueous gel," *J. Nonnewton. Fluid Mech.*, vol. 36, pp. 85–108, 1990.

[14] P. F. Davies, "Hemodynamic shear stress and the endothelium in cardiovascular pathophysiology," *Nat Clin Pr. Cardiovasc Med*, vol. 6, no. 1, pp. 16–26, 2009.

[15] J. VANTHIENEN, J. FLEDDERUS, R. DEKKER, J. ROHLENA, G. VANIJZENDOORN, N. KOOTSTRA, H. PANNEKOEK, and A. HORREVOETS, "Shear stress sustains atheroprotective endothelial KLF2 expression more potently than statins through mRNA stabilization," *Cardiovasc. Res.*, vol. 72, no. 2, pp. 231–240, Nov. 2006.

[16] A. Hamik, Z. Lin, A. Kumar, M. Balcells, S. Sinha, J. Katz, M. W. Feinberg, R. E. Gerszten, E. R. Edelman, and M. K. Jain, "Kruppel-like Factor 4 Regulates Endothelial Inflammation," *J. Biol. Chem.*, vol. 282, no. 18, pp. 13769–13779, May 2007.

[17] R. Magid, T. J. Murphy, and Z. S. Galis, "Expression of Matrix Metalloproteinase-9 in Endothelial Cells Is Differentially Regulated by Shear Stress: ROLE OF c-Myc," *J. Biol. Chem.*, vol. 278, no. 35, pp. 32994–32999, Aug. 2003.

[18] S. Kumar, C. W. Kim, R. D. Simmons, and H. Jo, "Role of Flow-Sensitive microRNAs in Endothelial Dysfunction and Atherosclerosis: Mechanosensitive Athero-miRs," *Arterioscler. Thromb. Vasc. Biol.*, vol. 34, no. 10, pp. 2206–2216, Oct. 2014.

[19] D. J. Son, S. Kumar, W. Takabe, C. Woo Kim, C.-W. Ni, N. Alberts-Grill, I.-H. Jang, S. Kim, W. Kim, S. Won Kang, A. H. Baker, J. Woong Seo, K. W. Ferrara, and H. Jo, "The atypical mechanosensitive microRNA-712 derived from pre-ribosomal RNA induces endothelial inflammation and atherosclerosis," *Nat. Commun.*, vol. 4, p. 3000, Dec. 2013.

[20] N. Segovia, P. Dosta, A. Cascante, V. Ramos, and S. Borrós, "Oligopeptide-terminated poly(β-amino ester)s for highly efficient gene delivery and intracellular localization.," *Acta Biomater.*, vol. 10, no. 5, pp. 2147–58, May 2014.

[21] P. Dosta, N. Segovia, A. Cascante, V. Ramos, and S. Borrós, “Surface charge tunability as a powerful strategy to control electrostatic interaction for high efficiency silencing, using tailored oligopeptide-modified poly(beta-amino ester)s (PBAEs),” *Acta Biomater.*, vol. 20, no. 0, pp. 82–93, Jul. 2015.

[22] R. Núñez-Toldrà, P. Dosta, S. Montori, V. Ramos, M. Atari, and S. Borrós, “Improvement of osteogenesis in dental pulp pluripotent-like stem cells by oligopeptide-modified poly(β-amino ester)s,” *Acta Biomater.*, vol. 53, pp. 152–164, Apr. 2017.

[23] P. Dosta, V. Ramos, and S. Borrós, “Development of new stable poly(β-amino ester) formulations for efficient siRNA delivery,” *Unpubl. Manuscr.*

[24] P. Dosta, V. Ramos, H. Jo, and S. Borrós, “Lysine/histidine oligopeptide-modified pBAEs preferentially deliver siRNA to endothelial cells of vasculature,” *Unpubl. Manuscr.*

[25] S. Tenzer, D. Docter, J. Kuharev, A. Musyanovych, V. Fetz, R. Hecht, F. Schlenk, D. Fischer, K. Kiouptsi, C. Reinhardt, K. Landfester, H. Schild, M. Maskos, S. K. Knauer, and R. H. Stauber, “Rapid formation of plasma protein corona critically affects nanoparticle pathophysiology.,” *Nat. Nanotechnol.*, vol. 8, no. 10, pp. 772–81, Oct. 2013.

[26] M. Agrawal, Ajazuddin, D. K. Tripathi, S. Saraf, S. Saraf, S. G. Antimisiaris, S. Mourtas, M. Hammarlund-Udenaes, and A. Alexander, “Recent advancements in liposomes targeting strategies to cross blood-brain barrier (BBB) for the treatment of Alzheimer’s disease.,” *J. Control. Release*, May 2017.

[27] J. Sudimack and R. J. Lee, “Targeted drug delivery via the folate receptor,” *Adv Drug Deliv Rev*, vol. 41, no. 2, pp. 147–162, 2000.

[28] A. Banerjee, S. Pathak, V. Devi S., D. Vasan, R. Murugesan, and R. S. Verma, “Strategies for targeted drug delivery in treatment of colon cancer: current trends and future perspectives,” *Drug Discov. Today*, vol. 6446, no. 17, May 2017.

[29] S. Muro, “Challenges in design and characterization of ligand-targeted drug delivery systems,” *J. Control. Release*, vol. 164, no. 2, pp. 125–137, Dec. 2012.

[30] M. A. Bruckman, K. Jiang, E. J. Simpson, L. N. Randolph, L. G. Luyt, X. Yu, and N. F. Steinmetz, “Dual-Modal Magnetic Resonance and Fluorescence Imaging of Atherosclerotic Plaques in Vivo Using VCAM-1 Targeted Tobacco Mosaic Virus,” *Nano Lett.*, vol. 14, no. 3, pp. 1551–1558, Mar. 2014.

[31] M. Nahrendorf, F. A. Jaffer, K. A. Kelly, D. E. Sosnovik, E. Aikawa, P. Libby, and R. Weissleder, “Noninvasive Vascular Cell Adhesion Molecule-1 Imaging Identifies Inflammatory Activation of Cells in Atherosclerosis,” *Circulation*, vol. 114, no. 14, pp. 1504–1511, Oct. 2006.

[32] S. Sadekar, a Ray, M. Janàt-Amsbury, C. M. Peterson, and H. Ghandehari, “Comparative biodistribution of PAMAM dendrimers and HPMA copolymers in ovarian-tumor-bearing mice.,” *Biomacromolecules*, vol. 12, no. 1, pp. 88–96, Jan. 2011.

[33] J. SOUČEK, P. POUČKOVÁ, J. STROHALM, D. PLOCOVÁ, D. HLOUŠKOVÁ, M. ZADINOVÁ, and K. ULBRICH, “Poly [N -(2-hydroxypropyl)methacrylamide] Conjugates of Bovine Pancreatic Ribonuclease (RNase A) Inhibit Growth of Human Melanoma in Nude Mice,” *J. Drug Target.*, vol. 10, no. 3, pp. 175–183, Jan. 2002.

[34] Y. Kaneda, Y. Tsutsumi, Y. Yoshioka, H. Kamada, Y. Yamamoto, H. Kodaira, S. Tsunoda, T. Okamoto, Y. Mukai, H. Shibata, S. Nakagawa, and T. Mayumi, “The use of PVP as a polymeric carrier to improve the plasma half-life of drugs,” *Biomaterials*, vol. 25, no. 16, pp. 3259–3266, Jul. 2004.

[35] S. Abe and M. Otsuki, “Styrene maleic acid neocarzinostatin treatment for hepatocellular carcinoma,” *Curr. Med. Chem. Agents*, vol. 2, no. 6, pp. 715–726, 2002.

[36] L. Sprincl, J. Exner, O. Sterba, and J. Kopecek, “New types of synthetic infusion solutions. III. Elimination and retention of poly-[N-(2-hydroxypropyl)methacrylamide] in a test organism,” *J. Biomed. Mater. Res.*, vol. 10, no. 6, pp. 953–963, Nov. 1976.

[37] K. Ulbrich, V. Šubr, J. Strohalm, D. Plocová, M. Jelínková, and B. Říhová, “Polymeric drugs based on conjugates of synthetic and natural macromolecules,” *J. Control. Release*, vol. 64, no. 1–3, pp. 63–79, Feb. 2000.

[38] V. Šubr and K. Ulbrich, “Synthesis and properties of new N-(2-hydroxypropyl)methacrylamide copolymers containing thiazolidine-2-thione reactive groups,” *React. Funct. Polym.*, vol. 66, no. 12, pp. 1525–1538, Dec. 2006.

[39] M. J. Yanjarappa, K. V Gujraty, A. Joshi, A. Saraph, and R. S. Kane, “Synthesis of copolymers containing an active ester of methacrylic acid by RAFT: controlled molecular weight scaffolds for biofunctionalization,” *Biomacromolecules*, vol. 7, no. 5, pp. 1665–1670, 2006.

[40] R. A. Black, “TIMP3 checks inflammation,” *Nat. Genet.*, vol. 36, no. 9, pp. 934–935, 2004.

[41] J. Suo, D. E. Ferrara, D. Sorescu, R. E. Guldberg, W. R. Taylor, and D. P. Giddens, “Hemodynamic Shear Stresses in Mouse Aortas Implications for Atherogenesis,” 2007.

[42] A. Kheirolomoom, C. W. Kim, J. W. Seo, S. Kumar, D. J. Son, M. K. J. Gagnon, E. S. Ingham, K. W. Ferrara, and H. Jo, “Multifunctional Nanoparticles Facilitate Molecular Targeting and miRNA Delivery to Inhibit Atherosclerosis in ApoE –/– Mice,” *ACS Nano*, vol. 9, no. 9, pp. 8885–8897, Sep. 2015.

[43] J. N. Topper, M. A. Gimbrone Jr, and M. a Gimbrone, “Blood flow and vascular gene expression: fluid shear stress as a modulator of endothelial phenotype.,” *Mol. Med. Today*, vol. 5, no. 1, pp. 40–46, Jan. 1999.

[44] M. A. Matthay, H. G. Folkesson, and A. S. Verkman, “Salt and water transport across alveolar and distal airway epithelia in the adult lung,” *Am. J. Physiol. Cell. Mol. Physiol.*, vol. 270, no. 4, pp. L487–L503, 1996.

[45] R. D. Bland, “Lung epithelial ion transport and fluid movement during the perinatal period,” *Am. J. Physiol. Cell. Mol. Physiol.*, vol. 259, no. 2, pp. L30–L37, 1990.

This page left blank intentionally

Chapter VII

Conclusions

This page left blank intentionally

Conclusions

Efficient and safe RNAi delivery vectors based on poly(β-amino ester)s with the ability to preferentially drive nucleic acids in a tissue-specific-manner have been developed and described in this thesis.

Firstly, polyplex cell-specificity features have been successfully achieved combining poly(β-amino ester)s with different mixtures of cationic and anionic oligopeptides formulations.

- pBAE end-capping using different oligopeptide moieties were successfully synthetized and characterized. Biophysical analysis showed that pBAEs are able to condense RNAi-based nucleic acids into discrete nanoparticles with tuneable surface features, such as oligopeptide composition and net surface charge.

- Higher cellular viability and silencing efficiency have been observed at *in vitro* level using mixtures of different oligopeptide formulations compared to commercial transfection reagents.

- The results obtained using different oligopeptide modified pBAEs have shown that is possible to tailor the polyplexes physicochemical proprieties that control the efficiency and specificity of RNAi delivery vectors. This open the window to design formulations for specific therapeutic applications.

In vitro proof of concept of this new delivery system in difficult-to-transfect and challenging cell lines has been performed. Specifically, Dental Pulp Pluripotent Stem Cells (DPPSC) gene expression has been regulated using oligopeptide-modified pBAE as RNAi delivery vector.

- Arginine- / aspartic acid- oligopeptide formulation has been identified as top-performing polyplex formulation to efficiently co-deliver siRNA and plasmid DNA to DPPSCs. These polyplexes showed slightly negative surface charge allowing high rate of transfection without cytotoxicity, making them excellent vehicle to deliver high payloads of therapeutic nucleic acids.

- Downregulation of pluripotent genes, such as OCTA 3/4 and NANOG, and upregulation of osteogenic key genes, such as RUNX2, improved and accelerated the expression of crucial osteogenic markers, becoming a powerful technique to enhance bone tissue regeneration.

Secondly, stable nanoparticles based on previously developed cell-specific oligopeptides pBAE formulations have been developed, characterized, and tested.

- PBAE backbone has been modified using different hydrophobic structures, such as hexylamine, hexadecilamine, and cholesterol. Newly developed polymers are able to efficiently condense RNAi-based nucleic acids into smaller nanometric size than previously studied polymers, maintaining their surface charge tuneability.

- RNAi packaging capacity can be modulated playing with pBAE hydrophobicity as have been demonstrated by gel retardation assay. Therefore, newly developed polymers present higher packaging capacity than C32 polyplexes.

- Stability experiments demonstrated that polyplexes formulated with hexylamine or cholesterol exhibit improved stability, remaining stable for more than 24 hours in serum-containing medium. The most stable polyplexes correspond with the polyplexes with smaller hydrodynamic size and higher packaging capacity.

- Greater GFP knockdown efficiency than C32 formulation has observed when newly oligopeptide-modified pBAEs polymers have been used in *in vitro* assays. In addition, stable polyplexes allowed efficient GFP silencing in serum-containing medium, while silencing efficiency of previous C32 polymers in serum-containing medium is reduced.

- Stability and transfections studies have been demonstrated that hexylamine modified pBAE, called C6-50 polymer, is the most promising delivery formulation to be use for *in vivo* applications.

As a proof of concept, cell-specificity and stability of our new developed polyplexes have been test to preferentially deliver siRNA to endothelial cells from vasculature.

- *In vitro* assays demonstrated that lysine/histidine oligopeptide mixture preferential delivers siRNA to endothelial cells. In addition, efficient and safer gene knockdown has been achieved when a functional siRNA against ICAM-2 gene was used.

- *In vivo* results showed significant ICAM-2 knockdown effect, and a reduction of more than 55% in gene expression was achieved in endothelial cells from carotids compared to negative control. In contrast, no significant reduction of ICAM-2 was observed in other tissues, confirming the endothelial preferentiality of our newly designed polymer formulation.

- Biodistrubution studies further demonstrated that lysine/histidine oligopeptide mixture presents a selective delivery to endothelial cell line, which only ICAM-2 reduction was observed in high vascularized organs.

Targeted delivery has been presented as a promising alternative to achieve preferential delivery to inflamed endothelial cells from the vasculature, designing a potential atherosclerotic treatment. Then, RNAi polyplexes based on poly(β-amino ester)s have been modified and optimized for this propose.

- Targeted pBAEs have been successfully synthetized using a reactive hydrophilic coating called pHAM-TT. Results showed that polyplex surface charge was decreased when hydrophilic coating was added. In contrast, polyplex surface charge was increased when VHPK targeting peptide was linked.

- *In vitro* assay using TNF-α treated iMAECs demonstrated that nanoparticles enter the cells by receptor-mediated endocytosis when anti-miRNA was delivered using VHPK targeted nanoparticles. Uptake results were further corroborated using therapeutic anti-miR-712, where miR712 expression was decreased, recovering the expression of anti-atherogenic genes.

- At *in vivo* level, specific delivery of anti-miR712 to inflame endothelial cells of atherosclerotic mice model using VHPK targeted nanoparticles have been achieved without unspecific delivery to healthy endothelial cells. In addition, anti-atherogenic gens have been recovered in inflame endothelial cells after anti-miR-712 delivery. Therefore, targeting delivery have been corroborated at *in vitro* and *in vivo* atherosclerotic models.

- Biodistribution studies show that miR712 was downregulated in lung, spleen, and kidney when anti-miR-712 was delivered using VHPK-targeted nanoparticles. However, only anti-atherosclerotic genes upregulation was observed in the lungs, obtaining a 4-fold increase at gene level and 1.5-fold increase at protein level.

This page left blank intentionally

List of Publications and Presentations

Publications and Patents

P. Dosta, V. Ramos, M. Mahmoud, H.Jo*, S. Borrós*, **"Inflame endothelium delivery using VHKP targeted poly(β-amino ester)s**", Biomaterials (prepared for submission).

P. Dosta, V. Ramos, M. Mahmoud, H. Jo* and S. Borrós*, "**Lysine/histidine oligopeptide-modified pBAEs preferentially deliver siRNA to endothelial cells of vasculature**", ACS Nano (prepared for submission).

P. Dosta, V. Ramos, and S. Borrós, **"Stable and efficient generation of poly(β-amino ester)s for RNAi delivery",** ACS Biomacromolecules (submitted).

R. Núñez-Toldrà*, P. Dosta*, S. Montori, V. Ramos, M. Atari, and S. Borrós, "**Improvement of osteogenesis in dental pulp pluripotent-like stem cells by oligopeptide-modified poly(ß-amino ester)s**" Acta Biomater., Feb. 2017.

P. Dosta, N. Segovia, A. Cascante, V. Ramos, and S. Borrós, "**Surface charge tunability as a powerful strategy to control electrostatic interaction for high efficiency silencing, using tailored oligopeptide-modified poly(β-amino ester)s (PBAEs)**," *Acta Biomater.*, vol. 20, pp. 82–93, Jul. 2015.

N. Segovia, P. Dosta, A. Cascante, V. Ramos, S. Borrós, "**Oligopeptide-terminated poly(β-amino ester)s for highly efficient gene delivery and intracellular localization**"., Acta Biomater. Vol. 10, pp. 2147–58, May 2014.

V. Ramos, S. Borros, N. Segovia, P. Dosta, **Chemical compounds for gene delivery** G054086PT, EU, filed March 2013

Seminars and Courses

Pere Dosta, Nathaly Segovia, Víctor Ramos, Salvador Borròs. **Surface charge tunability as a powerful strategy to control electrostatic interaction for highly efficient delivery of nucleic acids, using tailored oligopeptide-modified poly(β-amino ester)s (PBAEs**). 10th World Biomaterials Congress. May 2016. Montreal, Canada. Poster presentation

Pere Dosta, Hanjoong Jo, Victor Ramos, Salvador Borros. **Development of nanocarriers for RNA interference delivery in humans therapeutic applications**. 2016 Suddath Symposium - Mechanobiology of the Cell. February 2016. Atlanta, USA. Poster presentation.

Pere Dosta, Nathaly Segovia, Víctor Ramos, Salvador Borròs. **Nanoparticles with Tuneable Surface Properties Prepared from Oligopeptide-terminated poly(β-amino ester)s for Highly Efficient Gene Delivery**. European Society of Gene and Cell Therapy. October 2014. The Hague. Poster presentation.

Salvador Borrós, Anna Cascante, Pau Brugada, Nathaly Segovia, Gemma Molins, Pere Dosta, Victor Ramos. **Novel peptide-modified poly(ß-amino ester)s for highly efficient gene delivery intracelular localization and specific BBB targeting**. Roche - Nature Biotechnology Symposium 2014. September 2014. Roche, Switzerland. Poster presentation.

Nathaly Segovia, Pere Dosta, Víctor Ramos, Salvador Borròs. **New oligopeptide-terminated poly(β- aminoester)s for efficient gene delivery and controlled intracellular localization**. European Society of Gene and Cell Therapy. October 2013. Madrid, Spain. Poster presentation.

Nathaly Segovia, Pere Dosta, Víctor Ramos, Salvador Borròs**. A new family of biodegradable Poly(β- aminoester)s for efficient DNA and siRNA delivery**. Workshop - European Project Alexander. November 2012. Frankfurt am Main. Poster presentation.